

THE USE OF ORGANOPHOSPHORUS EXTRACTANTS IN f-ELEMENT SEPARATIONS

By

JENIFER CLAIRE BRALEY

A dissertation submitted in partial fulfillment of
the requirements for the degree of

DOCTOR OF PHILOSOPHY

WASHINGTON STATE UNIVERSITY
Department of Chemistry

AUGUST 2010

To the Faculty of Washington State University:

The members of the Committee appointed to examine the dissertation of JENIFER CLAIRE BRALEY find it satisfactory and recommend that it be accepted.

Kenneth L. Nash, Ph.D., Chair

Sue B. Clark, Ph.D.

Guy P. Meier, Ph.D.

James O. Schenk, Ph.D.

ACKNOWLEDGMENT

“Ah but I was so much older then, I’m younger than that now”

Bob Dylan

The journey through the Washington State University chemistry department would not be complete unless I acknowledged all who supported my travels. I hope this dissertation, and the consequences of it, justifies the support they’ve invested in me over the course of the past four years.

I have to begin with giving thanks to the support of my husband Andrew, regardless his location in the world at a given time. Many times during the advancement of this degree I was uncertain I would actually complete the process. Despite my continued assertions that I would falter, his faith was unwavering. I now have to write three words I hope I never have to utter again in his general direction: You Were Right.

My advisor Ken Nash has been integral in my development as a scientist and a person (the latter he might be cringing at as he reads this acknowledgment). For me, the completion of this degree would not be complete without some personal evolutions. I thank Ken for helping to ensure those changes were positive (at least 90% of the time...).

The grace of my reactor officemates, Mark Ogden and Tom Shehee, should also be recognized. Since Mark was the first to share the office space with me, he in particular had to deal with odd sets of neuroses that would have driven a weaker man mad. Your assistance in helping me manage these will not be forgotten. Tom’s zen-like demeanor is something I deeply

appreciate, but realize I will never be able to attain in this lifetime. The guidance provided by Micke Nilsson, Peter Zalupski and Jana Sulakova should also be noted. To all people who made my time in Pullman more enjoyable, you know who you are, you have my gratitude.

The time spent at EichromNPO, in particular with Phil Horwitz, Dan McAlister and my cousin Vinny, was invaluable. The opportunity to solidify my chromatographic understanding and confidence in my scientific method was immeasurable. Vince was kind enough to let me sleep on his sofa and disturb his lifestyle without financial compensation for two months as I completed my project in Chicago. I guess that's what family is for.

While on the topic of family, I would like to thank my mom and Aunt Ellen for always stressing the value of being an educated woman in our society. When I was younger, my mother, always respectful of balancing the needs of my siblings and I, took seven years to finish the last two years of her college education. I guess I wanted to complete as much of my education as possible, as soon as possible.

Finally, this dissertation requires a committee of four brave souls to approve its existence. Kan Nash, Sue Clark, Pat Meier and Jim Schenk have been kind enough to serve on this committee. Thank you for doing this. I assure you, the rest of the document is far less interesting.

THE USE OF ORGANOPHOSPHORUS EXTRACTANTS IN f-ELEMENT SEPARATIONS

Abstract

by Jenifer Claire Braley, Ph.D.
Washington State University
August 2010

Chair: Kenneth L. Nash

Used nuclear fuel reprocessing has been typically performed using solvent extraction. Different organic extractants have been developed containing nitrogen, sulfur and phosphorus; however, the only current reprocessing separation (PUREX) applied at a large scale utilizes tri-n-butyl phosphate, an organophosphorus extractant. The lower impact of radiolysis on reagent lifetime is one reason organophosphorus extractants have seen such success in used fuel separations. This dissertation will focus on defining several applications of organophosphorus extractants to manage used fuel, using solvent extraction and extraction chromatographic separations.

The first application will focus on the development of a sludge phase minimization process to be employed at Hanford's Waste Treatment Plant. The localization of actinides in the sludge phase makes minimizing the volume of waste produced particularly important. Aggressive acidic or oxidative scrubs have been proposed; however, undesired transuranic radionuclide migration from the solid sludge to the acidic waste stream is possible. A contaminated acidic waste stream would require cleanup prior to disposal. An extraction chromatographic decontamination has been proposed using tri-n-butyl phosphate or tri-n-octyl phosphine oxide impregnated resins. Results indicate that successful removal of Eu, U, Np and Pu from the

aluminum and chromium aqueous phase is possible. An extension of these studies was initiated by examining the uptake capabilities of a resin with covalently bound phosphate moieties. The resins were ultimately determined highly susceptible to acidic degradation.

The second issue addressed by the use of organophosphorus extractants is the separation of trivalent lanthanides from trivalent actinides using organophosphorus acids in the TALSPEAK (Trivalent Actinide Lanthanide Separation by Phosphorus reagent Extraction from Aqueous Komplexes) process. Much circumstantial support exists for the aggregation of extractant molecules in the organic phase (a precursor to third phase formation). To address the possibilities of third phase formation, variations of TALSPEAK using extraction chromatography or an organophosphonic acid were developed. Results show chromatographic Am/Ln separations were comparable to separations performed using solvent extraction. Studies indicate the phosphonic acid is capable of providing a separation of comparable quality to “classical” TALSPEAK, but may be less prone to aggregation.

TABLE OF CONTENTS

	Page
ACKNOWLEDGEMENTS.....	iii
ABSTRACT	v
LIST OF TABLES	xii
LIST OF FIGURES	xi
CHAPTER ONE: INTRODUCTION	
1. INTRODUCTION.....	1
2. HANFORD REMEDIATION.....	2
3. EXTRACTION CHROMATOGRAPHY (EXC)	5
4. COVALENTLY BOUND RESIN (CBR) CHARACTERIZATION	12
5. TALSPEAK	16
6. REFERENCES.....	21
CHAPTER TWO PREFACE	28
CHAPTER TWO: EXTRACTION CHROMATOGRAPHIC BEHAVIOR OF EUROPIUM AND THE ACTINIDES BETWEEN ACIDIC AQUEOUS $Al(NO_3)_3$ AND NEUTRAL PHOSPHORUS LIGANDS	
1. ABSTRACT.....	30
2. INTRODUCTION.....	30
3. EXPERIMENTAL.....	33
Materials and Instrumentation.....	33
Resin Preparation.....	34

Extraction in Batch Experiments	35
Column Experiments	40
4. RESULTS	42
Batch Extractions.....	42
Dynamic (Column) Experiments.....	50
5. DISCUSSION	55
HNO ₃ Partitioning	55
Europium Distribution	56
Actinide Distribution	59
Uptake Kinetics	62
Static and Dynamic Capacity Determination.....	63
Single Analyte Elution Curves	66
Simulated Waste Stream Remediation.....	68
6. CONCLUSIONS	69
7. REFERENCES.....	71
 CHAPTER THREE PREFACE.....	 75
 CHAPTER THREE: INVESTIGATIONS INTO THE UPTAKE CAPABILITIES OF PHOSPHATE BASED SOLVATING EXTRACTANT RESINS	
1. ABSTRACT.....	77
2. INTRODUCTION	77
3. EXPERIMENTAL.....	83
Materials.....	83
Instrumentation.....	84

Batch Extraction	85
Infrared Characterization of pTris	89
4. RESULTS	89
Nitric Acid Dependence for U(VI)	89
Nitric Acid & Sodium Nitrate Dependence for U(VI) in the Presence of Eu and Th	90
Acidic Impurities of the pPenta and pTris Resins	90
Investigation into Acid Promoted Hydrolysis of the Solvating Extraction Resins	94
Uranium Kinetic Studies	94
The Effect of Carbonate Media on Resin Hydrolysis and Uranium Uptake..	97
Minimization of Cation Exchange by Metal Ion Pre-equilibration	97
Resin Reproducibility Studies	97
Infrared Characterization of pTris	101
5. DISCUSSION	104
Uranyl Nitrate Extraction from Nitric Acid	104
Uranyl Uptake by pPenta, pTris and pTris-Mono resins from HNO ₃	108
Extraction of U(VI) as a Function of HNO ₃ or NaNO ₃ in the Presence of Th(IV) and Eu(III)	113
Acidic Impurities of the pPenta and pTris Resins	114
Investigation into Acid Promoted Hydrolysis of the Solvating Extraction Resins	115
The Effect of Carbonate Media on Resin Hydrolysis and Uranium Uptake	116

Minimization of Cation Exchange by Metal Ion Pre-equilibration	117
Resin Reproducibility Studies	118
Infrared Characterization of pTris	119
6. CONCLUSIONS	121
7. REFERENCES	122
 CHAPTER FOUR PREFACE	 126
 CHAPTER FOUR: EXPLORATIONS OF TALSPEAK CHEMISTRY IN EXTRACTION CHROMATOGRAPHY: COMPARISONS OF TTHA WITH DTPA AND HDEHP WITH HEH[EHP]	
1. ABSTRACT	128
2. INTRODUCTION	129
3. EXPERIMENTAL	133
Reagents	133
Resin Preparation	134
Procedures	134
4. RESULTS	137
Batch Studies	137
Am/Eu Column Investigations	145
SLW Column Investigations	145
5. DISCUSSION	150
Previous Uses of Phosphonic Acids and TTHA for TALSPEAK	150
Equilibrium Constants of Significance	151
DTPA & TTHA Metal Binding	152
Organic Phase Composition	155

pH Dependence.....	155
Kinetics Investigation	157
Lactate Dependence.....	158
Lanthanide + Yttrium Uptake.....	160
Polyaminopolycarboxylic Acid Dependence	161
Am/Eu Column Behavior (LN2 Resin)	161
SLW Column Investigation.....	162
6. CONCLUSIONS	164
7. REFERENCES.....	165
CHAPTER FIVE PREFACE.....	168
CHAPTER FIVE: INSIGHT TO TALSPEAK: EXCHANGING HDEHP FOR HEH[EHP] AND DTPA FOR TTHA	
1. ABSTRACT.....	170
2. INTRODUCTION.....	171
3. EXPERIMENTAL.....	175
Materials.....	175
Methods.....	176
4. RESULTS	178
Trans-lanthanide Kinetics Investigation	178
pH Investigation	178
Lactate, Sodium & Water Partitioning.....	180
5. DISCUSSION	185
Previous Uses of Phosphonic Acids and TTHA for TALSPEAK.....	185

DTPA & TTHA Metal Binding.....	188
Kinetics	189
Metal Partitioning in TALSPEAK.....	192
Organic Phase Composition	194
6. CONCLUSIONS	197
6. REFERENCES.....	199

CHAPTER SIX: CONCLUSIONS

1. HANFORD SITE REMEDIATION.....	202
2. COVALENTLY BONDED RESINS WITH PHOSPHATE ESTER MOIETIES	205
3. EXTRACTION CHROMATOGRAPHIC EXAMINATIONS OF TALSPEAK CHEMISTRY.....	208
4. THE EXAMINATION OF HEH[EHP] & TTHA FOR TALSPEAK SOLVENT EXTRACTION SYSTEMS	211

LIST OF TABLES

1. CHAPTER ONE: INTRODUCTION	1
Table 1.1. Preliminary uptake results uranium from a 20 ppm UO_2^{2+} aqueous phase using pPenta, pTris and pTris-Mono. Errors indicate $\pm 1\sigma$ standard deviation.....	14
2. CHAPTER TWO: EXTRACTION CHROMATOGRAPHIC BEHAVIOR OF EUROPIUM AND THE ACTINIDES BETWEEN ACIDIC AQUEOUS $\text{Al}(\text{NO}_3)_3$ AND NEUTRAL PHOSPHORUS LIGANDS:	30
Table 2.1. Preliminary uptake results uranium from a 20 ppm UO_2^{2+} aqueous phase using pPenta, pTris and pTris-Mono.	36
Table 2.2 Defined parameters for various TOPO-XAD7 n-dodecane wetted resins	41
Table 2.3 Time required for various concentrations of Eu^{3+} and UO_2^{2+} to reach equilibrium using different modifications of the TOPO-XAD7 resin. The aqueous phase initially contained 0.1 M HNO_3 , 0.25 M $\text{Al}(\text{NO}_3)_3$, 1 mM K_2CrO_4 and 2 mM ascorbic acid. $V:m = 1$ mL aqueous solution : 50 mg resin.....	48
Table 2.4. Neptunium redox reaction significant to understanding simulated acidic aqueous raffinate of the Hanford tanks.....	57
3. CHAPTER THREE INVESTIGATIONS INTO THE UPTAKE CAPABILITIES OF PHOSPHATE BASED SOLVATING EXTRACTANT RESINS	78
Table 3.1. Infrared vibrational modes significant to the analysis of pTris resin...	103
4. CHAPTER FOUR: EXPLORATIONS OF TALSPEAK CHEMISTRY IN EXTRACTION CHROMATOGRAPHY: COMPARISONS OF TTHA WITH DTPA AND HDEHP WITH HEH[EHP].....	128
Table 4.1. Column performance for Am/Eu separation with LN2 resin using 5 mM DTPA or TTHA at a pH of 2.78 or 3.5, respectively. $[\text{Eu}] = 1$ mM, $[\text{Lac}]_{\text{tot}} = 1$ M, $[\text{NO}_3^-] = 1$ M, flow rate and temperature 1 mL / min and 25° C, unless otherwise noted.....	148

	Table 4.2. Optimized Lanthanide elution curve separation using LN (HDEHP) S-grade (50-100 μm) Amberchrom GC71 resin. Flow rate: 1 mL / min. Column rinse volume: 20 mL. Column strip volume: 10 mL Load: 1 M Lactate, pH 3.3. Simulated Waste Concentrations of Lanthanides TALSPEAK Rinse: 2.5 mM TTHA, 1 M NO_3 , pH 3.5 Wash: 0.001 M HNO_3 Strip: 1 M HNO_3	150
	Table 4.3. Available equilibrium constants of significance for examining TALSPEAK systems within this report	153
5.	CHAPTER FIVE: INSIGHT TO TALSPEAK: EXCHANGING HDEHP FOR HEH[EHP] AND DTPA FOR TTHA.....	170
	Table 5.1. Distribution of select lanthanides + Y as a function of pH for the HEH[EHP]/DTPA TALSPEAK system for both 30 minute and 48 hour contact times. Error bars indicate a $\pm 1 \sigma$ error.....	184
	Table 5.2. Equilibrium constants for the MR_2^- species under various ionic strengths. “Model” value describes values used to fit lanthanide distribution shown in Figure 3.5	184

LIST OF FIGURES

1. CHAPTER ONE: INTRODUCTION	1
<p>Figure1.1. Waste phases in a typical Hanford tank. The sludge phase creates the most significant remediation challenge as it contains a majority of the actinides. Also problematic is the inconsistent chemical composition of the sludge from tank to tank.....</p>	3
<p>Figure1.2. Components of an extraction chromatographic resin</p>	7
<p>Figure 1.3. Schematic showing how to obtain significant terms for the calculation of a distribution value for an a) elution curve and b) a breakthrough curve. Definitions: V_m- Mobile phase (mL); V_s – Stationary phase volume (mL); $V_{mr} = V_r + V_m$ – Total Retention volume (mL); V_r – Retention volume (mL); V_b – Breakthrough volume (mL); $V_{mb} = V_m + V_b$ – Total breakthrough volume (mL); V^* – Eluent volume when the concentration of the eluent reaches $0.157C_0$ (mL); C_0- Initial concentration; β – Peak width at $c = 0.368 c_{max}$ (mL); N – Number of theoretical plates in the bed; N^* – Number of theoretical plates from the center of the sample application band to the bed end; D- Concentration distribution ratio; C_s – Concentration of the analyte in the stationary phase; C_m – Concentration of the analyte in the mobile phase [M]</p>	10
<p>Figure 1.4. Chemical Structure of Amberlite XAD-7HP polymeric adsorbant.....</p>	12
<p>Figure 1.5. Structures of immobilized: a) pentaerythritol triethoxylate (<i>pPenta</i>) b) Tris(hydroxymethyl)amino methane (<i>pTris</i>) c) Mono-Tris (hydroxymethyl)aminomethane (<i>pTris-Mono</i>)</p>	14
<p>Figure 1.6. a) Interaction of phosphorylated pentaerythritol with divalent and trivalent ions b) Interaction of phosphate ligands with the amine moiety through hydrogen bonding and with Fe(III)</p>	15
<p>Figure 1.7. a) Structures of the components used in these studies; a: bis(2-ethylhexyl) phosphoric acid (HDEHP) b: diethylenetriamine-N,N,N',N'',N'''-pentaacetic acid (DTPA) c: 2-ethylhexyl 2-ethylhexylphosphonic acid (HEH[EHP]) d: triethylenetetramine-N,N,N',N'',N''',N''''-hexaacetic acid, (DTPA) e: lactic acid (HL)</p>	18
<p>Figure 1.8. Equilibrium constants for DTPA and TTHA with the lanthanides</p>	

and americium in 0.1 M ionic media at 25 °C.....	20
2. CHAPTER TWO: EXTRACTION CHROMATOGRAPHIC BEHAVIOR OF EUROPIUM AND THE ACTINIDES BETWEEN ACIDIC AQUEOUS $\text{Al}(\text{NO}_3)_3$ AND NEUTRAL PHOSPHORUS LIGANDS:	30

Figure 2.1. *a)* Distribution of HNO_3 between acidic $\text{Al}(\text{NO}_3)_3$ and resin as $\text{Al}(\text{NO}_3)_3$ is varied between 0.01 to 1.5 M in 60% TBP-XAD7 (left y-axis) and 58% TOPO-XAD7 (right y-axis) resin *b)* Nitric acid uptake in mmol as a function of aqueous $[\text{Al}(\text{NO}_3)_3]$ from 0.01-1.5 M for 58% TOPO-XAD7 resin. Concentrations of nitric acid were held constant and are noted in legend. The dashed line and the dotted line represent the saturating mmol of HNO_3 in the organic solid phase for the TOPO· HNO_3 and (TOPO) $_2$ · HNO_3 species, respectively.....44

Figure 2.2. Nitric acid or aluminum nitrate dependences for europium nitrate adsorption into TBP or TOPO XAD7 resin. Initially present in each aqueous solution was 1.0 mM K_2CrO_4 and 2 mM ascorbic acid. *a)* Aluminum nitrate was varied from 0.01 to 1.5 M ■ 0.01 M HNO_3 ● 0.10 M HNO_3 ▲ 1.00 M HNO_3 . Organic phase: 50 mg TBP-XAD7 *b)* Aluminum nitrate was varied from 0.01 to 1.5 M ■ 0.01 M HNO_3 ● 0.10 M HNO_3 ▲ 1.00 M HNO_3 . Organic phase: 100 mg TOPO-XAD7 *c)* Nitric acid varied from 0.01 to 1.5 M ■ 0.01 M $\text{Al}(\text{NO}_3)_3$ ● 0.1 M $\text{Al}(\text{NO}_3)_3$ Organic phase: 50 mg TBP-XAD7 *d)* Nitric acid varied from 0.01 to 1.5 M ■ 0.01 M $\text{Al}(\text{NO}_3)_3$ ● 0.1 M $\text{Al}(\text{NO}_3)_3$ Organic phase: 100 mg 60% TOPO-XAD7.45

Figure 2.3. Metal distribution values as a function of aqueous $[\text{Al}(\text{NO}_3)_3]$ with $[\text{HNO}_3]$ equal to *a)* 0.01 M *b)* 0.1 M and *c)* 1 M. The various elements and redox conditions described as follows: ■ Th^{4+} , No Cr ● UO_2^{2+} , No Cr ▲ Eu, No Cr ○ Np, No Cr □ Np, 1 mM CrO_4^{2-} ▲ Np, 1 mM CrO_4^{2-} , 2 mM ascorbic acid Organic phase: 100 mg TOPO-XAD7.47

Figure 2.4. Isotherms comparing the uptake behavior of Eu with the 58% TOPO-XAD7, 58% TOPO-XAD7n and 38% TOPO-XAD7n resins. Uranium isotherm also shown for the 38% TOPO-XAD7n resin. Initial aqueous phase: 0.1 M HNO_3 , 0.25 M $\text{Al}(\text{NO}_3)_3$, 1 mM K_2CrO_4 , 2 mM ascorbic acid. Resin phase: 50 mg of the appropriate resin.49

Figure 2.5. Breakthrough curves comparing the column saturation behavior of Eu with the 58% TOPO-XAD7n and 38% TOPO-XAD7n resin. Uranium behavior also shown for the 38% TOPO-XAD7n resin. Aqueous phase: 0.1 M HNO_3 , 0.25 M $\text{Al}(\text{NO}_3)_3$, 1 mM K_2CrO_4 , 2 mM ascorbic acid. Concentration of metal are 50 mM unless otherwise noted52

Figure 2.6. Elution curves showing the load and strip capabilities of Eu, U, Np and Pu with 38% TOP-XAD7n resin. The loading aqueous phase for europium studies included 0.1 M HNO_3 , 0.25 M $\text{Al}(\text{NO}_3)_3$,

1 mM K ₂ CrO ₄ , 2 mM ascorbic acid unless noted. The load concentration of europium or uranium was 50 mM. Neptunium and plutonium studies were only performed at tracer conditions. The loading aqueous phase for all actinide studies contained 0.1 M HNO ₃ , 0.25 M Al(NO ₃) ₃ , 1 mM K ₂ CrO ₄ . Europium strip conditions are indicated by their appropriate chromatogram. All actinide strips conditions included 0.1 M HDEPA and 1 mM K ₂ CrO ₄ . Exceptions to the general experimental parameters presented are noted. within the figure	53
Figure 2.7. Loading and elution of U, Pu, Np and Eu by 38% TOPO-XAD7n column from simulated waste stream containing 1 mM K ₂ CrO ₄ , 0.1 M HNO ₃ and 0.25 M Al(NO ₃) ₃ shown on a semi-log scale to allow viewing of column tailing. Elution of Eu was performed using 3 M HNO ₃ and 1mM KBrO ₃ to maintain Np and Pu in the hexavalent state in the absence of chromate. Elution of actinides was performed using 0.1 M 1-hydroxyehtane-1,1-diphosphonic acid (HEDPA) and 1 mM KBrO ₃	54
3. CHAPTER THREE INVESTIGATIONS INTO THE UPTAKE CAPABILITIES OF PHOSPHATE BASED SOLVATING EXTRACTANT RESINS	78
Figure 3.1. Structure of tri-n-butyl-phosphate (TBP).....	81
Figure 3.2. Diagram showing the affect of the removal of oxygen on the basicity of common types of neutral phosphorus functional groups.....	81
Figure 3.3. Structures of immobilized resins: a) pentaerythritol triethoxylate (pPenta) b) tris-(hydroxymethyl)amino methane (pTris) c) mono-tris(hydroxymethyl)amino methane (pTris-Mono).....	82
Figure 3.4. Structure of bis-(2-ethylhexyl) phosphoric acid.	82
Figure 3.5. Extraction of UO ₂ ²⁺ as a function of the activity of nitric acid between 6.4 X 10 ⁻³ M to 4 M HNO ₃ . The green data displays the UO ₂ ²⁺ extraction data reported byin Dr. Alexandratos's lab	92
Figure 3.6. Comparison of the extraction of UO ₂ ²⁺ as a function of the activity of nitric acid or sodium nitrate with 0.01 M HNO ₃ from 6.4 X 10 ⁻³ M to 4 M HNO ₃ /NaNO ₃ combinations. Europium and thorium are present at 10 ⁻⁴ M. The corrected weight distribution ratio, Dw ₀ , accounts for the presence of UO ₂ (NO ₃) ⁺ in the aqueous phase. Each resin has 0.05 meq of ligand present.....	93
Figure 3.7a. Change in pH of DI H ₂ O after contact with 200 mg and 100 mg of pPenta and pTris, respectively. Figure 3.7b. Titration study showing the mmol of H ⁺ released per contact with 1 mL DI H ₂ O for the pTris resin. Legend indicates the length of time allowed per DI H ₂ O contact with pTris.....	94

Figure 3.8. Extraction of 1×10^{-4} M $\text{UO}_2(\text{NO}_3)_2$ as a function of the activity of HNO_3 between 6.4×10^{-3} to 4 M HNO_3 by 0.05 meq of the appropriate resin. Filled data points indicate resin that had no pre-equilibration performed prior to contact. Open data points indicate resin that was pre-equilibrated 3X at the appropriate acid concentration prior to uranium extraction. Axes descriptions apply to all axes.....	96
Figure 3.9. Extraction of uranium as a function of time by the pTris and pPenta resins using 0.025 and 0.5 meq of resin, respectively. The aqueous phase volume was 10 mL and 0.5 mL for the pPenta and pTris studies, respectively. The uranium concentration was decreased for the pTris resin in an attempt to improve the uptake kinetics.....	97
Figure 3.10. The carbonate concentration dependence of uranium uptake using 0.025 meq of the pTris resin. It should be noted that for Na_2CO_3 concentrations above 0.1 M, no detectable extraction of uranium was observed....	99
Figure 3.11. The nitric acid dependence of uranium uptake using 0.025 meq of the pTris resin. Preequilibrations were performed with 0.4 mL of the appropriate Zr or Fe solution listed. The percentages show the meq of Fe or Zr present relative to the total meq of phosphorus present in the pTris	100
Figure 3.12. The nitric acid dependence of uranium uptake using 0.05 meq of the pTris resin. The 1 st contact indicates the uptake of uranium from resin that had not previously been used for uranium extraction . The 2 nd contact indicates the use of that same resin after an attempted reconditioning had been performed.....	101
Figure 3.13. From left to right, infrared spectra obtained initially and nine months after receiving the pTris.....	103
Figure 3.14. IR spectra for the pTris resin when the resin is wetted with water, dried in an oven for three hours, then wetted again. Inset 3.14a and 3.14b highlight the aromatic and phosphorus IR absorptions , respectively, for all resin conditions. Inset 3.14c and 3.14d zoom towards the IR baseline to allow observation of spectral activity for the dried resin.....	104
Figure 3.15. The IR spectra pTris after a 34 day contact with 1, 2 and 4 M HCl. Three days were allowed for drying of the resins under vacuum	106
Figure 3.16. The IR spectra of pTris after a 34 day contact with 1, 2 and 4 M HCl. Five days were allowed for drying of the resins under vacuum	107
Figure 3.17. Extraction of $\text{UO}_2(\text{NO}_3)_2$ by TBP as a function of nitric acid concentration. "D" is the distribution ratio defined as $D = [\text{U}_{\text{org}}]/[\text{U}_{\text{aq}}]$ at equilibrium.	108

Figure 3.18. Tributyl phosphate/nitric acid complex speciation in the organic phase as a function of nitric acid concentration for 1.035 M (30% v/v) TBP.	110
Figure 3.19. Proposed base catalyzed pathway for degradation of pPenta resin..	111
Figure 3.20. Potential interaction of pTris-Mono hydroxyl groups with ammonia linker. This interaction may decrease the probability of alcoholic oxygens interaction with the partial positive charge of the phosphoryl group.	112
Figure 3.21. Proposed acid catalyzed pathway for degradation of pTris resin.....	112
4. CHAPTER FOUR: EXPLORATIONS OF TALSPEAK CHEMISTRY IN EXTRACTION CHROMATOGRAPHY: COMPARISONS OF TTHA WITH DTPA AND HDEHP WITH HEH[EHP].....	128
Figure 4.1. Structures of the components used in these studies; a: bis (2-ethylhexyl) phosphoric acid (HDEHP) b: diethylenetriamine-N,N,N',N'',N'''-pentaacetic acid (DTPA) c: 2-ethylhexyl 2-ethylhexylphosphonic acid (HEH[EHP]) d: triethylenetetramine-N,N,N',N'',N''',N''''-hexaacetic acid (TTHA) e: lactic acid (HL)	131
Figure 4.2. Equilibrium constants for DTPA and TTHA with the lanthanides and americium in 0.1 M ionic media at 25 °C.....	132
Figure 4.3. Uptake of europium and americium as a function of pH using 900 mg of LN (HDEHP) resin. Aqueous phase was 0.5 mL and included 1 mM Eu, 1 M total lactic acid, 1 M NO ₃ ⁻ and 5 mM DTPA or TTHA. Contact time was one hour. Values next to lines describe the slope of the data on a logarithmic scale. All errors presented are estimated at 10%. <i>DTPA</i> -- ● Eu ■ Am <i>TTHA</i> -- ○ Eu □ Am.....	139
Figure 4.4. Uptake of europium and americium as a function of pH using 900 mg of LN2 (HEH[EHP]) resin. Aqueous phase was 0.5 mL and included 1 mM Eu, 1 M total lactic acid, 1 M NO ₃ ⁻ and 5 mM DTPA or TTHA. Contact time was one hour. Values next to lines describe the slope of the data on a logarithmic scale. All errors presented are estimated at 10%. <i>DTPA</i> -- ● Eu <i>TTHA</i> -- ○ Eu □ Am	140
Figure 4.5. Comparison of the rate of uptake of americium and europium by 900 mg of LN or LN2 resins under TALSPEAK conditions. The aqueous phase was 0.5 mL and included 1 mM Eu, 1 M total lactic acid, 1 M NO ₃ ⁻ and 5 mM DTPA or TTHA. All errors presented are estimated at 10% of the weight distribution values. The aqueous phase pH for each system is as follows: DTPA/LN – 2.39, DTPA/LN2 – 2.78, TTHA/LN – 3.03, TTHA/LN2 – 3.49. <i>DTPA/LN</i> – ■ Eu □ Am <i>DTPA/LN2</i> – ● Eu ○ Am <i>DTPA/LN2/Eu</i> – ▲	

<i>TTHA/LN2/Eu</i> – ▼	141
------------------------------	-----

Figure 4.6. The uptake of Eu and Am as a function of the total formal concentration of lactate by 900 mg of LN or LN2 resins. Aqueous phase was 0.5 mL at a pH of 3.6 and included 1 mM Eu, 1 M NO₃⁻ and 5 mM DTPA or TTHA. Values next to lines describe the slope of the data on a logarithmic scale. All errors presented are estimated at 10% of the weight distribution values. Contact time was one hour. LN/Eu – ■ TTHA □ DTPA LN2/Eu – ● TTHA ○ DTPA LN/Am/TTHA – ▲

.....	142
-------	-----

Figure 4.7. Lanthanide + Y uptake under TALSPEAK conditions by 900 mg of LN and LN2 resins. The aqueous phase was 0.5 mL at a pH of 3.6 (DTPA) or 3.9 (TTHA) and included 1 mM Eu, 1 M total lactate, 1 M NO₃⁻ and 5 mM DTPA or 10 mM TTHA. Lanthanide concentrations ranged from 8 to 60 ppm to provide the maximum detection limits possible by the ICP-AES. All experiments were performed at a lanthanide resin loading of less than 3%. Contact time was one hour. All errors presented are estimated at 10%.

■ LN/DTPA □ LN/TTHA ● LN2/DTPA ○ LN2/TTHA	143
---	-----

Figure 4.8. Dependence of americium distribution on the concentration of select polyaminopolycarboxylic acids with 900 mg of LN or LN2 resin. The aqueous phase was 0.5 mL at a pH of 2.8 (DTPA) and 3.5 (TTHA) and included 1 mM Eu, 1 M total lactate and 1 M NO₃⁻. Values next to lines describe the slope of the data on a logarithmic scale. All errors presented are estimated at 10% of the weight distribution ratios. Contact time was one hour.

■ LN/DTPA □ LN2/DTPA ● LN/TTHA ○ LN2/TTHA	145
---	-----

Figure 4.9. Optimized Am(III), Eu(III) elution curve separation using LN2 (HEH[EHP]) S-grade (50-100 μm) Amberchrom GC71 resin. Flow rate: 1 mL / min. Temperature: 50° C. **Load:** 5 mM TTHA, 1 M NO₃⁻, pH 3.6, 1 mM Eu, Trace Am **TALSPEAK Rinse:** 5 mM TTHA, 1 M NO₃⁻, pH 3.6 **Wash:** 0.001 M HNO₃ **Strip:** 1 M HNO₃. ■ Am ● Eu.....

.....	147
-------	-----

Figure 4.10. Separation factors of Am from simulated liquid waste lanthanides using the LN resin (unless otherwise noted) under the conditions supplied. [NO₃⁻] = 1 M, [Lac] = 1 M. Lanthanide concentrations defined in Table 2. *DTPA (mM, pH)* -- ■ 0.5, 3.4 ● 2.5, 3.5 *TTHA (mM, pH)* -- □ 5, 3.5 (LN2 resin) ○ 2.5, 3.5 △ 10, 3.8.....

.....	149
-------	-----

Figure 4.11. Speciation diagram showing DTPA and lactic acid calculated using protonation constants at 0.1 M ionic strength, 25.0°C. The dotted rectangle outlines approximate working conditions for the TALSPEAK system

.....	154
-------	-----

5. CHAPTER FOUR: INSIGHT TO TALSPEAK: EXCHANGING HDEHP

FOR HEH[EHP] AND DTPA FOR TTHA.....170

Figure 5.1. Structures of the components used in these studies; a: di (2-ethylhexyl) phosphoric acid (HDEHP) b: diethylenetriamine-N,N,N',N'',N''',N''''-pentaacetic acid (DTPA) c: 2-ethylhexyl 2-ethylhexylphosphonic acid (HEH[EHP]) d: triethylenetetramine-N,N,N',N'',N''',N''''-hexaacetic acid (TTHA) e: lactic acid (HL)173

Figure 5.2. Equilibrium constants for DTPA and TTHA with the lanthanides and americium in 0.1 M ionic media at 25 °C.....174

Figure 5.3. The affect of lactate concentration on the extraction kinetics of the lanthanides for several modifications of the TALSPEAK process. For all studies, the following were present. *Aqueous phase*: 1 M NO₃⁻, pH = 3.6, 20 mM DTPA or TTHA *Organic Phase*: 0.1 M HDEHP/HEH[EHP] in n-dodecane. All lactate concentrations presented indicate the formal concentration of lactate. Additional data shown for the HDEHP/TTHA system when data was presentable with minimal overlap. Error bars indicate 1σ error179

Figure 5.4. Distribution of europium and americium as a function of pH for several modifications of the TALSPEAK process after a thirty minute contact. For all studies the following were present: *Aqueous phase*: 1 M total lactic acid, 1 M NO₃⁻, 20 mM DTPA *Organic phase*: 0.1 M HDEHP or HEH[EHP] in n-dodecane. Error bars indicate ±3σ error. Thermodynamic equilibrium constants used in distribution calculations for DTPA and TTHA were at 0.1 and 0.5 M ionic strength, respectively. ■ Eu □ Am Solid lines indicate calculated trends for Eu. Dashed lines indicate calculated trends for Am181

Figure 5.5. Distribution of europium and americium as a function of pH for several modifications of the TALSPEAK process after a thirty minute contact. For all studies the following were present: *Aqueous phase*: 1 M total lactic acid, 1 M NO₃⁻, 20 mM TTHA *Organic phase*: 0.1 M HDEHP or HEH[EHP] in n-dodecane. Error bars indicate ±3σ error. Thermodynamic equilibrium constants used in distribution calculations for DTPA and TTHA were at 0.1 and 0.5 M ionic strength, respectively. ■ Eu □ Am Solid lines indicate calculated trends for Eu. Dashed lines indicate calculated trends for Am182

Figure 5.6. Distribution of select lanthanides and Y as a function of pH for the HEH[EHP]/DTPA TALSPEAK system using a 48 hour contact time. For all studies the following were present: *Aqueous phase*: 1 M total lactic acid, 1 M NO₃⁻, 20 mM DTPA *Organic phase*: 0.1 M HDEHP or HEH[EHP] in n-dodecane. All error bars indicate ±1σ error. a) Metal-DTPA constants included in calculations were at 0.1 M ionic strength. Lines indicate the calculated extraction patterns based on thermodynamic data. - La - - - Eu •••Dy - - - - Y •••• Lu. b) Metal-DTPA constants included in calculations were

manipulated to fit data. Lines here show calculated extraction patterns with adjustment to $\log \beta_{101}$ metal-DTPA equilibrium constant. — La - - - Eu •••Dy
 -.-.- Y •••• Lu.....183

Figure 5.7. Water and lactate partitioning as a function of formal lactate concentration. For all studies the following were present: *Aqueous phase*: 1 M total lactic acid, 1 M NO_3^- , 20 mM DTPA, $\text{pH}(\text{final}) = 3.5$ *Organic phase*: 0.2 M HDEHP or 0.1 M HEH[EHP] in n-dodecane. Samples were contacted for 15 minutes. Error bars indicate $\pm 1\sigma$ error. *HDEHP*- ■ H_2O □ HL *HEH[EHP]*- ● H_2O ○ HL •••Calculated concentration of lactic acid in organic phase based on K_d into n-dodecane -.-.- Calculated concentration of water in organic phase based on K_d into kerosene.186

Figure 5.8. Sodium partitioning as a function of formal lactate concentration or pH. For all lactate dependence studies the following were present: *Aqueous phase*: 1 M NO_3^- , 20 mM DTPA *Organic phase*: 0.1 M HDEHP or HEH[EHP] in n-dodecane. The pH was 3.5 for all lactate dependence studies. For pH dependence studies, the total lactic acid concentration was 1 M. All data corresponding to pH dependence study are correlated to the top and right axes. All data corresponding to the lactate dependence study are correlated to the bottom and left axes. Samples were contacted for 15 minutes. Error bars indicate $\pm 1\sigma$ error187

Figure 5.9. Speciation diagram showing DTPA and lactic acid calculated using protonation constants at 0.1 M ionic strength, 25.0°C. The dotted rectangle demarcates approximate working conditions for the TALSPEAK system190

6. CHAPTER SIX: CONCLUSIONS202

Figure 6.1. Structures of immobilized: a) pentaerythritol triethoxylate (**pPenta**) b) tris (hydroxymethyl)amino methane (**pTris**) c) mono-tris(hydroxymethyl)amino methane (**pTris-Mono**)206

Figure 6.2. Structures of the components used in these studies; a) bis (2-ethylhexyl) phosphoric acid (HDEHP) b) diethylenetriamine-N,N,N',N'',N'''-pentaacetic acid (DTPA) c) 2-ethylhexyl 2-ethylhexylphosphonic acid (HEH[EHP]) d) triethylenetetramine-N,N,N',N'',N''',N''''-hexaacetic acid (TTHA) e) lactic acid (HL)212

Dedication

To Andrew: who tolerates my wild ideas.

CHAPTER ONE

INTRODUCTION

In 1978 James Earl “Jimmy” Carter, 39th President of the United States, signed into law the Nuclear Non-Proliferation Act thus fating any used nuclear fuel from commercial reactors in the US for final disposal in a geological repository without reprocessing. The Yucca Mountain Nuclear Waste Repository was designated by Congress in 2002 as the final disposal site for much of the United State’s nuclear waste. Funding for the Yucca Mountain repository was halted on February 26, 2009 by the 44th President of the United States, Barack Obama. As an effect of these actions, the USA currently lacks a plan for the final disposal of used nuclear fuel arising from as high level waste from nuclear weapons productions.

Two factors press for an increased understanding of nuclear waste management, reprocessing and remediation. As energy costs continue to rise throughout the world, the use of nuclear power becomes more acceptable. Today, roughly 17% of the world’s electricity is derived from nuclear power^[1], but the need for a more diversified energy plan is expected to drive that percentage higher. It is predicted that uranium resources will last over 100 years at current consumption rates.^[2] While 100 years seems noteworthy, increased consumption could have significant effects on the amount of uranium available for the long term if reprocessing does not occur. Further, the remediation of the Hanford and Savannah River sites, plutonium production facilities used during World War II, requires continuing innovation and creativity due to the storage methods and numerous separations processes used during the 45 years of plutonium production.^[3] Both the possibility of reprocessing and the requirement of remediation have helped to drive the research of the nuclear materials separations community.

Hanford Site Remediation

The Department of Energy's Hanford Site, located in south central Washington state, was the first facility that produced weapons grade Pu for use in nuclear weapons. Application of the Bismuth Phosphate, REDOX and PUREX processes employed at the Hanford Site during 40+ years of Pu production resulted in the creation of $\sim 2 \times 10^5$ m³ of highly radioactive waste, stored in 177 underground waste tanks.^[4] The raffinates from plutonium production, initially acidic, were made alkaline with excess NaOH prior to dispositioning to the underground tanks. Alkaline conditions favored precipitation of the metal species and reduced corrosion of the carbon steel liner of the tanks. This precipitation created a metal hydroxide/oxide sludge containing the bulk of the actinides in the waste. A schematic of a typical Hanford tank is shown in [Figure 1.1](#).

The wastes eventually partitioned into three phases: the saltcake, sludge and supernatant. The top, saltcake layer predominantly contains sodium salts of CO_3^{2-} , SO_4^{2-} , NO_2^- , NO_3^- and OH^- . The bottom, sludge layer is composed of oxide, hydroxide, sulfate, phosphate and silicate solids of metallic fission products. The middle, supernatant phase is a solution/slurry comprised of the saltcake components above, the sludge components below and any water left after evaporation during several decades in storage.^[5]

The Waste Treatment Plant, to which the tank waste will be sent to separate sludge components into Low Level Waste (LLW) and High Level Waste (HLW), is currently under construction at Hanford to facilitate tank waste management and disposition. The LLW will be disposed of at the Hanford Site, while the HLW will be incorporated into a borosilicate glass matrix and stored at a government sponsored geologic repository.^[6] The phase that poses the most significant challenges in this process is the sludge. Two of the most problematic

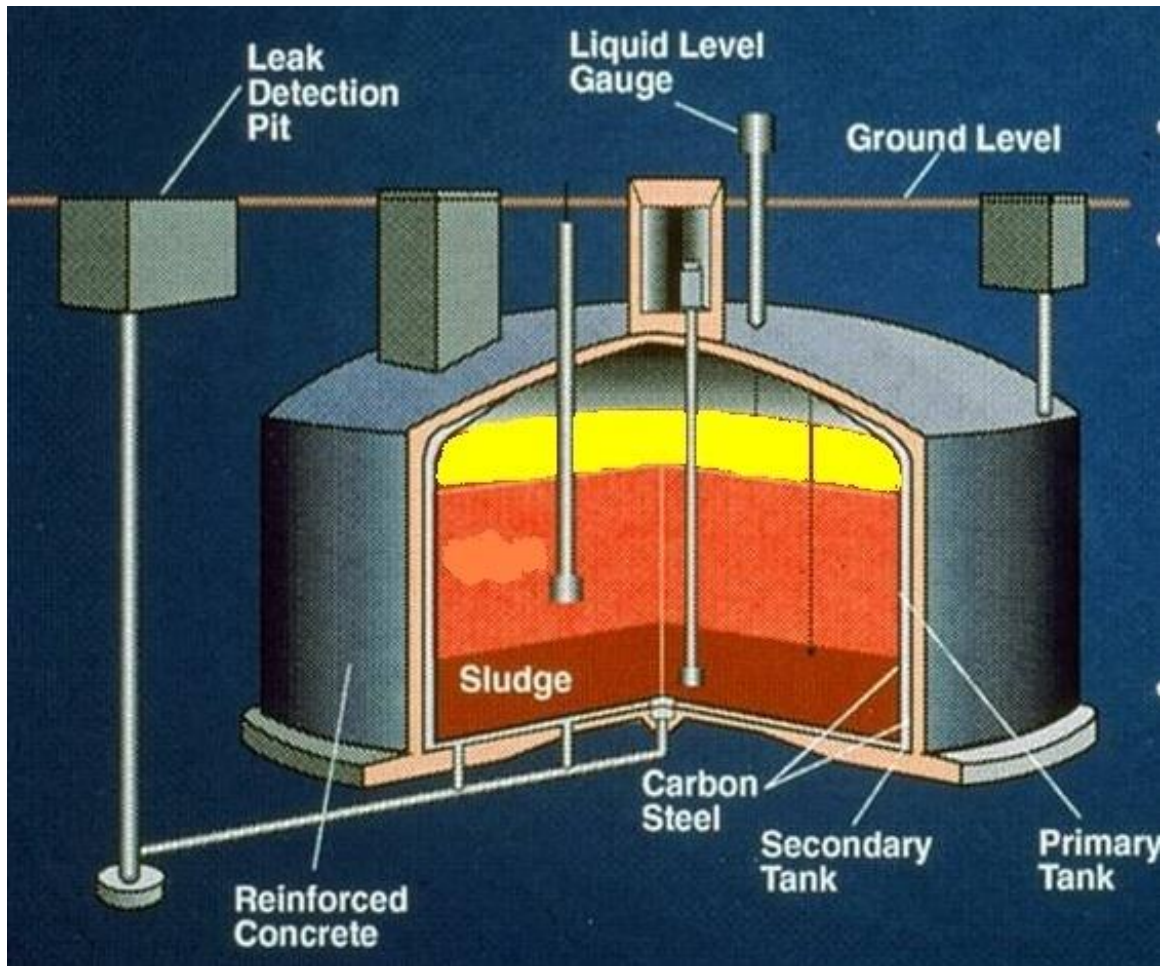


Figure 1.1 Waste phases in a typical Hanford tank. The sludge phase creates the most significant remediation challenge as it contains a majority of the actinides. Also problematic is the inconsistent chemical composition of the sludge from tank to tank.

nonradioactive elements that plague the tank sludge remediation efforts are aluminum and chromium. Aluminum metal was used as fuel cladding and aluminum nitrate was used as a salting agent in the REDOX process since methyl isobutyl ketone was not a sufficient strong extractant for the actinides and nitric acid would degrade the extractant. Chromate was commonly used in REDOX to oxidize plutonium to PuO_2^{2+} for removal from other aqueous raffinate. Currently, chromium is primarily present as a hydroxide, $\text{Cr}(\text{OH})_3$ and aluminum is present in two mineral phases, Gibbsite, $\gamma\text{-Al}(\text{OH})_3$, and Boehmite, $\gamma\text{-AlO}(\text{OH})$. The Boehmite phase is a more stubborn remediation challenge and emerged as radiolytic heating removed water from the Gibbsite phase.^[5] Removing Al and Cr solids from the sludge for separate disposal as low-level waste would greatly reduce the volume, and consequently the overall cost for the HLW sludge disposal operations.^[7] Numerous Al and Cr removal processes have been proposed and investigations have been performed over the course of the past decade.^[8-10]

Leaching of the sludge with caustic aqueous solutions to reduce their Al and Cr content has emerged as the preferred technique for sludge waste volume reduction. Contacting sludge samples with 2 M NaOH leaching solutions (alkaline leaching) has accomplished significant Al removal from some sludge samples and simulants. Excellent Cr removal has been demonstrated by treating the radioactive sludges with 2-3 M NaOH solutions that contain an oxidizing agent such as KMnO_4 (oxidative alkaline leaching).^[11] However, variability in the chemical composition of each tank sludge inhibits the complete removal of Al by caustic leaching.^[12]

The materials resistant to mobilization by alkaline leaching could respond to alternative leaching protocols. The results of a series of investigations into the use of acidic solutions or complexants as alternative leachants have been reported.^[9,13] These studies employed a sequential sludge treatment technique following an initial NaOH leaching step with a series of

increasingly aggressive acidic leachants, including dilute HNO₃ solutions. The acidic leaching treatments achieved a substantial increase in the efficiency of Al leaching in most of the sludge simulants. However, enhanced Al dissolution was accompanied by slight increases in the amount of radioactive species Am, U, Np and Pu present in the resultant leachate.

Previous reports from this lab have examined the use of SX with tri-n-butyl phosphate (TBP) or tri-n-octyl phosphine oxide (TOPO) extractants in n-dodecane organic phase as a means of removing potentially mobilized radioactive components if Al leaching was attempted with HNO₃ solutions.^[14] Selective extraction of Eu³⁺ and UO₂²⁺ from an aqueous solution of HNO₃ and Al(NO₃)₃ in the presence of low concentrations of Cr³⁺ and ascorbic acid was observed. The TOPO displayed an increased extraction of Eu in accordance with an increase in basicity of the extracting oxygen compared to TBP. The success observed in these studies warranted further investigation to TBP and TOPO extraction of Eu³⁺ and other actinides in an extraction chromatographic system.

Extraction Chromatography (EXC)

Any chemical process used for separations will immediately draw comparison to solvent extraction (SX). Solvent extraction is a method used to separate analytes based on their relative solubilities in two immiscible liquid phases; this technique has been a boon to separations community due to the high efficiency of separation that can be achieved with small energy requirements. One necessity of a viable separations process is a well-established knowledge of chemical processes occurring within both phases. The abundant understanding of SX is attractive to engineers and scientists designing a process. For any process to be competitive with

SX it must offer what SX cannot and, in addition, some improvements not typically achievable through conventional liquid-liquid extraction methods, such as, preconcentration, minimized possibilities of third phase formation, and avoiding the use of organic diluents.

A common complaint against SX is the large amount of organic waste resulting from the hydrolytic and radiolytic degradation of organic extractants and diluents.^[15-18] Solvent extraction requires a multi-stage setup for extraction, stripping and solvent washing. The multiple stages require individual instrumentation and equipment, ultimately producing additional contaminated material. Therefore, a separations technique that uses minimal amounts of solvent and compact equipment is desired for high level waste (HLW) partitioning.^[19] Several so called green candidates are available to alleviate the use of organic diluents. These include, but are not limited to: ionic liquids^[20], liquid membranes⁺ and cloud point extraction.^[22,23] The feasibility and capabilities of these recently developed green separation methods have been and are still under investigation.

An alternative to a diluent demanding SX process and some of these recently developed methods is extraction chromatography (EXC).^[24] Several variables still remain unknown regarding solid-support separation methods. Nevertheless, chromatography has been scaled to industrial level use^[25,26] and been studied for over a hundred years^[27], making extraction chromatography (EXC) an attractive option. Other benefits of EXC are similar to SX and include simplicity in equipment and operation arising from continuous flow functionality. Unique to EXC is the potential use of extractants that may not dissolve readily in organic diluents that are practical for large scale SX processes and the ability to minimize extractant loss through covalently binding the extractant to the inert support. The preconcentration capabilities further increase the attractiveness of EXC.^[24,28,29]

The presence of an inert solid support in EXC rather than an “inert” liquid diluent in SX makes for an interesting discussion when comparing EXC and SX systems. An EXC system has three major components: the inert support, the extractant and the mobile phase (Figure 1.2). The inert support may provide different impregnation and extraction results as an effect of different

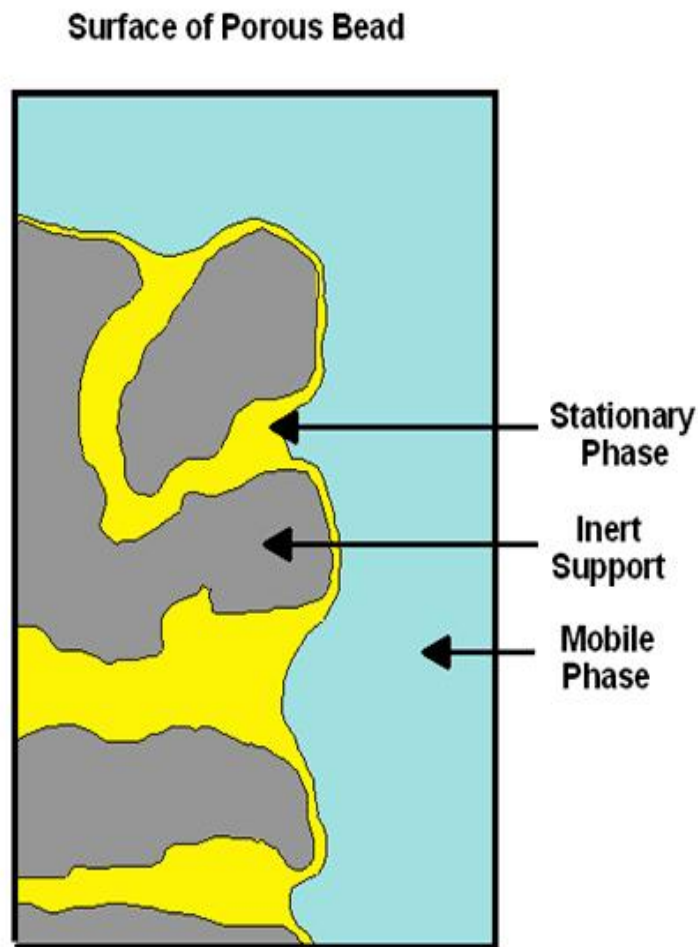


Figure 1.2. Components of an extraction chromatographic resin.^[30]

pore size, bead size and hydrophobic/hydrophilic nature.^[24] The extractant can be either covalently bound^[31-33] or, as in solvent impregnated resins^[34,35], SIRs, held by nonpolar Van der Waals or London Dispersion interactions. Covalently bound resins (CBRs) are the ideal option for an extraction column since the lack of covalent interactions in SIRs can lead to issues with extractant bleed off; however, preliminary screening of solid extractant behavior with quickly impregnated SIRs allows determination of whether more time should be invested developing synthetic pathways required for a particular CBR.

Preparing SIRs requires little or no time consuming synthesis. Typical dry impregnation methods involve dissolving an extractant in a low boiling point diluent, such as methanol, and contacting the extractant/diluent mixture with the polymer.^[36] The diluent is slowly removed under vacuum or by heating, leaving impregnated resin. When using SIRs, several variables must be balanced. A column must be run fast enough to be cost effective and slow enough for equilibrium to be obtained between the two phases and for extractant bleed off to be minimized. The impact of extractant bleed off depends on the solubility of the extractant in the mobile phase and on the sheer force of the mobile phase on the extractant. The extractant bleed off is a compromise considering the shorter time required to prepare the SIR compared to the CBR.

Separations based in extraction chromatography can either be performed in batch mode or column mode. Batch mode may be considered more analogous to SX and allow for easy comparison between the two methods since both require the single equilibrium of two bulk phases, whereas column mode does not contain discrete extraction steps, but instead continuous equilibration between two phases.^[37] The continuous equilibration between two phases allows many theoretical plates to be present in column mode, where as batch mode has only one theoretical plate. During batch mode extraction, a typical analytical scale study will involve

milligram amounts of resin being contacted with milliliters of aqueous solution containing the analyte of interest. The aqueous phase will be analyzed and a weigh distribution ratio (D_w) can be obtained by Equation 1.1 where $[M]_{aq}^o$ is the known concentration of metal added, is the

$$D_w = \frac{[M]_{aq}^o - [M]_{aq}}{[M]_{aq}} * \frac{V_{aq}}{M_{resin}} \quad (1.1)$$

concentration of metal at equilibrium in the aqueous phase after contact with the solid extractant and V_{aq} and M_{resin} are the volume in milliliters and mass in grams of the aqueous and solid phases, respectively.

The distribution ratio for a system, D (Equation 1.2), typically used in SX, can be obtained

$$D = \frac{[M]_{org}}{[M]_{aq}} \quad (1.2)$$

from breakthrough or elution curves, Figure 1.3, used in column chromatography. An elution curve is obtained by placing a finite sample at the beginning of the column and eluting, where as a breakthrough curve involves the continuous addition of analyte until saturation of the column has been obtained. Although both can provide distribution ratios, when the column is run under equilibrium conditions, an elution curve will provide separation information; a breakthrough curve is more ideal for a system with very high distribution ratios, species present in large initial concentrations and determination of column capacity. The number of free column volumes to peak maximum, or the resin capacity, k' , can also be availed from an elution curve and this value can be helpful in determining a distribution ratio (Equation 1.3a & 1.3b).^[37-39]

$$\begin{aligned} \text{a) } k' &= \frac{V_r}{V_m} \\ \text{b) } D &= k' * \left(\frac{V_m}{V_s} \right) \end{aligned} \quad (1.3)$$

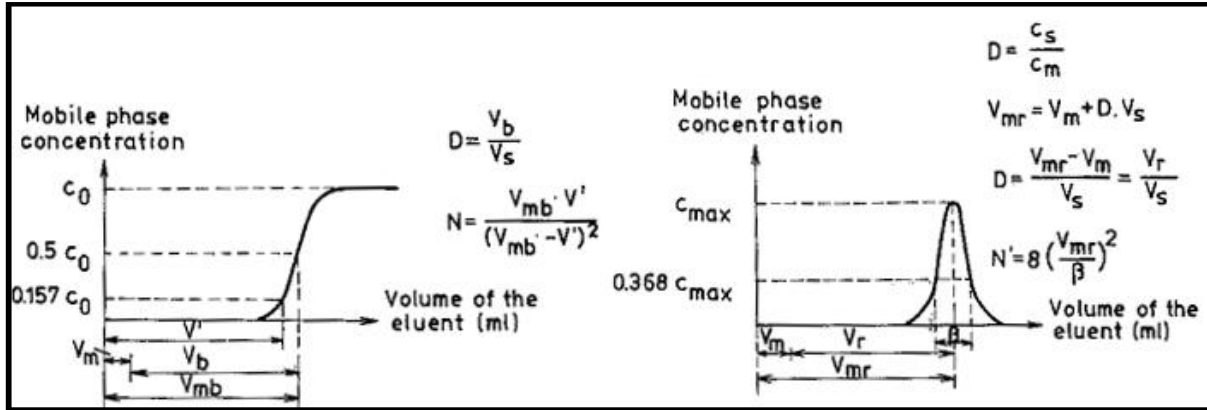


Figure 1.3 Schematic showing how to obtain significant terms for the calculation of a distribution value for an a) elution curve and b) a breakthrough curve. Definitions: V_m - Mobile phase (mL); V_s - Stationary phase volume (mL); $V_{mr} = V_r + V_m$ - Total Retention volume (mL); V_r - Retention volume (mL); V_b - Breakthrough volume (mL); $V_{mb} = V_m + V_b$ - Total breakthrough volume (mL); V' - Eluent volume when the concentration of the eluent reaches $0.157C_0$ (mL); C_0 - Initial concentration; β - Peak width at $c = 0.368 c_{max}$ (mL); N - Number of theoretical plates in the bed; N' - Number of theoretical plates from the center of the sample application band to the bed end; D - Concentration distribution ratio; C_s - Concentration of the analyte in the stationary phase; C_m - Concentration of the analyte in the mobile phase [M].

Several parameters must be examined when characterizing a column, including: flow rate, free column volume, and saturation concentrations. The equilibrium flow rate is the maximum flow rate allowed for the system to reach equilibrium and is often directly related to the kinetics of extraction. Slower SX kinetics often require slower equilibrium flow rates. The free column volume can be determined by subtracting the mass of a column from the mass of the column saturated with a liquid of a known density. Saturation concentrations can be availed through an isotherm determination. An extraction isotherm is a plot wherein the concentration of analyte in the solid phase is plotted as a function of the equilibrium concentration of analyte in the aqueous phase. The equilibrium concentrations of a radioactive analyte in the liquid and solid phases can be calculated from [Equation 1.4a](#) and [1.4b](#), where A_o and A are the count rates (using radiometric

$$\begin{array}{l}
 \text{a) } c = \frac{A}{A_o} * c_o \\
 \text{b) } q = \left(\frac{A_o - A}{A_o} \right) * \frac{V}{m} * c_o
 \end{array} \quad (1.4)$$

techniques) of the aqueous solution before and after equilibration, respectively, with V mL of solution and m grams of resin; c_o is the initial concentration of analyte in the aqueous solution and q is the mmol analyte recovered per gram of resin. The obtained data can be fitted by the Langmuir isotherm, Equation 1.5^[40], where Q_{max} is the maximum concentration of analyte in

$$q = Q_{max} * \frac{K * c}{1 + K * c} \quad (1.5)$$

the resin phase and K is a system specific relating to the distribution ratio of the analyte.

Several inert supports are available for the development of extraction chromatographic materials including cellulose, silica gel, diatomaceous earth, alumina and polymers.^[24] Many of these supports are considered unsuitable for extractant impregnation without preliminary treatments to render a hydrophobic surface on the support to reduce or eliminate functionalities capable of ion exchange.^[41] Warshawsky has noted the advantages of a macroporous, high surface area styrene-divinylbenzene- and acrylic ester-based polymers, the “XAD” series by Rohm and Haas.^[36] The supports were noted to have good “wettability” by most extractants, do not swell appreciably with solution composition changes, exhibit good mechanical stability and are relatively inexpensive.

Literature has shown Amberlite XAD-7, Figure 1.4, to successfully retain TBP for SIR purposes and preliminary results from this lab indicate the support works well with both TBP and TOPO.^[35] Amberlite XAD-7 is a white, nonionic, polyacrylic polymer. In this work the extraction of Eu, U, Th, Np by a TBP or TOPO XAD-7 resin under varied HNO_3 and $\text{Al}(\text{NO}_3)_3$ conditions that mimic what might be expected during an acidic remediation of the Hanford Site will be examined.

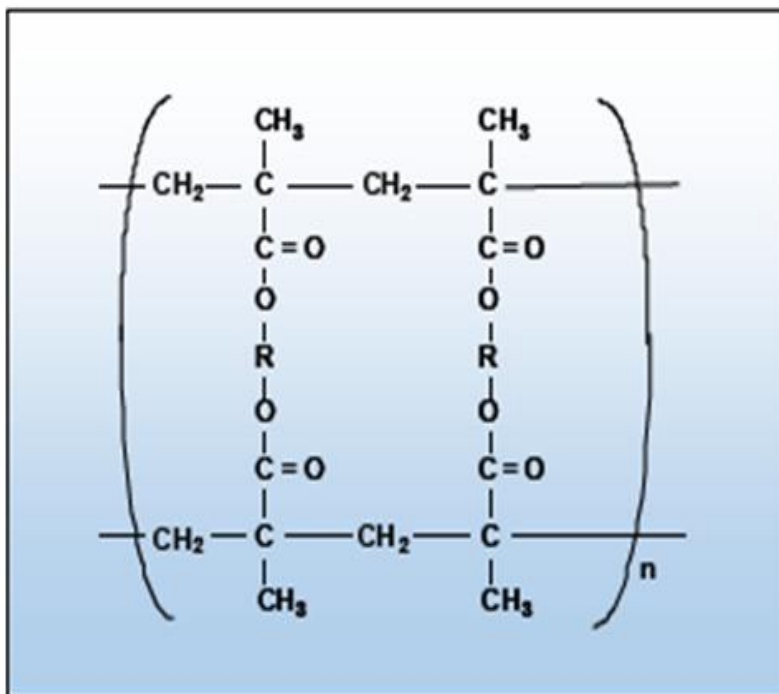


Figure 1.4 Chemical Structure of Amberlite XAD-7HP polymeric adsorbant.

Covalently Bound Resin (CBR) Characterization

During the past decade there has been a growing interest in the use of extraction chromatography, for both nuclear and non-nuclear applications.^[25] Some process scale extraction chromatography studies have included removal of toxic or hazardous materials from industrial effluents, the recovery of rare earths and the remediation capabilities of acidic nuclear waste solutions (Hanford).^[14,29,41] Although success has been attained, commonly these process scale efforts are plagued by the leaching of unbound extractant in to the effluent stream, which often leads to a change in column performance, even when only minimal leaching has occurred.

Covalently binding an extractant group to a resin could alleviate extractant leaching issues. Although leaching is more common for SIRs, leaching is present in SX systems and, when SX

separations are run at process scale, the cost associated with metal recovery may not be sufficient to offset the loss of an expensive extractant.^[42] Aside from covalently binding an extractant to a polymer, which can be difficult due to cross-linking, an ideal CBR should allow metal ion recovery, have high regenerability and be radiolytically stable (if designing a CBR for a nuclear waste process). The initial cost of the resin can be high, but sufficient regenerability should offset cost issues.

Numerous functional groups have been bound to resins including, but not limited to, polyethylene(imines)^[43], 8-hydroxyquinolinol^[44], iminodiacetic acids^[45] and varying phosphorus acids^[46]. Notably missing from the literature is a significant investigation into adduct forming, neutral organophosphorus ligands. The group of Prof. Spiro Alexandratos at Hunter College, CUNY, has been developing neutral organophosphorus CBRs that ideally undergo metal-extractant complexation at a phosphoryl moiety. Synthesized resins have shown uptake of several metal species, including the uranyl ion.^[31,47] This proposal will focus on outlining an investigation to further characterize the pPenta, pTris and pTris-Mono resins, [Figure 1.5](#). All compounds have shown affinity for UO_2^{2+} , [Table 1.1](#), and the pPenta resin has shown an affinity for metal ions that will bond covalently such as, Pb^{2+} , Cd^{2+} , Cu^{2+} , Ni^{2+} .^[Personal Communication,31,48] The percent extracted can be related to the distribution ratio through [Equation 1.6](#). The high uptake of UO_2^{2+} by pTris, at both high and low acidity, makes pTris an

$$\boxed{\%E = \frac{D}{D + 1} * 100 \quad (1.6)}$$

optimal candidate for further explorations. The pTris-mono will also be quite helpful in elucidating the roles that the groups surrounding the phosphoryl oxygen may have. The

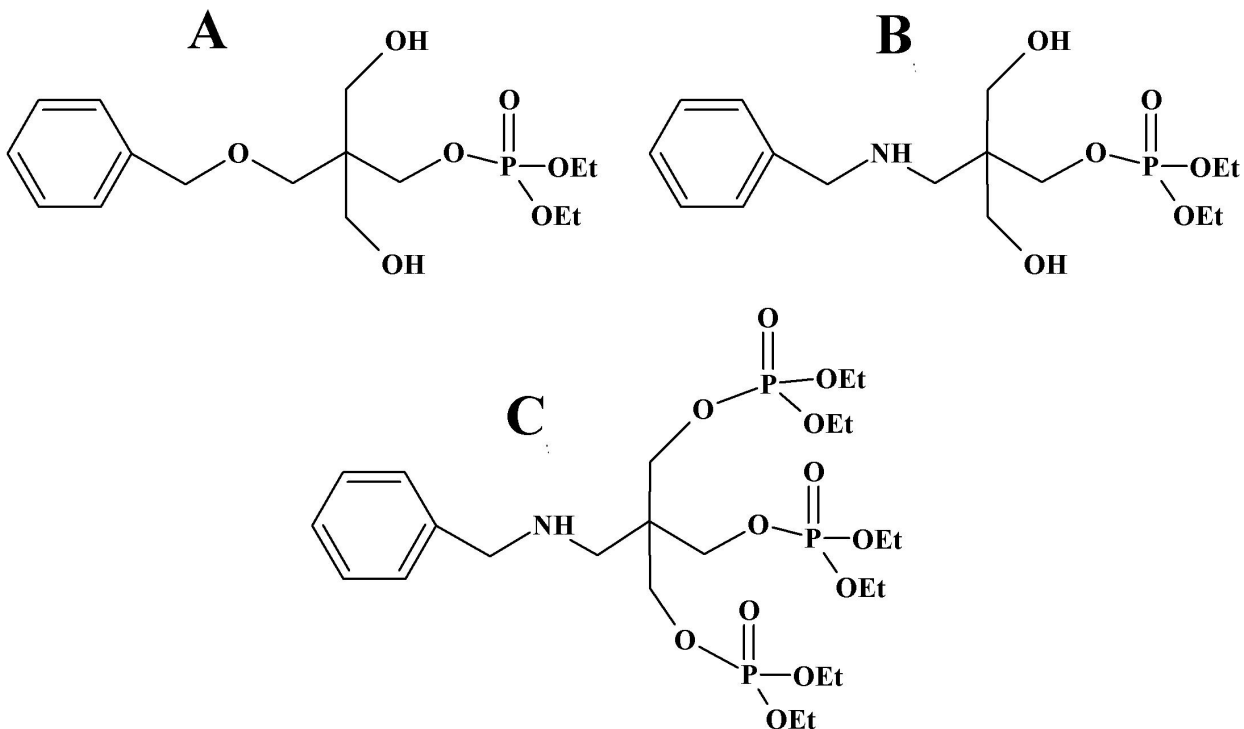


Figure 1.5 Structures of immobilized: *a*) pentaerythritol triethoxylate (*pPenta*) *b*) Tris(hydroxymethyl)amino methane (*pTris*) *c*) Mono-Tris(hydroxymethyl)aminomethane (*pTris-Mono*).

Table 1.1 Preliminary uptake results uranium from a 20 ppm UO_2^{2+} aqueous phase using pPenta, pTris and pTris-Mono. Errors indicate $\pm 1\sigma$ standard deviation.

[HNO ₃]	pPenta		pTris		pTris-Mono	
	<i>D</i>	%Extracted	<i>D</i>	%Extracted	<i>D</i>	%Extracted
$6.4 \cdot 10^{-3}$ M	1440 ± 70	96.2	1270 ± 50	93.9	21 ± 1	32.5
4 M	141 ± 13	71.3	15300 ± 450	99.5	97 ± 6	68.7

roles that the groups surrounding the phosphoryl oxygen may have. The Alexandratos approach uses the linkages (between functional groups and the hydrophobic polystyrene backbone) to create a local microenvironment more hospitable (hydrophilic) to the target ions, improving metal performance.

Studies indicate that the auxiliary group of the pPenta and pTris/pTris-Mono resins, -OH and NH-, respectively, significantly affect the basicity of the phosphoryl group through hydrogen bonding interactions, [Figure 1.6](#). This interaction has been supported by metal recovery and IR trends.^[31,48] Of further interest is the interaction of the pPenta resin with softer divalent metal ions.^[48] Significant interaction between divalent metal ions and phosphoryl groups is typically

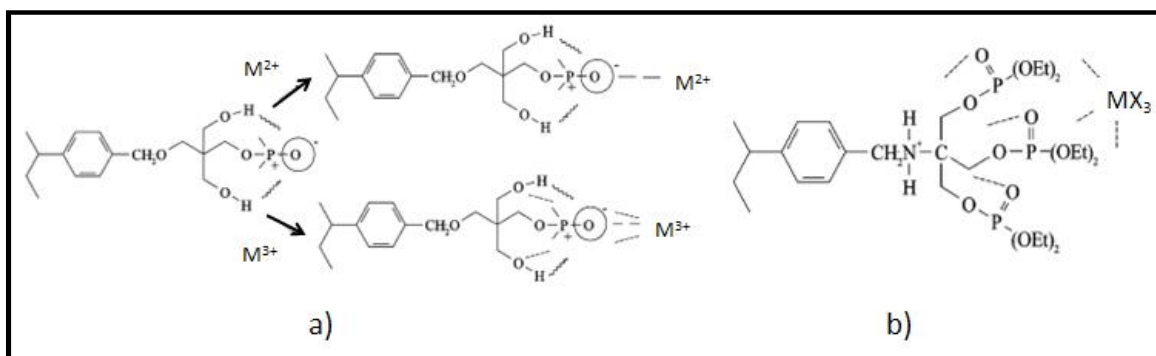


Figure 1.6 a) Interaction of phosphorylated pentaerythritol with divalent and trivalent ions b) Interaction of phosphate ligands with the amine moiety through hydrogen bonding and with Fe(III).

not observed because the metal ion is not acidic enough. The FTIR spectra show an increased polarizability of phosphoryl oxygen. The interaction with more covalently interacting actinides could prove valuable.

The recovery of uranium by these neutral organophosphorus resins begs further investigation into other actinide extraction behavior. The in depth mechanistic, kinetic and stoichiometric characterization provides an interesting challenge. Chairizia and Horwitz et al. published a

series of papers in the early and mid 90's characterizing a new chelating ion-exchange resin, Diphonix^(R).^[49-51] Although the characterized resin in these papers is a cation-exchanger, the methodical approach used provides a helpful outline for the characterization of adduct forming resins. The uptake, uptake efficiency and stripping behavior of An^{3+} , An^{4+} , AnO_2^+ and AnO_2^{2+} ions in NO_3^- systems needs to be examined. Variation of pH and ionic strength will begin to illustrate which conditions would be optimal if such adduct forming resins were to be used for nuclear waste management or remediation.

Trivalent Actinide - Lanthanide Separation by Phosphorus reagent Extraction from Aqueous Komplexes (TALSPEAK)

For reprocessing or disposal purposes of spent nuclear fuel, removal of americium from the lanthanides is a necessary step. The UREX+ nuclear fuel reprocessing suite currently emphasizes the TALSPEAK process for separation of the lanthanides from trivalent actinides. If the goal is to burn Americium in a fast neutron spectrum reactor, extraneous lanthanides would compete with americium for fission neutrons. Considering the hard-cation^[52] nature and the comparable charge density of Am and the lanthanides, this separation is unusually challenging. The most successful separations have involved exploiting the slightly covalent nature of Am^{3+} , brought on by the extension of the 5f orbitals.^[53-56] The interaction of nitrogen and sulfur donating ligands occurs with Am^{3+} preferentially over the lanthanides; thus allowing group separation.

Several propositions exist for separation of Am^{3+} from the lanthanides based on the manipulation of this chemistry. Sulfur donating ligands developed at Idaho National Labs^[57] and pyridine based ligands preferred in the SANEX process^[58] have achieved Am/Eu separations of

100 or higher. Unfortunately, the relatively polarizable molecular orbitals encountered in sulfur and pyridine based separations increase the propensity for radiolytic breakdown of the ligand.^[59] The alternative use of "TALSPEAK-Like" chemistry has less severe radiolysis concerns; however, the myriad of actors involved in TALSPEAK separations chemistry makes understanding the significance of the organic extractant, the aqueous holdback reagent and the supposedly inert buffer difficult. The most successful TALSPEAK separations have used bis-(2-ethylhexyl) phosphoric acid (HDEHP), diethylene triamine pentaacetic acid (DTPA), and lactic acid as the acidic phosphorus extractant, the polyaminocarboxylic acid complexant, and the carboxylic acid buffer, respectively (Figure 1.7). Recently, the Nash group at Washington State University has focused on fundamental examinations regarding the TALSPEAK solution chemistry.^[60,61] These examinations could be advanced by performing comparable studies while manipulating key variables. This study aims to obtain further understanding of TALSPEAK solution chemistry by immobilizing the organic phase on a polymeric support, and carefully contrasting the use of TTHA or organophosphonic acid with "classical" TALSPEAK chemistry.

The original Oak Ridge report, published in 1964, did provide a brief examination of triethylenetetraminehexaacetic acid (TTHA) as a holdback reagent, Figure 1.7.^[62] The conclusion was reached that the organophosphonic provided better separation of Eu from Am. TTHA was shown to insufficiently compete with the organophosphorus acid for the Americium. Stability constants for Am and the lanthanides have since shown the TTHA to have significant promise. Figure 1.8 shows the stability constants for DTPA and TTHA with the lanthanides and Americium.^[63] Sufficient recovery of Am using DTPA ($\log K_{Am} = 22.9$)

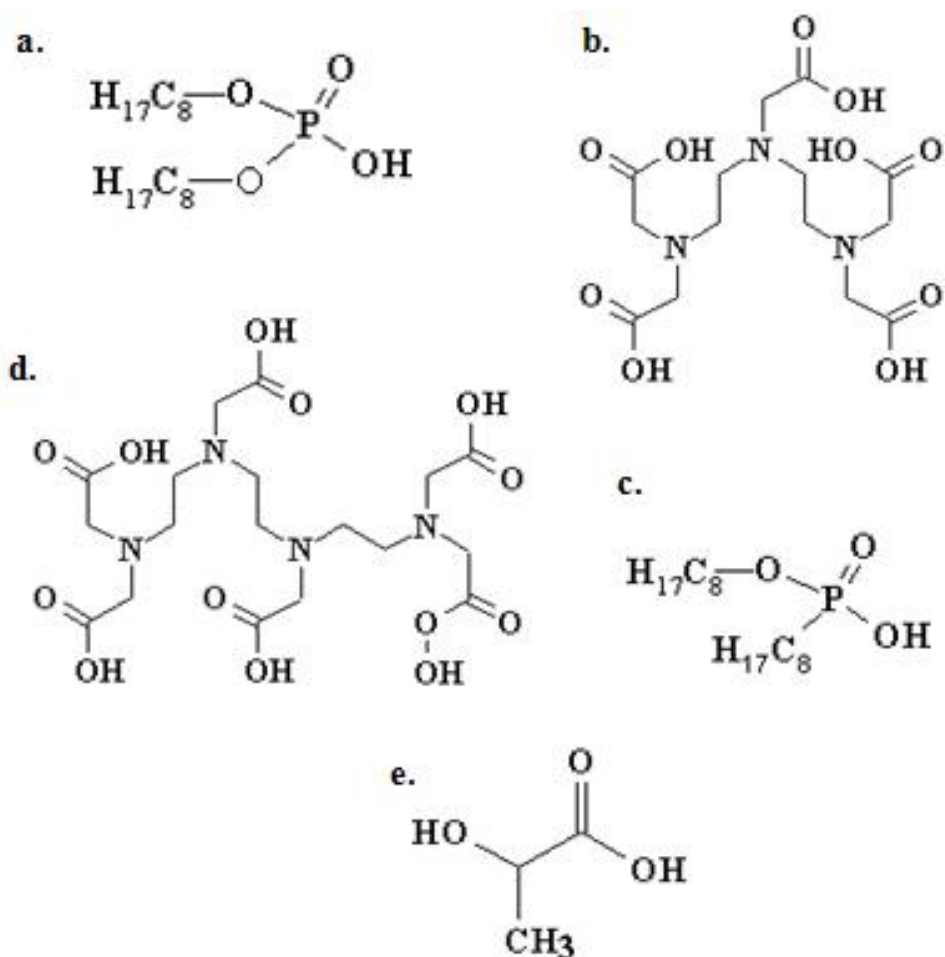


Figure 1.7 Structures of the components used in these studies; a: di(2-ethylhexyl) phosphoric acid (HDEHP) b: diethylenetriamine- *N,N,N',N'',N'''*-pentaacetic acid (DTPA) c: di(2-ethylhexyl) phosphonic acid (HEH[EHP]) d: triethylenetetramine- *N,N,N',N'',N''',N''''*-hexaacetic acid (DTPA) e: lactic acid (HL)

from HDEHP has been observed with separation factors typically around 100. If the reported stability constant for Am with TTHA ($\log K_{Am} = 26.6$) is correct, TTHA should be a more than sufficient competitor for HEDHP with americium. Examining the kinetics behavior of TTHA could also progress understanding of kinetics issues observed for the heavier lanthanides in TALSPEAK.^[64]

The original Oak Ridge report also examined DTPA dependence of two phosphonic acids: 2-ethylhexyl phenylphosphonic acid (HEH[ϕ P]) and decyl (decyl) phosphonic acid HD[DP].^[62] Separation factors for HEH[ϕ P] were comparable to those obtained by HDEHP, but the phosphonic acid gave considerably higher distribution coefficients. Studies with HD[DP] noted slightly lower separation factors and much lower distribution values compared to HEH[ϕ P]. These two phosphonic acid demonstrations are currently the only literature examples using a phosphonic extractant to perform TALSPEAK-type chemistry. Performing studies with TALSPEAK chemistry using another phosphonic extractant, bis-2-ethyl(-hexyl) phosphonic acid (HEH[EHP], [Figure 1.7](#)), varying pH, lactate, and contact times may elucidate a better understanding when compared to the "classical" system using HDEHP. The use of HEH[EHP] is particularly helpful since the molecule is structurally analogous to HDEHP; therefore minimizing discussion of any metal distribution differences to almost exclusively the difference in the basicity of the extractant.

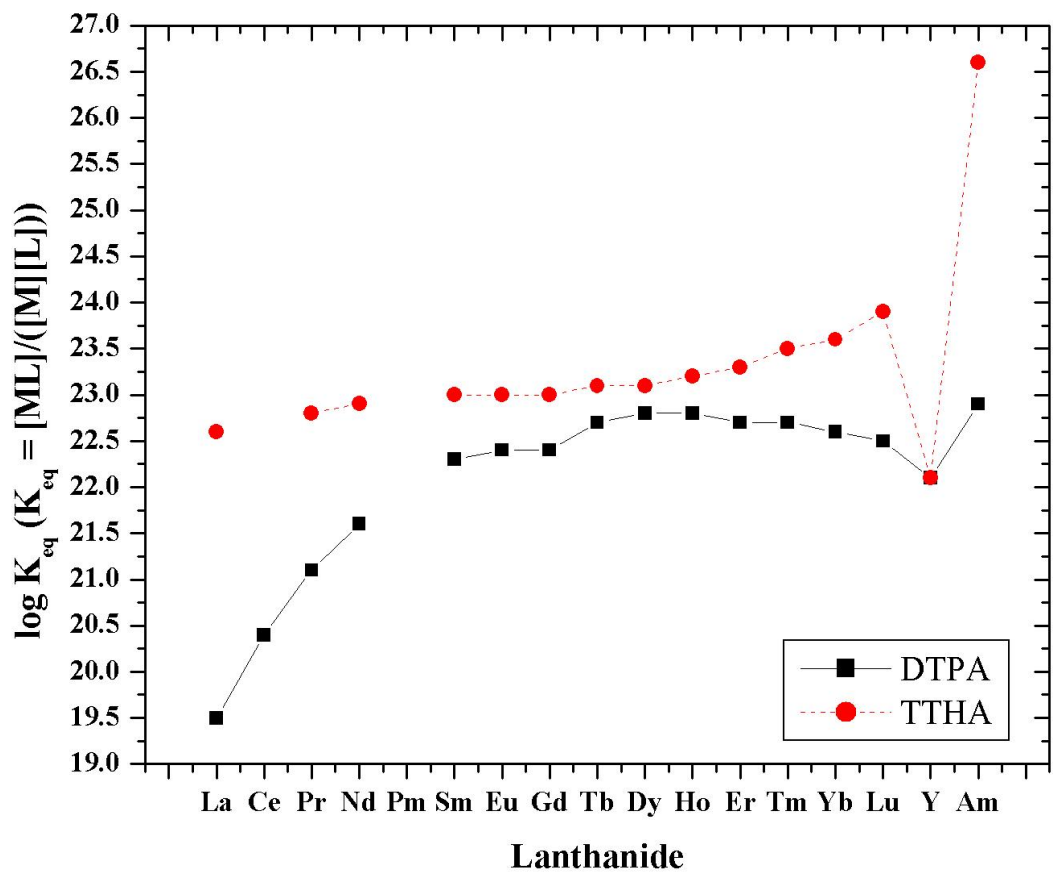


Figure 1.8 Equilibrium constants for DTPA and TTHA with the lanthanides and americium in 0.1 M ionic media at 25 °C.

References

- [1] OECD Publications. *Actinide and Fission Product Partitioning and Transmutations – Status & Assessment Report*, **1999**.
- [2] Deffeyes, K. S.; MacGregor I. “World Uranium Resource”, *Sci. Am.* 242, 1 **1980**.
- [3] Hanford Federal Facility Agreement and Consent Order; 89–10 Rev. 5.
- [4] DOE. Plutonium: The First 50 Years, United States Plutonium Production, Acquisition, and Utilization from 1944 through 1994. **1996** *DOE/DP-0137*, U.S Department of Energy, Washington, D.C.
- [5] Agnew, S.F. Hanford Defined Wastes: Chemical and Radionuclide Compositions. **1995** *LAUR-94-2657* Rev. 2, Los Alamos National Laboratory, Los Alamos New Mexico.
- [6] Orme, R.M.; Manuel, A.F.; Shelton, L.W.; Slaathaug, E.J. TWRS privatization process technical baseline **1996** *WHC-SD-WM-TI-774* Westinghouse Hanford Company: Richland, WA.
- [7] DeMuth, S.F.; Thayer, G.R. An Updated Cost Study for Enhanced Sludge Washing of Radioactive Waste. *Remediation* **2002** Spring 2002, 87–97.
- [8] Lumetta, G.J.; Rapko, B.M. Colton, N.G.; Washing and Caustic Leaching of Hanford Tank Sludge. **1994** *PNL-SA-23598* Pacific Northwest National Laboratory, Richland, Washington.
- [9] Martin, L.R.; Routt, A.; Olsen, R.; Neeway, J.; Nash, K.L. New (and old) approaches to cleanup of Hanford sludge leachate solutions Abstracts of Papers, 230th ACS National Meeting, Washington, DC, United States, Aug. 28-Sept. 1, 2005. **2005**.
- [10] Rapko, B.M; Geeting, J.G.H.; Sinkov, S.I.; Vienna, J.D.; Oxidative Alkaline Leaching of Washed 241-SY-102 and 241-SX1-01 Tank Sludges. **2004** *WTP-RPT-117* Rev 0, Pacific Northwest National Laboratory, Richland, WA.

[11] Rapko, B.M.; Lumetta, G.J.; and Wagner, M.J.; Oxidative dissolution of chromium from Hanford Tank sludges under alkaline conditions **1996 PNNL-11233** Pacific Northwest Lab: Richland, WA.

[12] Rapko, B.M.; Blanchard, D.L.; Colton, N.G.; Felmy, A.R.; Liu, J.; Lumetta, G.J.; The chemistry of sludge washing and caustic leaching processes for selected Hanford tank wastes. **1996 PNNL-11089** Pacific Northwest National Laboratory: Richland, WA.

[13] Bond, A.H.; Nash, K.L.; Gelis, A.V.; Sullivan, J.C.; Jensen, M.P.; Rao, L. Plutonium mobilization and matrix dissolution during experimental sludge washing of bismuth phosphate, Redox, and PUREX waste simulants. *Sep. Sci. Tech.* **2001** 36 (5&6) 1241–1256.

[14] Harrington, R.; Martin, L.; Nash, K. Partitioning of U(VI) and Eu(III) between acidic aqueous $\text{Al}(\text{NO}_3)_3$ and tributyl phosphate in n-dodecane. *Sep. Sci. & Tech.* **2006** 41 (10) 2283–2298.

[15] Zhang, A.; Wei, Y.Z.; Hoshi, H.; Kumagai, M.; Kamiya, M.; Koyama, T.; Resistance properties of a macroporous silica-based N,N, N'-N-tetraoctyl-3-oxapentane-1,5-diamide impregnated polymeric sorption material against nitric acid, temperature and γ -irradiation. *Radiat. Phys. Chem.* **2005** 72 (6) 669–678.

[16] Nash, K.L.; Gatrone, R.C.; Clark, G.A.; Rickert, P.G.; Horwitz, E.P.; Hydrolytic and radiolytic degradation of OΦD(iB)CMPO: Continuing Studies. *Sep. Sci. Technol.* **1988** 23 (12–13) 1355–1372.

[17] Zhang, A.; Wei, Y.Z.; Kumagai, M.; Koma, Y.; Koyama, T.; Resistant behavior of a novel silica-based octyl-(phenyl)-N, N-diisobutylcarbamoymethylphosphine oxide extraction resin against nitric acid, temperature and γ -irradiation. *Radiat. Phys. Chem.* **2005** 72 (4) 455–463.

[18] Chiarizia, R.; Horwitz, E.P.; Hydrolytic and radiolytic degradation of octyl-(phenyl)-N, N-diisobutylcarbamoymethylphosphine oxide and related compounds. *Solvent Extr. Ion Extr.* **1986** 4 (4) 677–723.

[19] Zhang, A.; Wei, Y.Z.; Hoshi, H.; Koma, Y.; Kamiya, M.; Partitioning of cesium from a simulated high level liquid waste by extraction chromatography utilizing a macroporous silica-based supramolecular calix[4]arene-crown impregnated polymeric composite. *Solvent Extr. Ion Extr.* **2007** 25 (3) 389–405.

- [20] Binnemans, K. Lanthanides and actinides in ionic liquids. *Chem. Rev.* **2007** 107 (6) 2592–2614.
- [21] Dam, H.H.; Reinhoudt, D.N. Multicoordinate ligands for actinide/lanthanide separations. *Chem. Soc. Rev.* **2007** 36 (2) 367–377.
- [22] Favre-Reguillon, A.; Draye, M.; Lebusit, G.; Thomas, S.; Foos, J.; Cote, G.; Guy, A. Cloud point extraction: an alternative to traditional liquid-liquid extraction for lanthanides(III) separation. *Talanta* **2004** 63 (3) 803–806.
- [23] Draye, M.; Thomas, S.; Cote, G.; Favre-Reguillon, A.; LeBusit, G.; Guy, A.; Foos, J. Cloud-point extraction for selective removal of Gd(III) and La(III) with 8-hydroxyquinoline. *Sep. Sci. & Tech* **2005** 40 (13) 611–622.
- [24] Braun, T.; Ghersine, G. *Extraction Chromatography*. Amsterdam; New York: Elsevier Scientific Pub. Co. **1975**.
- [25] Wenzel, U.; Ullrich W. Twin column chromatography for industrial-scale decontamination processes. *J. Chrom. A.* **2004** 1023 (2) 207–213.
- [26] Ganetsos, G.; Barker, P.E. *Preparative and Production Scale Chromatography*. CRC Press, **1992**
- [27] Archer J.P.; “The development of partition chromatography” Nobel Lecture, December 12, 1952. Nobel Lectures, Chemistry 1942-1962, Amsterdam; New York: Elsevier Scientific Pub. Co., **1964**.
- [28] Zhang, A.; Wei, Y.; Kumagai, M. Separation of minor actinides and rare earths from a simulated high activity waste by two macroporous silica based polymeric composites. *Sep. Sci. & Tech.* **2007** 42 (10) 2235–2253.
- [29] Dietz, M.; Yaeger, J.; Sajdak, L.R., Jr.; Jensen, M.P. Characterization of an improved extraction chromatographic material for the separation and preconcentration of strontium from acidic media. *Sep. Sci. & Tech* **2005** 40 (13) 349–366.

- [30] <http://www.eichrom.com/products/extraction.cfm>
- [31] Alexandratos, S.; Xiaoping, Z. Polyols as scaffolds in the development of ion selective polymer-supported reagents: The effect of auxillary groups on the mechanism of metal ion complexation. *Inorg. Chem.* **2008** 47 (7) 2831–2836.
- [32] Alexandratos, S.; Xiaoping, Z.; Immobilized phosphate ligands with enhanced ion affinity through supported ligand synergistic interaction. *Sep. Sci. & Tech.* **2008** 43 (6) 1296–1309.
- [33] Takeshita, K.; Matsumura, T.; Nakano, Y.; Separation of Am(III) and Eu(III) by thermal swing extraction using a thermosensitive polymer gel *Prog. Nucl. Energy* **2008** 50 (26) 466–469.
- [34] Metwally, E.; Salah, A.Sh.; El-Naggar, H.A. Extraction and separation of uranium(VI) and thorium(IV) Using tri-*n*-dodecylamine impregnated resins. *J. Nucl. & Radiochem. Sci.* **2005** 6 (2) 119–126.
- [35] Yamaura, M.; Matsuda, H.T. Actinides and fission products extraction behavior in TBP/XAD7 chromatographic column. *J. Rad. Nucl. Chem.* **1997** 224 (12) 83–87.
- [36] Warshawski, A.; “Extraction with Solvent Impregnated Resins” *Ion Exchange & Solvent Extraction.* **1981** Vol. 8, 229-310.
- [37] Rydberg, J.; Cox, M.; Claude, M.; Choppin, G.R.; Solvent Extraction: Principles and Practice. New York: Marcel Dekker, Inc. **2004.**
- [38] Horwitz ,E.P.; Chiarizia, R.; Dietz, M.L.; A novel strontium selective extraction chromatographic resin. *Solvent Extr. Ion Exch.* **1992** 10 (2) 313–336.
- [39] Horwitz, E.P.; Dietz, M.L.; Chiarizia, R.; Diamond, H.; Maxwell III, S.L.; Nelson, M.R. Separation and preconcentration of actinides by extraction chromatography using a supported liquid anion exchanger: application to the characterization of high-level nuclear waste solutions. *Anal. Chim. Acta* **1995** 310 (1) 63–78.
- [40] Strumm, W.; Chemistry of the Solid-Water Interface: Processes at the Mineral-Water and Particle-Water Interface in Natural Systems. New York: John Wiley & Sons, Inc. **1992.**

- [41] Cortina, J.L.; Warshwasky, A. *Ion Exchange and Solvent Extraction*. Marinsky, J. A., Marcus, Y., Eds.; Marcel Dekker: New York, **1997** Vol. 13, p. 195.
- [42] Barney, G.S.; Cowan, R.G.; *Chemical Pretreatment of Nuclear Waste for Disposal*. Schulz, W.W. Horwitz, E.P., Eds.; Plenum Press: New York, **1994** p. 51.
- [43] Alexandratos, S.D.; Crick, D.W.; Polymer supported reagents: Application to separation science. *Ind. Eng. Chem. Res.* **1996** 35 (3) 635–644.
- [44] Chanda, M.; Rempel, G.L.; Polyethyleneimine Adduct of poly(vinyl benzaldehyde): A highly selective sorbent for iron(III). *React. Polym.* **1993** 19 (3) 213.
- [45] Warshawsky, A.; Polymeric ligands in hydrometallurgy. *Syntheses and Separations Using Functional Polymers*. Sherrington, D.C., Hodge, P., Eds.; Wiley: New York, **1988** Chapter 10.
- [46] Mykytiuk, A.P.; Russell, D.S.; Sturgeon, R.E. Simultaneous determination of iron, cadmium, zinc, copper, nickel, lead, and uranium in seawater by stable isotope dilution spark source mass spectrometry. *Anal. Chem.* **1980** 52 (8) 1281.
- [47] Alexandratos, S. D.; Zhu, X.; High-affinity ion-complexing polymer-supported reagent: Immobilized phosphate ligands and their affinity for the uranyl ion. *React. Polym.* **2007** 67 (5) 375–382.
- [48] Alexandratos, S.D.; Zhu, X.; Bifunctional coordinating polymers: Auxiliary groups as a means of tuning the ionic affinity of immobilized phosphate ligands. *Macromolecules* **2005** 38 (14) 5981–5986.
- [49] Horwitz, E.P.; Chiarizia, R.; Diamond, H.; Gatrone, R.C.; Alexandratos, S.D.; Trochimczuk, A.Q.; Crick, D.W.; Uptake of metal ions by a new chelating ion-exchange resin. Part 1. Acid dependencies of actinide ions. *Solvent Extr. Ion Exch.* **1993** 11(5) 943–66.
- [50] Chiarizia, R.; Horwitz, E.P.; Gatrone, R.C.; Alexandratos, S.D.; Trochimczuk, A.Q.; Crick, D.W.; Uptake of metal ions by a new chelating ion-exchange resin. Part 2. Acid dependencies of transition and post-transition metal ions. *Solvent Extr. Ion Exch.* **1993** 11(5) 967–85.

- [51] Chiarizia, R.; Horwitz, E.P.; Alexandratos, S.D.; Uptake of metal ions by a new chelating ion-exchange resin. Part 4. Kinetics. *Solvent Extr. Ion Exch.* **1994** 12(1) 211–37.
- [52] Aspinnall, H. Chemistry of the f-Block Elements. Gordon & Breach: Australia. 5st Ed. 2001
- [53] Jensen, M. P.; Bond, A. H. Influence of aggregation on the extraction of trivalent lanthanide and actinide cations by purified Cyanex 272, Cyanex 301, and Cyanex 302. **2002** *Radiochim. Acta* 90, 205-209.
- [54] Jensen, M. P.; Bond, A. H. Comparison of Covalency in the Complexes of Trivalent Actinide and Lanthanide Cations. **2002** *J. Am. Chem. Soc.* 124, 9870-9877.
- [55] Choppin, G. R.; Nash, K. L. Actinide separation science. **1995** *Radiochim. Acta* 70/71, 225-236.
- [56] Kozimor, S.A.; Yang, P.; Batista, E.R.; Boland, K.S.; Burns, C.J.; Clark, D.L.; Conradson, S.D.; Martin Wilkerson, M.P.; Wolfsberg, L.E. Trends in Covalency for d- and f-Element Metallocene Dichlorides Identified Using Chlorine K-Edge X-ray Absorption Spectroscopy and Time-Dependent Density Functional Theory. **2009** *J. Am. Chem. Soc.* 131, 12125–12136.
- [57] Peterman, D.R.; Martin, L.R.; Klaehn, J.R.; Harrup, M.K.; Greenhalgh, M.R.; Luther, T.A. Selective separation of minor actinides and lanthanides using aromatic dithiophosphinic and phosphinic acid derivatives. **2009** *J. Rad. Nucl. Chem.* 282, 527–531
- [58] Hill, C.; Guillaneux, D.; Berthon, L.; Madic, D. Sanex-Btp process development studies. **2002** *J. Nucl. Sci. Technol. Suppl.* 3 453-461
- [59] Mincher, B. J.; Modolo, G.; Mezyk, Stephen P.; Review Article: The Effects of Radiation Chemistry on Solvent Extraction: 1. Conditions in Acidic Solution and a Review of TBP Radiolysis. *Solvent. Extr. Ion Exch.* **2009** 27 (1), 1–25
- [60] Nilsson, M.; Nash, K.L. Trans-lanthanide extraction studies in the TALSPEAK system: Investigating the Effect of Acidity and Temperature. **2009** *Solvent Extr. Ion Exch.* 27, 354–377.
- [61] Nilsson, M.; Nash, K.L. Review Article: A Review of the Development and Operational Characteristics of the TALSPEAK Process **2007** *Solvent Extr. Ion Exch.* 25, 665–710.

[62] Weaver, B.; Kappelmann, F.A. Talspeak, A new method of separating americium and curium from the lanthanides by extraction from an aqueous solution of an aminopolyacetic acid complex with a monoacetic organophosphate or phosphonate. August 1964, ORNL-3559.

[63] Zhengshui, H., Ying, P., Wanwa, M., and Xun, F. Purification of organophosphorus acid extractants. **1995** *Sol. Extr. Ion Exch.* 13 965–976.

[64] Kolarik, Z.; Koch, G.; Kuhn, W. Acidic organophosphorus extractants. XVIII. Rate of lanthanide (III) extraction by bis(2-ethylhexyl) phosphoric acid from complexing media. *Jour. Inorg. Nucl. Chem.* **1974**, 36 (4), 905-909.

CHAPTER TWO

PREFACE

Many of the following chapters of this dissertation focus on addressing research problems that will hopefully aid in future approaches to dealing with nuclear waste using organophosphorus extractants. The remediation of the Hanford site serves as an interesting platform to initiate description of the findings of this dissertation since the remediation is already ongoing. As noted in the Introduction, clean up of Hanford waste tank sludge phases has been demonstrated using a caustic scrub containing 2 M NaOH to remove Al, or 2-3 M NaOH and oxidizing KMnO_4 for removal of Cr, from the actinide and lanthanide hydroxide precipitates. However; the aluminum is present in two mineral forms: Gibbsite ($\gamma\text{-Al(OH)}_3$) and Boehmite ($\gamma\text{-AlO(OH)}$). The Boehmite phase, which emerged as radiolytic heating removed water from the Gibbsite phase, is a more stubborn remediation challenge and resistant to caustic leaching. Some studies have shown acidic scrubs containing 0.1 HNO_3 would be particularly capable of dislodging Al solids from Hanford sludges. One caveat of this treatment plan would be the potential mobilization of the actinides to the acidic Al leachate. The following chapter addresses how a secondary clean up could be achieved using neutral, organophosphorus reagent containing extraction chromatographic materials.

While this chapter successfully addresses several of the issues presented by the use of an acidic leach, an interesting comparison between solvent extraction and extraction chromatography can also be performed. Previous work has examined the use solvent extraction with organophosphorus reagents to perform the secondary remediation of the Al leachates. Many comparable studies to the solvent extraction investigation were performed in this next chapter.

Some of the most interesting results arose from the chromatographic use of tri-n-octyl phosphine oxide (TOPO). When TOPO is used in a liquid-liquid system, the highest usable concentrations in n-dodecane are typically around 0.1 M. For the extraction chromatographic investigations, the concentration of TOPO on the resin was > 1 M in many cases. This led to some interesting discoveries.

While the remediation of simulated Al leachates using extraction chromatography was successful in many cases, the bleed off of extractant from the resin can be quite deleterious to the separation. Chapter 3 begins the investigation of some neutral organophosphorus extractant moieties which are covalently bound to the polymeric support. This sort of resin would also compete with liquid-liquid separations, since significant extractant loss to the aqueous phase can occur over the course of an industrial solvent extraction process.

CHAPTER TWO

**EXTRACTION CHROMATOGRAPHIC BEHAVIOR OF EUROPIUM AND
ACTINIDES BETWEEN ACIDIC AQUEOUS $\text{Al}(\text{NO}_3)_3$ AND NEUTRAL PHOSPHORUS
LIGANDS**

Abstract

As the Hanford site undergoes remediation, significant economies could be realized if aluminum and chromium are kept from High-Level Waste glass. An acidic scrub of the Hanford sludge could enhance Al removal, although such treatment could lead to the mobilization of transuranic elements. Such mobilization would require a secondary cleanup of the acidic waste stream. This study examines tri-n-butyl phosphate or tri-n-octyl phosphine oxide impregnated resins as a chromatographic means for the removal of transuranics from a secondary waste stream. Results indicate >99% of the radioactive material may be recovered using extraction chromatography; providing another valid avenue for tank remediation.

Introduction

The Hanford Site, in south central Washington state, was the first facility to produce plutonium for nuclear weapons. Three plutonium separations methods were used during the operation of the Hanford site: the Bismuth Phosphate (1945-1956), Redox (1951-1959) and

PUREX processes (1956-1972; 1983-1989).^[1] The use of multiple plutonium separations created a complex waste matrix; the remediation of such has been one of the most labyrinthine challenges faced by the Department of Energy. Both the volume and composition of waste resulting from Pu production are major remediation concerns.^[2] The most problematic waste component is the sludge created by the caustic environment of the tanks. Research and remediation efforts have focused on caustic leaching to remove problematic nonradioactive elements, aluminum and chromium. Removal of these species would decrease volume and improve the stability of the glass matrix of the vitrified high level waste (HLW). The precipitation of chromium spinels from the HLW could short the heating electrodes, clog the pour spout, or otherwise jeopardize the operation and life of the melter.^[3] While some significant successes have been experienced, the most stubborn Al phase, boehmite (γ -AlO(OH)) has been resistant to caustic leaching.

An alternative, acidic leaching, has been shown to enable complete dissolution of Al.^[4] A caveat of acidic leaching is the potential to mobilize radioactive species into the Al/Cr waste stream. If acidic leaching were to be performed, knowledge of how to remove radioactive species, predominantly actinides, from conditions of variable $[\text{HNO}_3]$, $[\text{Al}(\text{NO}_3)_3]$ and chromium oxidation states would be required. Chromium may be present in the trivalent or hexavalent state during the course of this remediation. If the chromium is present as chromate, reduction of chromium to the trivalent state using ascorbic acid may be preferable. In some instances, the extraction of chromate by tri-*n*-butyl phosphate (TBP) can impede the extraction of desired species.^[5] Previous studies have shown solvent extraction (SX) with 60% by volume (v/v) (TBP) or 0.1 M tri-*n*-octylphosphine oxide (TOPO) in *n*-dodecane to be a complementary and effective means of handling the secondary cleanup.^[6,7] If the mobilization of actinides is

minimal, preconcentration and decontamination may be desired. An extraction chromatographic remediation could serve to compliment the solvent extraction efforts.

Extraction chromatography (EXC) is a type of liquid-liquid chromatography that couples the selectivity and adjustability of solvent extraction with the inherently multistage character of chromatography to provide a higher purity or preconcentrated product.^[8] Solvent impregnated resins (SIRs) allow the benefits of a functionalized polymeric resin without the difficulties associated with synthesis. They also provide a unique environment wherein “neat” ligand can interact with an aqueous phase. Omission of the functionalized resin synthesis can lead to extractant bleed off from the polymeric support. This must be considered when examining separation goals. Comparison between similar EXC or SX systems can oftentimes provide better understanding of behavior in each system.^[9] As an organic diluent’s density, dielectric constant and hydrogen bonding characteristics will affect SX results, pore size, bead size and hydrophilic/phobic characteristics of the resin can affect EXC results.

In this work, a bench scale exploration of an actinide separation system including U, Th, Np, Pu and Eu from Al/Cr leachate solutions that could emerge if one were to attempt nitric acid leaching with Al-bearing solids using EXC has been developed. Europium was used to model the partitioning of americium. To achieve these studies, the polyacrylic XAD7 resin was used as the solid support for extractant immobilization. Previous studies have shown the XAD7 resin to successfully retain TBP and TOPO extractants for the purposes of metal uptake.^[10,11] Initial batch uptake studies were performed to determine the f-element uptake capabilities. The maximum equilibrium flow rate was indicated by batch kinetic experiments. Elution curves displayed the remediation capabilities of the chromatographic materials. For the EXC remediation to be successful, the uptake and elution of the metal ions must be quantitative

(>99%) under a wide range of $\text{Al}(\text{NO}_3)_3$ and nitric acid conditions. The uptake kinetics must also be competitive with current solvent extraction methods to encourage a high volume of waste throughput.

Experimental

Materials and Instrumentation

All aqueous solutions were prepared from analytical grade reagents and ultra pure (18 M Ω) deionized H_2O . A density determination was performed of all solutions using a calibrated 1 mL pipette and weighing the 1 mL volume of each solution at room temperature. Solutions of HNO_3 were prepared by mass using Fischer Scientific concentrated (15.8 M) HNO_3 solution. Sodium hydroxide solutions were prepared from dilutions of 50% w/w NaOH (Alfa Aesar) and standardized by titration with potassium hydrogen phthalate to a phenolphthalein end point. Solutions of K_2CrO_4 and $\text{Al}(\text{NO}_3)_3$ were prepared by mass using analytical grade J.T. Baker solids. The L-ascorbic and 1-hydroxyethane 1,1-diphosphonic acid (HEDPA) solutions were prepared by mass from Fisher Scientific ACS certified reagent and Alfa Aesar, respectively. Experiments done using $^{152/154}\text{Eu}(\text{NO}_3)_3$, $^{237}\text{Np}(\text{NO}_3)_3$, $^{233}\text{UO}_2(\text{NO}_3)_2$, $^{238}\text{UO}_2(\text{NO}_3)_2$, $^{238}\text{Pu}(\text{NO}_3)_4$, and $^{232}\text{Th}(\text{NO}_3)_4$ were prepared by dilution of standardized stocks from the Washington State University (WSU) inventory. Experiments using inactive $\text{Eu}(\text{NO}_3)_3$ were prepared by dilution of standardized stocks. Radioactive $^{152/154}\text{Eu}$ was created by neutron activation of 99.999% Eu_2O_3 (Arris International) using a Teaching, Research, Isotopes General Atomics (TRIGA) reactor with a neutron flux of 5×10^{12} n/cm²·sec at the Nuclear Radiation Center at WSU. The TBP

organic solutions (Acros Organics) were purified to remove organic acid impurities using Na_2CO_3 (Fisher) as described previously.^[12] Both TBP and TOPO were diluted volumetrically using methanol (>99%, SigmaAldrich). Amberlite XAD-7 (Rohm & Hass) was treated as described in the following section.

Radiotracer experiments using $^{152/154}\text{Eu}$ were analyzed on a NaI(Tl) solid scintillation counter, a Packard Cobra-II auto gamma, for gross gamma counting. Radiotracer experiments using ^{233}U , ^{237}Np and ^{238}Pu were analyzed using a Beckman LS6500 liquid scintillation counter for alpha detection and 5 mL of EcoScint® scintillation fluid. Light metals analysis (Cr, Al) and heavy metal analysis (^{238}U , ^{232}Th) was done using a Perkin Elmer Optima 3200 RL ICP-OES instrument and an Agilent 4500+ ICP-MS, respectively. All mixing was done using a VWR mini vortexer. All mass measurements were obtained using a Mettler Toledo XS105 Dual Range series analytical balance.

Resin Preparation

Amberlite XAD7 resin is a polyacrylic resin with a 20-60 mesh particle size and a surface area of $450 \text{ m}^2/\text{g}$. Removal of acidic impurities in the XAD7 resin was performed with deionized water rinse until a neutral pH was obtained. Drying of the resin was expedited by methanol (MeOH) addition and removal, followed by placement in an oven at 80°C . The dried resin was removed from the oven, allowed to cool in a vacuum dessicator, weighed and contacted for 15 minutes by vigorous shaking with 2.3 M TBP or 1 M TOPO in MeOH with excess impregnation solution. Excess impregnation solution after contact was removed and the impregnated beads were dried at 80°C overnight. The amount of impregnation can be defined as

the ratio of mass of organic extractant present to the total final mass of the impregnated resin. The impregnation provided 60% $m_{\text{TBP}}/m_{(\text{TBP}+\text{XAD7})}$ or 58% $m_{\text{TOPO}}/m_{(\text{TOPO}+\text{XAD7})}$. For 38% $m_{\text{TOPO}}/m_{(\text{TOPO}+\text{XAD7})}$ resin, dried resin was contacted in a ratio of 1.05 g XAD7 : 1.75 g TOPO in excess methanol.

Preliminary europium studies indicated the TOPO-XAD7 resin was the most capable extractant resin for remediation of the Al^{3+} leachate. The kinetics of the TOPO-XAD7 resin was determined to be significantly slower than other comparable solvent extraction systems. In an attempt to encourage faster metal uptake kinetics, the TOPO-XAD7 resin was wetted with n-dodecane (TOPO-XAD7n).^[13] To accomplish this, TOPO-XAD7 resins were contacted with a 50% v/v chloroform/n-dodecane solution. The ratios were selected to minimize the presence of excess n-dodecane and potential loss of TOPO from the resin during the wetting process.

The concentration of TOPO per gram of resin was calculated. Since the density of XAD7 resin is 0.97 g/mL, and literature has found success in assuming the density of solvent impregnated resins to be 1 g/mL, the density of the impregnated resin can be approximated to 1 g/mL for discussion purposes.^[14] The supplier notes the maximum solubility of TOPO in aliphatic diluents at 0.4 M. The percent of TOPO dissolution could be calculated using this information. The volumes of 50% v/v chloroform/n-dodecane solution used for n-dodecane wetting and final characteristics of prepared resins are shown in [Table 1.1](#).

Extraction in Batch Experiments

All batch extractions were performed in triplicate and the errors presented are for a 1σ standard deviation of the triplicate analysis. The weight distribution ratio of the analyte, D_w

Table 2.1 Characteristics of various TOPO-XAD7 extraction chromatographic resins used in this study.

% w/w TOPO	C12 ^a	μL 50% v/v CHCl ₃ /C12 ^{ac}	mmol C12 ^{ad}	[TOPO; M]	% TOPO Dissolution ^b
58%	No	--	--	1.41	0%
58%	Yes	100	0.39	1.33	30%
38%	Yes	160	0.62	0.75	53%

^an-dodecane abbreviated as C12 for the purposes of this table

^bassumes a maximum solubility of 0.4 M TOPO in C12

^c per 100 mg TOPO resin

^dper g of TOPO-XAD7n resin

(mL·g⁻¹), was calculated for most experiments according to the following equation:

$$D_w = \left(\frac{A_o - A_s}{A_s} \right) \times \frac{V}{m} \quad (2.1)$$

where A_o and A_s are the aqueous phase activity (counts per minute) before and after equilibration, m the mass of resin (g) and V the volume of the aqueous phase (mL). For radiotracer experiments, triplicate experiments showed the reproducibility of the distribution measurements was generally within 10%, although the uncertainty interval was somewhat higher for the highest distribution values ($D_w \geq 10^3$) due to a lack of discernable activity in the aqueous phase. When possible, weight distribution values (D_w) were corrected for nitrate complexation in the aqueous phase, as done previously, to provide the corrected weight distribution ratio, D_{w_o} .^[7]

HNO₃ Partitioning

Nitric acid extraction for 0.1 and 1 M HNO₃ was determined for Al(NO₃)₃ concentrations ranging from 0.01 to 1.5 M. Extractions used a 1 mL aqueous phase and either 50 mg of TBP-XAD7 resin or 100 mg of TOPO-XAD7 resin. Phases were contacted for 20 minutes by vigorous shaking. The higher molecular weight of TOPO relative to TBP and potentially significant competition with HNO₃ for Eu³⁺ warranted an increase in the mass of resin in the TOPO-XAD7 study.

The amount of HNO₃ in the aqueous phase after contact was determined by titration with standardized NaOH using a phenolphthalein indicator. For studies with Al³⁺ present, possible binding of Al³⁺ with phenolphthalein prevented direct titration of the aqueous raffinate and a strip of extracted HNO₃ was required. The HNO₃ rich resin was therefore centrifuged using 2 mL Durapore filters for five minutes to ensure complete removal of unbound acid. Stripping was performed by multiple washings with deionized water, to remove bound HNO₃ from the resin phase and this solution was titrated.

Eu³⁺ Partitioning

For the initial ^{152/154}Eu extraction experiments with TBP-XAD7 and TOPO-XAD7, the aqueous phase contained various amounts of HNO₃, Al(NO₃)₃, Cr(III/VI), and Eu(III). Chromium and ascorbic acid concentrations were maintained at 1 mM and 2 mM, respectively. To encompass a wider variety of aqueous phase conditions than could be encountered during HNO₃ leaching of Hanford tank sludges, different aqueous phases were studied. Investigations of the extraction behavior of Eu³⁺ with varying [HNO₃] in the presence of constant [Al(NO₃)₃] and of constant [HNO₃] with varying [Al(NO₃)₃] were completed.

Tracer concentrations of Eu^{3+} (10^{-6} M) were used to examine Eu^{3+} distribution while using the TBP resin. Concentrations of Eu^{3+} for the TOPO investigations were increased to 1 mM to highlight the uptake capabilities of the TOPO resin. Initial studies used 1 mL aqueous phase and either 50 mg of TBP-XAD7 resin or 100 mg of TOPO-XAD7 resin for the same reasons stated above. For later comparison with actinide investigations, 500 μL of aqueous phase and 50 mg of TOPO-XAD7 were used at tracer concentrations of Eu^{3+} . Phases were contacted for 20 minutes by vigorous shaking and aliquots of the aqueous phase were obtained. Analysis for $^{152/154}\text{Eu}$ in the aqueous phase was performed as described previously.

Actinide Partitioning

Batch investigations were performed for ^{238}U , ^{232}Th , ^{237}Np and $^{152/154}\text{Eu}$ at tracer concentrations ($<10^{-5}$ M) using a 500 μL aqueous phase and 50 mg of 58% TOPO-XAD7 resin. The concentration of $\text{Al}(\text{NO}_3)_3$ was varied between 0.01 and 1 M while maintaining constant concentrations of HNO_3 . Studies were performed with ^{233}U and ^{237}Np examining the distribution of the actinides between the aqueous phase and the resin with 1 mM K_2CrO_4 (Cr(VI)), 1 mM K_2CrO_4 and 2 mM ascorbic acid (AA) (producing Cr(III)), and no chromium present. Studies with ^{232}Th included 1 mM Cr K_2CrO_4 and 2 mM ascorbic acid. All contacts were for 20 minutes. Aliquots of the aqueous phase were obtained. Analysis for ^{238}U , ^{232}Th and ^{237}Np in the aqueous phase was performed as described previously.

Uptake Kinetics

Since extraction chromatographic kinetics are generally diffusion controlled, higher concentrations of analyte may take longer to reach equilibrium.^[15] To ensure metal transfer from the aqueous phase to the resin was reaching equilibrium at all analyte concentrations, the kinetics of Eu^{3+} and UO_2^{2+} , representative of trivalent and hexavalent ions, were examined. Median tank conditions of 0.25 M $\text{Al}(\text{NO}_3)_3$ and 0.1 M HNO_3 were isolated to provide an indication of average uptake behavior.^[4,6] The TOPO resin (50 mg) was contacted with 0.5 mL of the appropriate aqueous phase. Macro concentrations of Eu^{3+} and UO_2^{2+} were available through the use of $^{151/153}\text{Eu}$ and ^{238}U and these were appropriately spiked with $^{152/154}\text{Eu}$ or ^{233}U . Solid and liquid phases were vortexed for varying amounts of time.

Isotherm Determination

To determine saturating conditions of each TOPO resin, isotherms were generated by monitoring Eu^{3+} or UO_2^{2+} partitioning while varying the concentrations of Eu^{3+} or UO_2^{2+} starting at 0.01 mM and increasing the concentration of Eu^{3+} or UO_2^{2+} until the resin was sufficiently saturated. Median tank conditions of 0.25 M $\text{Al}(\text{NO}_3)_3$ and 0.1 M HNO_3 were isolated to provide an indication of average uptake behavior and to ensure previous kinetic experiments would be valid. Macro concentrations of Eu^{3+} and UO_2^{2+} were available through the use of $^{151/153}\text{Eu}$ and ^{238}U and these were appropriately spiked with $^{152/154}\text{Eu}$ or ^{233}U . Solid and aqueous phases were contacted for 30 minutes. Contact times were increased in this investigation after kinetics studies indicated the amount of time required for metal distribution to reach equilibrium was increased for systems containing higher concentrations of metal.

Column Experiments

All column experiments were performed with 0.1 M HNO₃ and 0.25 M Al(NO₃)₃ to ensure kinetics and isotherm experiments performed in batch mode would assist in describing observations from column experiments. Some elution volumes are described in terms of *bed volume*. A column's bed volume (BV) is synonymous with its column volume, but indicates the column is packed. Columns were Biorad® 1.27 BV PTFE. All columns were weighed before and after column packing with extraction material to provide the mass of the resin used.

A free volume determination was performed for each column by extracting a mixed 0.1 M HNO₃/0.25 M Al(NO₃)₃ solution into the resin-loaded column. The solution was expelled from the column and weighed. The density of nitric acid/aluminum nitrate solution was determined to be 1.032 ± 0.003 . Using the expelled mass and the known density, the free column volume was determined. The free column volume for all experiments was 0.42 ± 0.02 mL. Fractions were collected using a Biorad® 2120 series fraction collector. All samples were weighed prior to analysis to ensure knowledge of sample size.

Dynamic Capacity Determination

Breakthrough curves were obtained for 58% TOPO/XAD7, 58% TOPO/XAD7n (n ~ n-dodecane wetted) and 38% TOPO/XAD7n systems for Eu³⁺ with initially 1mM Cr(VI) and 2mM ascorbic acid present in solution. Europium concentrations and flow rates may be found in [Table 2.2](#), which also contains experimental results. The performance of the 38% TOPO/XAD7n

Table 2.2 Defined parameters for various TOPO-XAD7 n-dodecane wetted resins.

	Eu ³⁺			UO ₂ ²⁺
<i>% TOPO (m/m)</i>	58%	38%	38%	38%
<i>Redox Conditions</i>	1mM Cr(III)/ 2mM AA	1mM Cr(III)/ 2mM AA	1mM Cr(VI)	1mM Cr(VI)
<i>q_{max} (mmol Eu/g resin)</i>	0.308 ± 0.008	0.176 ± 0.003	-	0.51 ± 0.01
<i>Q(m) (mmol Eu/g resin)</i>	0.299 ± 0.009	0.172 ± 0.002	-	0.50 ± 0.02
<i>Flow Rate (μL/mL)</i>	50	50	-	50
<i>D</i>	1200	350	-	640
<i>% recovery</i>	98.3 ± 0.1	99.9 ± 0.3	99.2 ± 0.2	99.7 ± 0.2
<i>Eluent</i>	3 M HNO ₃	3 M HNO ₃	3 M HNO ₃	0.1 M HEDP
<i>Stoichiometry¹</i>	1:4	1:3.5	-	1:1

¹Metal:Ligand

system showed promise and additional breakthrough curves were performed with 1 mM Cr(VI) and 50 mM Eu³⁺ or UO₂²⁺.

Metal Elution

The elution studies were performed in a similar way as described above for dynamic capacity determination. Europium experiments involved elution from solutions containing either 1 mM K₂CrO₄ and 2 mM ascorbic acid or just 1 mM K₂CrO₄. Actinide experiments were only performed in the presence of 1 mM K₂CrO₄. The oxidizing conditions stabilized Np and Pu to the hexavalent oxidation state. Values obtained from performing the dynamic capacity determinations were used to calculate the amount of Eu³⁺ and UO₂²⁺ needed to load the column to 40% capacity. For all curves the flow rate was 50 μL/min. Columns were loaded to 40% of capacity by passing the appropriate amount of Eu³⁺ or UO₂²⁺ through the column. A 3 BV rinse,

3.81 mL, was performed after column loading using a mixed 0.001 M HNO₃/0.75 M Al(NO₃)₃ solution. After rinsing the column, elution of the analytes was accomplished as detailed for each experiment. Neptunium and plutonium elution curves had the same load and rinse volumes as the uranium experiments, but were performed with only tracer concentration. The focus of Np and Pu experiments was to confirm both Np and Pu were in the hexavalent oxidation state throughout the experiment by comparison with uranium elution data.

Results

Batch Experiment

HNO₃ Partitioning

The partitioning of HNO₃ as a function of Al(NO₃)₃ into the TBP-XAD7 and TOPO-XAD7 phases is presented in [Figures 2.1a](#). [Figure 2.1b](#) shows the molar amounts of nitric acid extracted by TOPO-XAD7. The dashed line indicates the saturating condition of HNO₃ in the resin phase for the (TOPO)₂·HNO₃ species. Formal concentrations of Al(NO₃)₃ and HNO₃ were used during analysis for simplicity, as the potential calculation of free nitrate was daunting giving the lack of knowledge regarding activity coefficients with the high concentrations of Al(NO₃)₃ and HNO₃ present.

The extraction of 0.1 M HNO₃ as a function of Al(NO₃)₃ concentrations by the TBP coated resin appears to have two distinguishable slopes. Between 0.01 and 0.5 M Al(NO₃)₃ the data is fit well by a line with a slope equal to 1, providing support for a TBP·HNO₃ species in the

organic phase. Increasing the $[\text{Al}(\text{NO}_3)_3]$ beyond 0.5 M provides a drastic shift in slope from 1 to 2, allowing argument for the $\text{TBP}\cdot(\text{HNO}_3)_2$ species. The extraction of 0.1 M HNO_3 as a function of $\text{Al}(\text{NO}_3)_3$ concentrations shows a slope of 1, regardless of the concentration of $\text{Al}(\text{NO}_3)_3$, suggesting that only one HNO_3 molecule is extracted by each TOPO complex. The stoichiometries of nitric acid/extractant complexes are difficult to determine for 1 M HNO_3 /TOPO system. For this system, slope analysis is surely impacted by saturation of the resin by HNO_3 .

Europium and Actinide Partitioning

Figure 2.2 presents Eu^{3+} distribution data as a function of the total, aqueous nitrate concentration for the TBP and TOPO-XAD7 systems. Extraction behaviors for TBP and TOPO-XAD7 were determined as a function of increasing $\text{Al}(\text{NO}_3)_3$ concentration (0.010 M – 1.50 M) at three constant concentrations of HNO_3 (Figures 2.2a and 2.2c, respectively), and also for varied concentrations of HNO_3 (0.01 M – 1.50 M) at two constant concentrations of $\text{Al}(\text{NO}_3)_3$ (Figures 2.2b and 2.2d, respectively). All distribution data are corrected for complexation of europium by nitrate in the aqueous phase. Corrections for the presence of $\text{Eu}(\text{NO}_3)^{2+}$ in comparable media have been previously derived.^[4,6]

The partitioning of Eu^{3+} into the TBP and TOPO-XAD7 resins from solutions of constant HNO_3 concentrations increased significantly with increasing concentrations of $\text{Al}(\text{NO}_3)_3$ (Figure 2.2a and 2.2b, respectively) over the $\text{Al}(\text{NO}_3)_3$ concentration range of 0.10 – 1.50 M. The highest value observed for both systems was at $[\text{HNO}_3] = 0.01$ M and $[\text{Al}(\text{NO}_3)_3] = 1.5$ M.

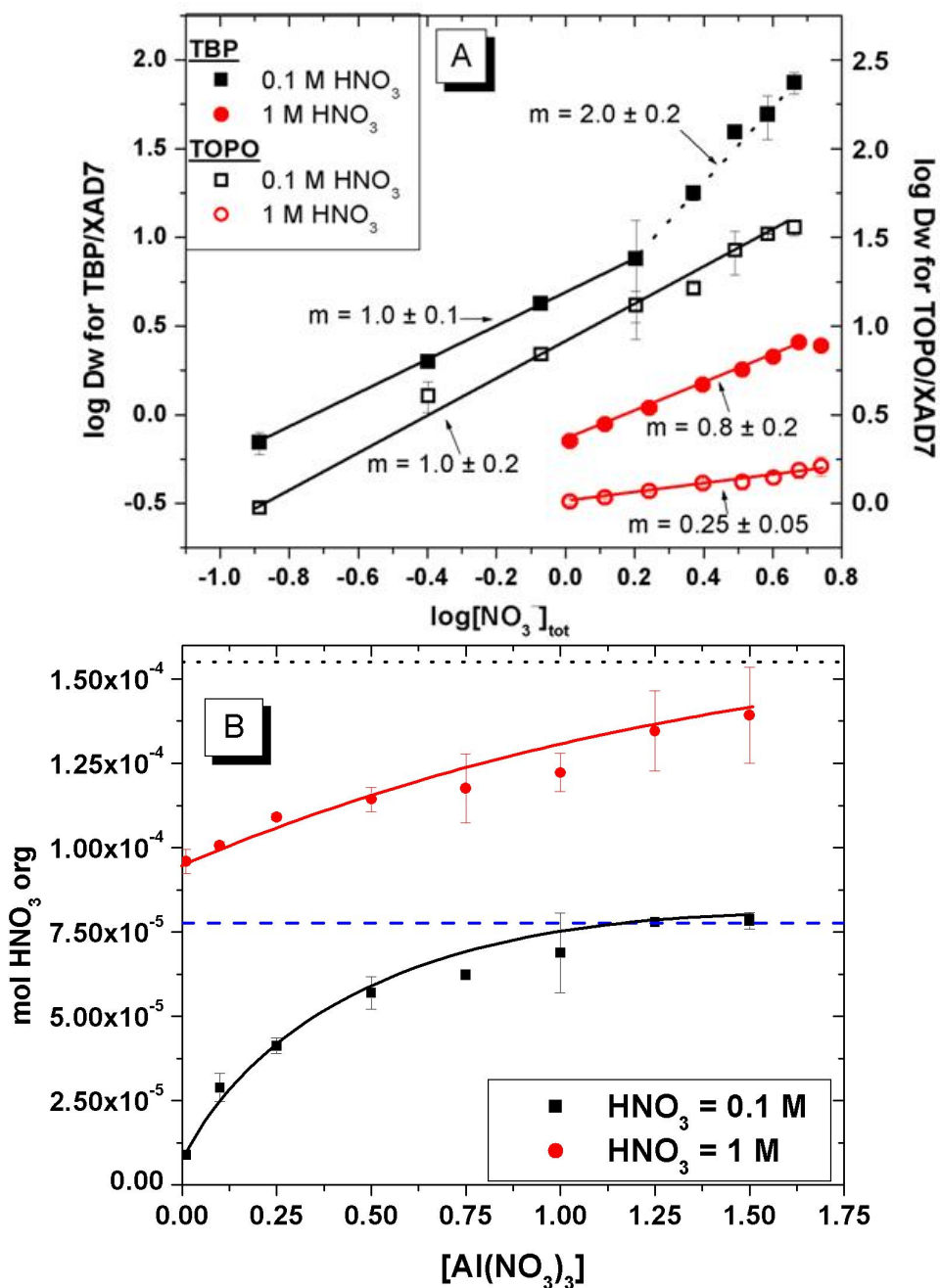


Figure 2.1 a) Distribution of HNO₃ between acidic Al(NO₃)₃ and resin as Al(NO₃)₃ is varied between 0.01 to 1.5 M in 60% TBP-XAD7 (left y-axis) and 58% TOPO-XAD7 (right y-axis) resin b) Nitric acid uptake in mmol as a function of aqueous [Al(NO₃)₃] from 0.01-1.5 M Al(NO₃)₃ for 58% TOPO-XAD7 resin. Concentrations of nitric acid were held constant at concentrations noted in legend. The dashed line and the dotted line represent the saturating mmol of HNO₃ in the organic solid phase for the TOPO·HNO₃ and (TOPO)₂·HNO₃ species, respectively.

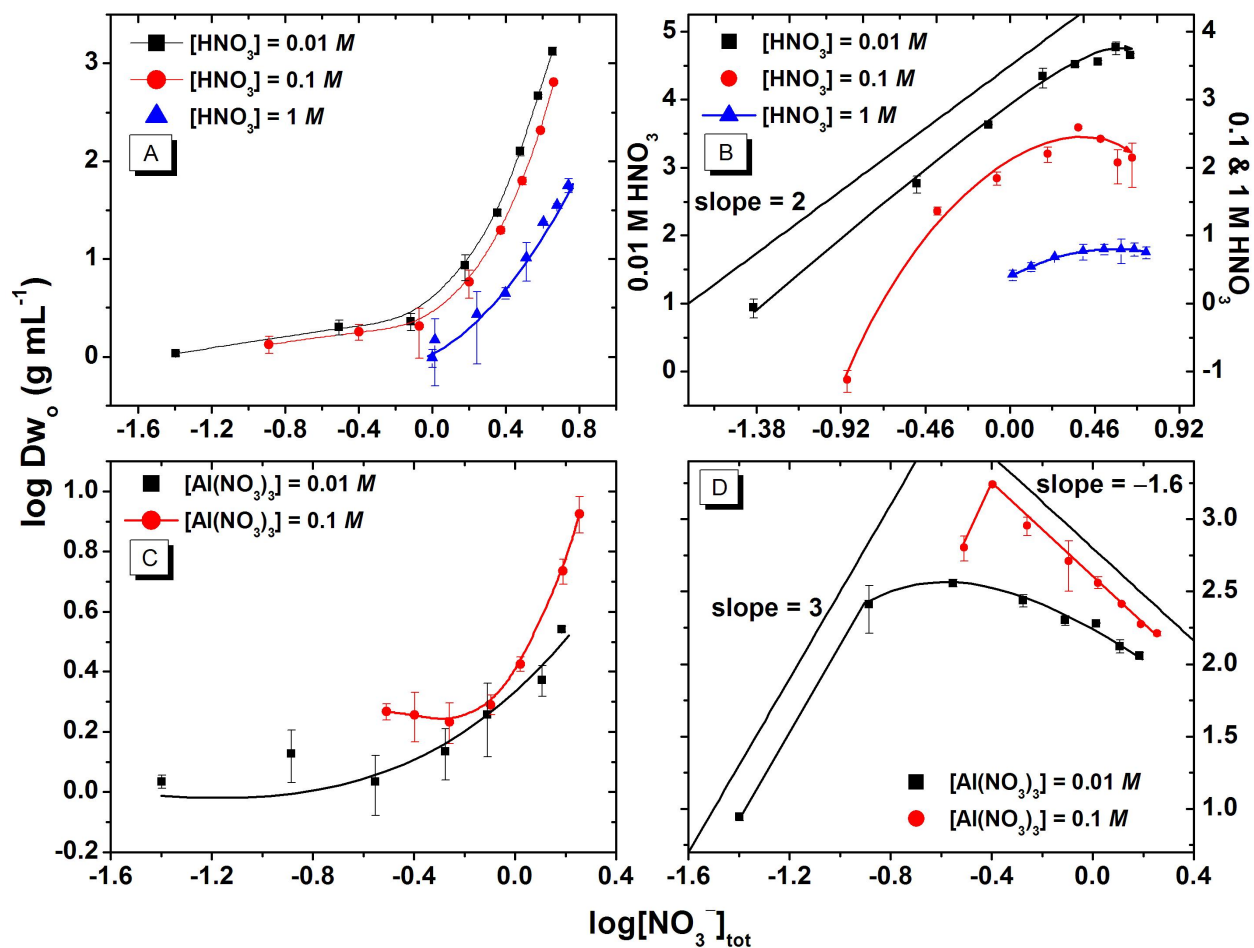


Figure 2.2 Nitric acid or aluminum nitrate dependences for europium nitrate adsorption into TBP or TOPO XAD7 resin. Initially present in each aqueous solution was 1.0 mM K_2CrO_4 and 2 mM ascorbic acid. a) Aluminum nitrate varied from 0.01 to 1.5 M ■ 0.01 M HNO_3 ● 0.10 M HNO_3 ▲ 1.00 M HNO_3 . Organic phase: 50 mg TBP-XAD7 b) Aluminum nitrate varied from 0.01 to 1.5 M ■ 0.01 M HNO_3 ● 0.10 M HNO_3 ▲ 1.00 M HNO_3 . Organic phase: 100 mg TOPO-XAD7 c) Nitric acid varied from 0.01 to 1.5 M ■ 0.01 M $Al(NO_3)_3$ ● 0.1 M $Al(NO_3)_3$. Organic phase: 50 mg TBP-XAD7 d) Nitric acid varied from 0.01 to 1.5 M ■ 0.01 M $Al(NO_3)_3$ ● 0.1 M $Al(NO_3)_3$. Organic phase: 100 mg 60% TOPO-XAD7.

The partitioning of Eu^{3+} between the TBP-XAD7 phase from solutions of constant $\text{Al}(\text{NO}_3)_3$ concentrations with increasing amounts of HNO_3 (Figure 2.2c) increased slightly over the HNO_3 concentration range of 0.10 – 1.50 M. The greatest Eu^{3+} recovery occurs under the highest acid and $\text{Al}(\text{NO}_3)_3$ concentrations. The partitioning of Eu^{3+} between the TOPO-XAD7 phase from solutions of constant $\text{Al}(\text{NO}_3)_3$ concentrations with increasing concentrations of HNO_3 (Figure 2.2d) increased slightly over the HNO_3 concentration range of 0.10 – 1.50 M. A maximum Eu^{3+} recovery occurs at $[\text{HNO}_3] = 0.25 \text{ M}$ and $[\text{Al}(\text{NO}_3)_3] = 0.1 \text{ M}$. A steep decrease, with an approximate slope of -1.6 on the log-log plot, is observed after this maximum.

Figure 2.3 shows the uptake of Th, U, Np, and Eu at tracer concentrations as a function of $\text{Al}(\text{NO}_3)_3$ concentration by TOPO-XAD7 resin. The uptake studies of Th^{4+} , UO_2^{2+} and Eu^{3+} served to model the distribution behavior of An^{4+} , AnO_2^{2+} , and An/Ln^{3+} cations, respectively. Comparing uptake behavior between redox active (Np) and redox inactive actinides/lanthanides (UO_2^{2+} , Th^{4+} , Eu^{3+}) allows an approximation of the anticipated redox state of Np in the sludge simulants for both potentially oxidizing and reducing conditions. Uptake studies were performed with no chromium present to examine the impact of chromium, in either oxidation state, on the partitioning of the analytes.

Eu and U Kinetics

Table 2.3 shows the contact time required for europium and uranium uptake to reach equilibrium for various types of TOPO impregnated resin. When using the 58% TOPO-XAD7n

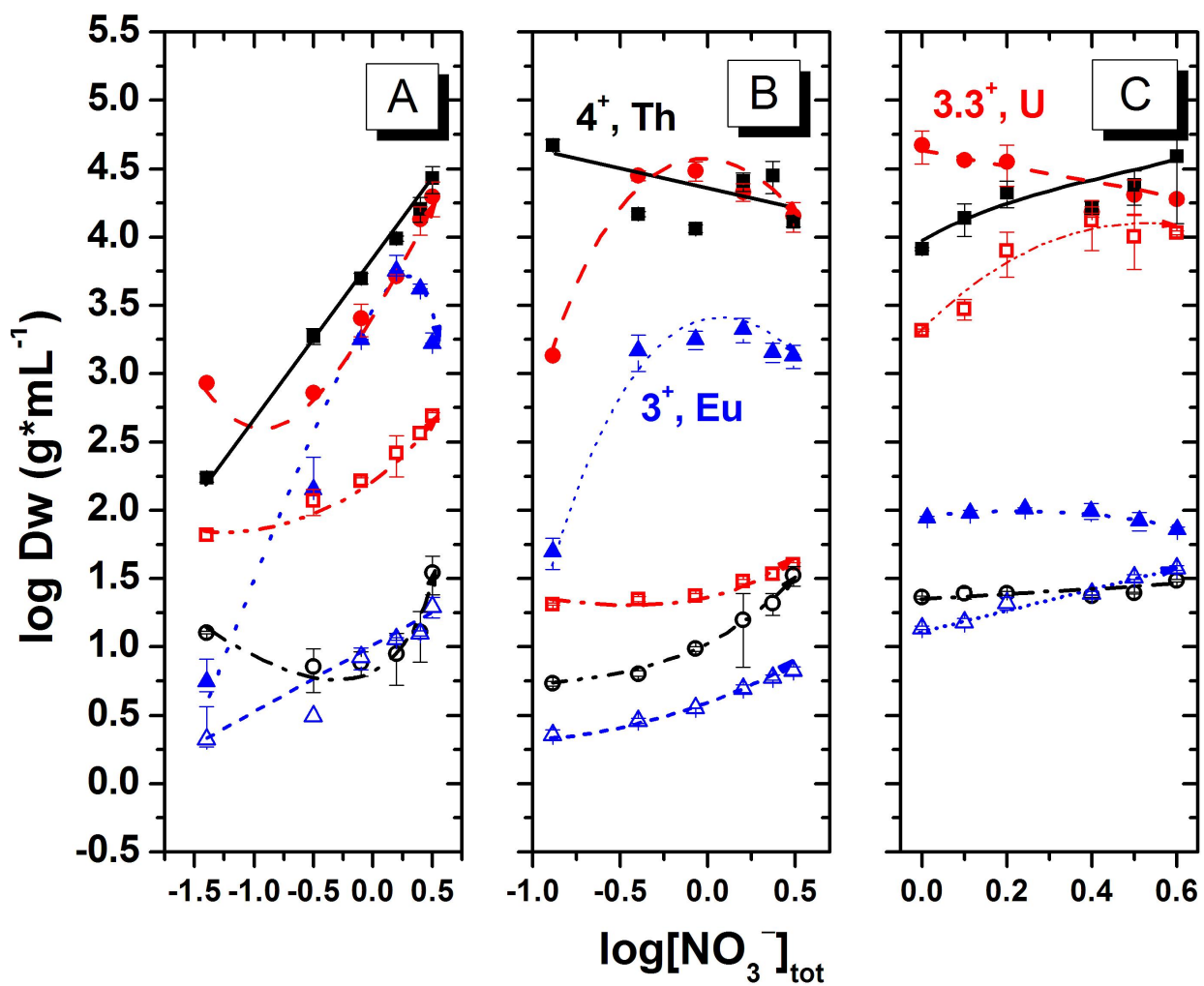


Figure 2.3. Metal distribution values as a function of aqueous $[Al(NO_3)_3]$ with $[HNO_3]$ equal to a) 0.01 M b) 0.1 M and c) 1 M. The various elements and redox conditions described as follows: \blacksquare Th⁴⁺, No Cr \bullet UO₂²⁺, No Cr \blacktriangle Eu, No Cr \circ Np, No Cr \square Np, 1 mM CrO₄²⁻ \triangle Np, 1 mM CrO₄²⁻, 2 mM ascorbic acid Organic phase: 100 mg TOPO-XAD7.

Table 2.3. Time required for various concentrations of Eu^{3+} and UO_2^{2+} to reach equilibrium using different modifications of the TOPO-XAD7 resin. The aqueous phase initially contained 0.1 M HNO_3 , 0.25 M $\text{Al}(\text{NO}_3)_3$, 1 mM K_2CrO_4 and 2 mM ascorbic acid. $V:m = 1$ mL aqueous solution : 50 mg resin.

Metal	[Metal]	n-dodecane	% impregnation	Uptake Equilibrium Time, min
Eu	10 mM	No	60	40
	1 mM	No	60	20
	Tracer	No	60	15
	10 mM	Yes	60	15
	1 mM	Yes	60	10
	10 mM	Yes	40	15
	1 mM	Yes	40	<1
	UO_2	10 mM	Yes	40
1 mM		Yes	40	25
Tracer		Yes	40	15

material, the concentration of TOPO is 1.33 M; an order of magnitude larger than typically used in solvent extraction.^[6,16,17] To provide a more thorough dissolution of TOPO for some experiments, the impregnation percentage was dropped to 38% (0.75 M). The increased percentage of dissolved TOPO would allow improved rearrangement possibilities for the extractant on the resin; ultimately expediting uptake kinetics.^[13]

Isotherm Determination

Figure 2.4 compares the Eu^{3+} isotherms of the 58% TOPO-XAD7, 58% TOPO-XAD7n systems and 38% TOPO-XAD7n resins. Data was fit using a Langmuir isotherm model where equilibrium concentrations of analyte in the liquid and solid phase, c and q , respectively, were calculated from through Equation 2.2 and 2.3, respectively;

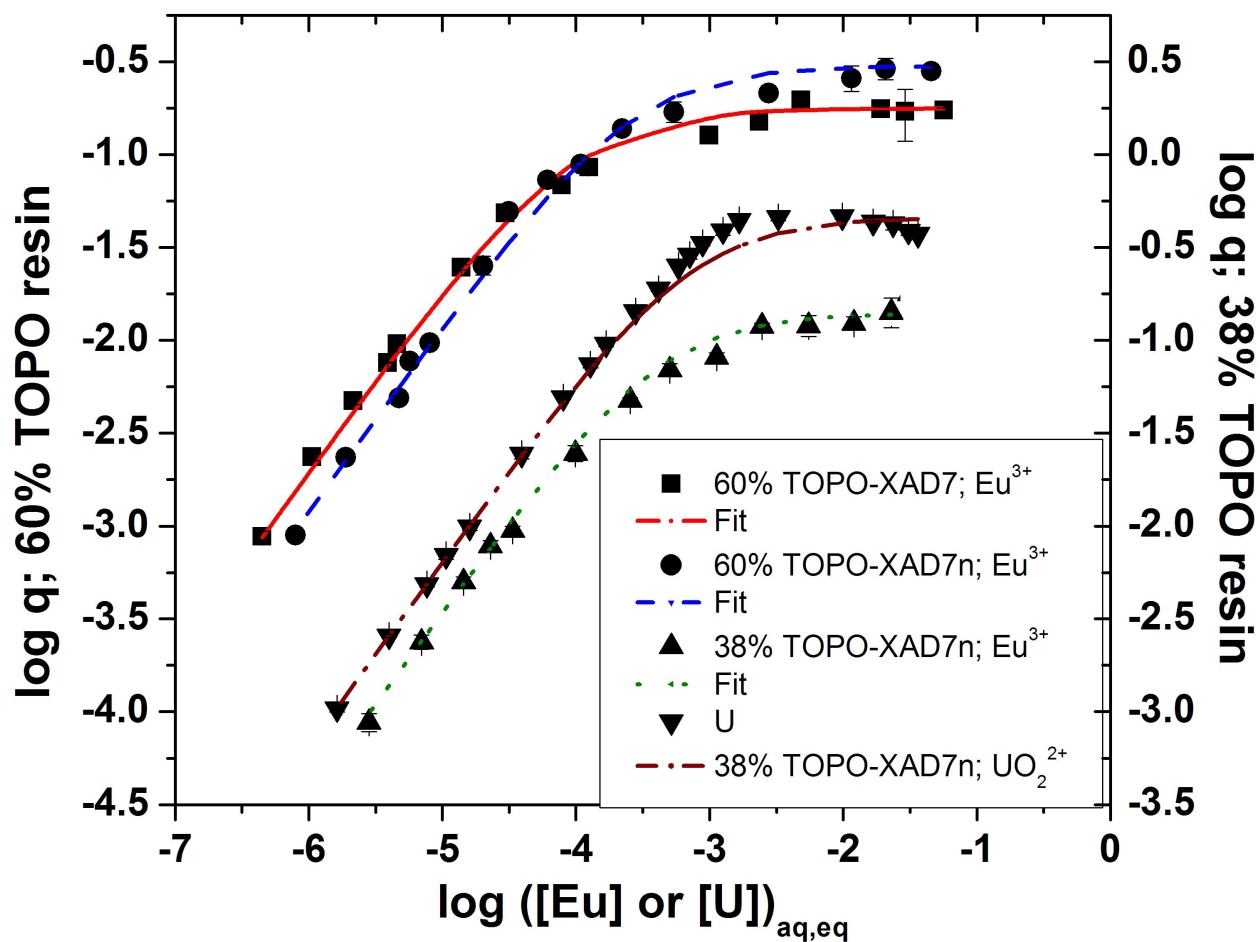


Figure 2.4. Isotherms comparing the uptake behaviors of europium by the 58% TOPO-XAD7, 58% TOPO-XAD7n and 38% TOPO-XAD7n resin. Uranium isotherm also shown for the 38% TOPO-XAD7n resin. Initial aqueous phase: 0.1 M HNO_3 , 0.25 M $Al(NO_3)_3$, 1 mM K_2CrO_4 , 2 mM Ascorbic Acid. Resin phase: 50 mg of the appropriate resin.

$$c = \frac{A}{A_o} \cdot c_o \quad (2.2)$$

$$q = \frac{A_o - A}{A} \cdot \left(\frac{V}{m}\right) \cdot c_o \quad (2.3)$$

where m is the mass of the resin, V is the volume of aqueous phase, A_o is the initial activity in the aqueous phase (cpm), A is the final activity in the aqueous phase after equilibration, and c_o is the initial concentration of analyte in the aqueous phase. Langmuir behavior was assumed for fitting purposes, Equation 2.4, where K is a system specific constant, c is the concentration of analyte in the aqueous phase and q_{max} is the maximum mole of analyte sorbed to the resin per gram.

$$q = q_{max} \cdot \left(\frac{Kc}{1 + Kc}\right) \quad (2.4)$$

The calculated saturation stoichiometry of the 38% TOPO-XAD7n resin is 1:3.5 (Eu:TOPO).

This indicates a mixture of 1:4 and 1:3 complexes in the solid phase.

Dynamic (Column) Experiments

Practical Dynamic Capacity

Determination of the practical dynamic capacity ($Q(m)$), the maximum mmol of analyte per gram of resin, was availed through Equation 2.5, where m is the mass of the solid, C_o is the initial concentration of analyte, V_o is the free volume of the column and $V(50\%)$ is the volume of solution eluted at 50% breakthrough. Under equilibrium conditions, the determined saturating

$$Q(m) = \frac{V(50) - V_o}{m_s} \cdot c_o \quad (2.5)$$

concentration of analyte in the solid phase should be within error for breakthrough curves ($Q(m)$) or isotherms (q_{max}). Table 2.2 has a summary of the q_{max} and $Q(m)$ values obtained for systems of interest.

Figure 2.5 shows the Eu^{3+} breakthrough curves for all materials examined. The saturating conditions are equivalent (i.e. $q_{max} = Q(m)$; within error) for the 58% TOPO-XAD7n and 38% TOPO-XAD7n isotherms and breakthrough curves. The solvation of TOPO in n-dodecane made the use of higher flow rates possible. A flow rate of 100 $\mu\text{L}/\text{min}$ was attempted for the 38% TOPO-XAD7n system. A higher flow rate led to a decrease in the practical dynamic capacity; indicating the system was no longer at equilibrium.

Using this information, flow rates for elution curves were determined to be at equilibrium when using a 50 $\mu\text{L}/\text{min}$ flow rate. Analyte elution was performed under various conditions and is shown in Figure 2.6. To assist in explaining the elution differences between the two solutions, a batch mode distribution study was performed monitoring Eu^{3+} uptake by the 38% TOPO-XAD7n resin as a function of nitric acid concentration for both resins not preequilibrated and preequilibrated with the appropriate nitric acid concentration (not shown).

To examine the ultimate remediation capabilities of the 38% TOPO-XAD7n resin for simulated Hanford waste, a simulated waste stream containing 1 mM K_2CrO_4 , tracer $^{152/154}\text{Eu}$, ^{233}U , ^{237}Np and ^{238}Pu , simultaneously, was loaded, the resin washed with 0.01 HNO_3 and 0.75 M $\text{Al}(\text{NO}_3)_3$, and material sequentially eluted with 3 M HNO_3 and 1 mM KBrO_3 to recover Eu, then 0.1 M HEDPA and 1 mM KBrO_3 to recover the actinides. The addition of potassium bromate insured the oxidation of Np and Pu to their hexavalent states in the absence of chromate. Figure 2.7 shows the semi-logarithmic elution curves obtained for the simulated waste experiment.

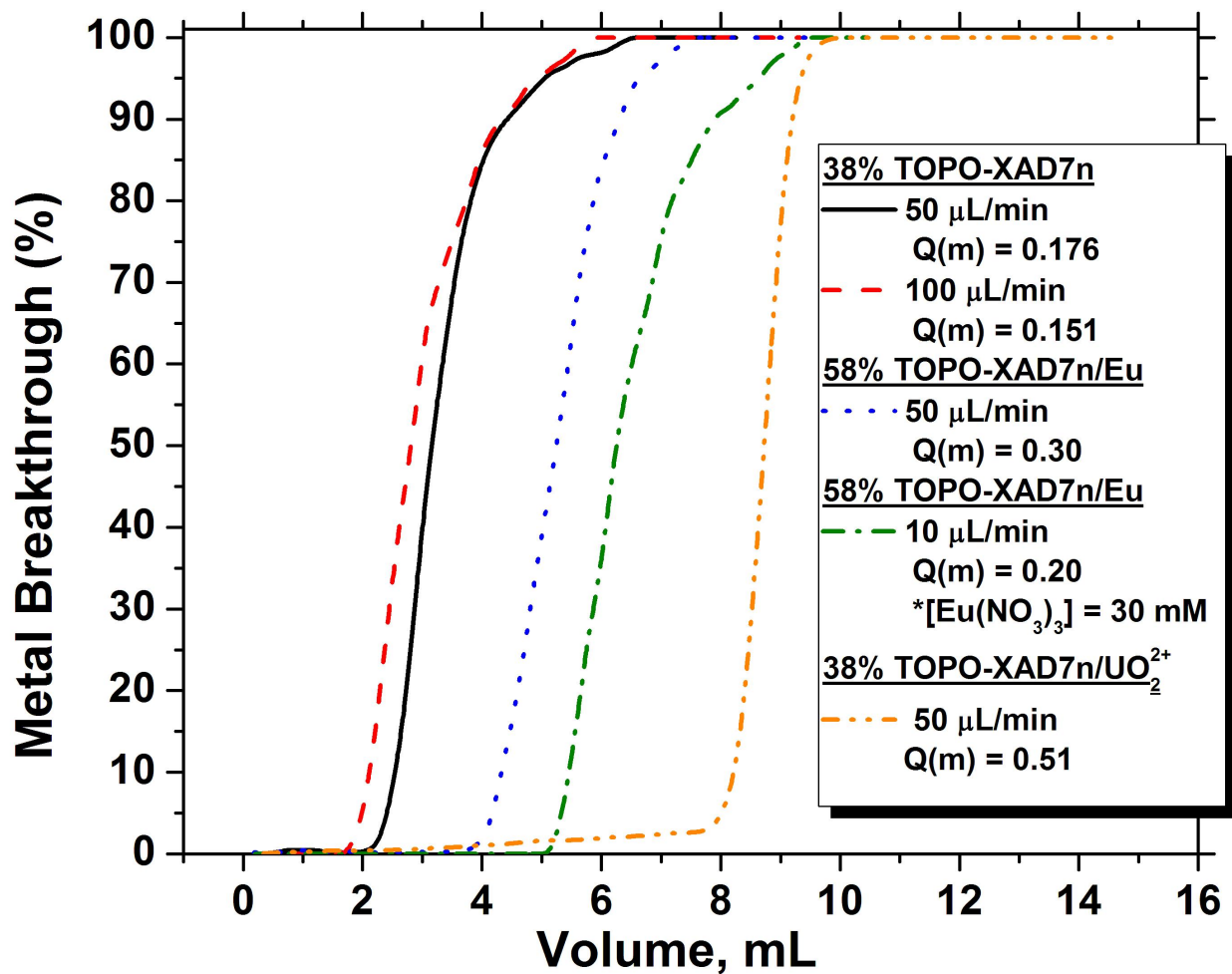


Figure 2.5. Breakthrough curves comparing the column saturation behaviors of europium by the 58% TOPO-XAD7n and 38% TOPO-XAD7n resin. Uranium behavior also shown for the 38% TOPO-XAD7n resin. Aqueous Phase: 0.1 M HNO_3 , 0.25 M $\text{Al}(\text{NO}_3)_3$, 1 mM K_2CrO_4 , 2 mM Ascorbic Acid. Concentration of metal 50 mM unless otherwise noted.

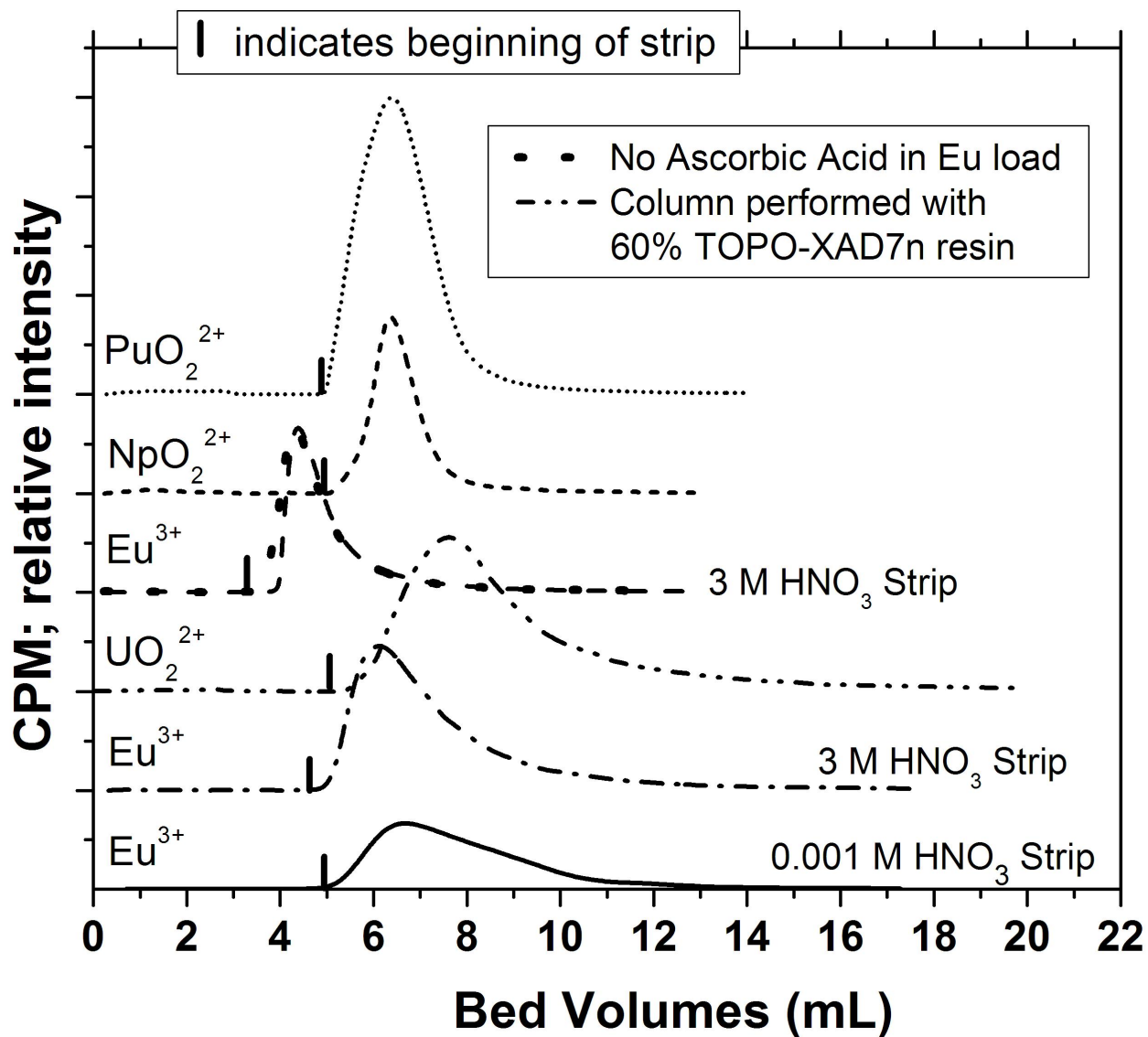


Figure 2.6. Elution curves showing the load and strip capabilities behaviors of Eu, U, Np and Pu by the 38% TOP-XAD7n resin. The loading aqueous phase for most europium studies included 0.1 M HNO₃, 0.25 M Al(NO₃)₃, 1 mM K₂CrO₄, 2 mM Ascorbic Acid unless noted. The load concentration of europium or uranium was 50 mM. Neptunium and plutonium studies were only performed at tracer conditions. The loading aqueous phase for all actinide studies contained 0.1 M HNO₃, 0.25 M Al(NO₃)₃, 1 mM K₂CrO₄. Europium strip conditions are indicated by their appropriate chromatogram. All actinide strips conditions included 0.1 M HDEPA and 1 mM K₂CrO₄. Exceptions to the general experimental parameters presented are noted within figure.

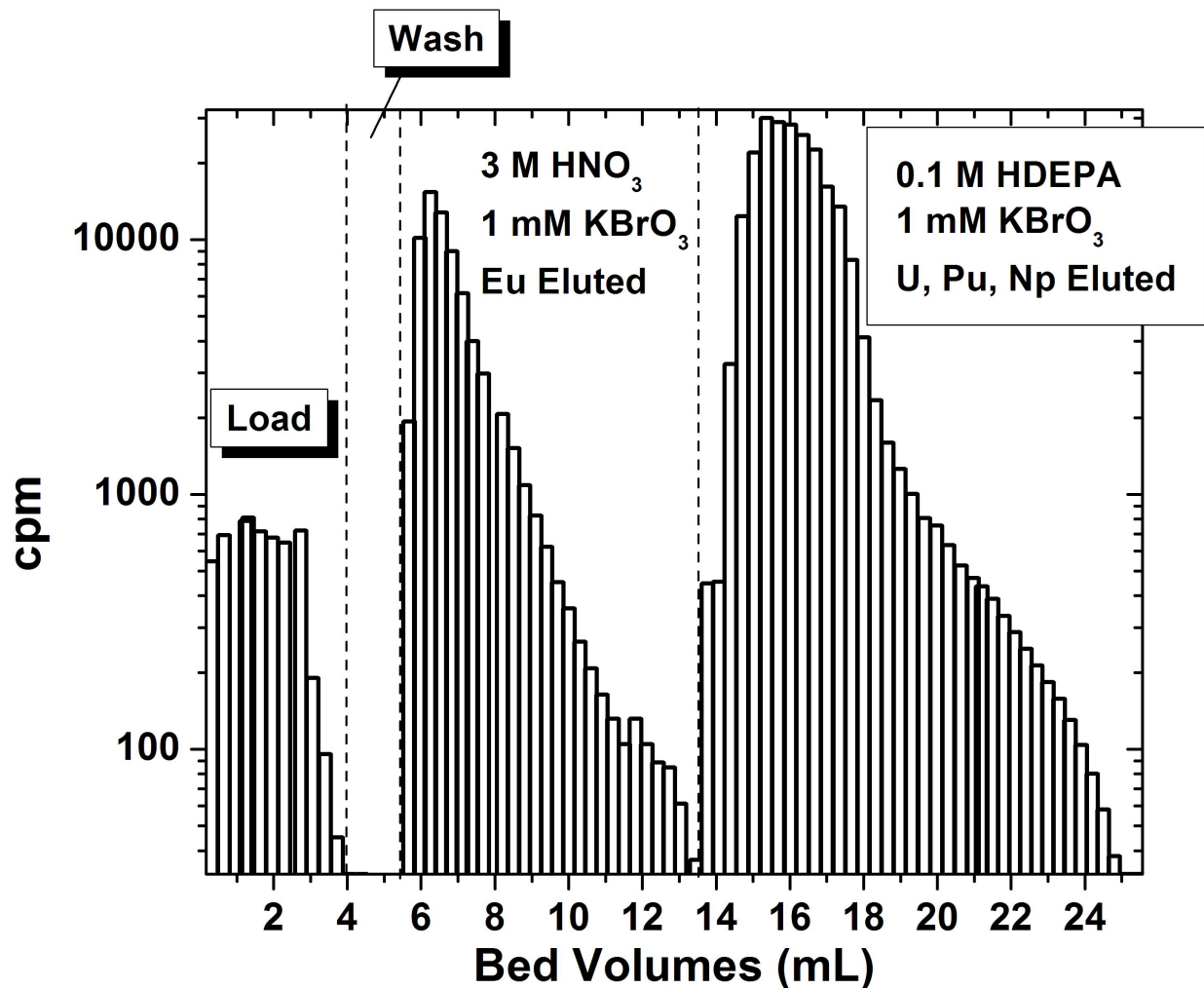


Figure 2.7. Loading and elution of U, Pu, Np and Eu by 38% TOPO-XAD7n column from simulated waste stream containing 1mM K_2CrO_4 , 0.1 M HNO_3 and 0.25 M $Al(NO_3)_3$ shown on a semi-log scale to allow viewing of column tailing. Elution of Eu was performed using 3 M HNO_3 and 1mM $KBrO_3$ to retain Np and Pu in the hexavalent state in the absence of chromate. Elution of actinides was performed using 0.1 M 1-hydroxyheptane-1,1-diphosphonic acid (HDEPA) and 1 mM $KBrO_3$.

Discussion

HNO₃ Partitioning

Nitric acid partitioning by TBP and TOPO is well established in the solvent extraction literature.^[18-23] Acid partitioning has not been investigated for extraction chromatographic TBP and TOPO systems and these studies were completed to provide further insight. Determination of the amount of nitric acid present in the organic solid phase allows for determination of unbound TBP or TOPO available for Eu³⁺ extraction. AnO₂²⁺ and An⁴⁺ extraction is thermodynamically favored over nitric acid extraction and therefore less affected by this particular competition.^[24] Several adduct extracted nitric acid species have been observed in the solvent extraction systems including: TBP/TOPO·HNO₃, TBP/TOPO·(HNO₃)₂, and TBP₂·HNO₃.^[18-23] The competition between HNO₃ and Eu³⁺ for extraction by TBP and TOPO warranted investigation as to the amount of HNO₃ extracted under various Al(NO₃)₃ conditions.

The comparable extraction of nitric acid by TBP and TOPO is noteworthy. Phosphine oxide type extractants are more basic than phosphate esters, thus improved extraction is typically seen. One possible explanation for the lack of additional HNO₃ extraction by TOPO is the presence of the (TOPO)₂·HNO₃ species. Thermodynamic modeling of the TBP·HNO₃ solvent extraction system has shown the (TBP)₂·HNO₃ species to be favored over the 1:1 species when there is an excess of extractant.^[13] Since the calculated concentration of TOPO in TOPO-XAD7 resin (1.33 M) is much larger than typically used in n-dodecane diluents (0.1 M)^[17], this could encourage the formation of a 2:1 extractant to acid species.

At 1 M HNO₃, the data converges to the calculated saturation line for the (TOPO)₂·HNO₃ for concentrations of Al(NO₃)₃ greater than 1 M. This observation, combined with the very low distribution of nitric acid displayed in Figure 2.1b, provides significant evidence for the (TOPO)₂·HNO₃ complex. The dashed line in Figure 2.1b indicates the moles of nitric acid that would saturate 100 mg of 58% TOPO-XAD7 (assuming the presence of the (TOPO)₂·HNO₃ species). The dotted line seen near the top of Figure 2.1b indicates the moles of nitric acid that would be required to saturate the resin in the presence of a 1:1 TOPO:HNO₃ species. A leveling of nitric acid uptake observed near the calculated saturation of the resin for the (TOPO)₂·HNO₃ species suggests the predominance of this species in the resin. This species has not been observed in the solvent extraction literature and this is most likely related to the relatively poor solubility of TOPO in unchlorinated organic diluents. In solvent extraction studies, the maximum concentration of TOPO in unchlorinated solvents is maintained a 0.1 M to minimize the potential for third phase formation.^[6,16,17] The analogous (TBP)₂·HNO₃ species is often the predominant form when the TBP and HNO₃ concentrations are approximately 1 M.^[19]

The initial objective of the HNO₃ extraction study was to determine values for the amount of free TOPO and TBP available for extraction of Eu³⁺. The varied organic species and their individual affect on Eu³⁺ extraction made a formal correction for the amount of free TBP and TOPO present currently incomplete and was not performed for Eu³⁺ extraction studies.

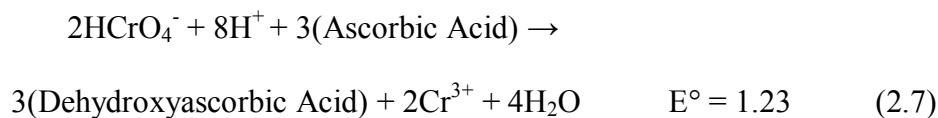
Europium Distribution

The availability of ^{152/154}Eu and comparable uptake behavior of europium to the lanthanides and the trivalent actinides for solvating organophosphorus extractants made this isotope an ideal

candidate to screen the potential of TBP and TOPO-XAD7 supports. For $^{152/154}\text{Eu}$ investigations, the aqueous phase conditions were similar to previous solvent extraction investigations, with concentrations of HNO_3 and $\text{Al}(\text{NO}_3)_3$ ranging from 0.01-1.50 M and 1 mM K_2CrO_4 was reduced to Cr^{3+} using 2 mM ascorbic acid.^[6,7,17] These conditions have been selected to represent a wide range of possible solutions that could be encountered during tank sludge leaching with HNO_3 solutions. For discussion purposes, “oxidizing conditions” or “reducing conditions” are defined as the inclusion of 1 mM K_2CrO_4 or 1 mM K_2CrO_4 /2 mM ascorbic acid in the aqueous phase, respectively. Chromate has been shown to be extracted by the organophosphorus ligands in this study, as shown in Equation 6.^[5,6] The overall reduction of chromium by ascorbic acid can be calculated using redox potentials listed in Table 2.4 and is shown in Equation 2.7 with the calculated reaction potential.

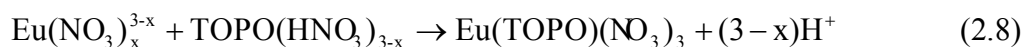
Table 2.4. Neptunium redox reaction significant to understanding simulated acidic aqueous raffinate of the Hanford tanks.^[27,35,40,41]

Reaction	E° (V)
$\text{NpO}_2^+ + 4\text{H}^+ + \text{e}^- \rightarrow \text{Np}^{4+} + 2\text{H}_2\text{O}$	0.567
$\text{NpO}_2^{2+} + \text{e}^- \rightarrow \text{NpO}_2^+$	1.236
$\text{NO}_3^- + 3\text{H}^+ + 2\text{e}^- \rightarrow \text{HNO}_2 + \text{H}_2\text{O}$	0.94
$\text{NpO}_2^{2+} + \text{HNO}_2 + \text{H}_2\text{O} \rightarrow \text{NpO}_2^+ + \text{NO}_3^- + 3\text{H}^+$	0.296
Dehydroascorbic Acid + $2\text{H}^+ + 2\text{e}^- \rightarrow$ Ascorbic Acid	0.390
$\text{HCrO}_4^- + 7\text{H}^+ + 3\text{e}^- \rightarrow \text{Cr}^{3+} + 4\text{H}_2\text{O}$	1.20



Increasing the concentration of nitric acid increased europium uptake by the TBP-XAD7 resin; however europium uptake was higher when the concentration of $\text{Al}(\text{NO}_3)_3$ was increased (Figure 2.2a and 2.2c). This was to some extent anticipated since the competition between HNO_3 is minimized at lower acid concentrations and a large excess of nitrate is available for formation of the neutral europium/TBP adduct. The steep increase in europium extraction as HNO_3 or $\text{Al}(\text{NO}_3)_3$ increases was observed in the solvent extraction system.

Europium extraction by the TOPO-XAD7 resin also increased as the concentration of $\text{Al}(\text{NO}_3)_3$ increased (Figure 2.2b). In contrast to the TBP-XAD7 resin, an increasing concentration of HNO_3 did not always increase metal extraction (Figure 2.2d). The slope of -1.6 observed on the logarithmic plot of Figure 2.2d could be generated by the presence of an ion exchange mechanism being utilized for Eu^{3+} uptake. This mechanism is shown in Equation 2.8, where $X \leq 2$. Cation exchange mechanisms occurring with an adduct forming extractant at high acid concentrations



have been suggested in the previous literature.^[25] To verify this as the case, the activity of the solution would need to be accounted for in the mixed electrolyte solution. In agreement with previous liquid-liquid studies, the results here indicate higher concentrations of $\text{Al}(\text{NO}_3)_3$ would be preferential to encourage decontamination of Al^{3+} leachates regardless the use of TBP or TOPO impregnated resins.

The extraction increase as the concentration of $\text{Al}(\text{NO}_3)_3$ increases can be related to the decline in the activity of water, allowing more effective release of the Eu^{3+} to the organic phase, i.e. Eu^{3+} is salted out of the aqueous phase. Corrected $D_{\text{W}_{\text{Eu}}}$ values shown in Figure 2.2d

decrease as the aqueous concentration of HNO_3 increases; in large part because of the increased association of the solvating extractants with HNO_3 in the resin phase.

A slope of three would be expected for the nitrate dependencies of the TBP and TOPO-XAD7 systems based on the requirement of charge neutrality for the extraction of Eu^{3+} . The TBP-XAD7 system shows slopes ranging from 1-5 when the acid concentration is held constant and the aluminum nitrate is varied, [Figure 2.2a](#). This changing slope could be attributed to a salting of TBP out of the aqueous phase and an increased concentration of TBP could lead to increased extraction. The maximal concentration of TBP in an aqueous phase is low at 0.42 g per liter.^[26] Increasing the concentration of HNO_3 has shown to have little impact on the solubility of TBP in water, but AgNO_3 has been shown to decrease the solubility of TBP by 31%.^[26] The impact of $\text{Al}(\text{NO}_3)_3$ could be larger given the salting out capabilities the Al^{3+} has historically shown.

The slope is more constant for the TOPO system, however, a lower NO_3^- dependency is observed than expected. The trends observed for both systems are comparable to previous solvent extraction investigations.^[6,17] The changes in slope are not attributable to a change in NO_3^- stoichiometry of the extracted complex, but rather several other possible effects such as change in nitrate ion activity at high $\text{Al}(\text{NO}_3)_3$ concentrations or Al^{3+} extraction.

Actinide Distribution Studies with TOPO-XAD7

The TOPO-XAD7 resin shows the most promise for tank remediation from the observable results of the Eu^{3+} extraction studies. Early Eu^{3+} uptake studies showed ample uptake of Eu^{3+} by 100 mg TOPO-XAD7 resin and warranted a decrease to 50 mg of TOPO impregnated resin.

Actinide extraction experiments dealt with the additional intricacy of redox chemistry. Therefore; studies regarding variable concentrations of $\text{Al}(\text{NO}_3)_3$ only were performed to allow a more thorough study of this additional variable.

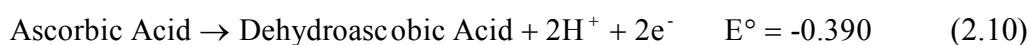
Neptunium and plutonium can be found in multiple oxidation states in acidic solution complicating the extraction process. To provide appropriate distribution data for each oxidation state, the uptake of stable oxidation state f-elements, UO_2^{2+} , Th^{4+} and Eu^{3+} , were studied to model which oxidation state of Np was dominant under the given conditions. The An^{4+} oxidation state is typically most extractable by TOPO and TRPO extractants with the AnO_2^{2+} oxidation state being a close second.^[16] AnO_2^+ species are generally poorly extracted by organophosphorus extractants.^[27] The ability of chromate to oxidize Np and Pu to the hexavalent state may offset the extraction competition encountered between the actinides/lanthanides and chromate. Plutonium is expected to be in the trivalent state^[28] in solutions containing ascorbic acid and in the hexavalent state for oxidizing conditions.^[29] Although predictions can be made, the redox speciation of Np in high ionic strength media and dilute nitric acid is relatively unknown. Uranium and neptunium extraction systems were investigated with no chromium present, 1 mM Cr(VI) and 2 mM ascorbic acid, and 1 mM Cr(VI) to provide the neutral, reducing and oxidizing conditions, respectively.

Expectedly, the presence of $\text{Al}(\text{NO}_3)_3$ had a similar “salting out” effect for both actinide and lanthanide uptake. Reactions in [Table 2.4](#) show the known list of governing equilibria for this system. An additional complication is that chromate and neptunium can be reduced and oxidized, respectively, by trace nitrate impurities.^[30-32]

Modeling of the system with UO_2^{2+} , Th^{4+} and Eu^{3+} shows the extraction preference for the TOPO-XAD7 system is $\text{An}^{4+} > \text{AnO}_2^{2+} > \text{An}^{3+}$ and AnO_2^+ is least preferred. This trend can be

directly related to the effective charge, Z_{eff} , which is 4, 3.3, 3 and 2.2 for An^{4+} , AnO_2^{2+} , An^{3+} and AnO_2^+ , respectively.^[33] The extraction trend demonstrates an electrostatic interaction in that the extraction of actinides with a greater charge density are preferred by a hard oxygen donor such as TOPO.

In general, the solutions without chromium exhibited the poorest uptake of Np which is indicative of the Np being present predominantly NpO_2^+ . At $[\text{HNO}_3] = 0.1 \text{ M}$, there is a slight separation between the uptake of Np in the systems with reducing and redox neutral conditions. These observed trends could be possibly explained by the several redox active entities in the aqueous phase. As the concentration of nitric acid increases, the reducing capabilities of ascorbic acid decrease, Equation 2.10.^[34] Therefore the ascorbic acid would be more capable of



completely reducing the chromate present and holding Np in pentavalent oxidation state (NpO_2^+).

Since ascorbic becomes less capable of reducing the chromate initially present in the system at higher nitric acid concentrations, the oxidation of Np at 1 M HNO_3 , even in the presence of ascorbic acid, becomes more possible. Pourbaix diagrams note the formation of Np(VI) is stable in higher concentrations of nitric acid.^[35] As shown in Table 2.4, the large excess of oxidizing nitrate provides a pathway for the oxidation of NpO_2^+ to NpO_2^{2+} .^[30,31] Np^{4+} does not appear to be present in any of the potential waste conditions as significantly higher uptake would be anticipated if Np^{4+} were present based on the uptake results of Th^{4+} .

The oxidizing conditions produce a slightly less convoluted picture regarding the Np redox speciation. Np extraction shows a consistent increase with D_w expressed as $0.01 \text{ M} < 0.1 \text{ M} < 1 \text{ M HNO}_3$. This is the general expectation for AnO_2^{2+} species. The Pourbaix predominance

diagram shows water stability can be an issue when generating Np(VI) at concentrations of HNO_3 less than 0.01 M.^[35] Water stability becomes less of an issue as the concentration of acid continues to increase. Nitric acid is also known to be oxidizing and an increase in nitric acid concentration could lead to more oxidizing conditions in the aqueous tank leachates. At 1 M HNO_3 and high $\text{Al}(\text{NO}_3)_3$ concentrations, the Np extraction aligns very well with the UO_2^{2+} extraction indicating a complete presence of NpO_2^{2+} . If a secondary cleanup is required of the Hanford sludges (and conditions are not oxidizing), a balance would be required to keep nitric acid concentrations sufficient enough to allow oxidation of Np while preventing competition between H^+ and An^{3+} or Ln^{3+} for the TOPO available in the system.

Uptake Kinetics

Uptake kinetics of Eu^{3+} and UO_2^{2+} were examined carefully as the trivalent and hexavalent oxidation states are of primary concern for remediation efforts, particularly if tank leachates are oxidizing. Both the concentration of analyte and the presence of n-dodecane added to a resin impregnated by a solid extractant can dramatically increase uptake kinetics.^[13] Both variables were examined in this study.

More time is required to obtain equilibrium as the Eu^{3+} concentration increases. The slower uptake kinetics observed at higher Eu^{3+} concentrations are most likely related to slower diffusion of Eu^{3+} into the impregnated XAD7 support. Preliminary column runs (not shown here) demonstrated the slow kinetics of the neat TOPO system were prohibitive for practical application. In light of these results, dissolving the part of the solid TOPO to the liquid form by wetting the resin with n-dodecane seemed a promising route to improve uptake kinetics. Neat

TOPO is a white solid. The rearrangement required for metal binding is energetically high when ligands are in their solid form. Wetting the resin with n-dodecane decreases the energetic barrier to rearrangement.

Comparison between 58% TOPO-XAD7 and 58% TOPO-XAD7n uptake of Eu^{3+} shows wetting the resin with n-dodecane significantly decreased the time required to reach equilibrium. Another improvement in uptake kinetics was observed when the TOPO impregnation percentage was decreased from 58% to 38%. The improvement in uptake behavior encouraged most of the following studies to be performed using 38% TOPO-XAD7n.

UO_2^{2+} was used as a model to determine AnO_2^{2+} sorption times. The uptake of 1 mM and 10 mM UO_2^{2+} are remarkably similar. Tracer concentrations of UO_2^{2+} ultimately provide a significant decrease in time required for the sorption of AnO_2^{2+} to the TOPO-XAD7n resin. UO_2^{2+} uptake was slower than Eu^{3+} uptake for the 38% TOPO-XAD7n resin. This could be related to the diffusion time required for the larger uranium molecule to migrate throughout the resin.

Static and Dynamic Capacity Determination

If a chromatographic remediation of Al^{3+} leachate solutions is to be performed, separations would be performed in a dynamic mode. Therefore, studies were performed to examine the dynamic capabilities of the TOPO-XAD7 for actinide decontamination. Isotherms and breakthrough curves allow determination of resin saturation for batch (static) and column (dynamic) modes, respectively. Saturation can be helpful in elucidating metal stoichiometry

when high concentrations of metal are present. Examining column behavior at heavy metal loading will show if the column maintains reasonable performance at higher load concentrations.

If analyte uptake is reaching equilibrium, the resin should behave comparably regardless the mode of operation. Comparable behavior allows validation of the values obtained for analyte uptake. The flow rate for the column experiments was dictated by the initial batch mode kinetic experiments (Table 2.3). A summary of parameters determined for both static and dynamic mode behavior is shown in Table 2.2. Overall, the 38% TOPO-XAD7n resin showed the excellent reproducibility between static and dynamic modes and also provided the best kinetics.

Static Extraction Capacity Determinations

Several assumptions are required for the Langmuir model to be valid: the surface of the adsorption must be uniform, the adsorbed molecules must not interact, all adsorption must occur through the same mechanism, and at maximum sorption only a monolayer can be formed.^[36] Given the ability for extractant and analyte to migrate through the pores of the polymer support, a monolayer would most certainly not be formed under saturating conditions. Figure 2.4 shows the Langmuir fit of the saturation isotherm is capable of providing a general description of europium and uranium uptake and the analyte concentrations that provide a saturated resin. Saturation conditions were observed for all 58% TOPO-XAD7 resins at concentrations of Eu^{3+} greater than 30 mM. For 38% TOPO-XAD7n resin, the saturating concentrations for Eu^{3+} and UO_2^{2+} were greater than 25 mM of metal. Knowing these concentrations ensures the column will be saturated for breakthrough curves and partitioning equilibria obtained from batch

experiments were not impacted by metal loading. To ensure saturation, breakthrough experiments later were performed with at least 30 mM Eu^{3+} or UO_2^{2+} .

The n-dodecane wetted material appears to show a slight decrease in the uptake of Eu^{3+} compared to the non-wetted material; however, this does not account for the decrease in weight percent of TOPO impregnated on the XAD7 resin after the wetting process. The 23% increase in weight of the 58% TOPO-XAD7 resin after wetting with n-dodecane actually produces a 46% TOPO-XAD7n resin. Using 50 mg of TOPO-XAD7 or TOPO-XAD7n resin provided 77 and 59 μmol TOPO in each experiment, respectively. This information, combined with the maximum amount of Eu sorbed (q_{max}), provides saturating stoichiometries (Eu:TOPO) of 1:5 and 1:4 for the 58% TOPO-XAD7 and 58% TOPO-XAD7n resins, respectively. This coincides with a more efficient usage of the n-dodecane wetted material.

Typical stoichiometries in solvent extraction systems have noted 1:3 Eu:TOPO extracted species^[37]; however, since the concentration of TOPO on the resin (>1 M) is an order of magnitude greater than typically used in solvent extraction systems, this excess of TOPO could lead to additional extractant molecules binding with Eu. Nitrates can be bound to a metal ion in a monodentate or bidentate fashion. Assuming the binding of three nitrates and bidentate behavior of the bound nitrates, this could lead to a coordination number of 10 for the extracted metal. Coordination numbers of 8-9 are typically observed with lanthanides in a solution matrix. Crystal structures have shown lanthanides to have coordination numbers as high as 12 in the solid state. Since the extraction chromatographic system represents a hybrid between the solution phase and a crystalline phase, a higher coordination number may not be unreasonable.

The information obtained through initial europium experiments narrowed uranium saturation investigations to only the 38% TOPO-XAD7n resin. Stoichiometries for Eu^{3+} and UO_2^{2+} using

the 38% TOPO-XAD7 resin were 1:3.5 for Eu:TOPO and 1:1 for UO_2 :TOPO complexes, respectively. The additional dissolution of TOPO appears to have aided in creating an environment similar to the solvent extraction system. The 1:1 stoichiometry of the UO_2^{2+} :TOPO complex was unanticipated. Typically a 1:2 stoichiometry is observed between uranium and TOPO in solvent extraction systems.^[38] However; the favorable excess of uranium may have forced a 1:1 complex.

Dynamic Extraction Capacity Determination

Figure 2.5 shows the breakthrough curves obtained for the TOPO-XAD7n resin with Eu^{3+} and UO_2^{2+} . As noted in the previous section, initial europium screening showed analyte uptake kinetics of the 38% TOPO-XAD7n where favorable compared to the 58% TOPO-XAD7n. Uranium behavior was just observed with the 38% TOPO-XAD7n resin. Given the unique data obtained regarding Eu:TOPO stoichiometries, the practical dynamic capacity, $Q(m)$, obtained from the breakthrough curves was particularly useful in validating the saturating values for Eu^{3+} for each of the n-dodecane wetted materials examined thus far. Table 2.2 notes the agreement between $Q(m)$ and q_{max} for the n-dodecane wetted materials.

Individual Analyte Elution Performance

The elution performance of Eu, U, Pu and Np was studied individually on TOPO-XAD7n resin and is shown in Figure 2.6. Specific aqueous phase conditions and concentrations of TOPO are noted within the figure. When examining europium performance on the 58% TOPO-

XAD7n resin, the elution peak obtained using an 0.001 M HNO₃ elution solution is significantly broad compared to the elution peak obtained using 3 M HNO₃. This could be related to the ongoing equilibration of the aqueous phase with the resin. The active displacement of Eu³⁺ by H⁺ encourages immediate elution. The elution of Eu³⁺ by 0.001 M HNO₃ occurs passively, as the Eu(NO₃)₃ extracted species slowly dissociates from the resin and into Eu³⁺ and 3NO₃⁻. To further examine the impact of preequilibration on metal uptake, batch studies were performed examining uptake from material both preequilibrated and not preequilibrated resin as a function of nitric acid concentration (not presented). Results show uptake of Eu³⁺ from by the 38% TOPO-XAD7 resin is less impacted by preequilibration as the concentration of nitric acid increases. This batch distribution study correlates with the elution observations.

The broad elution of Eu³⁺ from the 58% TOPO-XAD7n resin compared to the 38% TOPO-XAD7n resin is related to the slower kinetics of the 58% TOPO-XAD7n resin. The quick kinetics and sharp elution of the 38% TOPO-XAD7n resin made this material the primary focus for remediation of the Hanford site.

Studies also investigated europium uptake and elution in the presence of the extractable chromate ion potentially present in Hanford tank wastes. One remediation option is to leave oxidized chromium present as chromate. The extraction of chromate by TOPO could compete for extraction desired radioactive materials; however, chromate could help control the oxidation state of Np and Pu to the highly extractable AnO₂²⁺ cation. For these studies, no ascorbic acid was added. [Figure 2.6](#) shows no breakthrough of Eu³⁺ was observed during the load or wash steps of the elution curve and Eu³⁺ elutes in almost an identical fashion, regardless the oxidation state of the chromium. These initial results indicate when chromate is present, there may be a larger remediation benefit than disadvantage.

Actinide column behavior is also shown in [Figure 2.6](#). Macroscopic concentrations of uranium (30 mM) were used for loading to indicate the performance of the column when loaded with macro amounts of AnO_2^{2+} . Actinide elution was accomplished using 0.1 M HDEPA. During the loading process using the mixed aluminum nitrate/nitric acid/chromate solution, analyte breakthrough of 0.1 % was observed. No breakthrough was observed during the wash step at 0.01 M HNO_3 with 0.75 M $\text{Al}(\text{NO}_3)_3$. The stripping of uranium was immediate and quantitative. Similar experiments were performed using tracer amounts of ^{238}Pu and ^{237}Np . Potassium bromate was included in wash and elute steps to maintain Pu and Np in the AnO_2^{2+} state (in the absence of chromate). The breakthrough observed during the column loading for uranium was comparable for the plutonium and neptunium experiments. The elution of the tracer quantities of Np and Pu was sharper than the elution of the macroscopic uranium. The identical elution of the Np and Pu confirms the elution will be comparable for the AnO_2^{2+} cations, regardless of elemental composition.

Simulated Waste Stream Remediation

The simulated waste stream contained 0.1 M HNO_3 , 0.25 M $\text{Al}(\text{NO}_3)_3$, 1 mM K_2CrO_4 , 30 mM Eu and U, and tracer Pu and Np. The 0.1 % breakthrough observed during the loading step in the single, Pu, Np and U experiments and the lack of breakthrough during the wash step was also observed with the simulated waste stream. No evidence of Eu^{3+} breakthrough during the load step was observed using either gamma or liquid scintillation spectroscopy. Europium elution occurred without any detectable evidence for alpha activity observed using liquid scintillation detection. The elution of Eu^{3+} was quantitative within error. Removal of the

actinides was comparable to the single element experiments. The higher actinide loading for the simulated waste stream increased the column tailing, observed in the semi-log curve (Figure 2.7); however, recovery was still quantitative, within error.

Although the decontamination of the simulated Al^{3+} leachate waste stream using extraction chromatography is comparable to the decontamination obtained in solvent extraction investigations, throughput and column blockage can be drawbacks to the implementation of chromatography on a large scale. Extractant loss occurs in both liquid-liquid and extraction chromatographic methods. If the extractant were covalently bound to a polymer (instead of merely held in place by solubility preferences), chromatographic separations of nuclear fuel may become preferential. Several such resins are currently in development.^[43,44]

Conclusions

This investigation has addressed the concept of applying extraction chromatography methods to the task of decontaminating radioactive sludge leachate solutions that could result if acidic leaching procedures were adopted for the cleanup of recalcitrant, aluminum-containing tank waste sludge residues at the Hanford Site. The results presented indicate TOPO-XAD7 resin shows more desirable decontamination capabilities, especially regarding the uptake of trivalent f-elements, than the TBP-XAD7 resin. This was expected considering the increased basicity of the phosphoryl oxygen of the TOPO extractant compared to TBP. Quantitative removal of An/Ln^{3+} and AnO_2^{2+} from solutions containing HNO_3 , $\text{Al}(\text{NO}_3)_3$ and chromate when $[\text{NO}_3^-]_{\text{total}} > \sim 0.25$ M. The results for Eu^{3+} may be taken as generally characteristic of the behavior of the light lanthanides and trivalent actinide cations in a system of this type. Success was observed in

employing the potentially oxidizing conditions present in the Hanford tanks as chromium competition proved insubstantial, even when using macro concentrations of AnO_2^{2+} or Eu^{3+} . If conditions are not oxidizing, recovery of neptunium could prove problematic when the concentration of nitric acid is less than 1 M.

Behavior of TOPO-XAD7 in a column arrangement was improved by varying the concentration of the extractant on the support and wetting the impregnated support with n-dodecane. Isotherms and column experiments performed in this work allowed determination of maximum metal loading and stoichiometry under saturating conditions. The comparable stoichiometries obtained for static and dynamic modes of operation support separations performed by TOPO-XAD7n resins are reproducible and reaching equilibrium. Dynamic studies were performed to examine the performance of the TOPO-XAD7n resins as they would be used for remediation of Al^{3+} leachate solution. Recovery of Eu from the 38% TOPO-XAD7n resin was >99% using 3 M HNO_3 and 1 mM KBrO_3 to retain the actinides in the hexavalent state. Actinide recovery was also >99% using 100 mM etidronic acid and 1 mM KBrO_3 .

For extraction chromatography to be preferential over solvent extraction for the remediation of Al^{3+} leachate solutions, the chromatographic benefits would need amplification. Further studies could examine the use of stacked columns for a single elution that would separate Np, Pu and U sequentially, ultimately decreasing the overall cost of remediation. The minimization of extractant loss by using a covalently bound, solvating, organophosphorus resin could also reduce the cost of remediation.

References

- [1] Agnew, S.F. Hanford Defined Wastes: Chemical and Radionuclide Compositions. *LAUR-94-2657 Rev 2*, Los Alamos national Laboratory, Los Alamos, New Mexico.
- [2] DeMuth, S.F.; Thayer, G.R. An Updated Cost Study for Enhanced Sludge Washing of Radioactive Waste. *Remediation Spring*, **2002**, 87 – 97.
- [3] Vienna, J.D.; Hrma, P.; Crum, J.V.; Mika, M. Liquidus temperature-composition model for multi-component glasses in the Fe, Cr, Ni, and Mn spinel primary phase field. *J. Non-cryst. Sol.* **2001**, 292 (1-3), 1-24.
- [4] Bond, A.H.; Nash, K.L.; Gelis, A.V.; Sullivan, J.C.; Jensen, M.P.; Rao, L. Plutonium mobilization and matrix dissolution during experimental sludge washing of bismuth phosphate, Redox, and PUREX waste simulants. *Sep. Sci. Tech.* **2001**, 36 (5&6), 1241-1256.
- [5] Federov, Y.S.; Blazheva, I.V.; Zilberman, B.Y. Coextraction of Cr(VI) and U(VI) from nitric acid solutions with tributyl phosphate. *Radiochemistry.* **2000**, 42 (1), 69-73.
- [6] Harrington, R.C. *Separation of Hanford Tank Wastes by Liquid-Liquid Extraction Employing Organophosphorus Extractants*. M.S. Thesis, Washington State University: Pullman, 2006.
- [7] Harrington, R.C.; Martin, L.; Nash, K.L.; Partitioning of U(VI) and Eu(III) between acidic Al(NO₃)₃ and tributyl phosphate in n-dodecane. *Sep. Sci. Tech.* **2006**, 41 (10), 2283-2298.
- [8] Dietz, M.L.; Horwitz, E.P.; Bond, A.H. Extraction Chromatography: Progress and Opportunities, *Metal-ion Separation and Preconcentration*. Bond, A.H., Dietz, M.L., Rogers, R.D. Eds.; ACS Symposium Series 716, American Chemical Society, Washington, D.C., 1999, 234-250.
- [9] Horwitz, E.P.; McAlister, D.R.; Dietz, M.L. Extraction chromatography versus solvent extraction: How similar are they? *Sep. Sci. Tech.* **2006**, 41 (10), 2163-2182.
- [10] Yamaura, M.; Matsuda, H.T. Actinides and fission products extraction behavior in TBP/XAD7 chromatographic column. *J. Rad. Nucl. Chem.* **1997**, 224 (1-2), 83-87.

[11] Navarro, R.; Gallardo, V.; Saucedo, I.; Guibal, E. Extraction of Fe(III) from hydrochloric acid solutions using Amberlite XAD-7 resin impregnated with trioctylphosphine oxide (Cyanex 921). *Hydrometallurgy*. **2009**, *98* (3-4), 257-266.

[12] Martin, L.R. Actinide co-ordination chemistry and solvent extraction with phosphate and phosphine oxide ligands. Ph.D Thesis, The University of Manchester: U.K., 2003.

[13] Sulakova, J. Study of solid extractants for separation of minor actinides from high active liquid waste, Ph.D. Thesis, Czech Technical University: Prague, 179, 2007.

[14] Braun, T.; Ghersine, G. *Extraction Chromatography*. Elsevier Scientific Publishing Co.: New York, NY, 1975.

[15] Horwitz, E.P.; Bloomquist, C.A.A. The Preparation, Performance and Factors Affecting Band Spreading of High Efficiency Extraction Chromatographic Columns for Actinide Separations. *J. Inorg. Nucl. Chem.* **1972**, *34* (12), 3851-3871.

[16] Sushanta, S.K.; Reddy, M.L.P.; Romamohan, T.R.; Chakravorty, V. Solvent extraction of uranium(VI) and thorium(IV) from nitrate media by Cyanex 923. *Radiochim. Acta.* **2000**, *88* (1), 33-37.

[17] Braley, J.C.; Harrington, R.C.; Nash, K.L. Partitioning of U(VI) and Eu(III) between Acidic Aqueous $\text{Al}(\text{NO}_3)_3$ and Trioctylphosphine Oxide in *n*-Dodecane. *manuscript in preparation*

[18] Orekhov, V.T.; Minaev, V.A.; Federov, V.D. Extraction of nitric acid by various organophosphorus compounds in the presence of salting-out agents. *Zhurnal Neorganicheskoi Khimii.* **1968**, *13* (8), 2230-2233.

[19] Chaiko, D.J.; Vandegrift, G.F. A thermodynamic model of nitric acid extraction by tri-*n*-butyl phosphate. *Nucl. Technol.* **1988**, *82* (1), 52-59.

[20] Siddall, T.H. Thermodynamics for the extraction of uranyl nitrate and nitric acid by esters of the types $(\text{RO})_3\text{P}[\text{UNK}]\text{O}$ and $(\text{RO})_2\text{RP}[\text{UNK}]\text{O}$. *J. Am. Chem. Soc.* **1959**, *81* (16), 4176-4180.

[21] Niitsu, M.; Sekine, T. Solvent extraction equilibriums of acids. I. Extraction of nitric and perchloric acid with trioctylphosphine oxide. *J. Inorg. Nucl. Chem.* **1975**, *37* (4), 1054-1056.

- [22] Leene, H.R.; De Vries, G.; Brinkman, U.A.Th. Reversed-phase extraction chromatography using solutions of nitric acid as eluants. *J. Chromatography*. **1973**, *80* (2), 221-232.
- [23] Mikhailichenko, A.I. Extraction of inorganic acids by tri-n-octylphosphine oxide. *Radiokhimiya*. **1970**, *12* (4), 594-600.
- [24] Marcus, Y.; Kertes, A.S.; Yanir, E. *International Union of Pure and Applied Chemistry: Equilibrium Constants of Liquid-Liquid Distribution Reactions*, Part 1; Butterworths: London, U.K., 1973. p. 1-69.
- [25] Alexandratos, S.D.; Zhu, X. Bifunctional coordinating polymers: Auxiliary groups as a means of tuning the ionic affinity of immobilized phosphate ligands. *Macromolecules*. **2005**, *38* (14), 5981-5986.
- [26] Higgins, C.E.; Baldwin, W.H.; Soldano, B.A. Effects of electrolytes and temperature on the solubility of tributyl phosphate in water. *J. Phys. Chem.* **1959**, *63* (1), 113-118.
- [27] Tochiyama, O.; Nakamura, Y.; Hirota, M.; Inoue, Y. Kinetics of nitrous acid-catalyzed oxidation of neptunium in nitric acid-TBP extraction system. *J. Nucl. Sci. Tech.* **1995**, *32* (2), 118-124.
- [28] Poczvnajlo, A.; Janiszewski, Z.; Al-Shukrawi, H. The use of ascorbic acid for reductive separations of plutonium from uranium. *Nukleonika*. **1988**, *33* (7-9), 203-218.
- [29] Weigel, F.; Katz, J.J.; Seaborg, G.T. in *The Chemistry of the Actinide Elements, Second Edition, Vol. 1*, J.J. Katz, G.T. Seaborg and L.R. Morss, Eds. Chapman and Hall: London, U.K. 1986, p. 499.
- [30] Escure, H.; Gourisse, D.; Lucas, J. Dismutation du neptunium pentavalent en solution nitrique—I: Etudes a l'equilibre. *J. Inorg. Nucl. Chem.* **1971**, *33* (6), 1871-1876.
- [31] Ananiev, A.V.; Shilov, V.P.; Moisy, Ph.; Madic, C. Heterogenous catalytic oxidation of neptunium (IV) in nitric acid solutions. *Radiochimica Acta*. **2003**, *91* (9), 499-503.
- [32] Hsu, C-L.; Wang, S-L.; Tzou, Y-M. Photocatalytic presence of NO_3^- and Cl^- electrolytes as influenced by Fe(III). *Env. Sci. Tech.* **2007**, *41* (22), 7907-7914.

[33] Choppin, G.R.; Rao, L.F. Complexation of pentavalent and hexavalent actinides by fluoride. *Radiochimica Acta*. **1984**, *37* (3), 143-146.

[34] Ruiz, J.J.; Aldaz, A.; Dominguez, M. Mechanism of L-ascorbic acid oxidation and dehydro-L-ascorbic acid reduction on a mercury electrode. I. Acid medium. *Can. J. Chem.* **1977**, *55* (15), 2799-2806.

[35] Pourbaix, M.J.N. *Atlas of Electrochemical Equilibriums in Aqueous Solutions*, 2nd ed.; Natl. Assoc. Corrosion Eng.: Houston, TX, 1974.

[36] Strumm, W. *Chemistry of the Solid Water Interface: Processes at the Mineral Water and Particle Water Interface in Natural Systems*. John Wiley & Sons, Inc.: New York, NY, 1992.

[37] Foffart, J.; Duyckaerts, G. Extraction of lanthanides and actinides by alkylphosphine oxides. IV. Extraction of trivalent cations by tri-n-butylphosphine oxide or tri-n-octylphosphine oxide. *Analyt. Chim. Acta*, **1969**, *46* (1), 91-9.

[38] Watanabe, K. Extraction of thorium and uranium from chloride solutions by tributyl phosphate and tri-n-octylphosphine oxide. *J. Nuc. Sci. Tech.* **1964**, *1* (5), 155-62.

[39] Alexandratos, S.D.; Zhu, X. High-affinity ion-complexing polymer-supported reagent: Immobilized phosphate ligands and their affinity for the uranyl ion. *React. Polym.* **2007**, *67* (5), 375-382.

[40] Alexandratos, S.; Xiaoping, Z. Immobilized phosphate ligands with enhanced ion affinity through supported ligand synergistic interaction. *Sep. Sci. & Tech.* **2008**, *43* (6), 1296-1309.

[41] Burney, G.A.; Harbour, R.M. Radiochemistry of Neptunium. **1974**, *NAS-NS-3060* US Atomic Energy Commission.

[42] Harris, D.C. *Quantitative Chemical Analysis 3rd Ed.* W. H. Freeman and Company: New York, NY, 1991.

CHAPTER THREE

PREFACE

The success of the extraction chromatographic decontamination of Al leachates arising from remediation of the Hanford waste tanks led to creation of resins with covalently bound extractant groups. Covalently binding the reactive group to a polymeric support reduces extractant leaching to the aqueous phase. This sort of extractant loss can be problematic for both solvent extraction and extraction chromatographic separation methods. This work focused on evaluation of the actinide sorption properties of a polystyrene resin functionalized with neutral organophosphorus extractants covalently bonded to the backbone. These extractants are analogous to the tri-n-butyl phosphate extractant used for the decontamination of Al leachates in the Chapter 2. To encourage sufficient partitioning of the aqueous phase to a more hydrophobic resin, hydrophilic alcohol groups were placed in several of the developed resins. Some preliminary studies have been published examining uranium, lanthanide and transition metal uptake by the resins from nitric acid media. This chapter initially sought to expand these opening investigations with investigations examining transuranic metal partitioning from varied nitrate media.

The original plan quickly changed course as metal partitioning patterns indicated that the ethoxy groups of the organophosphorus extractant were hydrolyzing. Hydrolysis of phosphate esters leads to the formation of an acidic organophosphorus extractant, which would partition metals using a cation-exchange mechanism, was thought to be the product of the hydrolysis reaction. To confirm the presence of ion-exchange groups, several studies were performed. Iron generally has a higher affinity for cation-exchange materials than uranium. Examining uranium

uptake in the presence of iron at lower pH's did show some circumstantial evidence for the presence of ion exchange groups on the resin. Infra-red spectra of the resins, before and after acid contact, were obtained. Peaks were observed in areas consistent with phosphoric acid wags at $\sim 2300\text{ cm}^{-1}$; however, the asymmetric stretch of CO_2 is also present in this region (and spectra were taken in air). Since the IR was not purged with N_2 before spectra were obtained, the definitive observation of the phosphoryl wag was not possible.

Overall the results of the investigation were informative but disappointing. Currently, resins with malonamide covalently bound to a polystyrene support are showing comparable metal extraction patterns to known malonamide solvent extraction systems. Studies of this dissertation returned to extraction chromatography. A fundamental examination of TALSPEAK (Trivalent Actinide - Lanthanide Separation by Phosphorous reagent Extraction from Aqueous Komplexes) extraction chromatographic chemistry had yet to be performed in the literature. Chapter 4 examined this chemistry. An expansion of the typical TALSPEAK system was performed to include bis-2-ethyl(hexyl) phosphonic acid and triethylenetetraminehexaacetic acid.

CHAPTER THREE

INVESTIGATIONS INTO THE UPTAKE CAPABILITIES OF NOVEL PHOSPHATE BASED SOLVATING EXTRACTANT RESINS

Abstract

Characterization of three solvating organophosphate polystyrene resins functionalized with pentaerythritol triethoxylate (pPenta), tris(hydroxymethyl)amino methane (pTris), and mono-tris(hydroxymethyl)amino methane (pTris-Mono) has been completed. Infrared spectra, sodium hydroxide titrations and IR spectra performed initially after synthesis of these resins has demonstrated that the fresh resin has no cation exchanging groups. Lanthanide and actinide partitioning studies produce results that can be interpreted to indicate the presence of exchangeable protons on the resin. This communication describes the potential capabilities for the pPenta, pTris and pTris-Mono resins regarding a chromatographic PUREX process.

Introduction

The separation of a desired analyte from a bulk solution is commonly achieved through the use of two immiscible phases and the placement of a selective ligating agent in a preferred phase. Solvent extraction (SX) is a method used to separate analytes based on their relative solubilities in two immiscible *liquid* phases; this technique offers the possibility of high separation efficiency and requires only small energy differences. Chromatographic extraction, a typically less utilized technique compared to SX, can utilize the immiscible nature of organic solids and

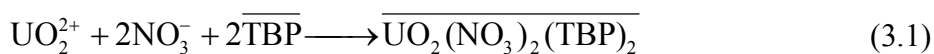
water solvents with the advantages of chromatography. One requirement for a viable separations process is a well established knowledge of chemical processes occurring within both phases. The abundant understanding of SX is attractive to engineers and scientists designing a process. For any process to be competitive with SX it must offer what SX cannot and, in addition, some improvements not typically achievable through conventional liquid-liquid extraction methods, such as, preconcentration, minimized possibilities of third phase formation, and avoiding the use of organic diluents.

A common complaint against SX is the large amount of organic waste resulting from the hydrolytic and radiolytic degradation of organic extractants and diluents.^[1-4] At the industrial scale, solvent extraction requires a multistage setup for extraction, stripping, and solvent washing. The multiple stages require individual instrumentation and equipment, ultimately producing additional contaminated material. A separations technique that uses minimal amounts of solvent and compact equipment offers some advantages for high level radioactive waste partitioning.^[5] Several so called “green” candidates are available to alleviate the use of organic diluents. These include, but are not limited to: ionic liquids^[6], liquid membranes^[7], and cloud point extraction.^[8,9] The feasibility and capabilities of these recently developed separation methods have been, and are still, under investigation globally.

An alternative to a diluent demanding SX process and some of these recently developed methods is chromatographic extraction (CX).^[10] Several variables still remain unknown regarding solid support separation methods. Nevertheless, chromatography has been scaled to industrial level use^[11,12] and has been studied for over a hundred years^[13], making CX an attractive option. Other benefits of CX are similar to SX, including simplicity in equipment and operation arising from continuous flow functionality. Unique to CX is the potential use of

extractants that may not dissolve readily in organic diluents that are practical for large scale SX processes and the ability to minimize extractant loss through covalently binding the extractant to the inert support. The preconcentration capabilities further increase the attractiveness of CX.^[5,14,15]

One of the most commonly used extractants in SX is tri-n-butyl phosphate (TBP, [Figure 3.1](#)). TBP is a neutral, organophosphorus extractant which extracts metals through a *solvation* mechanism. Solvating extractants require soluble anion(s) from the hydrophilic phase to neutralize the charge of the metal cation to allow partitioning into an organic phase. Since the solution anion plays a crucial role in extraction, increasing the concentration of the anion typically increases metal extraction. Equation 3.1 shows the extraction of Uranium by TBP with



NO_3^- as the solution anion. The overbar denotes a species is in the organic phase. Many solvating extractants, such as TBP, contain a phosphoryl oxygen (P=O) and metal interaction with the ligand primarily occurs through the oxygen of this functional group. The basicity of the phosphoryl oxygen increases as surrounding oxygens are removed, [Figure 3.2](#).^[16] The ability to fine tune the basicity of the phosphoryl oxygen adds to the attractiveness of these neutral extractants.

The PUREX (Plутonium URanium EXtraction) process is the de facto standard aqueous nuclear reprocessing method for the recovery of uranium and plutonium from used (irradiated) nuclear fuel. PUREX utilizes TBP to extract U and Pu from nitric acid solutions into an organic phase (kerosene). The compatibility with highly concentrated nitric acid solutions, minimum issues with third phase formation, and ready extraction of actinides with a Z_{eff} charge greater than 3.3 have allowed PUREX to remain the standard nuclear fuel reprocessing method since

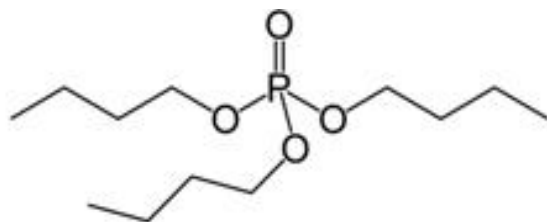


Figure 3.1. Structure of tri-n-butyl-phosphate (TBP).

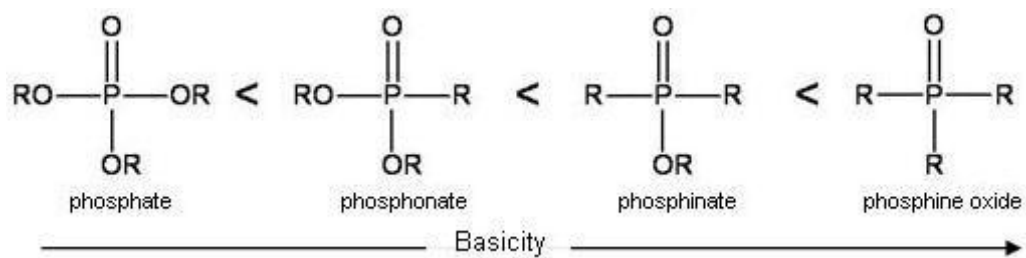


Figure 3.2. Diagram showing the affect of oxygen removal on the basicity of common types of neutral phosphorus functional groups.

1956. Actinides with a high Z_{eff} charge are particularly prone to hydrolysis and the compatibility of an organic extractant with concentrated nitric acid solutions can simplify reprocessing significantly.

The development of solid sorbents compatible with PUREX processing would have the potential to decrease the volume of these process radioactive waste streams. The group of Prof. Spiro Alexandratos at Hunter College, CUNY, has been developing neutral organophosphate resins that could be employed to perform a chromatographic PUREX process. Thus far, pentaerythritol triethoxylate (pPenta), tris(hydroxymethyl)amino methane (pTris), and mono-tris(hydroxymethyl)amino methane (pTris-Mono) functionalized resins, [Figure 3.3](#), have shown affinity for both divalent and trivalent transition metals, and trivalent and hexavalent lanthanides and actinides.^[17-20] The affinity for transition metals was unexpected, as the previous literature had shown neutral organophosphate extractants do not extract transition metals to a significant degree.^[21] Neutral, organophosphorus extractants frequently require purification to remove acidic impurities (organophosphorus acids).^[22]

Organophosphorus acids extract metal ions through a cation exchange process and require no assistance in neutralization of the metal ion since a discreet negative charge exists on the extractant. The pH of the aqueous phase can have a significant impact on extraction because many cation exchangers are acidic. If the aqueous phase pH is near or below the pK_a of the acid, H^+ competition for the binding site will become significant and a decrease in metal uptake will be observed. Metal extraction is expected to decrease as the acid concentration increases based on this H^+/M^{x+} binding site competition. Bis-2-ethyl(hexyl) phosphoric acid (HDEHP, [Figure 3.4](#)) is an example of a cation exchange extractant. The pK_a for HDEHP is approximately 3.47, depending on the organic diluent.^[23] Uranium extraction by HDEHP is shown in Equation 3.2.

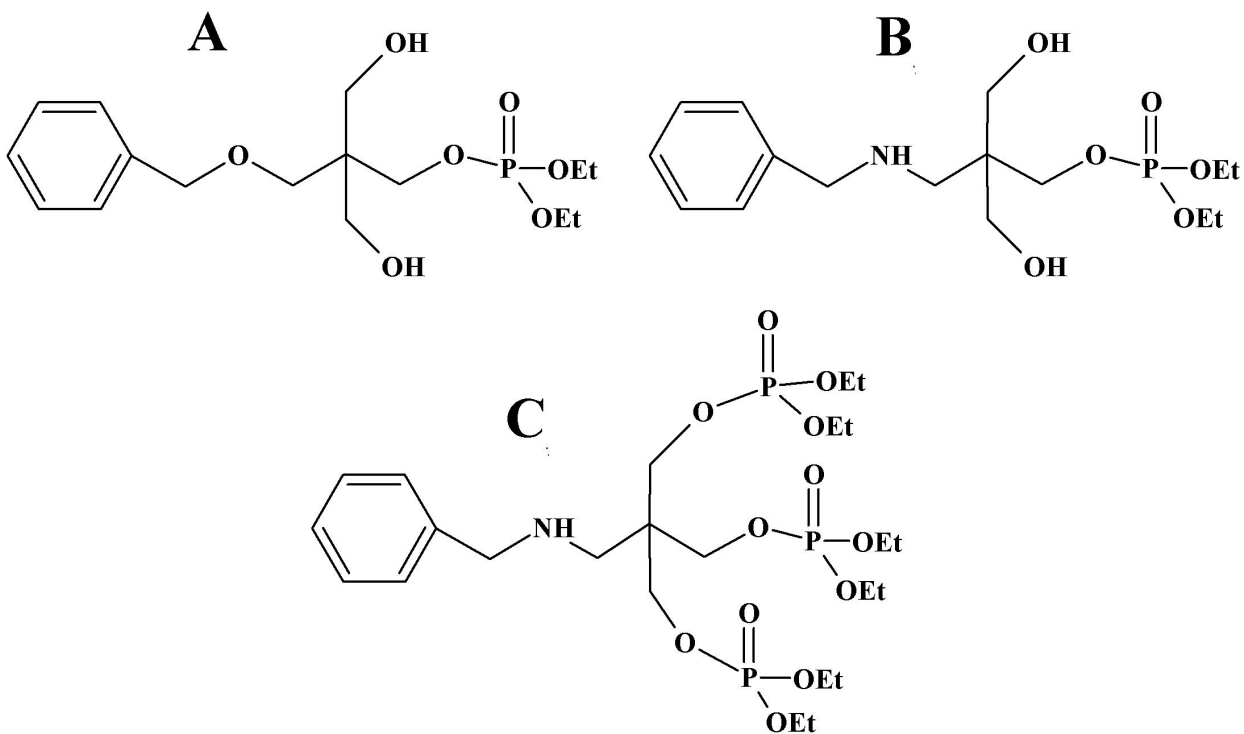


Figure 3.3. Structures of immobilized: a) pentaerythritol triethoxylate (**pPenta**) b) tris (hydroxymethyl)amino methane (**pTris**) c) mono-tris(hydroxymethyl)amino methane (**pTris-Mono**)

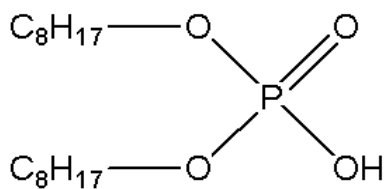


Figure 3.4. Structure of bis-2-ethylhexyl phosphoric acid.



Note should be made HDEHP generally exists as a dimer in SX systems and this may not be the case for a phosphoric acid functional group bound to a resin. Association of H^+ with the negatively charged extractant group at $\text{pH} < 3$ will begin to cause a dramatic decrease in metal uptake.

The difference in phase transfer reactions between neutral and cation exchange extractants has opposite effects on metal ion uptake between the two materials. For a neutral extractant, increasing acid concentration increases the amount of solution anion and an increase in metal partitioning is observed. For an acidic extractant, the proton (H^+) successfully competes for the extraction site and a decrease in metal extraction is observed as the nitric acid concentration increases.

This communication contains the results of actinide and lanthanide interactions between pPenta, pTris and pTris-Mono resins from various aqueous media. Since solvating phosphate materials have the potential to undergo acidic degradation to a cation exchange material, a combination of metal partitioning patterns and infrared spectroscopy will aid in describing their chemical state of the resin. Metal partitioning patterns will be particularly helpful in monitoring possible resin decomposition since very low concentrations ($\leq 10^{-4}$ M) are used relative to the amount of functionalized material present.

Experimental

Materials

All aqueous solutions were prepared from analytical grade reagents and ultra pure (18 M Ω) H₂O. All resins obtained from Dr. Alexandratos were in vials, sealed with parafilm and stored in a refrigerator when not being used for experiments. The synthesis and characterization of these materials has been described in previous publications.^[17-20] A density determination was performed of all solutions using a calibrated 1 mL pipette and weighing 1 mL of each solution at room temperature. All solutions were prepared by mass. Solutions of HNO₃, HCl and etidronic acid (1-hydroxyethane-1,1-diphosphonic acid - HEDPA) were prepared using Fischer Scientific concentrated (15.8 M) HNO₃, Fischer Scientific concentrated (12 M) HCl and Sigma Aldrich etidronic acid (60% w/w), respectively. Sodium hydroxide solutions were prepared from dilutions of 50% w/w NaOH (Alfa Aesar) and standardized by titration with potassium hydrogen phthalate to a phenolphthalein end point. Sodium hydroxide solutions were used for analysis of HNO₃ solutions used in extraction studies. Zirconium chloride (ZrCl₄) and Eu(NO₃)₃•(H₂O)₆ were Alfa Aesar Reactor grade reagents. Ferric nitrate (Fe(NO₃)₃•(H₂O)₉) and Na₂CO₃ were analytical reagent grade EMD and Mallinckrodt, respectively. Phenylphosphonic and phenylphosphoric acids were Alfa Aesar Reagent Grade. Experiments using ²³³UO₂(NO₃)₂, ²³⁸UO₂(NO₃)₂, and ²³²Th(NO₃)₄ were prepared by dilution of standardized stocks from the Washington State University (WSU) inventory. More emphasis was eventually based upon the characterization of the p-Tris resin as this material has shown the highest cation uptake capacities of the three resins examined and more pTris sample resin was provided relative to the other pPenta and pTris-Mono resins.

Instrumentation

Radiotracer experiments using ^{233}U were analyzed with a Beckman LS6500 liquid scintillation counter for alpha detection and 5 mL of EcoScint® scintillation fluid. Heavy metal analysis (^{238}U) was done using an Agilent 4500+ ICP-MS. For mixing times greater than 30 minutes, a carousel mixer was employed. Shorter mixing times utilized a VWR mini vortexer. All mass measurements were obtained using a Mettler Toledo XS105 Dual Range series analytical balance. Pipetting was accomplished using Finnpiquette adjustable volume micropipettes and tips. Fourier transform infrared spectra were obtained using a Thermo® Nicolet 6700 spectrometer.

Batch Extractions

All batch extractions were performed in triplicate and the errors presented are for a $\pm 1\sigma$ standard deviation of the triplicate analysis. The weight distribution ratio, D_w ($\text{mL}\cdot\text{g}^{-1}$), was calculated for most experiments according to Equation 3.3:

$$D_w = [(A_0 - A_s)/w]/(A_s/V) \quad (3.3)$$

where A_0 and A_s are the aqueous phase activity (counts per minute) before and after equilibration, w the weight of resin (g) and V the volume of the aqueous phase (mL). Most uranium distribution values have been corrected for nitrate complexation in the aqueous phase^[8], Reaction 3.4. The



Corrected distribution values are annotated as D_{w_0} . Triplicate experiments showed the reproducibility of the distribution measurements was generally within 10%, although the uncertainty interval was somewhat higher for the highest distribution values ($D_w \geq 10^3$).

Studies involving ^{238}U

To extend the availability of the pPenta, pTris and pTris-Mono samples provided, both the aqueous volume, 1 mL, and the resin equivalents, 0.05 meq, were dropped by two orders of magnitude relative to the studies performed in Dr. Alexandratos's lab.^[19,20] All other aspects including pre-equilibration times (15 minutes), the number of pre-equilibration contacts (three), the amount of time required for contacts (18 hours) and the concentration of $\text{UO}_2(\text{NO}_3)_3$ (10^{-4} M) were identical to those used previously. For studies also including Th^{4+} and Eu^{3+} , the concentration of each was 10^{-4} M. This made the total metal concentration 3×10^{-4} M and the total M:P loading 0.6%. Investigations involving the effects of NaNO_3 in the aqueous phase had 0.01 M HNO_3 in the aqueous phase to prevent uranium hydrolysis, which can become significant at $\text{pH} \geq 3$.^[24]

Evaluation of acidic impurities for the pTris and pPenta resins

Fresh samples of 0.200 g pPenta and 0.100 g pTris resins were contacted with 2 mL of 18 M Ω DI H_2O to evaluate the release of hydrogen ions (H^+) from fresh resin samples. A quantitative study was performed involving multiple contacts between fresh samples of DI H_2O (1 mL) with 100 mg of pTris resin. Five contacts were made. No further acid release was observed after three contacts. Water contacts were performed for five and ten minutes with no apparent change in the amount of acid produced. The water from individual contacts was titrated separately with 0.01 M NaOH to a phenolphthalein end point.

Studies involving ^{233}U

Uranium-233 became available for use at WSU midway through resin characterization. Studies that started with natural uranium and ICP-MS analysis continued with ^{233}U and radioanalytical methods of quantitation. The use of ^{233}U allowed several experimental benefits;

- A decrease in uranium concentration and therefore a decrease in the total resin required for distribution studies
- Simplified analysis of the aqueous phase
- Improved error analysis

Studies using ^{233}U were done with pTris exclusively. Extractions were generally performed with 0.5 mL aqueous volume, 0.025 meq pTris (6 mg) and 25 minute contact times unless otherwise noted.

Kinetics Investigation

Tracer concentrations of ^{233}U expedited uptake kinetics since chromatographic exchange kinetics are largely diffusion based.^[25] Oftentimes decreasing the concentration of analyte can accelerate the extraction. Kinetic studies involved varying contact times from 1 to 30 minutes. Previous studies performed by Dr. Alexandratos showed uranium uptake kinetics of the pPenta resin slowed as the concentration of nitric acid increased.^[19] To maximize sample availability, the kinetics investigation was isolated to 1 M HNO_3 as uptake kinetics for lower concentrations of acid was deemed more rapid by previous investigations. Aliquots of 400 μL were obtained of the aqueous phase and analyzed.

Carbonate media investigation

When the hydrolysis of phosphate esters seemed evident, the uptake behavior of carbonate media was examined. The literature has shown phosphates to have a maximum of stability around a pH of 8 and the expectation was ester hydrolysis could be minimized if extractions were performed around this pH.^[26] The pH of the aqueous phase was obtained before contact with the resin and after the uranium sorption to the resin using pH paper. The concentration of Na_2CO_3 was varied between 0.01 and 1 M. Aliquots of the aqueous phase (400 μL) were analyzed.

Minimization of ion exchange by metal preequilibration

To minimize the impact a potential cation exchanging group may have on extraction trends, pre-equilibrations with zirconium and iron were performed before examining the nitric acid dependence of uranium uptake. It was intended that these cations would be strongly absorbed by any existing cation exchange sites on the resin, thus allowing solvating functional groups to interact with the metal salts. Aliquots of the aqueous phase (300 μL) were counted via liquid scintillation. To prevent metal hydrolysis, Zr^{4+} and Fe^{3+} were in 1 M and 0.1 M HNO_3 , respectively. Hydrolysis for Zr^{4+} and Fe^{3+} of these species can become significant at $\text{pH} \geq 1$ and $\text{pH} \geq 2$, respectively.^[24]

Zirconium concentrations were investigated at 10, 2.5 and 0.5 mM using 0.8 mL of zirconium containing aqueous solution in one contact with 0.05 meq (12 mg) of pTris resin. The amount of pTris was increased to improve error analysis since Zr pre-equilibrations decreased the distribution of uranium to the resin phase. Iron concentrations were varied from 0.5 mM to 1

μM using 0.4 mL of iron solution in one contact with 0.025 meq of pTris resin. The aqueous phase volume for uranium distribution was 0.5 mL.

Resin reproducibility investigations

Due to acid hydrolysis concerns, a series of experiments investigating the reproducibility of the pTris resin by using repeat extraction methodology. To recondition the resins between extractions, three washes (5 minutes each) were performed with DI H₂O to obtain a neutral wash, one 25 minute contact was performed with 0.1 M etidronic acid (HEDPA) for uranium removal, followed by 2 washes (5 minutes each) with DI H₂O to obtain a neutral wash. Aliquots of 300 μL of the aqueous phase were analyzed radiometrically.

Infrared Characterization of pTris

All spectra were obtained between 400 and 4000 cm^{-1} using 200 scans and resolution of either 16 cm^{-1} or 32 cm^{-1} . Resins were ground using a mortar and pestle prior to obtaining spectra. The effect of hydration on resin swelling on produced spectra was examined by initially wetting the resin, followed by oven drying for three hours, then wetting the resin again. Spectra were obtained after both wetting periods and after drying in the oven. The IR signature of the pTris resin was monitored over several months. A separate experiment examined the affects of 1, 2 and 4 M HCl in contact with pTris for 38 days.

Results

U(VI) Uptake by pPenta, pTris, and pTris-Mono Resins as a Function of [HNO₃]

The initial studies (at WSU) of the resins provided by Dr. Alexandratos focused on reproducing ²³⁸UO₂²⁺ uptake results by the pPenta resin and determining ²³⁸UO₂²⁺ uptake capabilities by the pTris and pTris-Mono resins as a function of nitric acid concentration (Figure 3.5).^[17] The present pPenta results agree very well with that published previously. For the pPenta and pTris resins, high uranium uptake is observed at low acid concentrations and UO₂²⁺ uptake decreases as the [HNO₃] increases. For the pTris-Mono, UO₂²⁺ uptake displays an opposite trend where better uptake is observed with high acid concentrations and less uptake is observed at lower acid concentrations.

Extraction of U(VI) as a Function of HNO₃ or NaNO₃ in the Presence of Th(IV) and Eu(III)

To probe the effects of a salting agent on metal partitioning, sodium nitrate was introduced into the aqueous phase and the concentration was varied. Thorium and europium (1×10^{-4} M each) were included in part to minimize any potential interaction with cation exchange impurities. The presence of these heavy metals on ²³⁸UO₂²⁺ uptake was examined for all three resins by varying NaNO₃ or HNO₃ concentration (Figure 3.6). At the higher concentrations of nitrate, metal distribution from a sodium nitrate aqueous phase is higher than from a nitric acid aqueous phase. Metal partitioning is very similar, regardless the aqueous media, when nitrate concentrations are low.

Determination of Acidic Impurities in the pPenta and pTris Resins

Figure 3.7a shows the change in pH of the aqueous phase in contact with the resins as a function of time. The dramatic change in pH noted on successive contacts prompted a study intended to quantify the amount of exchangeable H^+ present in the pTris resin, Figure 3.7b. Five

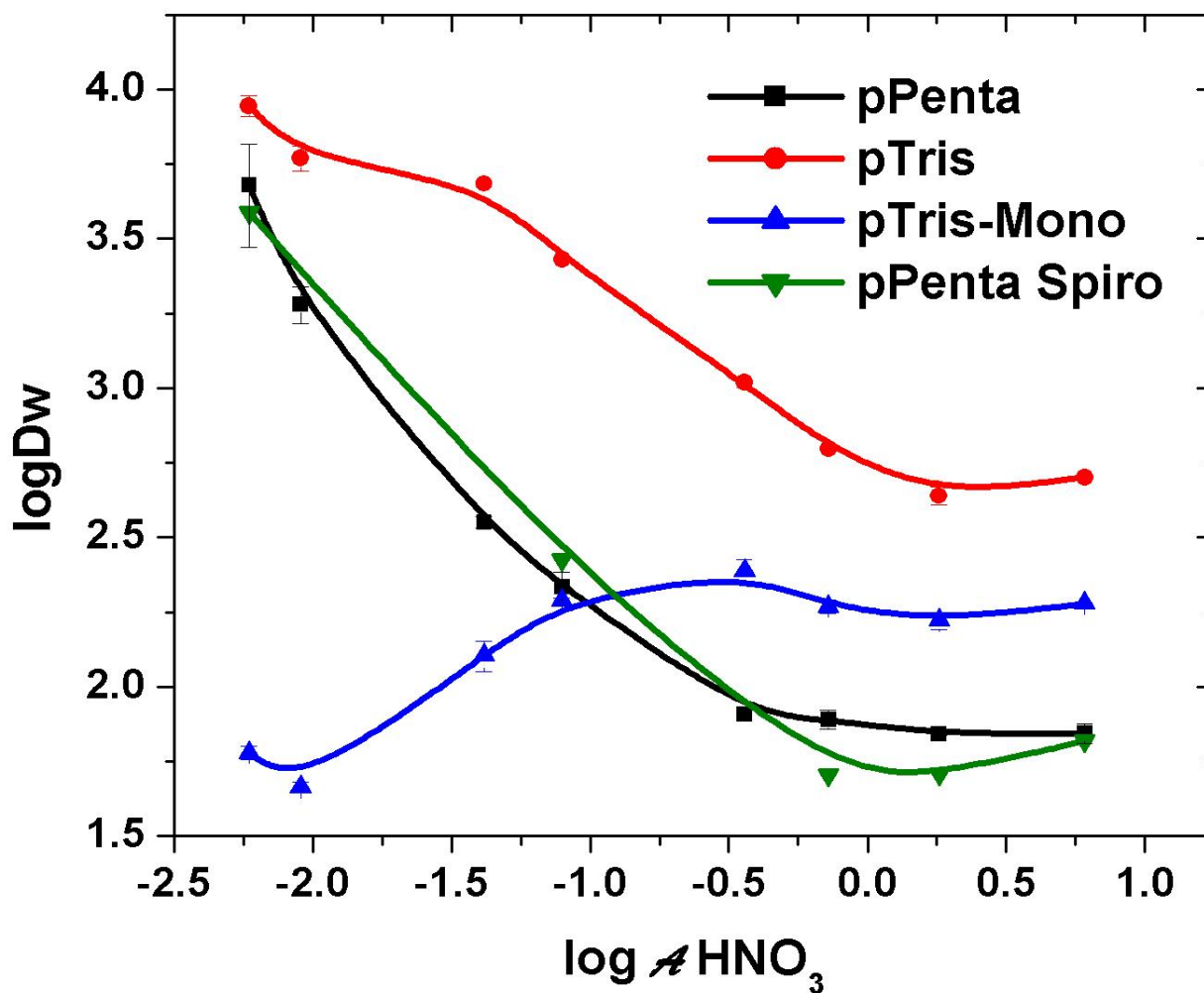


Figure 3.5. Extraction of UO_2^{2+} as a function of the activity of nitric acid from $6.4 \times 10^{-3} \text{ M}$ to 4 M HNO_3 . The \blacktriangledown indicates the UO_2^{2+} extraction reported in Dr. Alexandratos's lab.^[19]

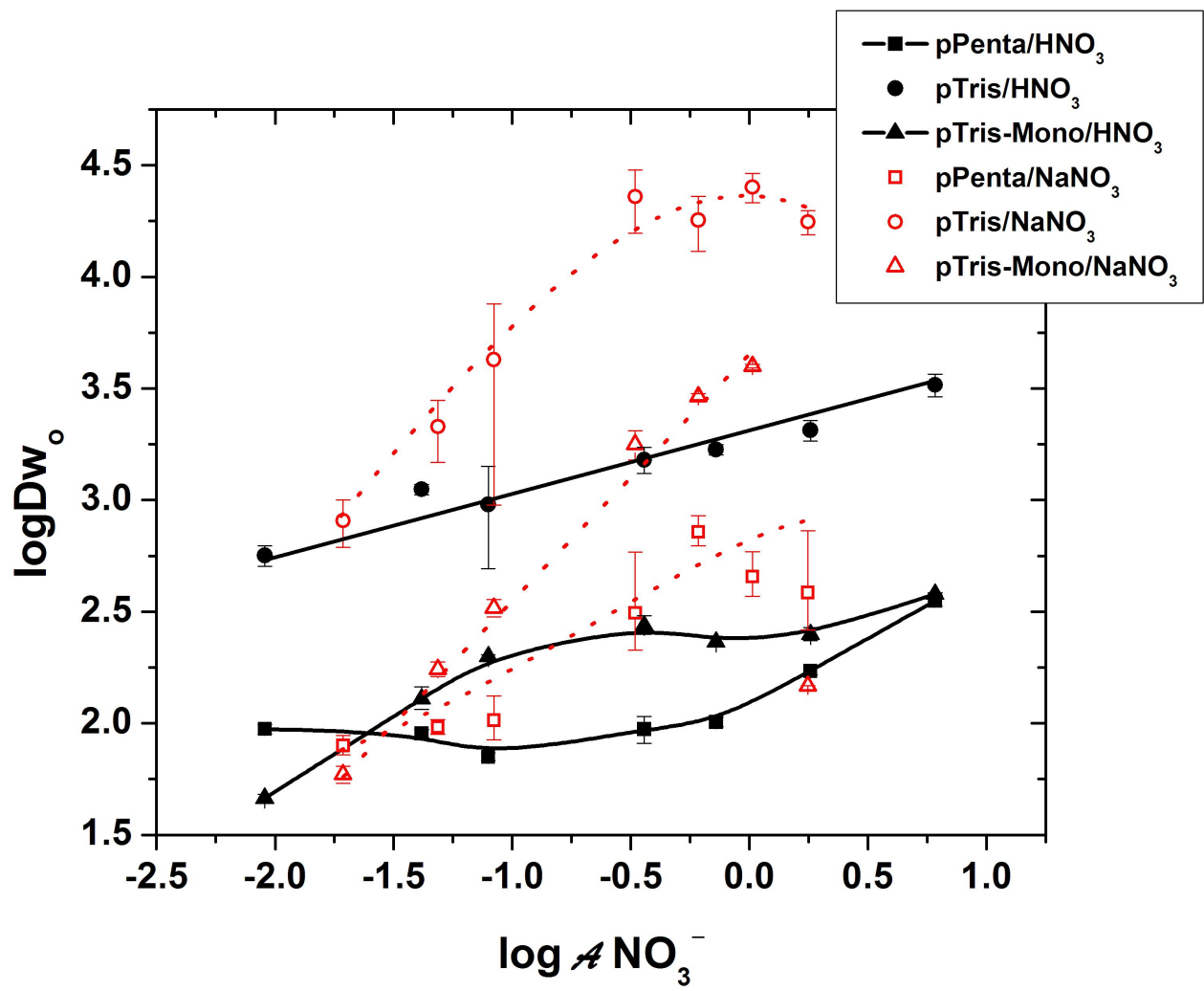


Figure 3.6. Comparison of the extraction of UO_2^{2+} as a function of the activity of nitric acid or sodium nitrate with 0.01 M HNO_3 from 6.4×10^{-3} M to 4 M $HNO_3/NaNO_3$. Europium and thorium are present at 10^{-4} M. The corrected weight distribution ratio, Dw_o , accounts for the presence of $UO_2(NO_3)^+$ in the aqueous phase. Each resin has 0.05 meq of material present.

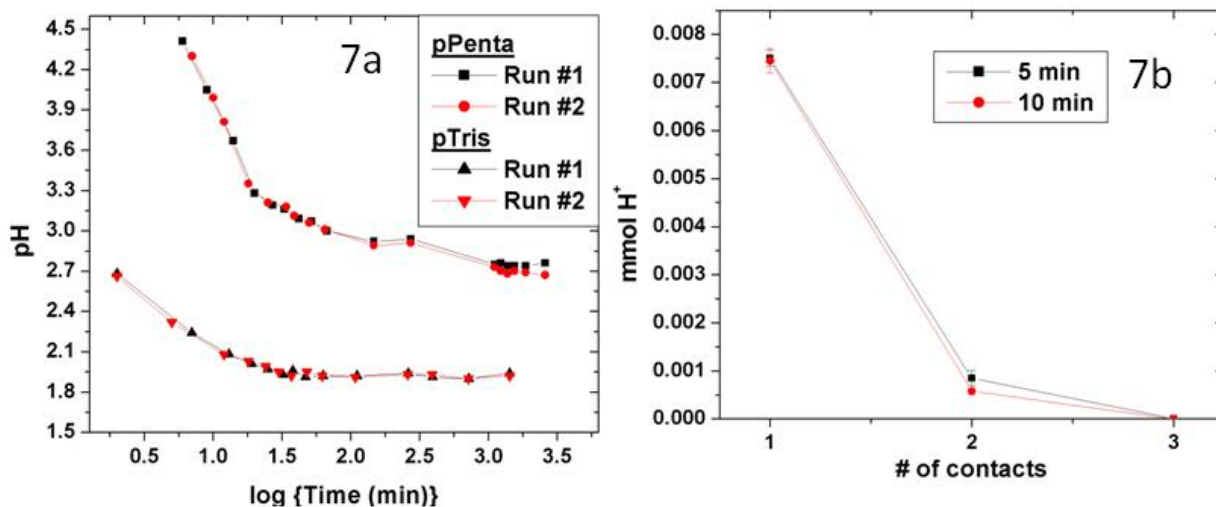


Figure 3.7a. Change pH of DI H₂O observed contact with 200 mg and 100 mg of pPenta and pTris, respectively. **Figure 3.7b.** Titration study showing the mmol of H⁺ released per contact with 1 mL DI H₂O for the pTris resin. Legend indicates the length of time allowed per DI H₂O contact with pTris.

contacts were made. [Figure 3.7b](#) shows three contacts were sufficient to remove all H^+ ; no further acid release was observed after three contacts. The summed release of H^+ indicates a 16% impurity based on the moles of H^+ released relative to the moles of phosphorus provided from pTris sample (remembering that every pTris functional group actually provides three equivalents of phosphorus).

Investigation into Acid Promoted Hydrolysis of the Solvating Extraction Resins

Concerns of acid promoted hydrolysis prompted a study investigating the affects of acid pre-equilibration with the resin before uranium sorption. [Figure 3.8](#) shows a comparison between resins pre-equilibrated three times at the appropriate HNO_3 concentration before ^{238}U contact and resins not pre-equilibrated before ^{238}U contact. Uranium uptake drops by an order of magnitude at all acid concentrations examined when the pTris-Mono resin is used. The pPenta and pTris resins show the same uptake at low acid concentrations regardless the condition of the resin. At acid concentrations greater than 0.5 M, uranium uptake displays the same order of magnitude drop observed for the pTris-Mono after preequilibration of the pPenta and pTris resins.

Uranium Kinetic Studies

[Figure 3.9](#) compares the uptake kinetics of pTris at the tracer level with previous experiments performed by Dr. Alexandratos' lab at $1 \times 10^{-4} \text{ M } ^{238}UO_2(NO_3)_2$ using the pPenta resin.^[19] Studies show the uptake is within error after 20 minutes and for later studies 25 minutes

was used to ensure equilibrium. This was a substantial decrease from previous kinetic studies where 17 hours were required for equilibration. The improvement in kinetics was expected. The

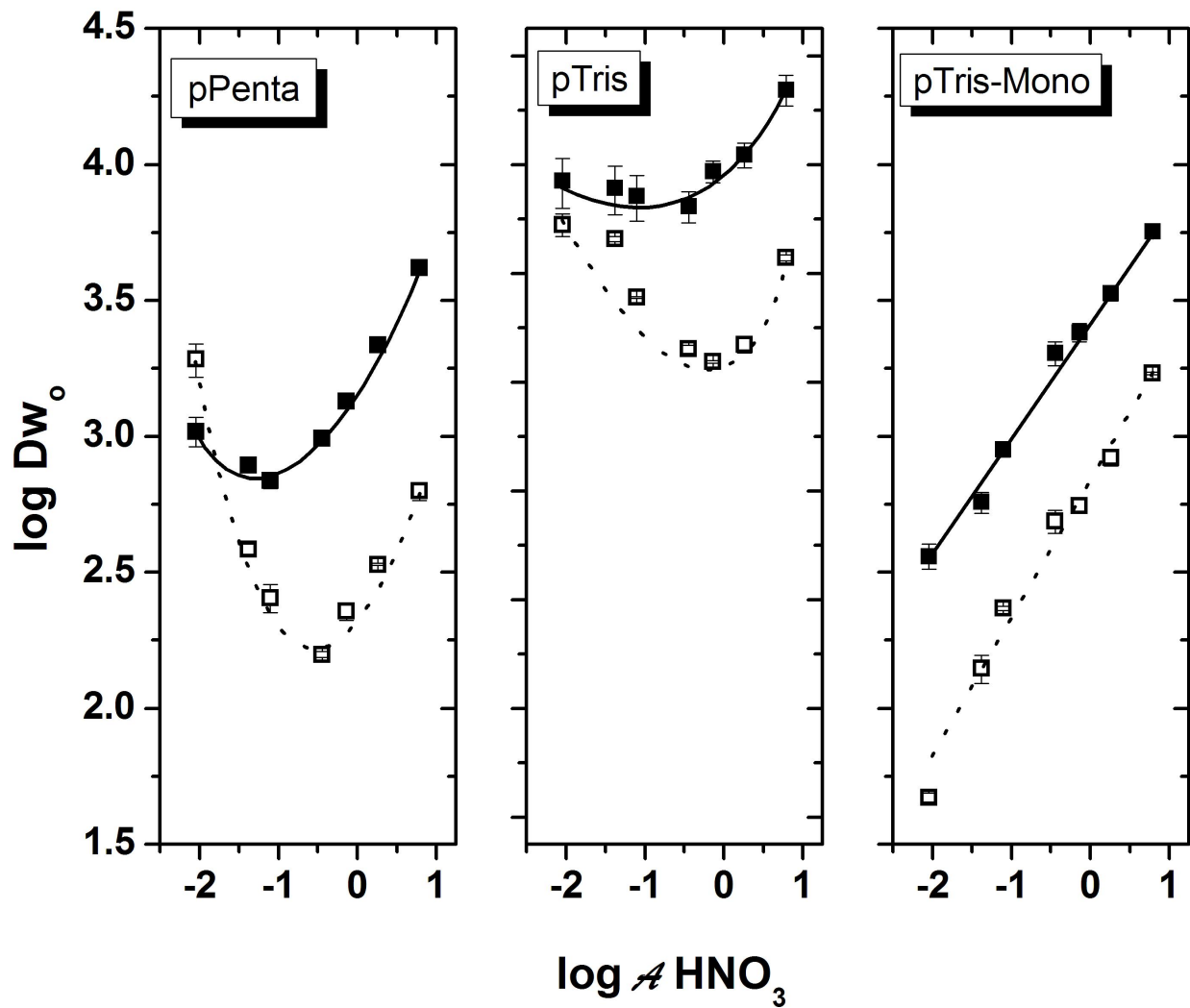


Figure 3.8. Extraction of 1×10^{-4} M $\text{UO}_2(\text{NO}_3)_2$ as a function of the activity of HNO_3 from 6.4×10^{-3} to 4 M HNO_3 by 0.05 meq of the appropriate resin. Filled data points indicate resin that had no pre-equilibration performed prior to contact. Open data points indicate resin that was pre-equilibrated 3X at the appropriate acid concentration prior to uranium extraction. Axes descriptions applies to all axes.

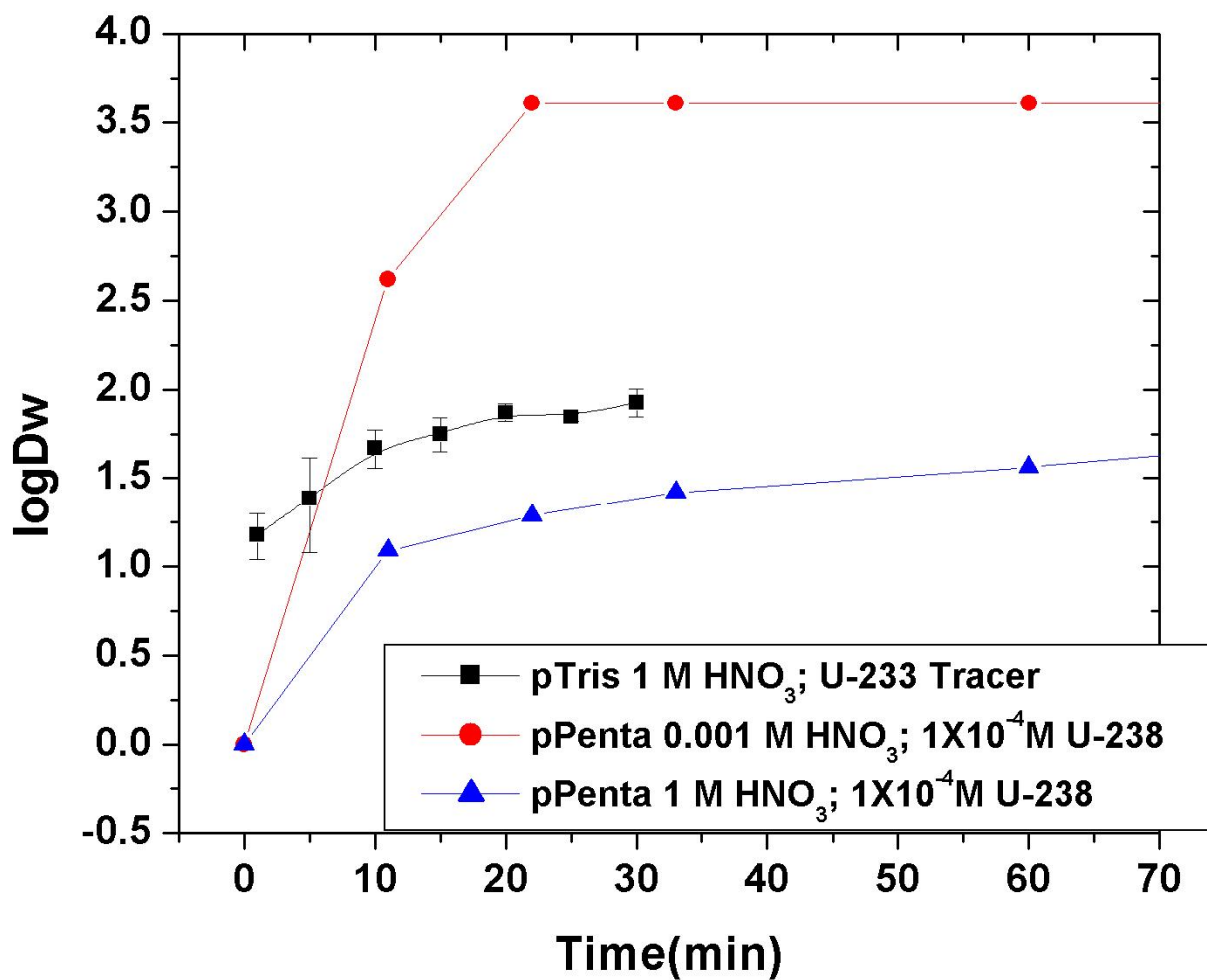


Figure 3.9. Extraction of uranium as a function of time by the pTris and pPenta resins using 0.025 and 0.5 meq of resin, respectively. The aqueous phase volume was 10 mL and 0.5 mL for the pPenta and pTris studies, respectively. The uranium concentration is decreased for the pTris resin in an attempt to improve the uptake kinetics.

diffusion based nature of chromatographic materials dictates decreasing the analyte concentration can expedite uptake kinetics significantly.^[25]

The Effect of Carbonate Media on Resin Hydrolysis and Uranium Uptake

For some potential applications, there might be interest in examining the uptake and removal of uranyl from carbonate media using these resins. [Figure 3.10](#) shows the influence of carbonate on the weight distribution ratio of uranium and the pH of the aqueous phase after extraction for each carbonate concentration. The extraction of uranium drops dramatically with increasing carbonate concentration. This is accompanied with a higher final pH of the aqueous solution.

Minimization of Cation Exchange by Metal Ion Pre-Equilibration

The nitric acid dependence for uranium uptake with zirconium and iron pre-equilibrations is shown in [Figure 3.11](#). For concentrations of iron greater than 0.01 mM, generally solvating extractant uptake trends are observed where better uranium distribution occurs at higher acid concentrations and lower distribution ratios are seen at lower acid concentrations. As the concentration of iron decreases, the uptake of uranium increases by more than two orders of magnitude at the lowest acid concentrations. Uranium extraction is affected even at a very low percentage of iron (0.0016 %) relative to the total resin capacity. The uptake of uranium at the highest concentrations of acid is relatively unaffected by changing the concentration of iron introduced to the system.

Figure 3.12 shows the uranyl distribution data as a function of $[\text{HNO}_3]$ for reconditioned

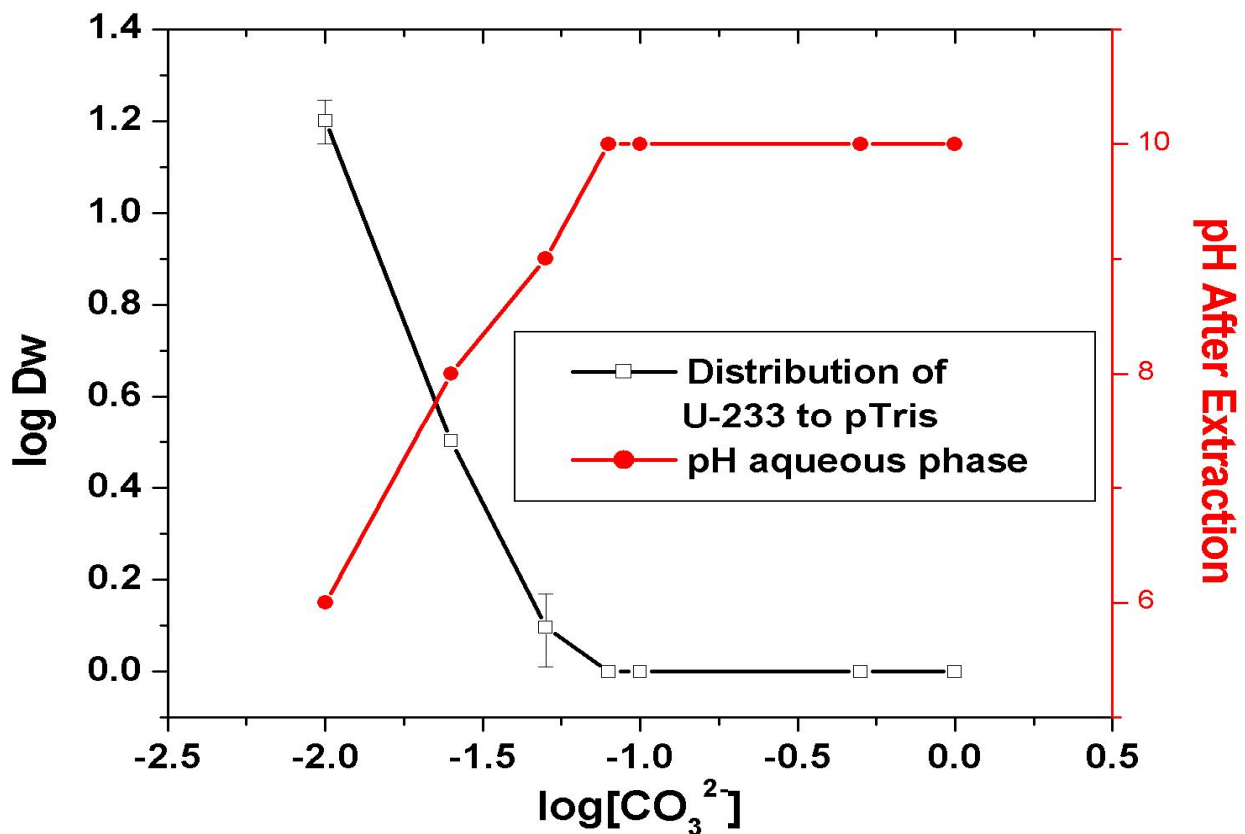


Figure 3.10. The carbonate concentration dependence of uranium uptake using 0.025 meq of the pTris resin. Note should be made for Na_2CO_3 concentrations about 0.1 M, no detectable extraction of uranium was present.

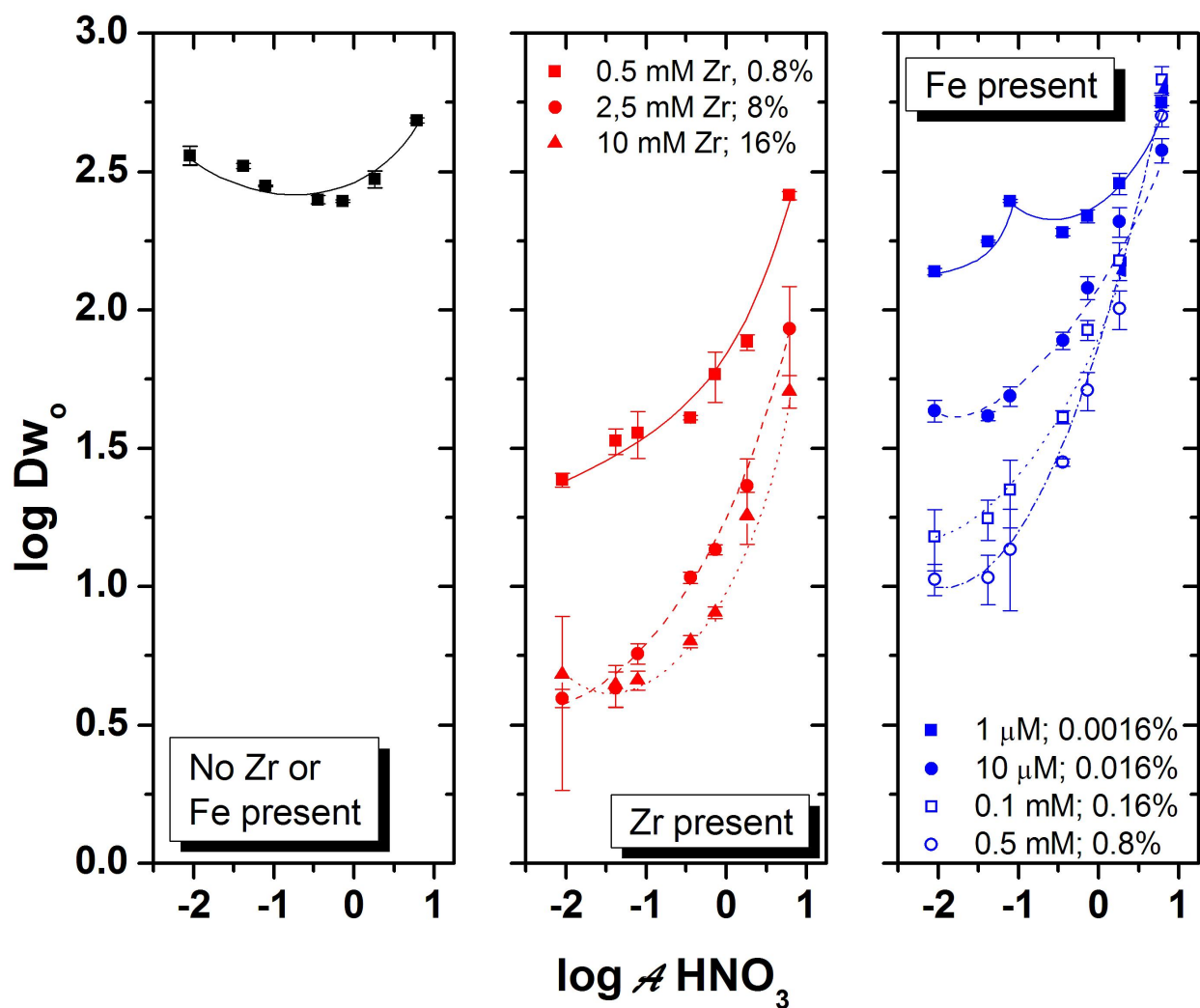


Figure 3.11. The nitric acid dependence of uranium uptake using 0.025 meq of the pTris resin. Preequilibrations were performed 0.4 mL of the appropriate Zr or Fe solution listed. The percentages show the meq of Fe or Zr present relative to the total meq of phosphorus present in the pTris.

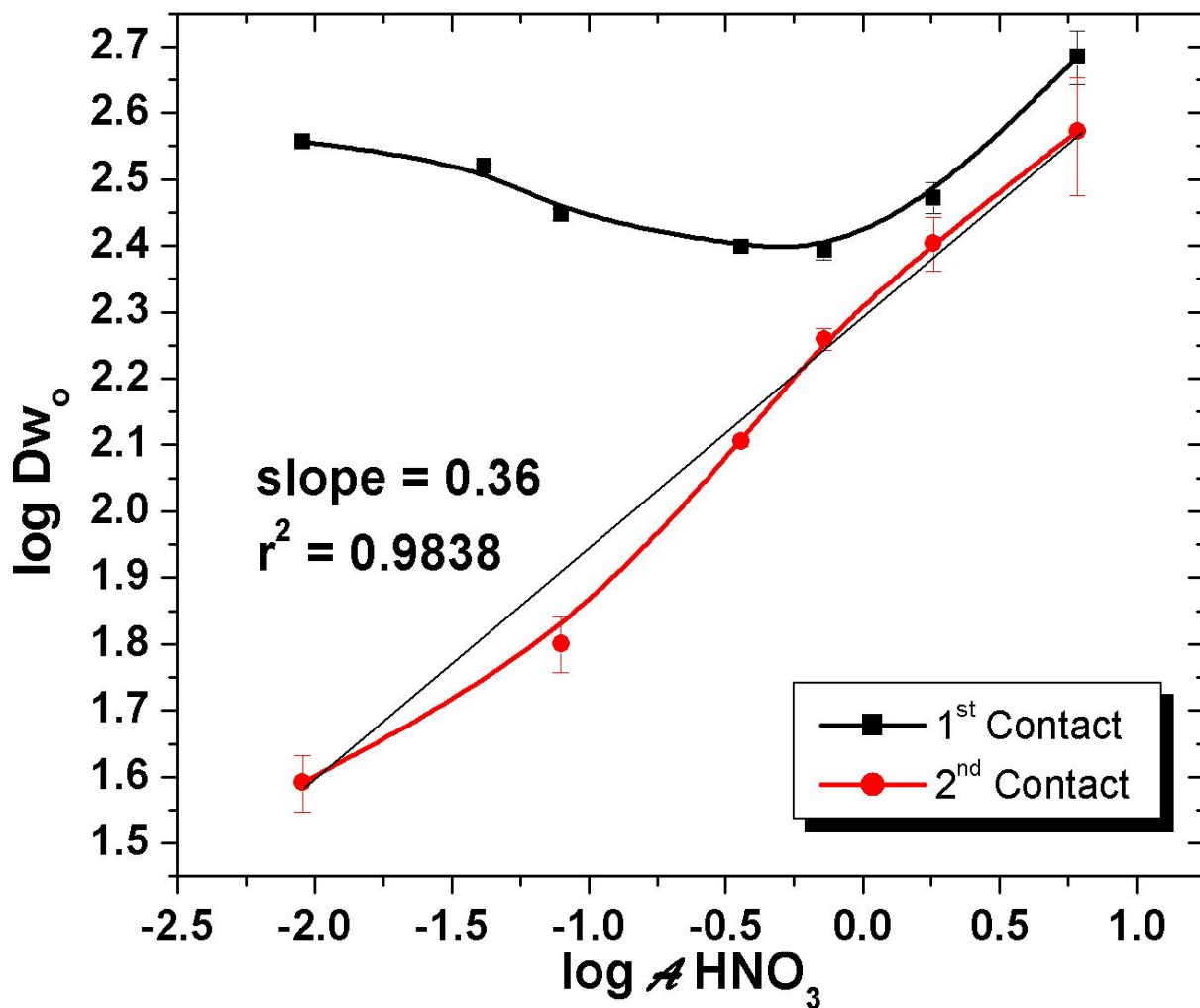


Figure 3.12. The nitric acid dependence of uranium uptake using 0.05 meq of the pTris resin. The 1st contact indicates the uptake of uranium from resin that has not been used for uranium extraction before. The 2nd contact indicates the use of that same resin after an attempted reconditioning has been performed

resin as compared with previously unused resin. The same resin has been used for each respective data point (i.e., pTris resin at 0.01 M HNO₃ was reconditioned and used again at 0.01 M HNO₃). A slope of 0.36 is observed at the lower acid concentrations, much less than the expected slope of 2 for such a graph. [Figure 3.12](#) does correct for the formation of UO(NO₃)⁺, therefore distribution values are annotated by D_{w_0} .

Infrared Characterization of pTris

The time-dependent spectra of pTris represent spectra obtained when the material was received from Dr. Alexandratos and a spectra nine months after the material had been received, [Figures 3.13a](#) and [3.13b](#), respectively. [Table 3.1](#) is provided to aid in deconvolution of spectral peaks.^[31] The spectrum obtained after the material was stored for nine months is considerably different. Bands potentially attributed aromatic stretching ($\nu = 2981, 2921 \text{ cm}^{-1}$) in [Figure 13a](#) have completely vanished in [Figure 3.13b](#). The phosphoryl stretching ($\nu = 1249 \text{ cm}^{-1}$), phosphate esters ($\nu = 1022, 798 \text{ cm}^{-1}$) bands still potentially seem present, but at a much lower intensity than when the material was initially received. The initially received materials did appear hydrated to some degree. Over the course of storage, the material appeared to have dried considerably.

To understand the impact of resin swelling on observed spectra, spectra were obtained for a single sample of resin that was initially wet, then vacuum dried, then wetted again with DI water. The results of this study are shown in [Figure 3.14](#). [Figure 3.14a](#) and [Figure 3.14b](#) highlight the

regions of aromatic and phosphorus based activity, respectively, for all three examined resin conditions. [Figure 3.14c](#) and [Figure 3.14d](#) highlight these same respective aromatic and phosphorus regions, but now only the dry resin conditions are shown and the figures zoom to the

Table 3.1. Infrared vibrational modes significant to the analysis of pTris resin.^[31]

Functional Group	1° Alcohol	Phosphate Acid	Phosphate Ester	Aromatic
Mode	Stretch	Bend; Wag	Stretch; Bend	Stretch
Characteristic Absorbance (cm ⁻¹)	1000-1075	2550-2700; 2500-2350	$\nu_{PO} = 1280$; $\nu_{COP}^* = 970-1050$ S 740-830 S	2850-3000

* Methoxy and ethoxy derivatives only

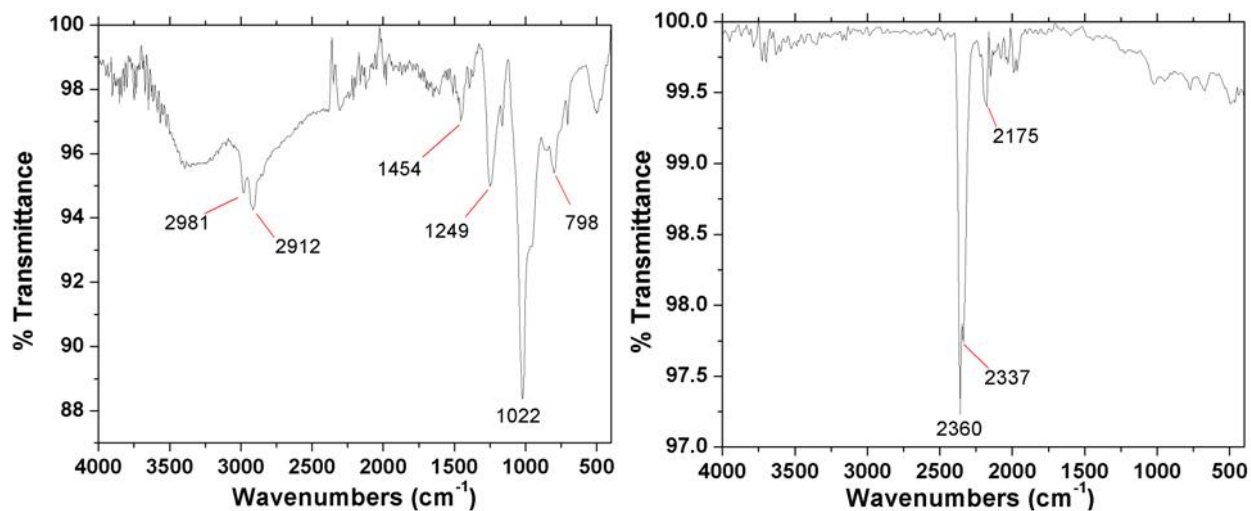


Figure 3.13. From left to right, infrared spectra obtained initially after receiving pTris and nine months after reception.

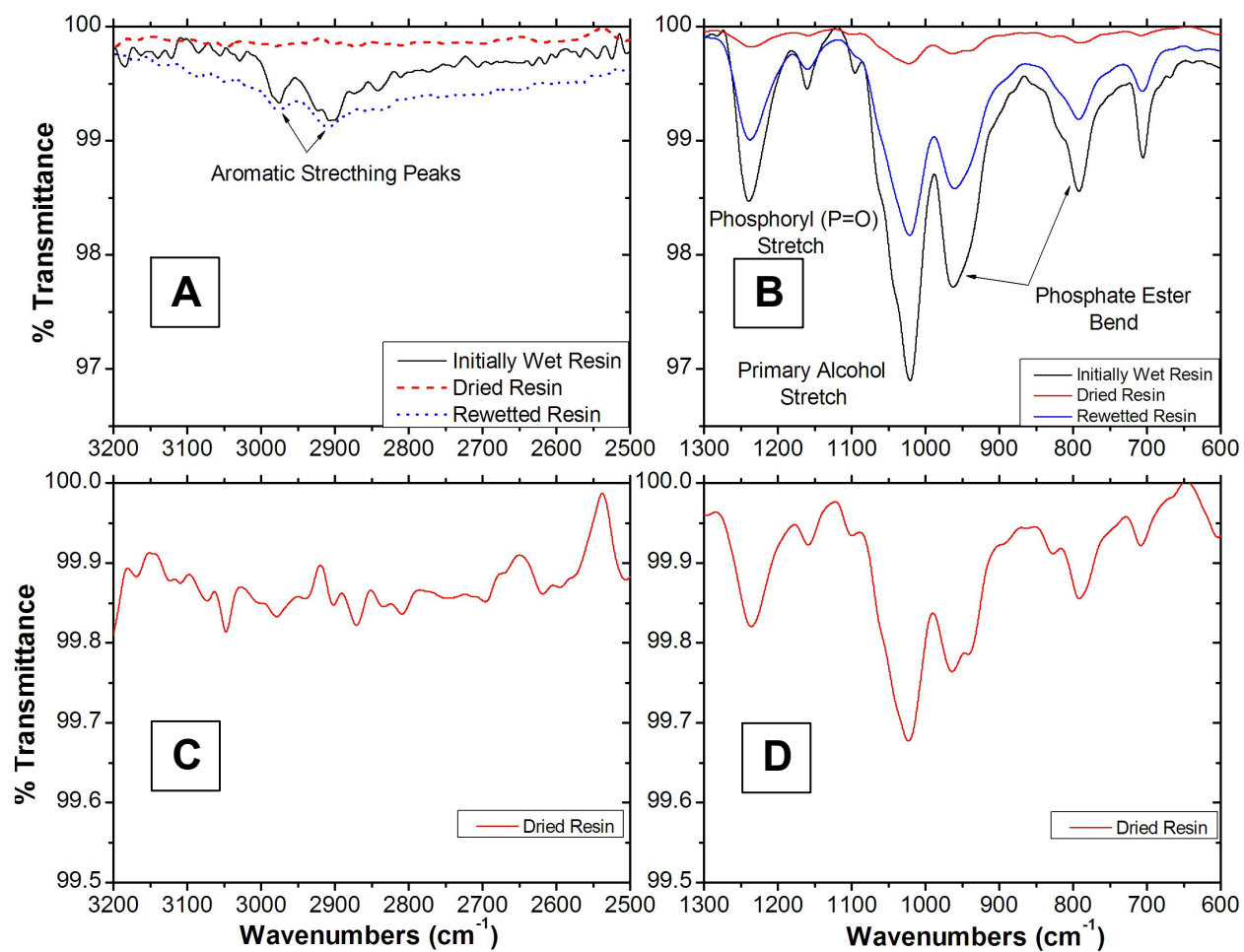


Figure 3.14. IR spectra for the pTris resin when the resin is wetted with water, dried in an oven for three hours, then wetted again. Inset 3.14a and 3.14b highlight the areas of observed aromatic stretching and phosphorus IR activity, respectively, for all resin conditions. Inset 3.14c

and 3.14d zoom towards the IR baseline to allow observation of spectral activity for the dried resin.

baseline of the spectra. When the resin is hydrated, all anticipated bands are present in the spectra. When the resin is dried, the aromatic stretching band is not detectable, but many of the anticipated phosphate and –OH bands are still present at a much weaker signal.

The affect of prolonged contact with hydrochloric acid for the pTris resin is shown in [Figure 3.15](#). Spectra in these figures were obtained with a resolution of 32 cm^{-1} . Hydrochloric acid was chosen over nitric acid to ensure resin degradation is not a result of the oxidizing nature of nitric acid. At 1 M HCl, the phosphate bands anticipated at roughly 1200 and 1000 cm^{-1} have greatly decreased in intensity and the phosphoric acid peak at 2360 cm^{-1} has become the most prominent peak. The spectrum of pTris in contact with 2 M HCl shows an increase in the peak at 2360 cm^{-1} . The aromatic stretch observed after contact with 1 M acid has decreased in intensity after contact with 2 M HCl. Aromatic stretching is not observed for resin contacted with 4 M HCl. After contact with 4 M HCl, the prominent band is still at 2360 cm^{-1} .

Resins contacted with acid were further vacuum dried and these spectra are shown in [Figure 3.16](#). The spectrum obtained at 1 M HCl shows a decrease in the peak at 2360 cm^{-1} and the addition of other significant peaks at 2159 and 2120 cm^{-1} . The aromatic stretching peaks are only observable when the spectra is zoomed very near the baseline. After contact of the pTris with 4 M HCl and five days of vacuum drying, any peaks are very hard to discern.

Discussion

Uranyl Nitrate Extraction from Nitric Acid

The nitric acid dependence of $\text{UO}_2(\text{NO}_3)_2$ extraction by 19% TBP in kerosene is shown in Figure 3.17.^[26] In general, uranyl nitrate extraction increases with increasing $[\text{HNO}_3]$. At

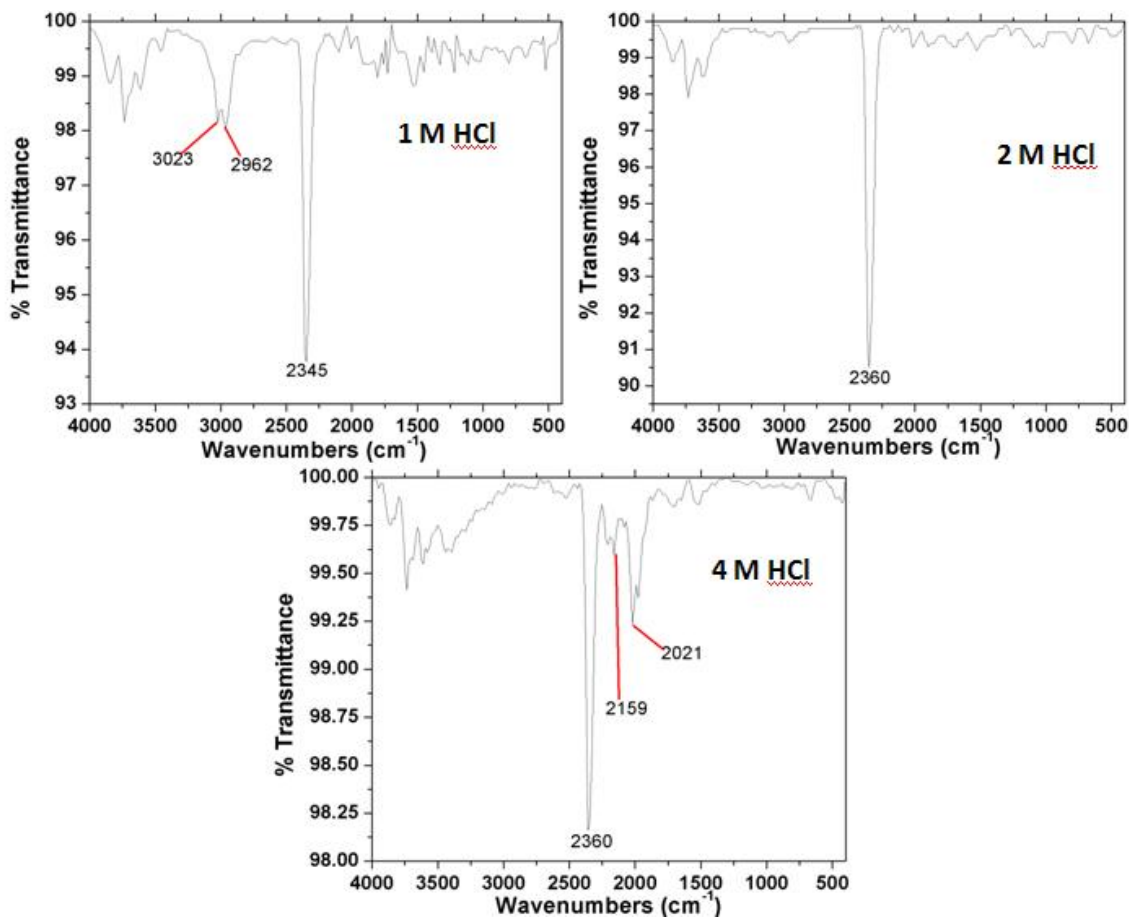


Figure 3.15. The IR spectra pTris after a 34 day contact with 1, 2 and 4 M HCl. Three days were allowed for drying of the resins using a vacuum dessicator.

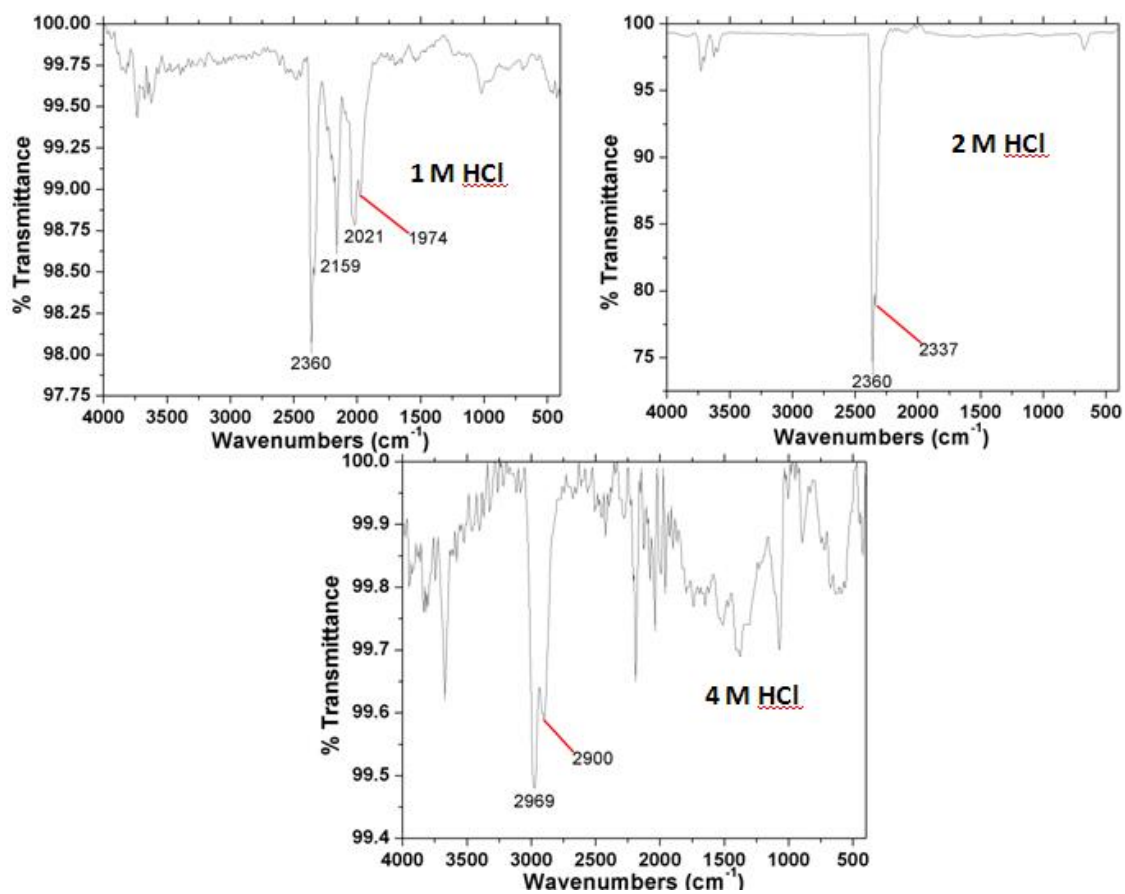


Figure 3.16. The IR spectra pTris after a 34 day contact with 1, 2 and 4 M HCl. Five days were allowed for drying of the resins using a vacuum dessicator.

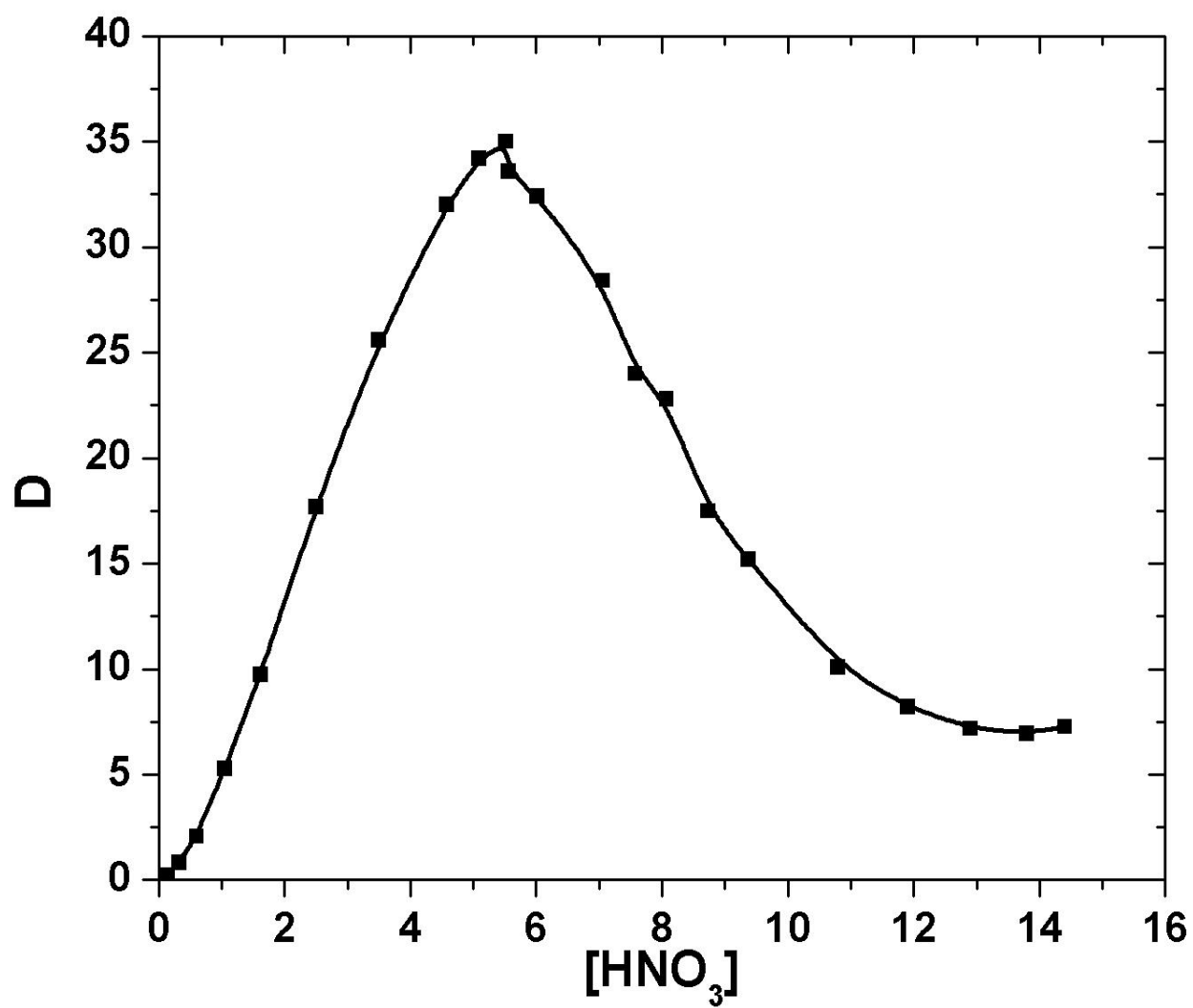


Figure 3.17. Extraction of $\text{UO}_2(\text{NO}_3)_2$ by TBP as a function of nitric acid concentration. "D" is the distribution ratio defined as $D = [\text{U}_{\text{org}}]/[\text{U}_{\text{aq}}]$ at equilibrium.^[28]

concentrations of nitric acid above 5 M, uranium extraction decreases. Numerous reports in the literature relate this to nitric acid extraction by the phosphoryl oxygen competing for metal extraction.^[26,27] Figure 3.18 shows the speciation of TBP/nitric acid complexes in the organic phase for 30% TBP as a function of nitric acid concentration. Comparison between Figures 2 and 3 show uranium extraction is not inhibited until the $\text{TBP}(\text{HNO}_3)_2$ species is present. To the extent that TBP can be considered a model for pPenta, pTris and pTris-Mono (solvating, phosphate type extractants), *uranium uptake should be largely unaffected by the presence of HNO_3 at acid concentrations less than 5 M.*

Experiments performed with these resins have produced metal uptake trends that closely match the patterns of a cation-exchanging material. The literature has shown a very small amount of phosphoric acid impurity in TBP, i.e. ~3%, can produce ion exchange uptake patterns if the metal concentration is less than or equivalent to 10^{-4} M.^[2] This level of impurity is probably too low to be reliably detectable by NMR or IR.

Uranyl Uptake by pPenta, pTris, and pTris-Mono Resins from HNO_3

The decrease in metal uptake as the concentration of nitric acid increases for the pPenta and pTris. One possible interpretation of the data in Figure 3.5 is competitive nitric acid partitioning

to the solvating resin could be inhibiting the uptake of uranium. However, the uptake at very low acid is unexpected; as nitrate anions are required for uranyl partitioning, lower nitrate concentrations should not correlate with high cation partitioning to the resin phase. The high D_U values seen at low acidity are more consistent with a pattern seen for a typical cation exchange resin, i.e., high uptake at low $[H^+]$.

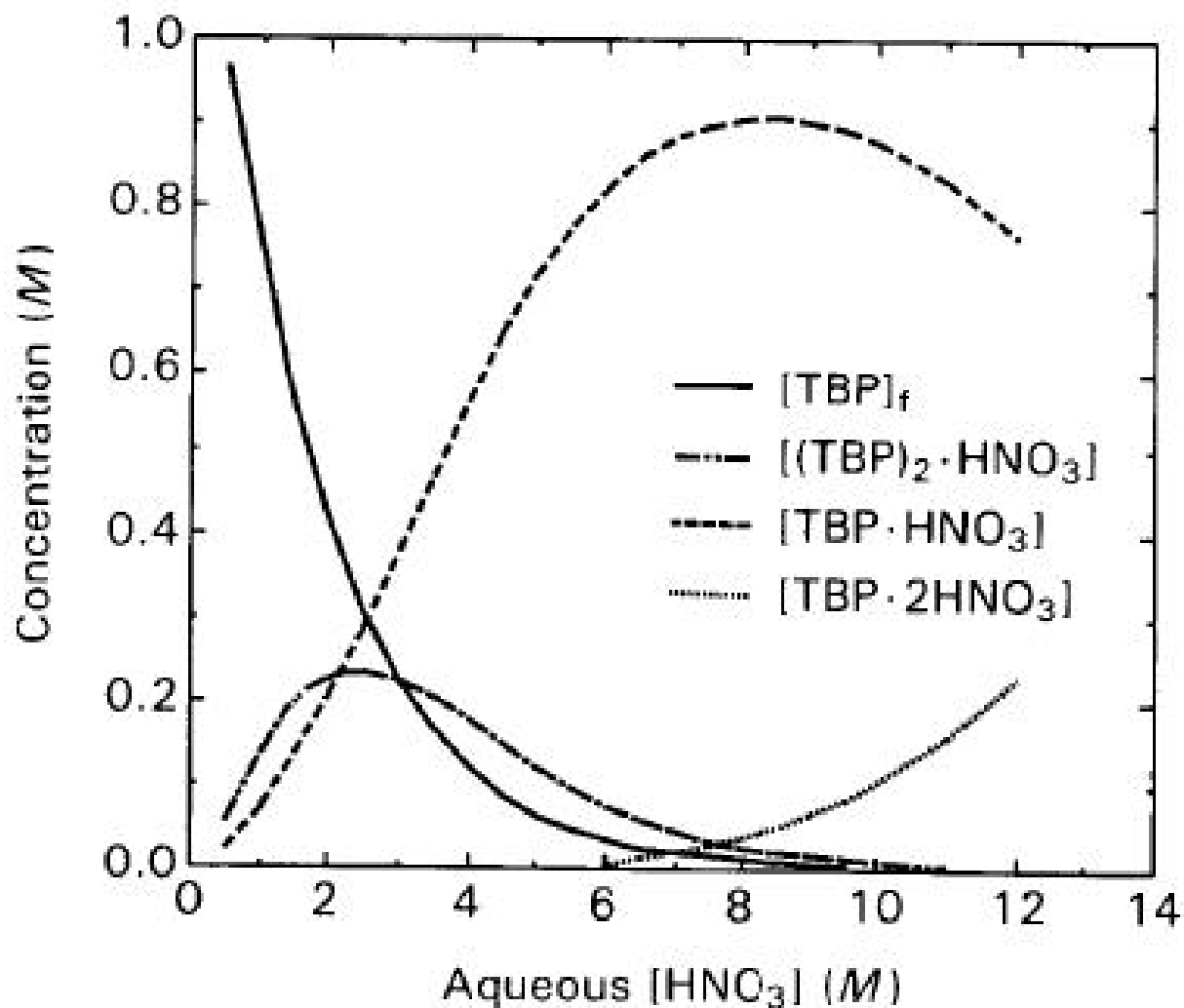


Figure 3.18. Tributyl phosphate/nitric acid complex speciation in the organic phase as a function of nitric acid concentration for 1.035 M (30% v/v) TBP.^[15]

A working hypothesis for the observations made to date is that the resin has a percentage of not fully esterified sites present that can engage in conventional cation exchange, swapping 2 x H^+ for 1 x UO_2^{2+} . Such an “impurity” would dictate high extraction at low nitrate (and acidity). A small resin impurity could have a large impact, since the metal loading of these studies is 0.2% of the total phosphorus capacity. A significant comment is metal ion partitioning studies are very sensitive indicators of the presence of cation exchanging impurities (or degradation products) in solvating extractant systems. This has been reported in studies of the extraction of various actinide ions in degraded PUREX and TRUEX process solvents.^[22,29]

The pTris-Mono shows more classical solvating extractant behavior. We speculate that this species may be less prone to hydrolysis than the pTris and pPenta resins, even though they are structurally very analogous. Even though acidic conditions are present, a base catalyzed process may be more likely because of the proximity of the linking ether.^[26] The proposed mechanism for this degradation is shown in [Figure 3.19](#). An intermediate phosphonate would be formed that and attacked through water. Eventually the phosphoric acid would be formed. Since the pTris-Mono resin has the ammonia linker, the base catalyzed pathway exploited by the pPenta would not be possible for the pTris-Mono. Furthermore, interaction of the pTris-Mono $-OH$ groups with the ammonia linker, [Figure 3.20](#), may also retard a potential acid-catalyzed degradation.

If the pPenta and pTris were both degrading to the phosphoric acid through an acid catalyzed pathway, the breakdown of the resins would be similar. However; metal partitioning patterns

shown in Figure 3.5 and 3.8 indicate the pPenta resin is more prone to de-esterification because a base-catalyzed pathway is possible. Degredation of the pTris would occur through the acid catalyzed pathway noted in Figure 3.21. Theoretically, the pTris-Mono should be subject to a

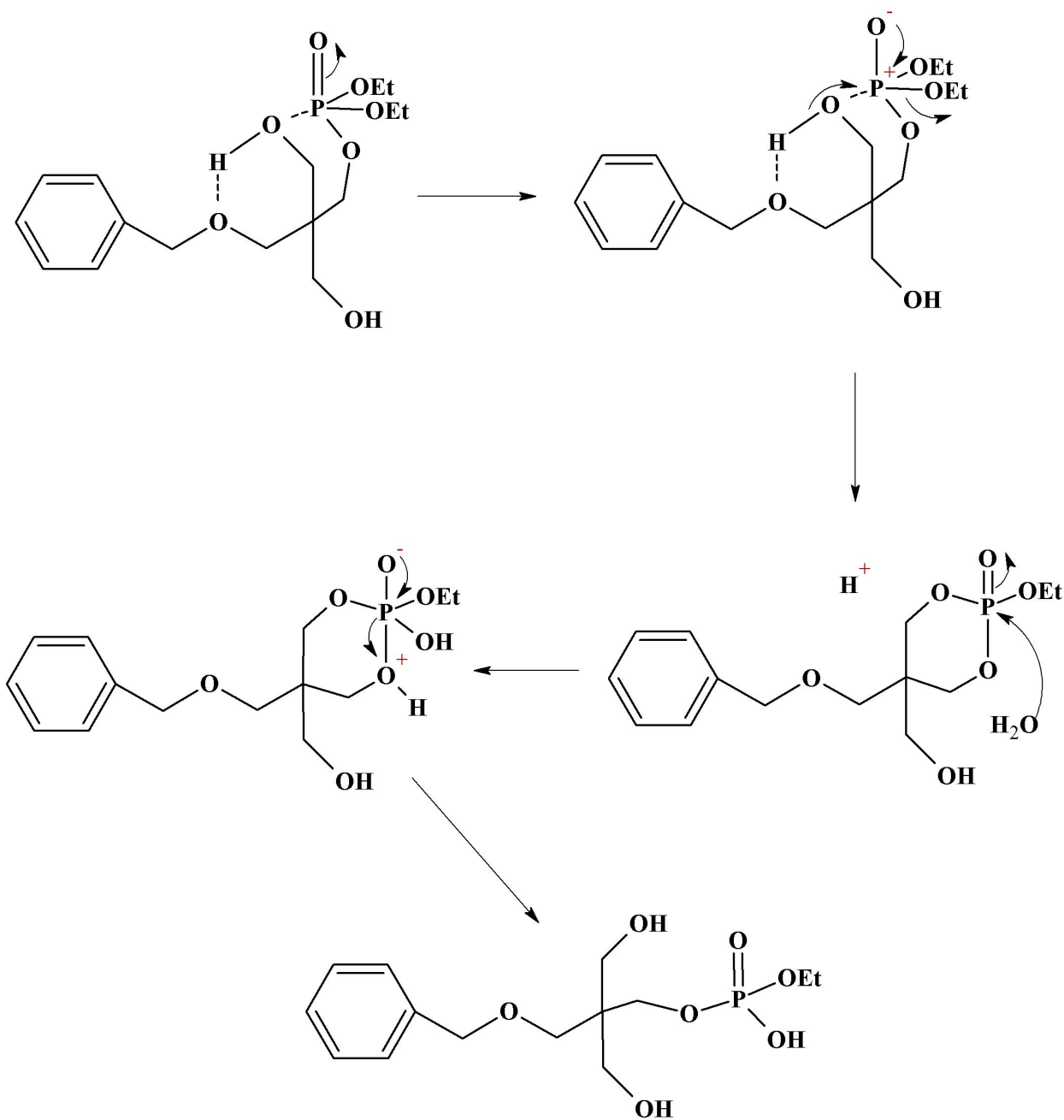


Figure 3.19. Proposed base catalyzed pathway for degradation of pPenta resin.

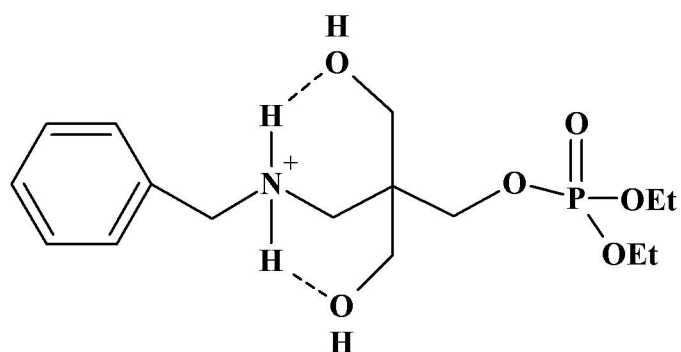


Figure 3.20. Potential interaction of pTris-Mono hydroxyl groups with ammonia linker. This interaction may decrease the probability of interaction with the partial positive charge existing on the phosphate.

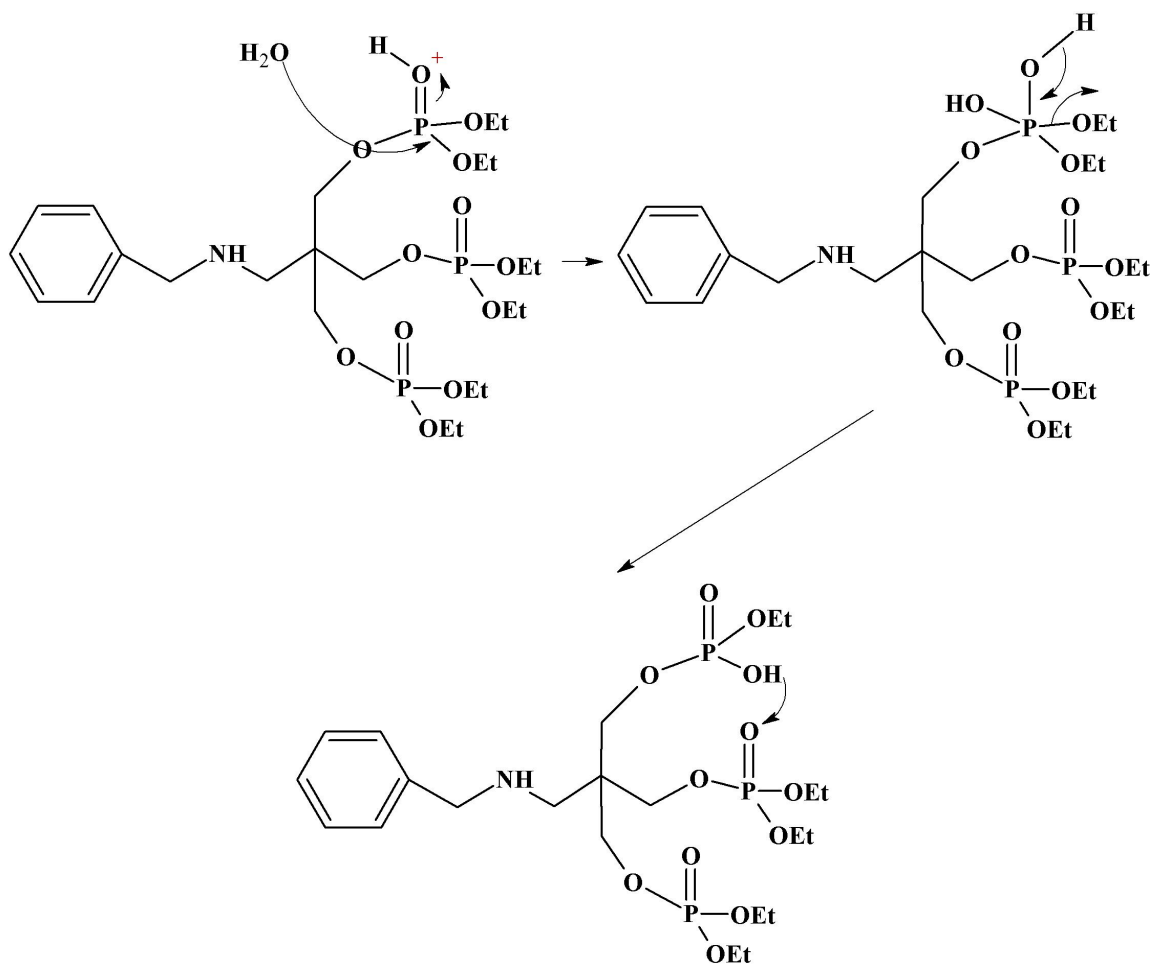


Figure 3.21. Proposed acid catalyzed pathway for degradation of pTris resin.

similar acid-catalyzed pathway^[26], but the closer proximity of phosphate groups to one another may lead to a higher local concentration of acid once the pTris functional group begins to degrade.

Uranium generally interacts less with a cation exchange site than some other elements, particularly thorium, europium, iron and zirconium. On the other side of this, thorium, europium, iron and zirconium will usually compete less with uranium for a solvating extractant. If cation exchange sites are providing the mechanism for uranium uptake, uranium partitioning at low concentrations of acid should greatly decrease in the presence of these other elements and remain largely unaffected at concentrations of acid greater than 1 M.

Extraction of U(VI) as a Function of HNO₃ or NaNO₃ in the Presence of Th(IV) and Eu(III)

Adding Th⁴⁺ and Eu³⁺ should suppress the influence of any cation exchanging functionality at low acidity, as Th⁴⁺ in particular should be more strongly retained (than UO₂²⁺) by the acidic phosphate groups (assumed to be Resin-OPO(Et)OH), thus decreasing the opportunity for uranium partitioning. The most dramatic difference between these results and those shown in [Figure 3.5](#) is the inversion of uptake trends. When only nitric acid is present in the system with Eu³⁺ and Th⁴⁺, cation exchange pathways appear to be at least partially blocked preventing the high uptake of UO₂²⁺ at lower acid concentrations. Comparison between [Figures 3.5](#) and [3.6](#) shows the uptake at acid concentrations greater than 1 M to be very comparable, independent of the presence of Eu³⁺ or Th⁴⁺. This is also consistent with expectation noted earlier, as both

$\text{Eu}(\text{NO}_3)_3$ and $\text{Th}(\text{NO}_3)_4$ interact less strongly with phosphate esters than does $\text{UO}_2(\text{NO}_3)_2$.^[21,22]

Introducing sodium nitrate produces uptake patterns representative of a solvating extractant.

Blocking the cation exchange sites with Th^{4+} or Eu^{3+} and adding a salting agent (NaNO_3) would encourage uptake of UO_2^{2+} by a solvation mechanism.

The slope of [Figure 3.6](#) for the sodium nitrate data displays of nitrate dependence of 1.5 for the pTris and pTris-Mono systems. The nitrate dependency for the pPenta data is lower (~1 at the steepest increase). Since the data are corrected for nitrate complexation of uranium in the aqueous phase, a slope of 2 would be anticipated to satisfy the charge neutralization required for uranium uptake. An acidic impurity not completely blocked by Th^{4+} or Eu^{3+} could produce higher uranium uptake at lower nitrate concentrations and ultimately a nitrate dependence not as steep. This could be the explanation for the much lower dependence of the pPenta from sodium nitrate aqueous media in [Figure 3.6](#) and pre-equilibration studies performed later ([Figure 3.8](#)) show pPenta appears to be the most prone to hydrolysis.

Another notable difference is the increased partitioning of uranyl into the pTris-Mono relative to the pPenta when the competition with HNO_3 is eliminated. This seems complimentary to previous discussion which noted the pTris-Mono appears more resistant acidic degradation of the ethoxy groups. When only nitric acid is present ([Figure 3.5](#)), the pPenta absorbs more uranium than the pTris-Mono until the concentration of HNO_3 passes 0.1 M, after which the pTris-Mono is a better uranium sorbent. When sodium nitrate is used as the salting agent and Th^{4+} or Eu^{3+} are present to block potential cation exchange sites, uranium sorption performance of the pTris-Mono is more than 10 times stronger; uptake onto pPenta is less affected.

Determination Acidic Impurities in the pPenta and pTris Resins

Concluding resin synthesis, Dr. Alexandratos performs a significant wash of the resins concluding with a 1 L wash with H₂O.^[17,18] After the series of washes is performed, the aqueous phase pH is neutral. Several months after synthesis, water washes (Figure 3.7a and 3.7b) indicate the presence of exchangeable hydrogen ions in the resin sample. This observed release of H⁺ does not demonstrate whether the H⁺ is being released from an ionized ethoxy group or if it is released from the nitrogen present on the resin. However, it does support the hypothesis of acidic groups being present on the resin. If acidic groups are present in the resin, the 16% calculated impurity would be large enough to impact metal partitioning patterns at the concentrations.^[22]

Investigation into Acid Promoted Hydrolysis of the Solvating Extraction Resins

It should also be noted that an organophosphorus cation exchange material will behave as a solvating extractant if the concentration of acid is sufficient to completely inhibit metal ion interaction with the cation exchange site and force interaction with the phosphoryl oxygen. This knowledge is central to providing a discussion regarding the uranium uptake patterns between resin that is pre-equilibrated and not pre-equilibrated before uranium uptake (Figure 3.8).

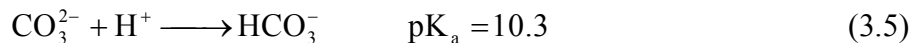
The pTris-Mono based resin continues to show uptake trends indicative of a solvating resin regardless of resin pre-equilibration with acid. The weight distribution values for the pTris-Mono resin decrease by almost an order of magnitude after acid contact at all concentrations of nitric acid investigated. This would be related to nitric acid competition for the phosphoryl oxygen and this is the behavior anticipated by a resin partitioning uranium through a solvation

mechanism. Introducing more acid to the resin through pre-equilibration will compete for uranium partitioning and a slight decrease in uranium uptake will be observed.

After pre-equilibration, all resins show approximately the same order of magnitude drop in uranium partitioning at concentrations of nitric acid greater than 0.5 M compared to uranium uptake by resins that have not been pre-equilibrated. However, the increase in uranium uptake at lower acid concentrations by the pPenta and pTris resins *after* pre-equilibration is not indicative of solvating reagents being present in the resin. As noted previously, the most metal partitioning will occur in dilute acid media when a cation exchange material is present. Acid contact with the resins during pre-equilibration may encourage dissociation of the ethoxy group and formation of the phosphoric acid before uranium is even introduced to the system. This would allow the uranium to partition through a cation-exchange mechanism using now introduced phosphoric acid impurity. If an acidic degradation of the resin is occurring, ultimately the phosphate group could be completely removed from the resin with time.

The Effect of Carbonate Media on Resin Hydrolysis and Uranium Uptake

The decrease in uranium extraction with increasing carbonate concentration (Figure 3.10) could be related to the presence of acidic functional groups in the resin and to the strength of the triscarbonato complexes of uranyl. As H^+ is released from the resin, the carbonate is most likely protonated. The protonation of carbonate would produce lower concentrations of the CO_3^{2-} species available for uranium binding in the aqueous phase. The protonation reactions and the associated pK_a s for carbonate, bicarbonate and carbonic acid are shown in Equations 3.5 and 3.6.^[24]





The lower pH observed after carbonate contact with the resin suggests that the acid present in the resin is being released in a way that is analogous to what was observed during the water wash steps. This would produce a deprotonated ion exchange material and decrease in the pH of the aqueous phase. At a lower pH, more sodium bicarbonate would be present. Since sodium bicarbonate is a weaker binding agent, uranium would not be retained in the aqueous phase through anion holdback and would be allowed to partition to the resin. For 0.01 M carbonate, the pH after extraction was roughly 6. This would be within the buffer range of the bicarbonate/carbonic acid reaction. As the carbonate concentration becomes sufficiently large, the acid present on the resin becomes insignificant and the final pH after extraction is 10. No uranium uptake is observed, within error for concentrations of carbonate greater than 0.1 M. Clearly the change in pH again indicates the presence of H^+ .

To compare numbers, assuming a 16% impurity of the pTris, roughly 4 μeq of protons would be present from the pTris resin (6 mg of resin were used). The aqueous phase contained 5 μeq of carbonate in 0.5 mL of 0.01 M Na_2CO_3 . The amount of theoretical acid released from the resin would be capable of producing an 80%/20% bicarbonate/carbonate system where ^{233}U uptake would be possible. At 0.1 M carbonate, 50 μeq of carbonate are present and the impurity represents the ability to neutralize only 8% of the carbonate present and no uranium uptake would be observed. This study is in alignment with the other studies within this manuscript which note the presence and amount of exchangeable H^+ within the resin.

Minimization of Cation Exchange by Metal Ion Pre-Equilibration

Adding low concentrations of a polyvalent cation to the resin could serve to block the cation exchanging sites and thus allow uranyl nitrate to interact with the remaining intact phosphate ester groups. Both Zr^{4+} and Fe^{3+} were examined as potential blocking cations. Iron was particularly well suited for this task, since metal hydrolysis is less problematic and extraction of iron at the phosphoryl oxygen generally less than Zr^{4+} from nitrate media.^[21,24] If the small amount of acidic impurity were dictating extraction trends, only a small amount of Fe would be needed to impact these trends (as is shown in [Figure 3.11](#)).

The resins pre-equilibrated with iron do not perfectly mimic well known solvating extractant systems where the uptake data would show a sharp increase in uptake from 0.01 to roughly 1 M, followed by similar uranium uptake at acid concentrations greater than 1 M. This could result from some competition of Fe with U for the phosphoryl oxygen. The pre-equilibration with iron at 1 μ M shows some blockage of the potential ion exchange groups at low acid and very similar uptake to the system with no iron pre-equilibration. Although the results from this study would partially indicate the presence of ion exchange groups present, a better agreement would be required with data already in the literature for solvating extractant systems.

Resin Reproducibility Studies

The observation of solvating extractant type behavior for the reconditioned resin in [Figure 3.12](#) was unexpected. At least several possible explanations exist for this observation: 1) HEDPA was not a sufficiently strong complexant to have removed the uranium from an ion exchange site, 2) an acidic impurity that had the potential for uranium extraction was removed from the resin as a part of the reconditioning process or 3) the HEDPA was not sterically capable

of insertion into the polymer network and therefore interaction between HEDPA and uranium was prohibited.

At all acid concentrations, uranium uptake by the reconditioned material is lower than initially used material. This could be related to uranium remaining on the resin from the previous contact. Etidronic acid ($\log K_{\text{HEDPA,U}} \sim 11.2$)^[30] would most certainly be a sufficiently strong complexant to remove UO_2^{2+} from a phosphate phosphoryl oxygen ($\log K_{\text{TBP,U}} \sim 1.8$)^[23] or a phosphoric acid ($\log K_{\text{HDEHP,U}} \sim 3.4$)^[23]; however insertion of HEDPA into the polymer matrix could be a kinetically slow process. Ultimately, it appears the incomplete removal of uranium would be related to slow recovery kinetics and insufficient contact times since the thermodynamics indicate all uranium should be recovered. Interestingly, the differences in uranium uptake between the materials is highly dependent on the concentration of nitric acid. Different uranium recovery kinetics could be indicative of a different HEDPA-uranium binding mechanisms being used if uranium is bound to the resin through a solvated mechanism ($[\text{HNO}_3] > 1 \text{ M}$) or through a cation exchange mechanism ($[\text{HNO}_3] < 1 \text{ M}$). A contact time longer than 25 minutes may be necessary to regenerate the resin.

Infrared Characterization of pTris

While some activity still remains near the region of phosphorus activity for [Figure 3.13b](#), the lack of aromatic stretching absorbance around 2900 cm^{-1} is interesting for a polystyrene resin. The absence of an aromatic stretch is noted in several of the acid contacted resins ([Figure 3.15](#)) and resins that were further vacuum dried after acid contact ([Figure 3.16](#)). The oxidation of the aromatic ring is not plausible under the concentrations of nitric acid present. A more likely

explanation is the resin swells in contact with water and when phosphate groups are bound to the backbone. As the resin is vacuum dried, or the phosphate groups are hydrolyzed, the resin shrinks. The infrared beam may have a decreased ability to penetrate through the resin. Since the aromatic groups would not be exposed to light, the anticipated aromatic stretch would not be observable.

This theory was tested by examining the IR spectra of a resin that had been wet, dried by vacuum, then re-wetted (Figure 3.14). It appears resin swelling, brought on by hydration, does allow increased visibility of functional groups on the pTris. Fortunately, the groups significant to determining phosphate ester hydrolysis are still visible (although the signal is weaker). There are some other visual indicators of degradation. Freshly received resins had varying amounts of yellow coloration. The pTris-Mono resin was almost white, the pPenta resin had a light yellow coloration and the pTris was yellow. After acid contact, the pTris-Mono resin would not change color significantly. The pPenta and pTris resins would display a definite increase in the amount of yellow coloring on the resin.

The spectra of the pTris resin after contact with acid is shown in Figure 3.15. The most intense peak is at 2360 cm^{-1} and could potentially be attributed to a phosphoric acid wag. The band increases in intensity from 1 to 2 M HCl, then decreases as the concentration of acid is increased to 4 M. The decreased intensity may be related to a near complete cleavage of the phosphate group from the resin support. Since no other signals seem prominent. An IR was taken of the 4 M HCl aqueous phase that had been in contact with the resin. No evidence of phosphate groups was present in this aqueous IR.

Spectra were also obtained with two days of additional vacuum drying after the initial IR spectra. These spectra in general had weakening of IR signals. This is concurrent with Figure

3.14 that displayed the significance of resin hydration state on IR spectra.. The exception to this is the phosphoric acid peak for pTris in 2 M HCl where a notable increase in signal is observed. This could be related to a continued degradation of the resin to the phosphoric acid. For 4 M HCl, the only significant peaks appear in the aromatic region of the spectra very near the baseline. All other peaks typically indicative of a phosphorus functional group have completely disappeared.

Conclusions

Significant evidence for ion exchanging impurities exists when examining extraction data and IR spectra. IR spectral results appear to indicate that prolonged contact with HCl results in complete de-esterification and possible removal of phosphate functional groups from the resin backbone. Future work will involve continued attempts at resin regeneration, examination of extraction patterns for DI H₂O washed resin, and investigation of acidic uptake of the pPenta, pTris and pTris-Mono resins, though the apparent instability of the phosphate esters appears to be an important limitation of these materials. The placement of ester t-butyl groups instead of ethyl groups could reduce the potential for hydrolysis of these novel resins, though steric crowding might become an issue.

References

- [1] Zhang, A.; Wei, Y.Z; Hoshi, H.; Kumagai, M; Kamiya, M.; Koyama, T. Resistance properties of a macroporous silica-based N,N,N'N-tetraoctyl-3-oxapentane-1,5-diamide impregnated polymeric sorption material against nitric acid, temperature and γ -irradiation. *Radiat. Phys. Chem.* **2005**, *72* (6), 669-678.
- [2] Nash, K.L.; Gatrone, R.C; Clark, G.A.; Rickert, P.G.; Horwitz, E.P. Hydrolytic and radiolytic degradation of OΦD(iB)CMPO: Continuing Studies. *Sep. Sci. Technol.* **1988**, *23* (12-13) 1355-1372.
- [3] Zhang, A.; Wei, Y.Z; Kumagai, M.; Koma, Y.; Koyama, T. Resistant behavior of a novel silica-based octyl-(phenyl)-N,N-diisobutylcarbamoymethylphosphine oxide extraction resin against nitric acid, temperature and γ -irradiation. *Radiat. Phys. Chem.* **2005**, *72* (4), 455-463.
- [4] Chiarizia, R.; Horwitz, E.P. Hydrolytic and radiolytic degradation of octyl-(phenyl)-N,N-diisobutylcarbamoymethylphosphine oxide and related compounds. *Solvent Extr. Ion Exch.* **1986**, *4* (4), 677-723.
- [5] Zhang, A.; Wei, Y.Z; Hoshi, H.; Koma, Y.; Kamiya, M.; Partitioning of cesium from a simulated high level liquid waste by extraction chromatography utilizing a macroporous silica-based supramolecular calix[4]arene-crown impregnated polymeric composite. *Solvent Extr. Ion Exch.* **2007**, *25* (3), 389-405.
- [6] Binnemans, K. Lanthanides and actinides in ionic liquids. *Chem. Rev.* **2007**, *107* (6), 2592-2614.
- [7] Dam, H.H.; Reinhoudt, D.N. Multicoordiante ligands for actinide/lanthanide separations. *Chem. Soc. Rev.* **2007**, *36* (2), 367-377.
- [8] Favre-Reguillon, A.; Draye, M.; Lebuzit, G.; Thomas, S.; Foos, J.; Cote, G.; Guy, A. Cloud point extraction: an alternative to traditional liquid-liquid extraction for lanthanides(III) separation. *Talanta*, **2004**, *63* (3), 803-806.
- [9] Draye, M.; Thomas, S.; Cote, G.; Favre-Reguillon, A.; LeBuzit, G.; Guy, A.; Foos, J. Cloud-point extraction for selective removal of Gd(III) and La(III) with 8-hydroxyquinoline. *Sep. Sci. & Tech* **2005**, *40* (13), 611-622.

- [10] Braun, T.; Ghersine, G. *Extraction Chromatography*. Elsevier Scientific Publishing Co.: New York, NY, 1975.
- [11] Wenzel, U.; Ullrich W. Twin column chromatography for industrial scale decontamination processes. *J. Chrom. A.* **2004**, *1023* (2), 207-213.
- [12] Ganetsos, G.; Barker, P.E. *Preparative and Production Scale Chromatography*. CRC Press, 1992.
- [13] Archer J.P. "The development of partition chromatography" Nobel Lecture, December 12, 1952. Nobel Lectures, Chemistry 1942-1962, Elsevier Scientific Pub. Co.: New York, NY 1964.
- [14] Zhang, A.; Wei, Y.; Kumagai, M. Separation of minor actinides and rare earths from a simulated high activity waste by two macroporous silica based polymeric composites. *Sep. Sci. & Tech.* **2007**, *42* (10), 2235-2253.
- [15] Dietz, M; Yaeger, J.; Sajdak, L.R., Jr.; Jensen, M.P. Characterization of an improved extraction chromatographic material for the separation and preconcentration of strontium from acidic media. *Sep. Sci & Tech.* **2005**, *40* (13), 349-366.
- [16] Rydberg, J.; Cox, M.; Musikas, C.; Choppin, G.R.; Solvent Extraction: Principles and Practice. New York: Marcel Dekker, Inc. 2004.
- [17] Alexandratos, S.D.; Zhu, X. Polyols as scaffolds in the development of ion-selective polymers supported reagents: The effect of auxiliary groups on the mechanism of metal ion complexations. *Inorg. Chem.* **2008**, *47* (7), 2831-2836.
- [18] Alexandratos, S.D.; Zhu, X. Bifunctional Coordinating Polymers: Auxiliary groups as a means of tuning the affinity of immobilized phosphate ligands. *Macromolecules.* **2005**, *14* (38), 5981-5986.
- [19] Alexandratos, S.D.; Zhu, X. High-affinity ion-complexing polymer-supported reagent: Immobilized phosphate ligands and their affinity for the uranyl ion. *React. Polym.* **2007**, *67* (5), 375-382.
- [20] Alexandratos, S.D.; Zhu, X. Immobilized Tris(hydroxymethyl)aminomethane as a Scaffold for Ion-Selective Ligands: The Auxiliary group Effect on Metal Ion Binding at the Phosphate Ligand. *Inorg. Chem.* **2007**, *46* (6), 2931-2147.

[21] Ishimora, T.; Watanabe, K. Inorganic Extraction studies on the system of tri-n-butyl phosphate – nitric acid. *Bull. Chem. Soc. Jap.* **1960**, *33* (10), 1443-1448.

[22] Schulz, W.W.; Navratil, J.D. *CRC Science and Technology of Tributyl phosphate: Volume I*. CRC Press: Boca Raton. 1984.

[23] Marcus, Y.; Kertes, A.S.; Yanir, E. *IUPAC Equilibrium Constants of Liquid-Liquid Distribution Reaction; Introduction, And Part 1: Organophosphorus Extractants*. Page Bros (Norwich) Ltd, Norwich: London. 1974.

[24] Martell, A.E.; Smith, R.M. Database 46: NIST Critically Selected Stability Constants of Metal Complexes, Version 8. 2004

[25] Horwitz, E.P.; Bloomquist, C.A.A. Preparation, performance, and factors affecting band spreading of high-efficiency extraction chromatographic columns for actinide separations. *J. Inorg. Nucl. Chem.* **1972**, *34* (12), 3851-71.

[26] Cox, M.; Castresana, M.E.; Castresana, J.; Miralles, W. Interfacial properties and metal extraction chemistry of Organophosphorus Acids: (RO)₂PO(OH), (RO)RPO(OH) and R₂PO(OH). **1983** Proc. of ISEC '83, 268.

[27] Alcock, K.; Best, G.F.; Hesford, E.; McKay, H.A.C.; Tri-n-butyl phosphate as an extracting solvent for inorganic nitrates – V. *J. Inorg. Nucl. Chem.* **1958**, *6* (4), 328-333.

[28] Sato, T. The extraction of uranyl nitrate from nitric acid solutions by tributyl phosphate. *J. Inorg. Nucl. Chem.* **1958**, *6* (4), 334-337.

[29] Nash, K.L.; Gatron, R.C.; Clark, G.A.; Rickert, P.G.; Horwitz, E.P. Hydrolytic and radiolytic degradations of O/Φ/DE(iB)CMPO; continuing studies. *Sep. Sci. Tech.* **1988**, *23* (12-13), 1355-1372.

[30] Nash, K.L. Stability and stoichiometry of uranyl phosphate coordination compounds in aqueous solution. *Radiochimica Acta.* **1993**, *61* (3-4), 147.

[31] Smith, A.L. *Applied Infrared Spectroscopy: Fundamentals, Techniques, and Analytical Problem-solving, Volume 54*. John Wiley & Sons: New York, NY. 1979

[32] Westheimer, F.H.; Eberhard, A. Hydrolysis of Phostonates. *J. Am. Chem. Soc.* **1965**, *87* (2), 253-259.

CHAPTER FOUR

PREFACE

The TALSPEAK separations method has been designated in the United States Department of Energy Fuel Cycle Research and Development program as the preferred approach to the separation of trivalent lanthanides from trivalent actinides. Although testing of the separation has been successful up to the lab scale with actual dissolved fuel, many aspects of the chemistry are still incompletely understood. This has led to much recent investigation regarding the underpinning solution chemistry of the HDEHP extractant, DTPA holdback reagent and lactic acid buffer. Furthermore; systematic investigations of an extraction chromatographic TALSPEAK system has yet to be performed. This chapter attempted to provide a thorough investigation of the chemistry involved in a TALSPEAK extraction chromatographic system. Alternative TALSPEAK reagents (HEH[EHP] and TTHA) were also investigated in this study.

The comparison of metal partitioning behavior in the presence of the larger TTHA holdback reagent with classical TALSPEAK reagents led to a better understanding of the processes occurring in the separation. Since TTHA is a larger polyaminopolycarboxylic acid, the coordination center of a lanthanide can be fully satisfied. A lanthanide will generally have at least one coordination site available for further interaction when binding with DTPA (and potential ternary complex formation). TTHA is also a weaker lanthanide complexant than DTPA in the pH range studied. Acknowledging these qualities of the two hold-back reagents, a more complete understanding of lanthanide ternary complex formation and metal partitioning at high concentrations of lactate was provided.

Comparison of metal partitioning using HDEHP and HEH[EHP] impregnated resin under TALSPEAK conditions also led to some interesting findings. Metal partitioning in TALSPEAK can partially be modeled using known thermodynamic parameters, but the observed pH dependence for metal partitioning is cannot currently be modeled. Experiments performed here displayed even further deviations from predicted patterns using extraction chromatographic HDEHP-TALSPEAK. However, HEH[EHP] impregnated resin appeared to be more resistant to deviations from predicted patterns regardless which holdback reagent (TTHA or DTPA) is used. The reason for the increased deviation of HDEHP extraction chromatographic TALSPEAK is not fully understood, but is thought to be related to the increased tendency of aggregation for the neat extractant present on the resin.

While the studies performed in this TALSPEAK chromatographic remediation were useful, the real significance of the studies was the continued solvent extraction experiments involving TTHA and HEH[EHP] in Chapter 5. Here the potential utility of the phosphonic acid extractant was observed in a way that could revolutionize TALSPEAK separations as they are currently conducted.

CHAPTER FOUR
EXPLORATIONS OF TALSPEAK CHEMISTRY IN EXTRACTION
CHROMATOGRAPHY: COMPARISONS OF TTHA WITH DTPA AND HDEHP WITH
[HEH]EHP

Abstract

The TALSPEAK (Trivalent Actinide - Lanthanide Separation by Phosphorus reagent Extraction from Aqueous Komplexes) process uses an organophosphorus acid ((RO)₂PO₂H; typically bis-(2-ethylhexyl) phosphoric acid (HDEHP)) for extraction of lanthanides to the organic phase and a polyaminopolycarboxylate complexant (typically diethylenetriamine-N,N,N',N'',N'''-pentaacetic acid, DTPA) to retain trivalent actinides in the aqueous phase. The potential of triethylenetetramine- N,N,N',N'',N''',N''''-hexaacetic acid (TTHA) and phosphonic acid extractants ((RO)(R)PO₂H) as alternative holdback reagents and extractants, respectively, has only been briefly considered. Furthermore, TALSPEAK has primarily been studied as a liquid-liquid separation with only minor examinations of chromatographic possibilities. This study aimed to obtain further understanding of TALSPEAK solution chemistry by immobilizing the organic phase on a polymeric support, and contrasting the use of TTHA or 2-ethylhexyl phosphonic acid mono-2-ethylhexyl ester acid (HEH[EHP]) with "classical" TALSPEAK chemistry. Results indicate the replacement of DTPA by TTHA generally provides an improvement in Eu³⁺ and Am³⁺ separation, but TTHA retains lanthanides lighter than Nd³⁺ in the aqueous phase. High concentrations of lactate (>1.0 M) seem to decrease metal extraction by

changing the composition of the organic phase, not through retaining lanthanides in the aqueous phase with the $M(\text{Lac})_4^-$ species. Since comparable lactate and pH dependences were observed using DTPA or TTHA (which saturates the coordination sphere of any lanthanide), the possibility of ternary complex formation, $M(\text{Lac})(\text{DTPA})^-$, in the aqueous phase seems unlikely. While much was learned about TALSPEAK chemistry through these experiments, none of the results indicate an obvious benefit for performing TALSPEAK separations chromatographically.

Introduction

For reprocessing or disposal purposes, the removal of americium from the lanthanides is a necessary step if transmutation is to be realized. Extraneous lanthanides compete for fast-spectrum neutrons needed for the fissioning of americium. Considering the hard-cation^[1] nature and the comparable charge density of Am^{3+} to the lanthanides, this separation is unusually challenging. The most successful approaches to group separation have involved exploiting the slightly greater covalency in Am^{3+} , which results from the slightly higher spatial extension of the 5f orbitals of Am^{3+} compared to Ln^{3+} .^[2-5] The interaction of “softer” nitrogen and sulfur donating ligands with Am^{3+} is stronger than with the lanthanides; thus allowing group separation.

There are several viable approaches for separation of Am^{3+} from the lanthanides based on the manipulation of this chemistry. Unfortunately, the relatively polarizable molecular orbitals encountered in sulfur and pyridine based separations increase the susceptibility for radiolytic breakdown of the ligand.^[6-8] The most tested, and arguably least understood, method for separating trivalent actinides from trivalent lanthanides is the TALSPEAK (Trivalent Actinide - Lanthanide Separation by Phosphorus reagent Extraction from Aqueous Komplexes) solvent

extraction process. The use of TALSPEAK chemistry has less severe radiolysis concerns; however, the complex nature of the TALSPEAK separation process makes understanding the chemistry of the system challenging. Applications of TALSPEAK generally use bis-(2-ethylhexyl) phosphoric acid (HDEHP, organic extractant), diethylenetriamine-N,N,N',N'',N'''-pentaacetic acid (DTPA, holdback reagent), and lactic acid (carboxylic acid buffer). Structures of these three species are shown in [Figure 4.1](#). Successful TALSPEAK separations using these reagents have been observed up to the pilot plant scale. Recent reports have addressed the basic chemistry of TALSPEAK to find that metal distribution data cannot be modeled using known thermodynamic equilibria.^[9-11]

This study aims to advance the understanding of TALSPEAK solution chemistry by comparing performance of triethylenetetramine- N,N,N',N'',N''',N''''-hexaacetic acid (TTHA) with DTPA and 2-ethylhexyl phosphonic acid mono-2-ethylhexyl ester acid (HEH[EHP]) with HDEHP. The alternative holdback reagents have some other benefits as well. Based on binding constants ([Figure 4.2](#)), the alternative use of TTHA may provide an improved separation factor between the lanthanides and americium. Since HEH[EHP] has a stronger P-C bond present (compared to HDEHP's three P-O bonds), the phosphonic acid should be more resistant to radiolytic degradation.

Another thoroughly unexplored area of investigations is the use of extraction chromatographic materials to perform TALSPEAK chemistry. Previous reports have examined chromatographic TALSPEAK separations using aqueous phase conditions observed in liquid-liquid systems that provide the highest separation factors and applying them to HDEHP immobilized on silica supports.^[12,13] While the "proof-of-concept" studies were successful in separating Am³⁺ from Eu³⁺ when using a column length >12 cm, a more indepth investigation

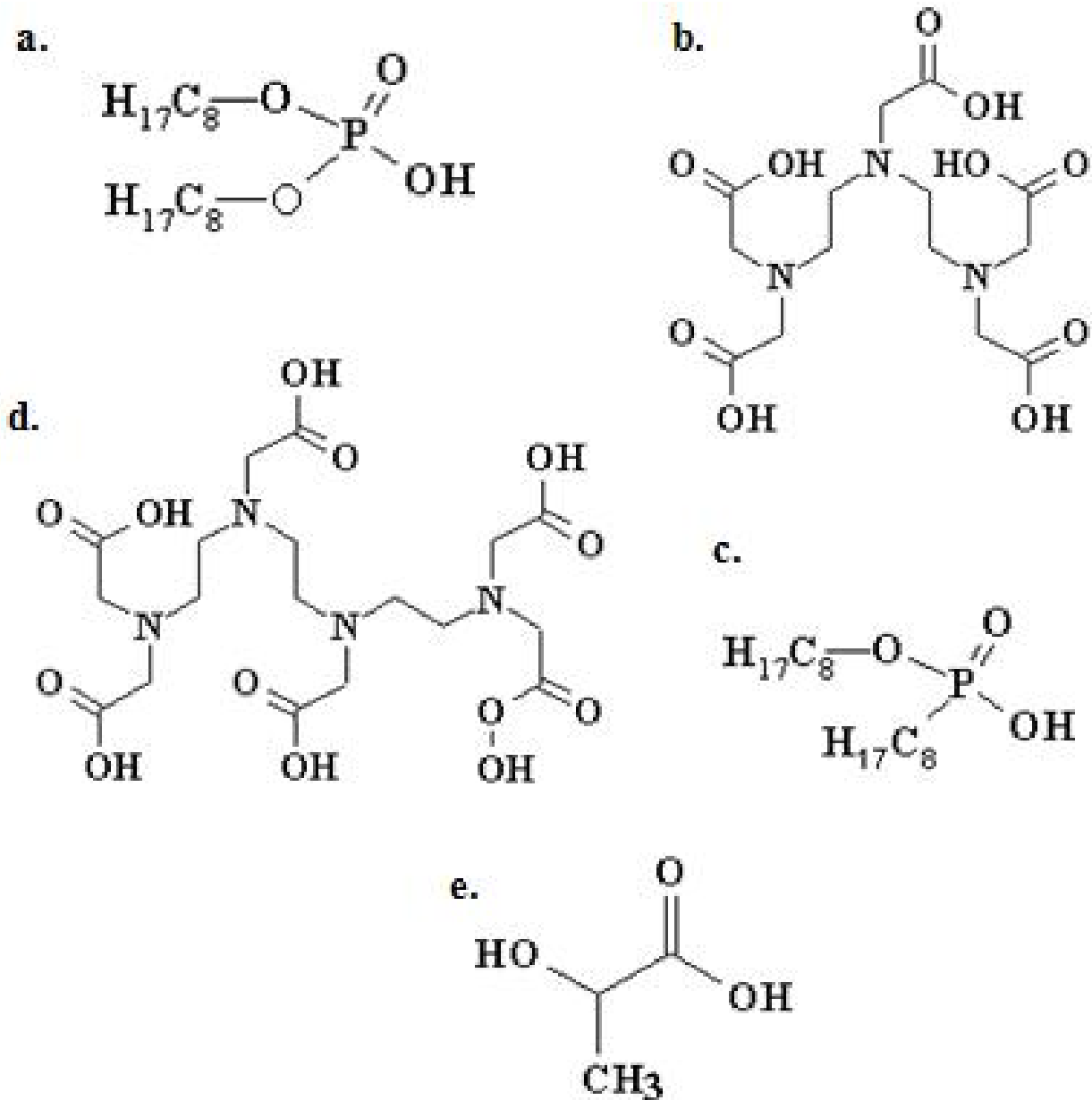


Figure 4.1. Structures of the components used in these studies; a: di(2-ethylhexyl) phosphoric acid (HDEHP) b: diethylenetriamine-N,N,N',N'',N'''-pentaacetic acid (DTPA) c: 2-ethylhexyl phosphonic acid mono-2-ethylhexyl ester acid (HEH[EHP]) d: triethylenetetramine-N,N,N',N'',N''',N''''-hexaacetic acid (TTHA) e: lactic acid (HL)

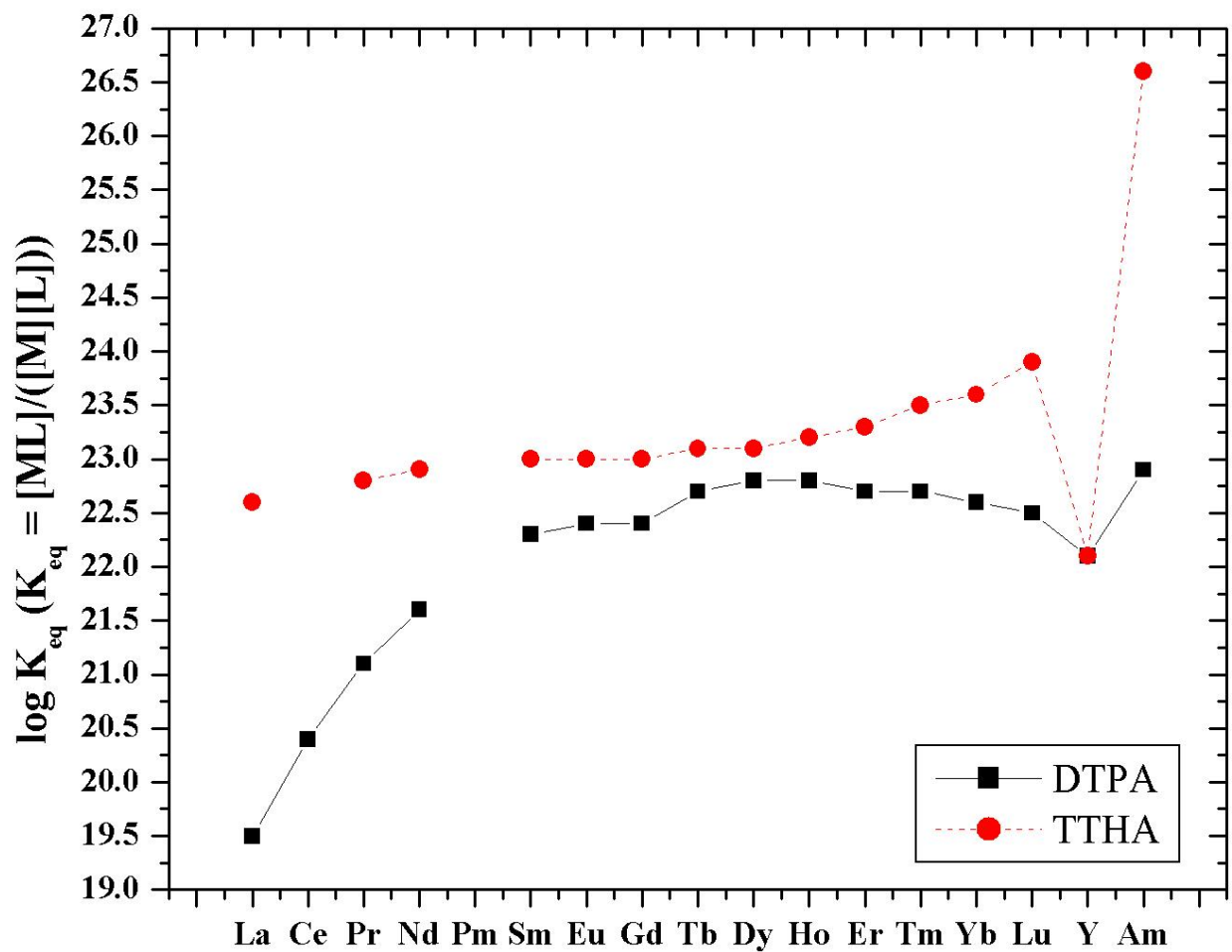


Figure 4.2. Equilibrium constants for DTPA and TTHA with the lanthanides and americium in 0.1 M ionic media at 25 °C.^[16,18]

studying the variation of each TALSPEAK component has not been reported. With this in mind, a systematic examination of TALSPEAK chemistry has been performed on a series of extraction chromatographic materials comprised of two different acidic organophosphorus extractants (HDEHP and HEH[EHP]). Each was sorbed onto Amberchrom CG-71, an aliphatic polymethacrylate polymer. Of particular interest in these studies was using the results of extraction chromatographic (EXC) experiments to understand the nuances of TALSPEAK chemistry.

Experimental

Reagents

Nitric acid solutions were prepared from Trace Metal Grade acids (Fisher Scientific) using deionized water obtained from a Milli-Q2 water purification system. Acid solutions were standardized using Fisher Certified 1.0 M NaOH and an Ag/AgCl pH electrode. All aqueous solutions were fixed at 1.0 M NO_3^- . Sodium nitrate (Ricca Chemical Company) was dissolved in deionized water, filtered through a 1.0 μm membrane, recrystallized from H_2O and redissolved in H_2O to prepare a 5.28 mol NaNO_3/kg solution, as determined through use of Eichrom, 4% crosslinked, cation exchange resin and potentiometric titration. Lanthanide oxides, 99.999%, purchased from Arris International, were used to prepare lanthanide nitrate stock solutions (La, Ce, Pr, Nd, Sm, Eu, Gd, Tb, Dy, Ho, Er, Tm, Yb, Lu, Y). Metal content and acid content of lanthanide solutions was determined using a Varian ICP-AES and Eichrom cation-exchange

resin, respectively. All radioactive isotopes were stored in 0.5 M HNO₃. ¹⁴⁷Pm, ¹⁵²Eu carrier-free nitrates were obtained from Isotope Product Laboratories. The ²⁴¹Am had an additional 10 µg/mL of Eu³⁺ carrier to prevent sorption of americium to the glass. DTPA and TTHA were obtained from Fluka and VWR, respectively. Stock solutions of polyaminopolycarboxylic acids were prepared by dissolving the solid acid in solution and adding 1.0 M NaOH to raise the pH to 3.6. A simulated liquid waste (SLW) lanthanide solution was prepared using information previously published.^[14] The composition of this solution is listed in [Table 4.2](#).

Resin Preparation

The extraction chromatographic materials were prepared from bis-(2-ethylhexyl) phosphoric acid (HDEHP, Sigma-Aldrich), 2-ethyl(hexyl) phosphonic acid mono-2-ethyl(hexyl) ester (HEH[EHP], Albright and Wilson) on Amberchrom CG71 (50-100 mm, polymethacrylate, Eichrom Technologies, Inc.). The HDEHP and HEH[EHP] prepared resins are marketed by Eichrom under the LN and LN2 trade names, respectively. The organophosphorus acids were purified by the third phase formation procedure prior to production of the EXC materials.^[15] In a typical preparation, 10 grams of purified extractant were dissolved in 100 mL of methanol and mixed with 15 grams of resin, then stirred for 1 h on a rotary evaporator. The methanol was removed by applying a vacuum and heating the mixture to 50°C using a water bath to yield a free flowing material comprising 40% (w:w) of extractant on the resin.

Procedures

Determination of Weight Distribution Ratios (D_w)

The uptake of metal ions by the EXC materials from acidic solutions was measured by contacting a known volume of solution (5.0 mL for ICP-AES analysis, 0.5 mL for radiotracer analysis) with a known mass of resin (200 mg for ICP-AES analysis and 900 mg for radiotracer analysis) in a borosilicate glass culture tube as described previously.^[16] Following equilibration with the resin, the aqueous phase was passed through a 0.45 μm PTFE filter to remove any resin particles. ^{147}Pm was determined using a Packard TriCarb 2550 TR/AB liquid scintillation counter and Ultima Gold scintillation cocktail. ^{152}Eu and ^{241}Am were determined using a Packard Cobra II Auto-Gamma NaI detector (sodium, lactate and polyaminocarboxylic acid dependencies) or a Canberra HPGe detector (pH dependence) when ^{241}Am and ^{152}Eu were present in the same solution.

For the studies examining lanthanide uptake by the resins, five stock solutions were prepared containing 4 – 80 ppm each of 5 – 6 adjacent lanthanides. Lanthanide concentrations were selected to maximize detection while preventing metal loading. Each stock solution contained a metal ion in common with at least one other solution, allowing accurate separation factors to be measured for the entire series of lanthanides and yttrium. Duplicate measurements for the same metal ions in different stock solutions agreed within 10%, therefore no corrections were applied to the acid dependency data. An equilibration time of one hour was used in all determinations of weight distribution ratios, except for data generated on the kinetics of uptake by the EXC materials, where equilibration times were varied from 1 to 120 minutes.

Weight distribution ratios (D_w) were calculated using Equation 4.1, where A_o and A_s are the

$$D_w = ((A_o - A_s / w)(A_s / V) \quad (4.1)$$

aqueous phase metal ion concentrations (ppm) before and after equilibration, w is the dry weight of the resin in grams and V is the volume of aqueous phase in milliliters. The weight distribution ratios were converted to the number of free column volumes to peak maximum, k' (the resin capacity factor), by first calculating the volume distribution ratio, D_v , using Equation 4.2, where

$$D_v = D_w \cdot d_{extr} / 0.4 \quad (4.2)$$

d_{extr} is the density of the extractant and 0.4 is the extractant loading in grams of extractant per gram of resin as provided from the manufacturer. The D_v values were then converted to k' by using Equation 4.3, where v_s and v_m are the volumes of stationary phase (extractant) and mobile

$$k' = D_v \cdot (v_s / v_m) \quad (4.3)$$

phase, respectively, for slurry packed columns of the EXC materials. The physical constants necessary to convert D_w to k' for packed columns of the EXC materials have been listed previously.^[16] By combining Equations 2 and 3, and using the conversion values reported^[16] for d_{extr} and v_s/v_m , one obtains Equation 4. The bed densities of the EXC materials were measured

$$k' = D_w \cdot (d_{extr} \cdot v_s) / (0.4 \cdot v_m) \quad (4.4)$$

by slurry packing a known mass of resin into a graduated cylinder and dividing the mass of resin by the volume of the bed.

Column Elution of Metal Ions

The column elution behavior of selected lanthanide ions was determined using the equipment detailed previously.^[16] For the purposes of this report, TALSPEAK conditions are defined as the aqueous phase containing 1.0 M NO_3^- and 1 M total lactate and the noted

concentration of polyaminopolycarboxylic holdback reagent. For Am/Eu studies, analyte loading was performed in 5 mL of 0.01 M HNO₃ or under the specified TALSPEAK conditions. For simulated waste studies, loading was performed in 2.5 mL of 0.001 M HNO₃ with 0.1 M lactate at a pH of 3.6 or under the specified TALSPEAK conditions. The increased amount of metal and addition of lighter (and typically less extractable) lanthanides justified the addition of a buffer, a decrease in the amount of metal loading and an increase in pH to ensure quantitative metal loading. For some columns, loading was performed in the presence of specified TALSPEAK conditions and solutions at all stages were heated to 50°C to potentially expedite uptake kinetics. All columns included a one bed volume wash of the column with the same nitric acid concentration used during the load and concluded with a strip of the remaining material with five bed volumes of 1.0 M HNO₃. HPGe analysis displayed no remaining activity on the column when gamma emitting isotopes of Am³⁺ or Eu³⁺ were investigated. Column investigations presented are composites from separate runs analyzing ²⁴¹Am, ¹⁴⁷Pm and the lanthanides. Lanthanide column investigations utilized the same instrumental parameters noted previously; however, since a single lanthanide column was run for each condition, all lanthanides present in the SLW were analyzed by the ICP-AES in the same solution.

Results

Batch Studies

A value of $k' \leq 1$ indicates behavior in which the analyte will be removed from the column after one bed volume of rinsing under the noted conditions. Therefore, metal uptake when $k' \leq 1$

is too low to be quantified. Figures presenting batch partitioning of analytes will only present data where the k' values were greater than 1. A note will be made when distribution to the resin phase was investigated, but too low to be quantified.

pH Dependence

An initial analysis was performed to examine the optimum pH for Am/Eu TALSPEAK separations using TTHA or DTPA with a combination of the LN or LN2 resin. The total concentration of lactate was 1 M for all conditions and 1.0 mM Eu was present. [Figures 4.3 and 4.4](#) show the separation tendencies for LN and LN2 resins, respectively. Europium partitioning into the LN resin from a DTPA aqueous phase was described with k' values less than one when the pH was greater than 3.8. Americium values of $k' < 1$ were observed at a pH of 3.5 and 2.8 for TTHA and DTPA systems, respectively, using LN and LN2 resins. These pH's were highlighted for future column investigations. An examination of americium partitioning by the LN2 resin from a DTPA aqueous media was investigated, but all k' values were less than 1 and therefore not shown in [Figure 4.4](#).

Kinetics Investigation

Reports regarding the liquid-liquid TALSPEAK system have shown phase transfer kinetics to be slow under some conditions. To develop some understanding regarding the kinetics of the extraction chromatographic system, Eu^{3+} and Am^{3+} uptake was monitored at a pH where both

Am^{3+} and Eu^{3+} partitioning would be quantifiable (i.e. $k' > 1$) for the LN system. Time traces are shown in Figure 4.5. Initial investigations with the LN resin indicated the time for Am^{3+}

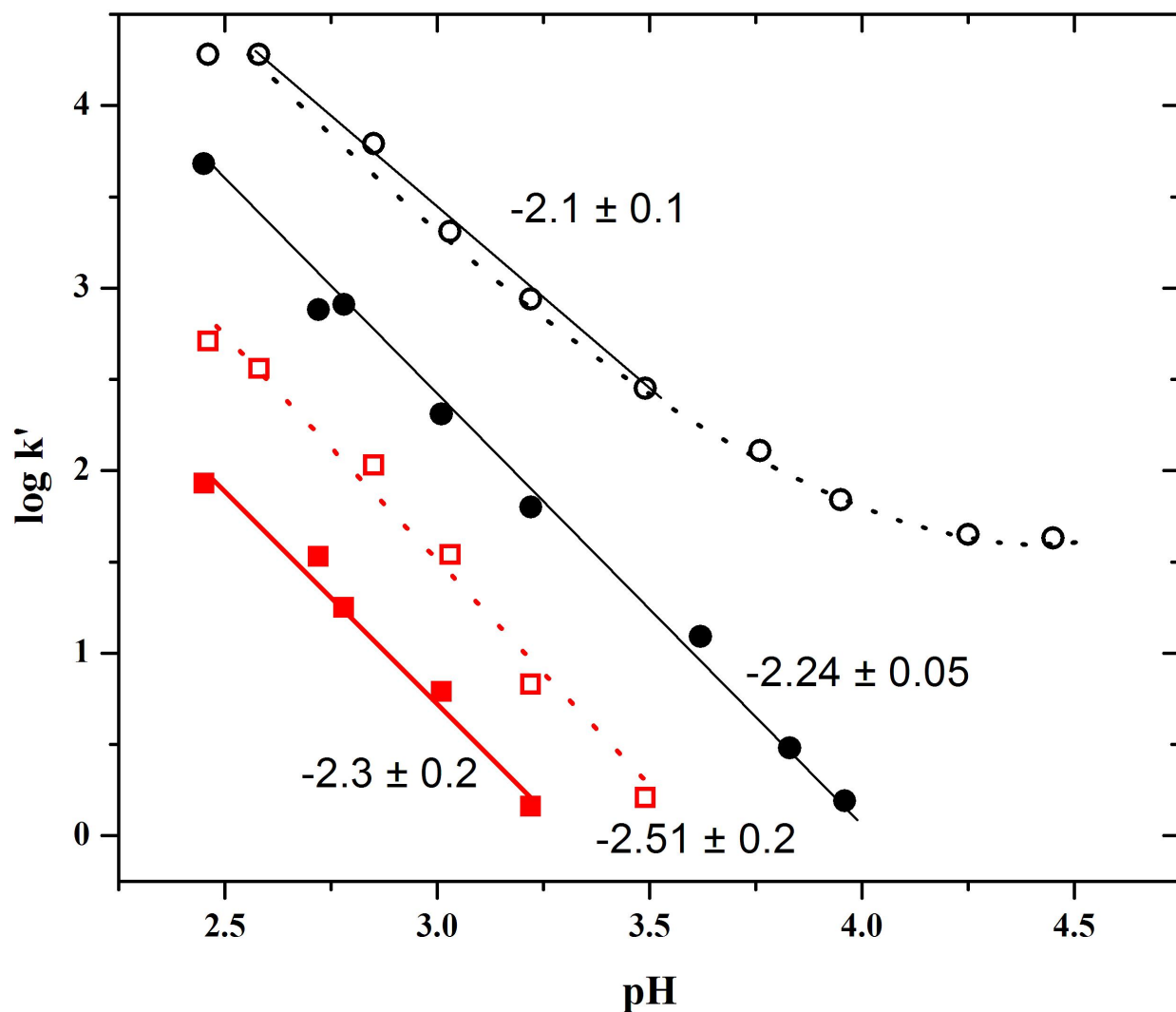


Figure 4.3. Uptake of europium and americium as a function of pH using 900 mg of LN (HDEHP) resin. Aqueous phase was 0.5 mL and included 1 mM Eu, 1 M total lactic acid, 1 M NO_3^- and 5 mM DTPA or TTHA. Contact time was one hour. Values next to lines describe the slope of the data on a logarithmic scale. All errors presented are estimated at 10%. *DTPA* -- ● *Eu* ■ *Am* *TTHA* -- ○ *Eu* □ *Am*

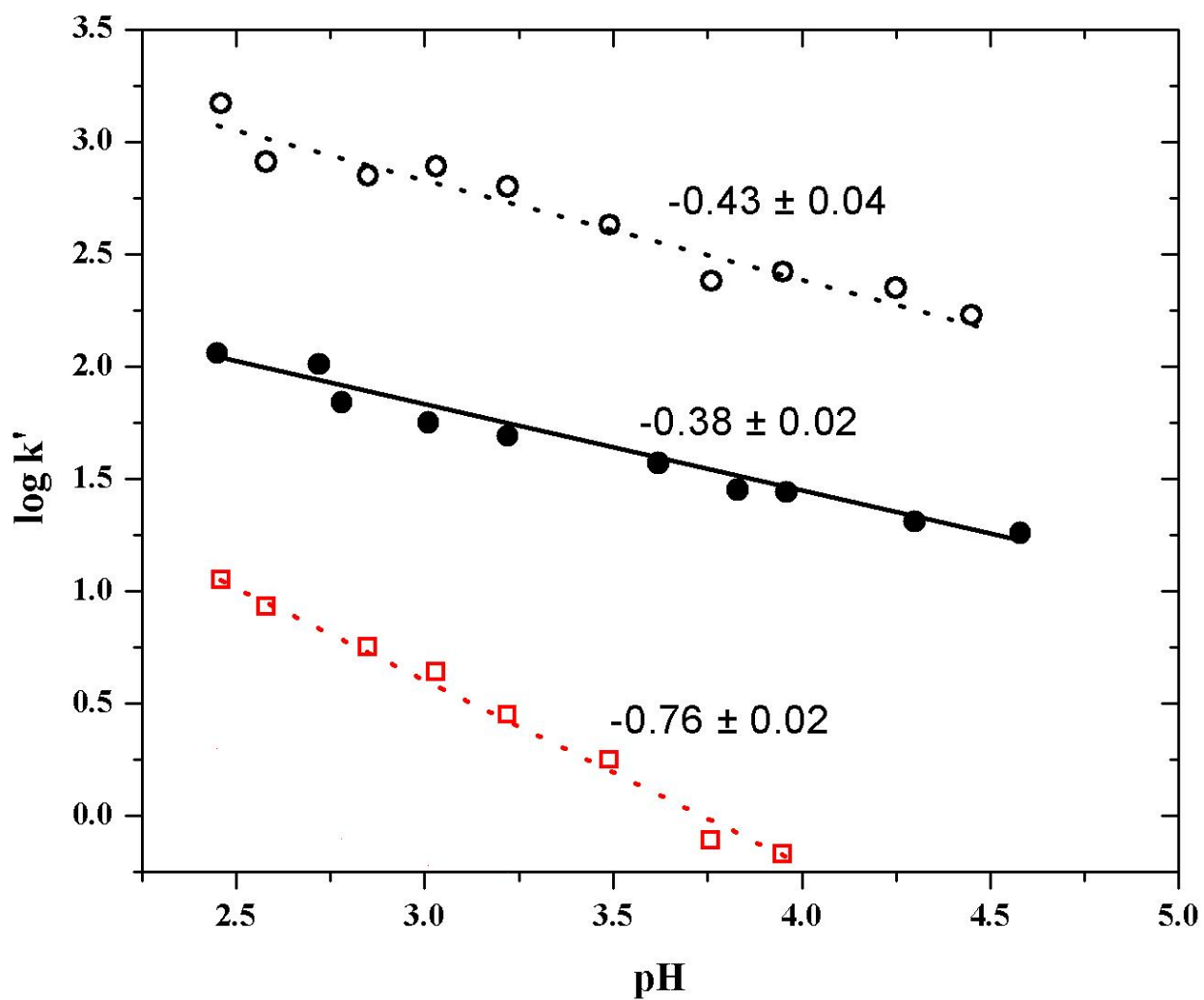


Figure 4.4. Uptake of europium and americium as a function of pH using 900 mg of LN2 (HEH[EHP]) resin. Aqueous phase was 0.5 mL and included 1 mM Eu, 1 M total lactic acid, 1 M NO_3^- and 5 mM DTPA or TTHA. Contact time was one hour. Values next to lines describe

the slope of the data on a logarithmic scale. All errors presented are estimated at 10%. *DTPA* -- ●
Eu ○ *Am* □

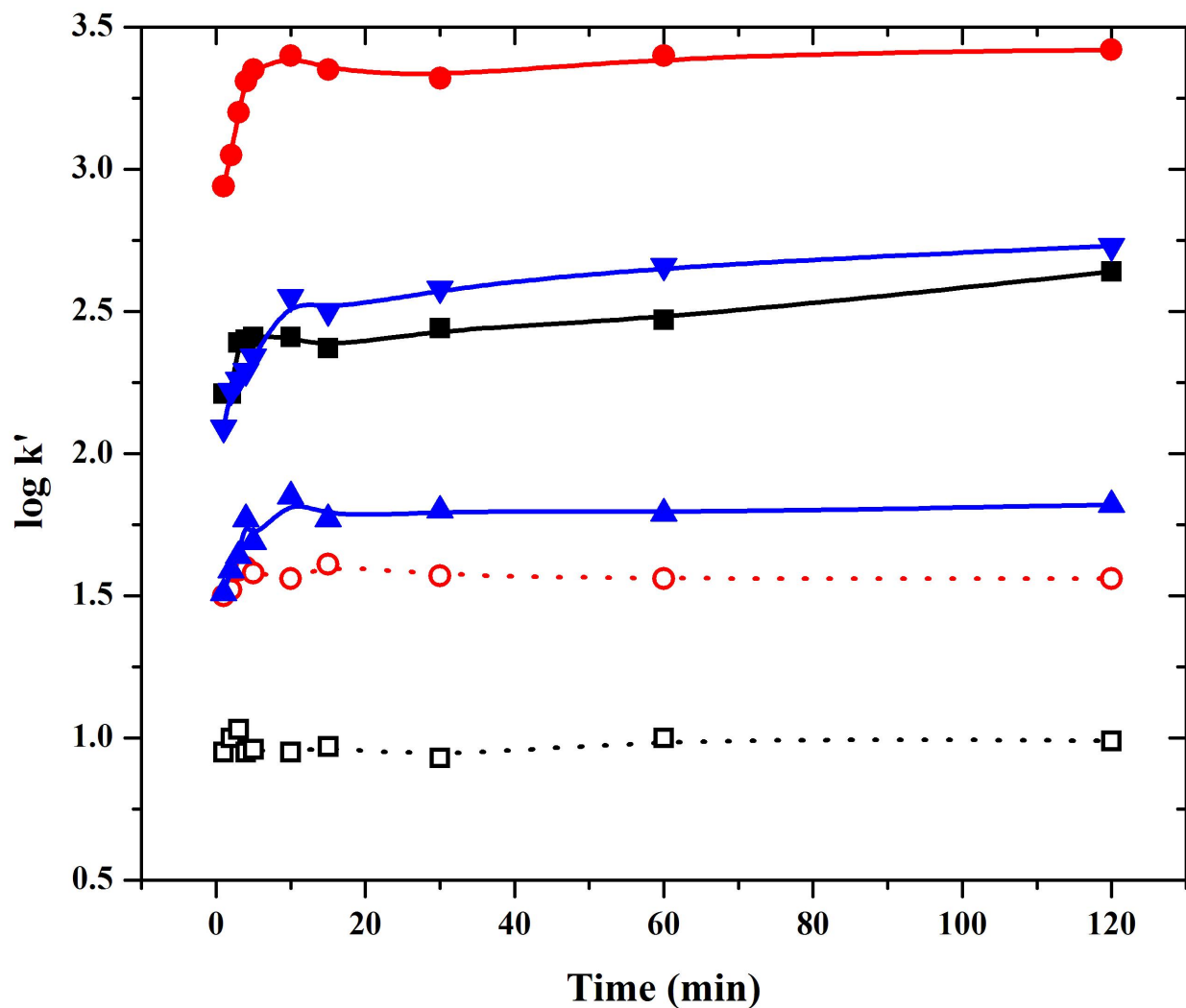


Figure 4.5. Comparison of the rate of uptake of americium and europium by 900 mg of LN or LN2 resins under TALSPEAK conditions. Aqueous phase was 0.5 mL and included 1 mM Eu, 1 M total lactic acid, 1 M NO_3^- and 5 mM DTPA or TTHA. All errors presented are estimated at 10%. The aqueous phase pH for each system is as follows: DTPA/LN – 2.39, DTPA/LN2 –

2.78, TTHA/LN – 3.03, TTHA/LN2 – 3.49. DTPA/LN – ■ Eu □ Am DTPA/LN2 – ● Eu ○ Am
DTPA/LN2/Eu – ▲ TTHA/LN2/Eu – ▼

equilibration was virtually negligible when compared to the time required for Eu^{3+} equilibration. For this reason, kinetics of the LN2 system were only observed with Eu^{3+} .

Lactate Dependence

Although intended primarily as a pH buffer in TALSPEAK chemistry, lactate has shown a more profound impact on Am/Eu separations. [Figure 4.6](#) shows the uptake of Eu^{3+} and Am^{3+} from a TTHA or DTPA TALSPEAK aqueous phase using either the LN (for Am^{3+} and Eu^{3+}) or the LN2 resin (Eu^{3+} only). The pH was consistent for both DTPA and TTHA to ensure appropriate comparisons. Increasing the lactate concentration leads to a decrease in analyte uptake for all systems. Increasing the concentration of lactate beyond 1.0 M for the LN/DTPA system, generates a dramatic decrease in Eu^{3+} uptake with a slope of -4.5 on the logarithmic plot. An examination of americium partitioning by the LN2 resin from a DTPA aqueous media was examined, but it was found all k' values were less than 1 and therefore not shown in [Figure 4.6](#).

Lanthanide + Yttrium Uptake

Figure 4.7 shows the uptake behavior of elements anticipated in a simulated TALSPEAK waste feed. The pH of the aqueous phase and concentrations of DTPA and TTHA were manipulated to encourage holdback (and detection) of the heavier lanthanides. For the lighter lanthanides, DTPA and TTHA produce different metal partitioning patterns. A greater retention of the lighter lanthanides was observed by TTHA when compared to DTPA. The familiar lanthanide partitioning pattern observed in TALSPEAK solvent extraction studies when DTPA is

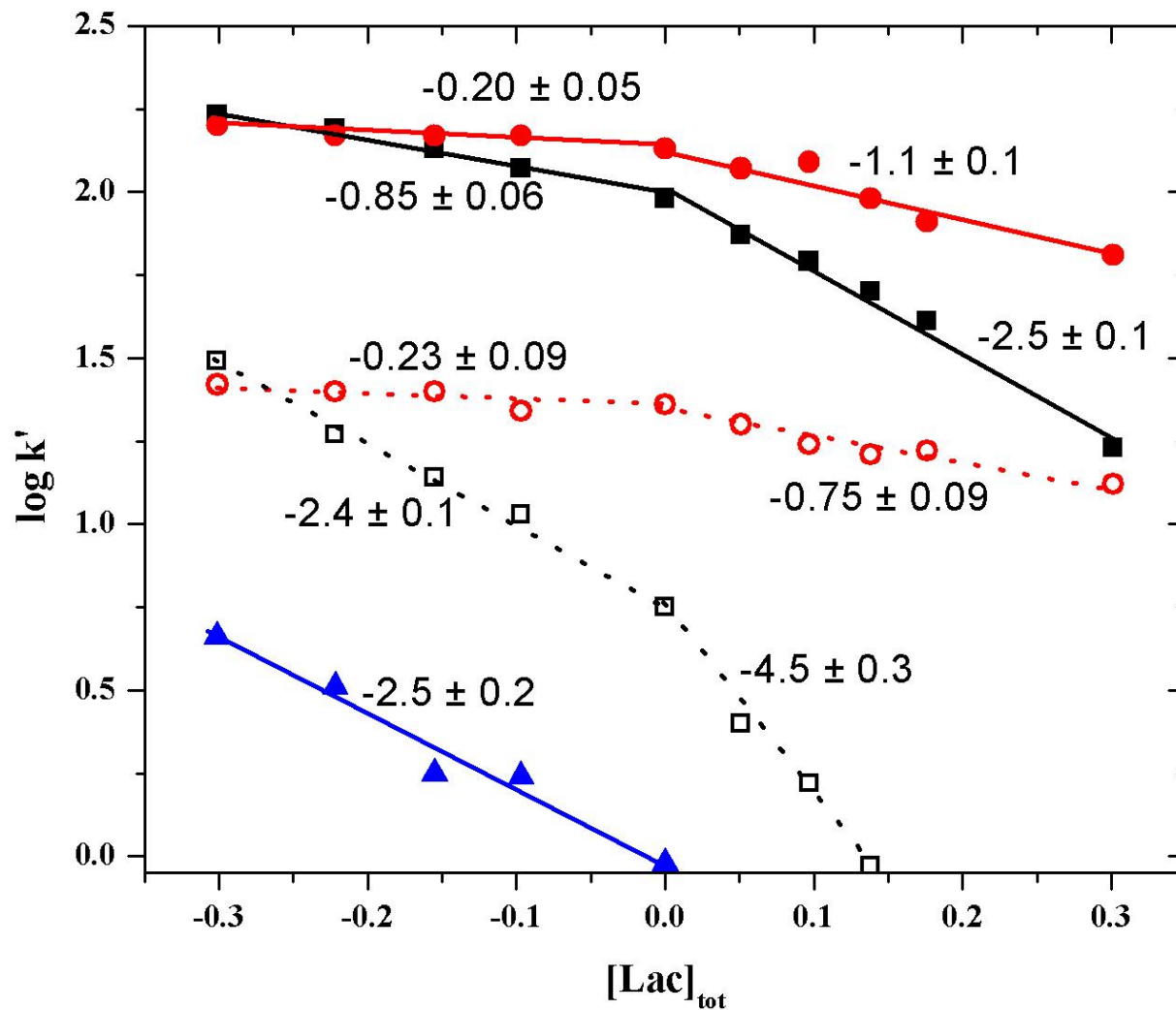


Figure 4.6. The uptake of Eu and Am as a function of the formal concentration of lactate by 900 mg of LN or LN2 resins. Aqueous phase was 0.5 mL at a pH of 3.6 and included 1 mM Eu, 1 M NO_3^- and 5 mM DTPA or TTHA. Values next to lines describe the slope of the data on a logarithmic scale. All errors presented are estimated at 10%. Contact time was one hour. LN/Eu – ■ TTHA □ DTPA LN2/Eu – ● TTHA ○ DTPA LN/Am/TTHA – ▲

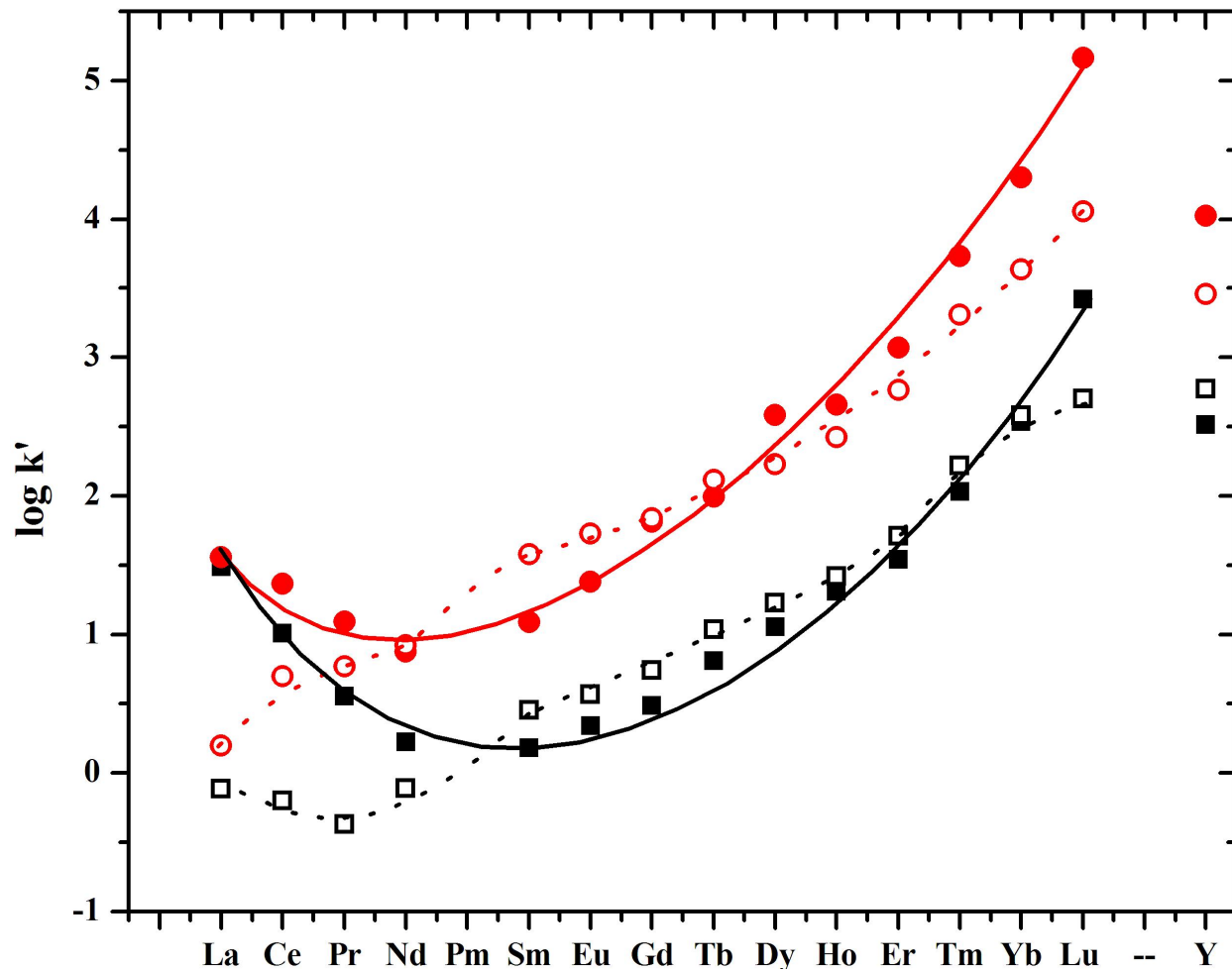


Figure 4.7. Lanthanide + Y uptake under TALSPEAK conditions by 900 mg of LN and LN2 resins. The aqueous phase was 0.5 mL at a pH of 3.6 (DTPA) or 3.9 (TTHA) and included 1 mM Eu, 1 M total lactate, 1 M NO_3^- and 5 mM DTPA or 10 mM TTHA. Lanthanide concentrations ranged from 8 to 60 ppm to provide the maximum detection limits possible by the ICP-AES. All experiments were performed at a lanthanide resin loading of less than 3%. Contact time was one hour. All errors presented are estimated at 10%. ■ LN/DTPA □ LN/TTHA ● LN2/DTPA ○ LN2/TTHA

present was observed in this study for both the LN and LN2 resins. The change in extraction of the lanthanides heavier than samarium is comparable for both hold-back reagents.

Polyaminopolycarboxylic Acid Dependence

To further optimize the purity of the initial Am^{3+} strip, the polyaminopolycarboxylic acid concentration was varied (Figure 4.8). Both the trends for the LN and LN2 resin were considered. The dependences were performed at the pH of 3.5 and 2.8 for TTHA and DTPA systems, respectively. Investigated DTPA and TTHA ranges were determined by preliminary studies. The pH of the TTHA study was higher to encourage retention of americium in the aqueous phase.

Am/Eu Column Investigations (LN2 Resin)

The separations behavior of Am^{3+} and Eu^{3+} was studied chromatographically with Am^{3+} and Eu^{3+} in the same solution. The percentage of Am^{3+} and Eu^{3+} in each stage of separation is noted in Table 4.1. The chromatogram for the most successful separation (using the LN2 resin with 0.05 M TTHA, pH=3.5 at 50°C) is shown in Figure 4.9. The separation factor between Am^{3+} and Eu^{3+} was 120 for this system.

SLW Column Investigations

The separation of an anticipated simulated trivalent f-element waste stream was studied

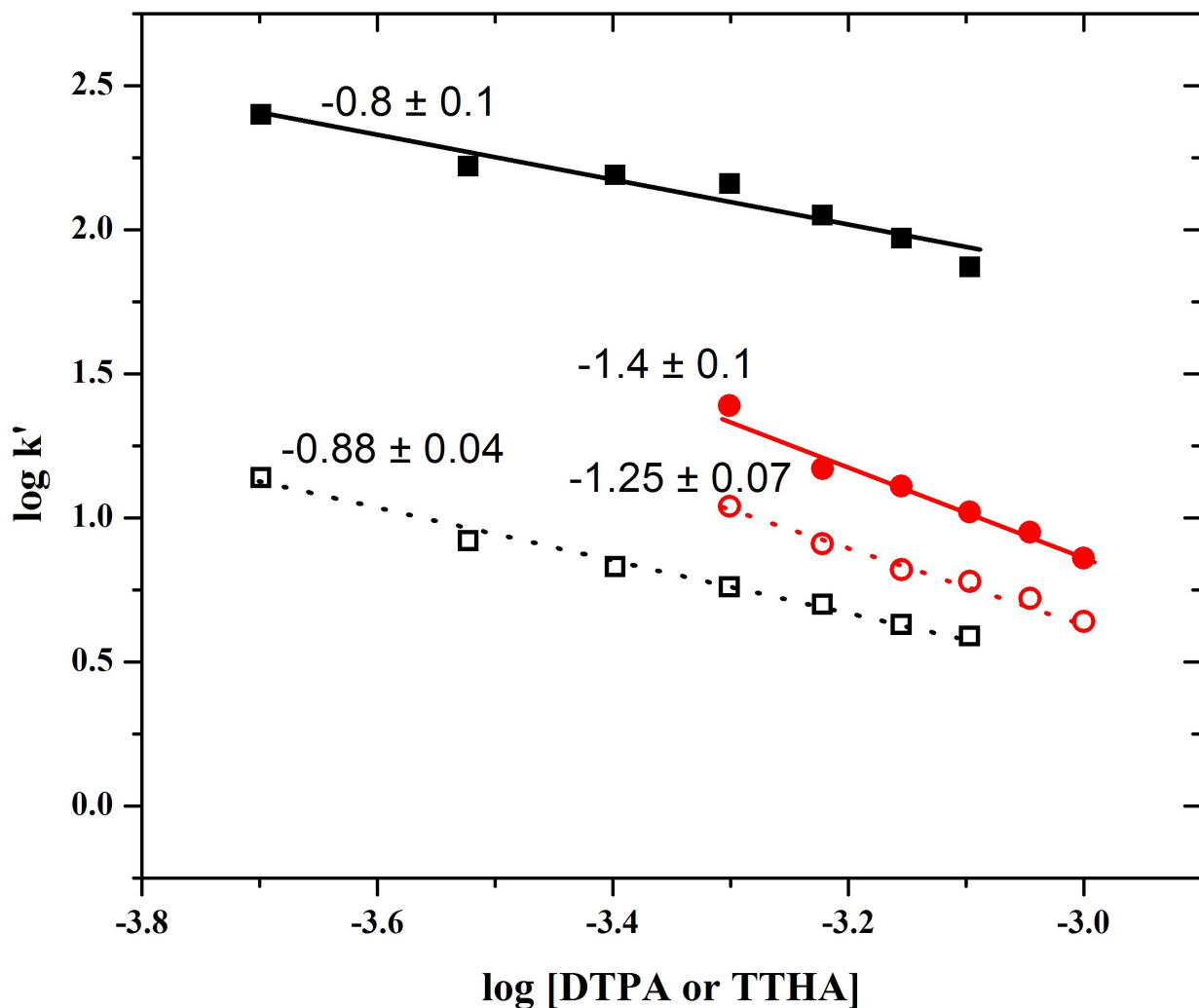


Figure 4.8. Dependence of americium distribution on the concentration of select polyaminopolycarboxylic acids with 900 mg of LN or LN2 resin. The aqueous phase was 0.5 mL at a pH of 2.8 (DTPA) and 3.5 (TTHA) and included 1 mM Eu, 1 M total lactate and 1 M NO_3^- . Values next to lines describe the slope of the data on a logarithmic scale. All errors presented are estimated at 10%. Contact time was one hour. ■ LN/DTPA □ LN2/DTPA ● LN/TTHA ○ LN2/TTHA

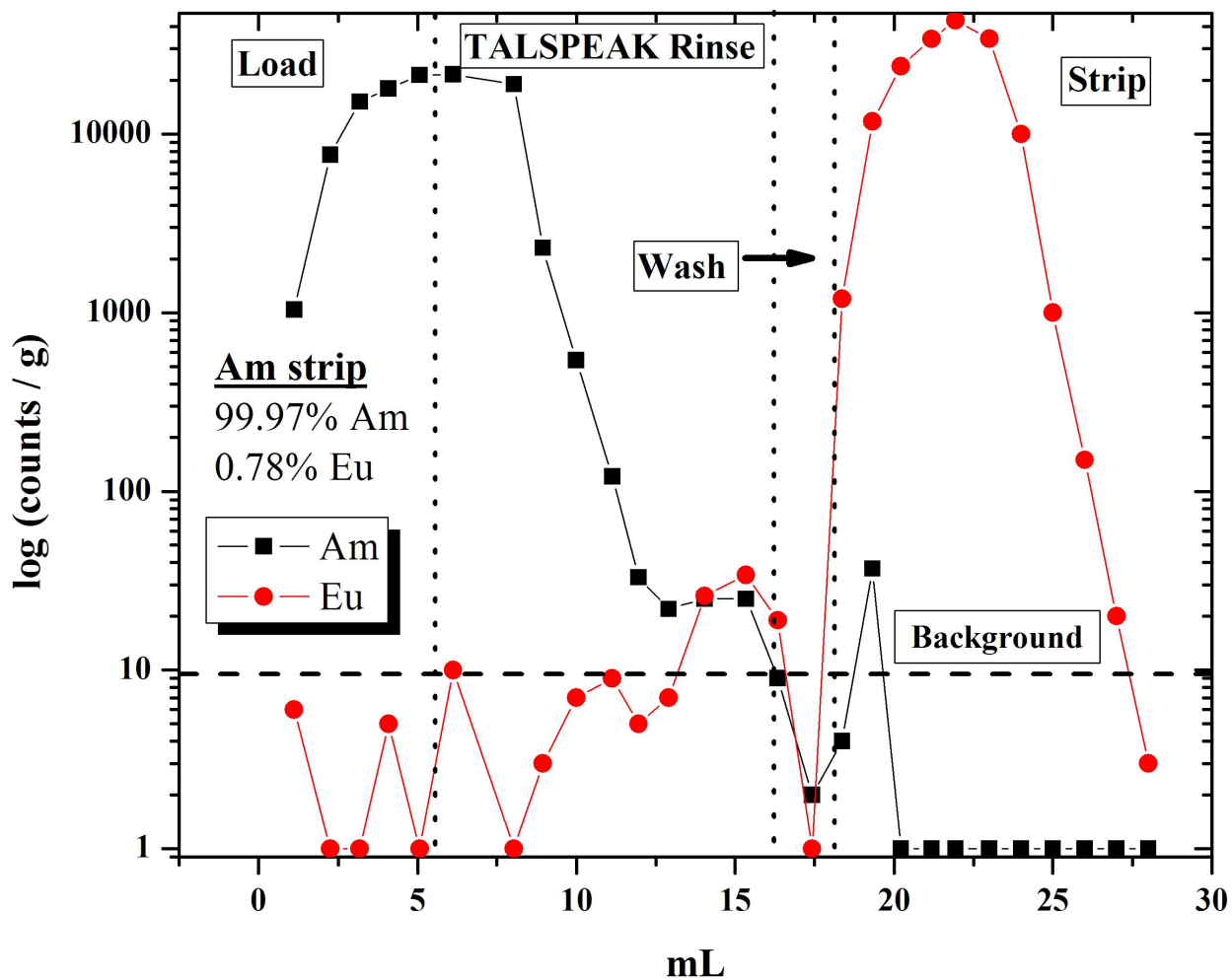


Figure 4.9. Optimized Am(III), Eu(III) elution curve separation using LN2 (HEH[EHP]) S-grade (50-100 μ m) Amberchrom GC71 resin. Flow rate: 1 mL / min. Temperature: 50° C. **Load:** 5 mM TTHA, 1 M NO_3^- , pH 3.6, 1 mM Eu, Trace Am **TALSPEAK Rinse:** 5 mM TTHA, 1 M NO_3^- , pH 3.6 **Wash:** 0.001 M HNO_3 **Strip:** 1 M HNO_3 . ■ Am ● Eu

Table 4.1. Column performance for Am/Eu separation with LN2 resin using 5 mM DTPA or TTHA at a pH of 2.78 or 3.5, respectively. [Eu] = 1 mM, [Lac]_{tot} = 1 M, [NO₃⁻] = 1 M, flow rate and temperature 1 mL / min or 25° C, respectively, unless otherwise noted.

	Varied Parameter					
	--		0.5 mL / min		50°C	
	% Am ^a	% Eu ^b	% Am ^a	% Eu ^b	% Am ^a	% Eu ^b
DTPA	100	31.8	100	31.4	99.9	13.7
TTHA	100	3.7	99.9	3.5	100	0.8

^aIndicates Am recovered during TALSPEAK rinse

^bIndicates Eu impurity recovered during TALSPEAK rinse

chromatographically. To expedite optimization, the majority of separations were performed observing Am³⁺ separation from Pm³⁺ in the presence of a SLW mixture. Column behavior of the lanthanides was examined for conditions providing the highest purity Am³⁺ or the best recovery of the lanthanides in the designed lanthanide strip. The column separation factors are noted in [Figure 4.10](#), as well as the percent Am³⁺ recovered in the designed TALSPEAK Am³⁺ strip. [Table 4.2](#) shows the concentrations of the lanthanides from a simulated liquid waste feed at each stage based on the best overall separation obtained between Am³⁺ and the lanthanides.

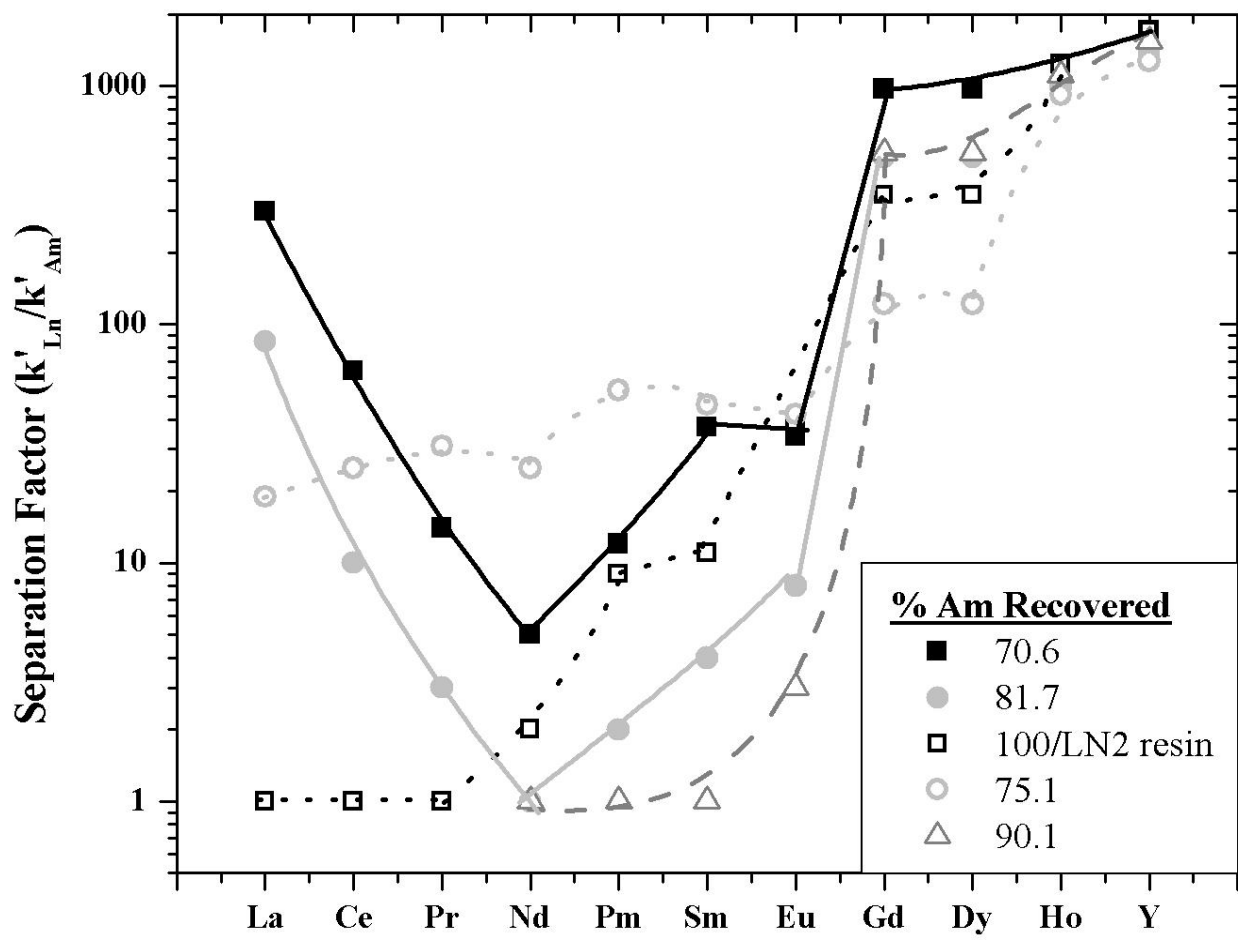


Figure 4.10. Separation factors of Am from simulated liquid waste lanthanides using the LN resin (unless otherwise noted) under the conditions supplied. $[\text{NO}_3^-] = 1 \text{ M}$, $[\text{Lac}] = 1 \text{ M}$. Lanthanide concentrations defined in Table 2. *DTPA* (*mM*, *pH*) -- ■ 0.5, 3.4 ● 2.5, 3.5 *TTHA* (*mM*, *pH*) -- □ 5, 3.5 (LN2 resin) ○ 2.5, 3.5 △ 10, 3.8.

Table 4.2. Optimized lanthanide elution curve separation using LN (HDEHP) S-grade (50-100 μm) Amberchrom GC71 resin. Flow rate: 1 mL / min. Column rinse volume: 20 mL. Column strip volume: 10 mL **Load:** 1 M Lactate, pH 3.3, simulated waste concentrations of lanthanides **TALSPEAK Rinse:** 2.5 mM TTHA, 1 M NO_3^- , pH 3.5 **Wash:** 0.001 M HNO_3 **Strip:** 1 M HNO_3

Lanthanide	[Ln], mM	Rinse %	Elution %	Total Recovery %
La	0.63	3.4	96.1	99.5
Ce	1.2	2.6	97.2	99.8
Pr	0.58	2.1	97.6	99.7
Nd	2.0	2.6	97.1	99.7
Pm	Trace	1.4	98.6	100
Sm	0.41	1.6	98.3	99.9
Eu	0.077	0.15	99.6	99.9
Gd	0.012	0.59	99.2	99.8
Tb	.0038	0.25	99.7	99.9
Dy	.0025	0.10	99.9	100
Y	1.7	>0.01	99.8	99.8
Am	Trace	75	25	100

Discussion

Previous Uses of Phosphonic Acids and TTHA for TALSPEAK

In the original Oak Ridge report, Weaver and Kappelmann briefly examined phosphonic acid extractants.^[12] It was concluded that various phosphonic acid extractants provided a comparable separation of Eu^{3+} from Am^{3+} in relationship to HDEHP. This is expected since lanthanide extraction with phosphoric or phosphonic acids increases in a comparable fashion across the lanthanide series.^[16,17] While HDEHP and HEH[HEP] are structurally analogous and contain comparable lanthanide extraction trends, the differences in dimerization constant, pKa and

sodium extraction provide an interesting basis for comparing lanthanide partitioning of both extractants in a TALSPEAK system.^[18]

The Oak Ridge report also examined the capabilities of TTHA as an americium hold-back reagent. Under the particular conditions examined in the study, TTHA was shown to insufficiently compete with the organophosphorus acid for the americium. Since separation efficiency is determined by both the relative strength of complexes with the polyaminopolycarboxylate and organophosphorus extractant, considering the relative stability of both complexes provides guidance for group selectivity. Figure 4.2 shows the stability constants for DTPA and TTHA with the lanthanides and americium.^[19] TALSPEAK separation factors between Am^{3+} and Nd^{3+} (the least extracted lanthanide) are range from 10-100 depending on the combination of DTPA and HDEHP concentrations used. The difference in $\log \beta$ for DTPA at 0.1 M ionic strength between Am^{3+} and Nd^{3+} is seen to be about 1.5. For TTHA, the difference in $\log \beta$ between Am^{3+} and Nd^{3+} is about 4. Therefore; much larger separation factors might be possible using TTHA as a holdback reagent if large enough concentrations are used to compete with HDEHP.

Equilibrium Constants of Significance

The complexity of TALSPEAK chemistry is emphasized when the number of active species in solution are taken into account. For the purposes of this investigation, the speciation of the additional extractant (HEH[EHP]) and hold-back reagent (TTHA) will need to be considered. Accounting for the varied speciation advances discussion of the individual components of the

system. Table 4.3 shows the reactions of significance to the TALSPEAK process and their equilibrium constants. An in depth review of these reactions and their impact on the overall chemistry of the system has been performed previously.^[9,10] Speciation calculations based on the pK_a's of DTPA and TTHA listed in Table 4.3 allow calculation of the polyaminopolycarboxylate species available for analyte binding. The speciation diagram for TTHA in relevant TALSPEAK pH ranges is shown in Figure 4.11. A comparable speciation diagram for DTPA has been provided previously.^[9] Thermodynamic data in Table 4.3 also note the binding of a trivalent cation with DTPA (D) or TTHA (T).

DTPA & TTHA Metal Binding

The lanthanide series shows a steady contraction in the ionic radii from La³⁺ to Lu³⁺.^[20] This decrease leads to a change in coordination number from 9 for the lighter lanthanides to 8 for the heavier lanthanides.^[21] Under some circumstances, larger coordination numbers can be observed.^[22] This change in coordination number leads to different binding behaviors for DTPA and TTHA depending on the lanthanide. Studies have shown that all DTPA interaction sites (three N atoms of the diethylene backbone and five O atoms from carboxylate groups) bind to a lanthanide.^[22] For lighter lanthanides with 9-coordinate tendencies, the additional coordination site is generally occupied by water. Studies have shown TTHA to bind in a 10-coordination fashion for the lightest lanthanides.^[22] For lanthanides heavier than neodymium, lanthanide-TTHA complexes have been shown to be 9-coordinate with one of the terminal carboxylates non-coordinating observed in both the solution and solid phases.

Under the same pH, TTHA was found to be a weaker holdback reagent than DTPA. While

Table 4.3. Available equilibrium constants of significance for examining TALSPEAK systems within this report. [12,16,18]

Component	Reaction	Log K_d , K_{ex} , K_{eq} or β
Acid Dissociation Constants		
DTPA	$H_5D \xrightleftharpoons{K_d} H_4D^- + H^+$	-2.00
	$H_4D^- \xrightleftharpoons{K_d} H_3D^{2-} + H^+$	-2.69
	$H_3D^{2-} \xrightleftharpoons{K_d} H_2D^{3-} + H^+$	-4.28
TTHA	$H_6T \xrightleftharpoons{K_d} H_5T^- + H^+$	-2.30
	$H_5T^- \xrightleftharpoons{K_d} H_4T^{2-} + H^+$	-2.76
	$H_4T^{2-} \xrightleftharpoons{K_d} H_3T^{3-} + H^+$	-4.08
Lactate	$HL \xrightleftharpoons{K_d} H^+ + L^-$	-3.67
HDEHP	$HA \xrightleftharpoons{K_d} H^+ + A^-$	-3.47
HEH[EHP]	$HA \xrightleftharpoons{K_d} H^+ + A^-$	-4.51
Metal Binding Constants		
DTPA	$Eu^{3+} + D^{5-} \longleftrightarrow EuD^{2-}$	22.39
	$Eu^{3+} + HD^{4-} \longleftrightarrow EuHD^-$	24.54
	$Am^{3+} + D^{5-} \longleftrightarrow AmD^{2-}$	22.9
	$Am^{3+} + HD^{4-} \longleftrightarrow AmHD^-$	24.47
TTHA	$Eu^{3+} + T^{6-} \longleftrightarrow EuT^{3-}$	23.1
	$Eu^{3+} + HT^{5-} \longleftrightarrow EuHT^{2-}$	--
	$Am^{3+} + T^{6-} \longleftrightarrow AmT^{3-}$	26.79
	$Am^{3+} + HT^{5-} \longleftrightarrow AmHT^{2-}$	--
Lactate	$Eu^{3+} + L^- \xrightleftharpoons{\beta_1} EuL^{2+}$	2.90
	$Eu^{3+} + 2L^- \xrightleftharpoons{\beta_2} EuL_2^+$	5.18
	$Eu^{3+} + 3L^- \xrightleftharpoons{\beta_3} EuL_3$	6.44
HDEHP	$Eu^{3+} + 3(HA)_2 \xrightleftharpoons{K_{ex}} Eu(AHA)_3 + 3H^+$	2.62
HEH[EHP]	$Eu^{3+} + 3(HA)_2 \xrightleftharpoons{K_{ex}} Eu(AHA)_3 + 3H^+$	0.38

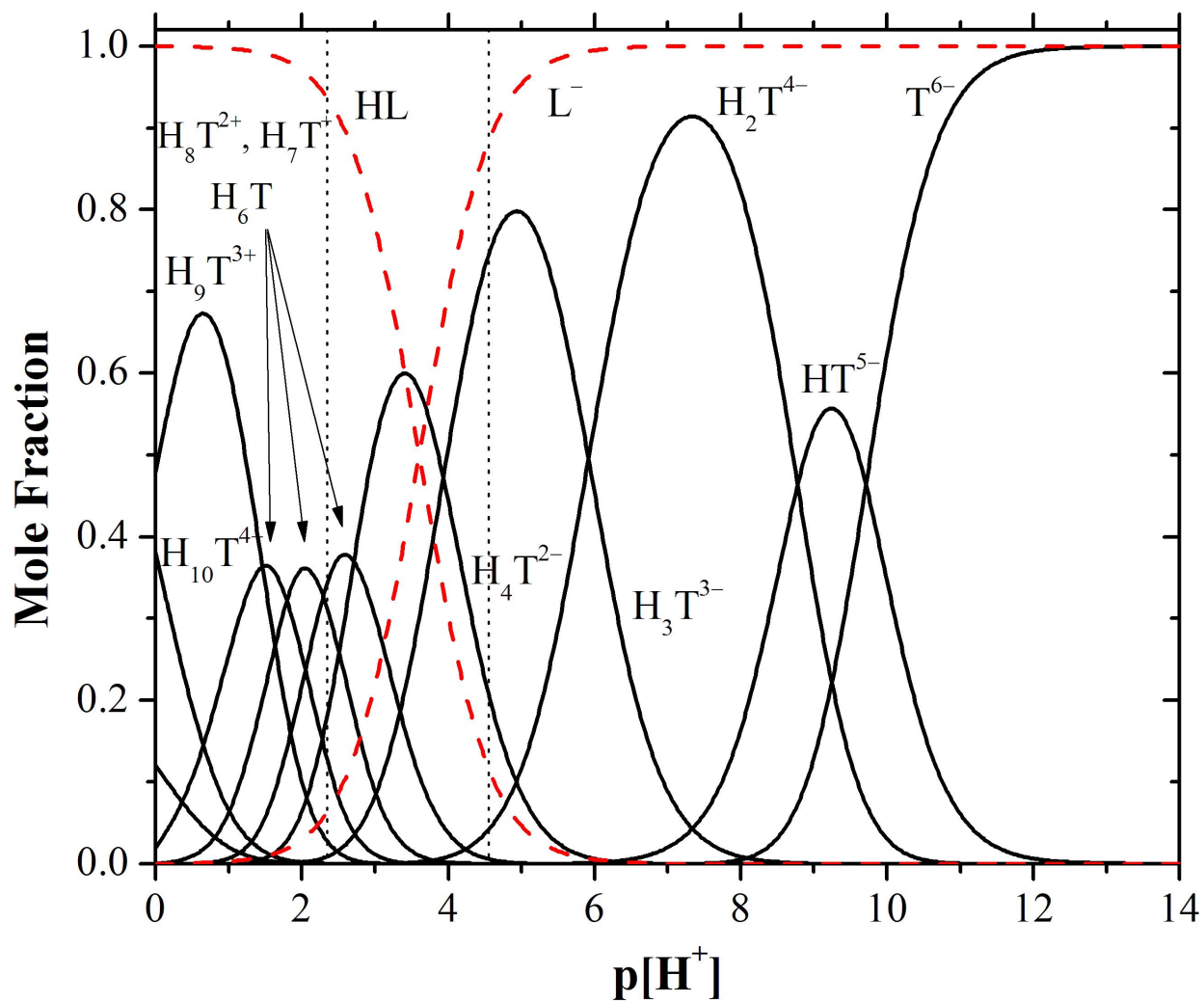


Figure 4.11. Speciation diagram showing DTPA and lactic acid calculated using protonation constants at 0.1 M ionic strength, 25.0°C.^[18] The dotted rectangle outlines approximate working conditions for the TALSPEAK system.

the binding constants for TTHA are higher, speciation calculations show lower concentrations of metal-binding TTHA species (T^{6-} and HT^{5-}) are present than the DTPA species (D^{5-} and HD^{4-}). This may be attributed to the higher final pK_a of TTHA (10.5) compared to DTPA (9.9).^[19] Experiments discussed later will show Am/Eu separation factors were higher when TTHA was used, but not as high as predicted by thermodynamic data presented in the literature for Am^{3+} and Eu^{3+} .

Organic Phase Composition

Recent examinations of the TALSPEAK solvent extraction system suggest evidence for the formation of micelles when HDEHP is used as the extractant.^[23,24] This evidence includes the rapid uptake of water, lactate and sodium to the organic phase when the total concentration of lactate is above 0.5 M. The partitioning of these species to the organic phase are the same within error of distribution of these analytes into n-dodecane for the HEH[EHP] system. Furthermore, when HEH[EHP] is used as the extractant, lanthanide extraction exhibits similar behavior to thermodynamically predicted models.^[9,24] In light of these results, much of the discussion will focus on the potential formation of micelles in LN resin phase. Other proposed reactions can be found in the literature.^[9]

pH Dependence

As the pH increases, [Figure 4.3](#) shows most LN partitioning data can be described by a slope -2 on a logarithmic plot. The exception is the Eu^{3+} uptake data by the LN resin from a TTHA

aqueous media. At lower pH's, the pH dependence is similar to all other investigated systems; however, the slope moves towards zero as the pH goes beyond 4.0. Europium uptake by the LN2 resin decreases as well when the pH increases (Figure 4.4), but now the magnitude of the slopes are smaller for all systems and there is no leveling of metal distribution at high pH. The variability in the pH dependence for the two resins, regardless the presence of DTPA or TTHA, warrants further examination.

Thermodynamic models calculate metal partitioning should decrease slightly as the pH increases. A minimum in partitioning should be observed at $\text{pH} = 3.5$. As the pH continues to increase beyond 3.5, metal partitioning should begin a slight increase.^[9] Although the decrease in metal extraction observed in Figures 4.3 and 4.4 is in theoretical disagreement, previous pH investigations of the “classical” TALSPEAK solvent extraction system using the same concentrations of lactate and an order of magnitude more DTPA (50 mM) have shown a dramatic decrease in analyte uptake as the pH increases.^[10] However, europium uptake deviates more from the predicted thermodynamic model for the HDEHP extraction chromatographic system than the HDEHP liquid-liquid system.

Several reasons for the deviation of the metal partitioning as the pH increases have been noted previously.^[9,11,23] The observed differences in the liquid-liquid and extraction chromatographic systems may be explained by micelle formation. If this sort of aggregation is occurring, the presence of neat HDEHP on the resin could encourage aggregation. Ultimately, a greater deviation from trends based on known thermodynamic parameters would arise.

The decreased deviation of the LN2 resin from the calculated models is interesting. If micelle formation is the cause of a decrease in metal extraction, two arguments can be provided regarding the decreased tendency of HEH[EHP] to form micelles: 1) The dimerization constant

for HEH[EHP] is lower than HDEHP.^[25] A decreased tendency to dimerize may make HEH[EHP] less likely to reorganize into larger molecular clusters. 2) The higher pK_a of the phosphonic acid buffer (4.51) compared to the phosphoric acid buffer (3.47) could be significant.^[18] At a pH of 3.6, more 50 % of the HDEHP has been deprotonated. Therefore the organic phase contains less $(HA)_2$ and more (Na^+AHA^-) (or some de-dimerized material like Na^+A^- in the organic phase). The addition of Na^+ and the dedimerization of HDEHP could increase the polarity of the organic phase. This could encourage partitioning of water and ultimately a rearrangement of the organic phase. The phosphonic acid has a higher pK_a and probably remains as primarily $(HA)_2$ beyond pH 4; therefore making it less prone to de-dimerization and the formation of micelles.

Kinetics Investigation

Previous reviews have noted the concentrations of lactate, hydrogen ion and polyaminopolycarboxylic acid can all have an impact on the kinetics of metal distribution.^[24,26,27] The concentration of lactate seems to have the largest kinetic impact on the system. Decreasing the concentration of lactate below 0.5 M has been shown to dramatically affect the distribution of lanthanides heavier than samarium. To ensure reasonably fast kinetics, the concentration of lactate was maintained above 0.5 M in all experiments. For most experiments, the concentration of lactate is at 1 M.

An extensive analysis of each kinetic effects for a particular TALSPEAK reagent is beyond the scope of this investigation. The goal of these kinetics studies was to evaluate the contact time required for metal partitioning to reach equilibrium in batch experiments and the type of

flow rate appropriate for column experiments. Figure 4.5 shows all systems are very near equilibrium within 10 minutes. For the LN/DTPA system, distribution values obtained at 10 minutes appear to be within 10% of equilibrium values (assuming the system is at equilibrium after two hours). For column investigations, the excess of resin to aqueous phase and a flow rate of 1 mL / min should allow lanthanide uptake to the resin phase to be within 10% of equilibrium distribution. This will also allow sufficient sample throughput. A flow rate of 1 mL / min is conservative when compared to lanthanide separation studies performed previously at 5 mL / min using the LN and LN2 resin.^[16]

Lactate Dependence

Earlier studies have investigated the lactate dependence of lanthanide partitioning into HDEHP in the absence of DTPA at a pH of 3.6.^[23] A comparable study was performed with extraction chromatography. The study was expanded to examine the europium partitioning for the LN/TTHA and LN2/DTPA or TTHA systems, as well as americium.

As noted previously, TTHA will saturate the coordination sphere of both light and heavy lanthanides. This decreases the probability of formation for a ternary Ln-TTHA-Lactate complex in the aqueous phase. Figure 4.6 shows systems involving TTHA seem relatively unaffected by the variance of lactate concentration. For the Eu/LN/TTHA system, initially a slope of -1 is observed on the logarithmic plot as the concentration of lactate increases. An eventual break is observed around 1.0 M, where the slope increases to -2.5. This compares to the LN/DTPA system, where an initial slope of -2.5 on the logarithmic plot progresses to a slope of -4.5 beyond 1 M lactate.

In earlier solvent extraction investigations, the slope of -4.5 in the presence of HDEHP has been interpreted to possibly indicate the formation of the $M(\text{Lac}_4)^-$ species retaining lanthanides in the aqueous phase.^[23] However, HEH[EHP] is a weaker extractant than HDEHP. Competition arising from the $M(\text{Lac}_4)^-$ species should be more likely when a weaker extractant is present in the organic phase. Since metal extraction by HEH[EHP] appears to be less dependent on higher concentrations of lactic acid, the -4.5 slope observed appears to be more indicative of changes in the organic phase than competing equilibria in the aqueous phase.

Figure 4.6 also shows the LN2 system, regardless the presence of DTPA or TTHA, seems to be almost completely unaffected by the presence of lactate when compared to any of the other LN data. The participation of lactate has been suggested in the probable organic phase extractant reorganization.^[23,24] If lactate dependent micellar aggregation is more likely for HDEHP than HEH[EHP], this could explain the metal partitioning dependence and independence of HDEHP and HEH[EHP], respectively, when concentrations of lactate and H^+ are varied.

The common slope of -2.5 for both the DTPA and TTHA data at different concentration ranges of lactate is interesting, especially since decreased metal partitioning seems to be related to changes in organic phase composition. If a ternary complex was being formed in the DTPA aqueous phase, changing the concentration of lactate should impact the DTPA and TTHA systems quite differently (remembering TTHA has saturated the metal center). These observations point to a ternary complex not being significant in the DTPA-based aqueous phase. This is in agreement with previous calorimetric and fluorescence work.^[11]

Lanthanide + Yttrium Uptake

Understanding lanthanide partitioning behavior is crucial to determining the ability for a complicated TALSPEAK-type system to be used for An/Ln separations. The lanthanide composition in spent nuclear fuel largely consists of the light lanthanides.^[14] The simulated waste solution, presented in [Table 4.2](#), notes lanthanides with a concentration greater than 1.0 μM anticipated in a waste stream. The addition of lanthanides heavier than gadolinium is largely present to develop our theoretical understanding of the system.

The lanthanide uptake of the LN/DTPA chromatographic system is very comparable to uptake patterns observed in the solvent extraction system.^[9] The lightest lanthanides are strongly extracted by HDEHP, with a decrease in extraction observed through Nd. This is in agreement with the equilibrium constants for the light lanthanides with DTPA. Extraction generally decreases as the equilibrium constant for the $\text{Ln}(\text{H}_n\text{DTPA})^{n-2}$ species increases. As the equilibrium constants for the lanthanide-DTPA species level ([Figure 4.2](#)), HDEHP controls the extraction trends. Heavier lanthanides are well extracted into the organic phase.

In contrast to DTPA, TALSPEAK chemistry containing TTHA as a hold-back reagent shows the lowest extraction for the lightest lanthanides. This can be largely explained by the very consistent equilibrium constants observed for TTHA with all the lanthanides. In contrast, DTPA shows an increase in the binding constant of nearly three orders of magnitude as lanthanides get heavier from La to Sm ([Figure 4.2](#)). If the additional separation factor observed with TTHA between Am and the middle lanthanides (Eu, Sm, Nd) is to be utilized, a sufficiently strong organic extractant must be present to ensure removal of the light lanthanides from the aqueous phase.

Polyaminopolycarboxylic Acid Dependence

In an attempt to further optimize conditions for column experiments, the influence of DTPA and TTHA concentrations on Am^{3+} hold-back to the aqueous phase were examined. The pH's were selected based on previous pH profiles. In general, the logarithmic dependences were consistent with literature values of -1.^[10,28] Americium uptake by the LN and LN2 resins was comparable when using TTHA in the aqueous phase. The higher pH used in the TTHA study was closer to the pK_a of HEH[EHP] (4.51).^[18] Both HDEHP and HEH[EHP] were less prone to acid competition at the higher pH of the TTHA study; therefore, americium uptake was similar. At the lower pH used in the DTPA study, acid competition was still significant for the LN2 resin and Am^{3+} uptake by the LN2 resin was noticeably less when compared to Am^{3+} uptake by the LN resin. The Am^{3+} retention at a pH of 2.8 using the LN resin clearly shows a higher pH will be required to maintain Am^{3+} in the aqueous phase using DTPA.

Am/Eu Column Behavior (LN2 Resin)

Americium/europium separations were initially used as a means of probing the selectivity of TTHA versus DTPA for americium. Even though light lanthanide retention in the aqueous phase was shown to be greater with TTHA in simulated waste studies, the improved separation of americium from europium observed when using TTHA coupled with the LN2 resin (compared to the LN resin with DTPA) seemed to warrant further examination. [Table 4.2](#) shows in all instances DTPA is out performed by TTHA for separations focusing exclusively on separating americium from europium. The highest separation factor ($\text{SF} \sim 120$) between Am^{3+} and Eu^{3+} was achieved when the solution was heated to 50°C ([Figure 4.9](#)).

Increasing the temperature in more classical DTPA/HDEHP solvent extraction systems has decreased the separation factor between americium and the lanthanides.^[9] This has been related to the exothermic extraction of lanthanides by HDEHP in a TALSPEAK system. DTPA and TTHA both displayed an improved separation factor when using the HEH[EHP] resin at a higher temperature. A certain (incorrect) oversimplification is arguing that lanthanide extraction using HDEHP is overall an exothermic process, whereas lanthanide extraction using HEH[EHP] is an endothermic process. The complete inversion of thermochemical properties by changing the basicity of the interacting oxygen does seem unlikely. The fundamental differences in organic phase structure, if micelle formation were actually occurring, for HDEHP versus HEH[EHP] could account for this dramatic thermochemical inversion.

SLW Column Investigation

To complete the examination of chromatographic materials in the TALSPEAK process, several variations of the aqueous phase were attempted using the LN resin. The LN resin was selected for these more applied applications after lanthanide investigations indicated the poor competition between the LN2 for the light lanthanides versus TTHA. [Figure 4.10](#) shows the separation factors (α) obtained for a simulated waste stream versus americium.

TTHA appears to be an insufficient hold-back reagent for TALSPEAK purposes for two reasons; 1) The small separation factor obtained between the light lanthanides and americium 2) TTHA cannot compete sufficiently with the LN resin for americium. Indeed, unless the LN2 resin is used, quantitative removal of americium from the resin is not achieved during the designed reverse TALSPEAK strips. Quantitative removal of americium from the resin appears

possible using DTPA (noting the relatively small concentrations of DTPA used), but the separation factors between americium and the lanthanides lighter than samarium are so slight the attempted separation would not meet desired goals. Since the goal of this separation is to completely recover americium to avoid geological disposal, quantitative recovery of americium is crucial. In light of this, the best overall separation factors were observed using 2.5 mM TTHA and 1 M lactate in the aqueous phase at a pH of 3.5. Table 4.3 shows the individual lanthanide percentages during TALSPEAK strip and acid strip of the optimized column.

Previous literature^[12,13] has reported successful americium separation from simulated waste when using a DTPA/lactate system with HDEHP impregnated on a silica support producing >99% pure americium. The largest contributing factor to the differences between previous studies and the observations in this paper is most likely the length of the column. The column length in previous studies reporting >99% pure americium were six times longer (12 cm) than the columns used in this study (2 cm). The increased column length most likely provided additional theoretical plates, aiding in the separation of americium from the light lanthanides. Using Equation 4.5, the number of theoretical plates for a system can be calculated, where L is the column length and w is the width of the peak and N is the theoretical number of plates. Based on these calculations, columns in these investigations contained 1.6 theoretical plates.

$$N = \frac{16L^2}{w^2} \quad (4.5)$$

Higher separation factors obtained in the literature utilized at least 28.4 theoretical plates. The lowest separation factors in the optimized simulated waste column separation were between Am and Nd or Ce (SF = 28). Doubling the length of the column (and therefore the number of theoretical plates) increases the separation by the square root of 2.^[29] To obtain a separation factor equal to 100, the column length would need to be doubled 2.5 times (ultimately providing

a required column length of 12 cm). The column length required is in good agreement with previously successful separations in the literature. Therefore; this study concludes TALSPEAK-type chromatographic studies can be successful, however the number of plates provided for the system must be considered carefully.

Conclusions

A fundamental examination of solid-liquid TALSPEAK chemistry has been performed. The substitution of TTHA for DTPA in some experiments displayed the potential for improved Am/Eu separations; however, increased retention of the light lanthanides in the aqueous phase was undesired. Since comparable lactate and pH dependences were observed using DTPA or TTHA (which saturates the coordination sphere of any lanthanide), the possibility of ternary complex formation, $M(\text{Lac})(\text{DTPA})^-$, in the aqueous phase seems unlikely. Fundamental differences in extraction trends were observed when HEH[EHP] was used in place HDEHP as the TALSPEAK organic extractant. The differences in extraction trends may suggest reorganization of the extractant. High concentrations of lactate ($>1.0\text{ M}$) seem to decrease metal extraction by changing the composition of the organic phase, not by retaining lanthanides in the aqueous phase through the $M(\text{Lac})_4^-$ species. While separation factors as high as 20 were observed for the lanthanide series versus americium; none of these results indicate an obvious benefit for performing TALSPEAK separations chromatographically.

References

[1] Aspinall, H. *Chemistry of the F-Block Elements*. Gordon & Breach: Amsterdam, the Netherlands. 5th Ed. 2001. 61-104.

- [2] Jensen, M. P.; Bond, A. H. Influence of aggregation on the extraction of trivalent lanthanide and actinide cations by purified cyanex 272, cyanex 301, and cyanex 302. *Radiochim. Acta.* **2002**, *90* (4), 205-209.
- [3] Jensen, M. P.; Bond, A. H. Comparison of covalency in the complexes of trivalent actinide and lanthanide cations. *J. Am. Chem. Soc.* **2002**, *124* (33), 9870-9877.
- [4] Choppin, G. R.; Nash, K. L. Actinide separation science. *Radiochim. Acta.* **1995**, *70/71*, 225-236.
- [5] Kozimor, S.A.; Yang, P.; Batista, E.R.; Boland, K.S.; Burns, C.J.; Clark, D.L.; Conradson, S.D.; Martin Wilkerson, M.P.; Wolfsberg, L.E. Trends in covalency for d- and f-Element metallocene dichlorides identified using chlorine k-edge x-ray absorption spectroscopy and time-dependent density functional theory. *J. Am. Chem. Soc.* **2009**, *131* (34), 12125–12136.
- [6] Peterman, D.R.; Martin, L.R.; Klaehn, J.R.; Harrup, M.K.; Greenhalgh, M.R.; Luther, T.A. Selective separation of minor actinides and lanthanides using aromatic dithiophosphinic and phosphinic acid derivatives. *J. Rad. Nucl. Chem.* **2009**, *282* (2), 527-531.
- [7] Hill, C.; Guillaneux, D.; Berthon, L.; Madic, D. Sanex-BTP process development studies. *J. Nucl. Sci. Technol.* **2002**, *Suppl. 3*, 453-461.
- [8] Mincher, B. J.; Modolo, G.; Mezyk, S. P. Review article: The effects of radiation chemistry on solvent extraction: 1. Conditions in acidic solution and a review of TBP radiolysis. *Solvent Extr. Ion Exch.* **2009**, *27* (1), 1-25.
- [9] Nilsson, M.; Nash, K.L. Trans-lanthanide extraction studies in the TALSPEAK system: Investigating the effect of acidity and temperature. *Solvent Extr. Ion Exch.* **2009** *27*(3), 354-377.
- [10] Nilsson, M.; Nash, K.L. Review article: A review of the development and operational characteristics of the TALSPEAK process. *Solvent Extr. Ion Exch.* **2007** *25*(6), 665-710.
- [11] Leggett, C.J.; Liu, G.; Jensen, M.P. Do Aqueous Ternary Complexes Influence the TALSPEAK Process? *Solvent. Extr. Ion Exch.* 2010 *28* (3), 313-334.

- [12] Weaver, B.; Kappelmann, F.A. Talspeak, A new method of separating americium and curium from the lanthanides by extraction from an aqueous solution of an aminopolyacetic acid complex with a monoacetic organophosphate or phosphonate. August 1964, ORNL-3559.
- [13] Kosyakov, V.N.; Yerin, E.A. Separation of transplutonium and rare-earth elements by extraction with HDEHP from DTPA solution. *J. Rad. Nucl. Chem.* **1978**, *43* (1), 37-51.
- [14] Bond, W.D.; Leuze, R.E. Feasibility studies of the partitioning of commercial high-level wastes generated in spent nuclear fuel reprocessing: Annual progress report for FY-1974, ORNL-5012, January 1975.
- [15] Hu, Z.; Pan, Y.; Ma, W.; Fu, X. Purification of organophosphorus acid extractants. *Solvent Extr. Ion Exch.* **1995**, *13* (5), 965-976.
- [16] Horwitz, E.P.; McAlister, D.R.; Dietz, M.L. Extraction chromatography versus solvent extraction: How similar are they? *Sep. Sci. Tech.* **2006**, *41*(10), 2163-2182.
- [17] Kubota, F.; Goto, M.; Nakashio, F. Extraction of Rare Earth Metals with 2-ethylhexyl phosphonic acid mono-2-ethylhexyl Ester in the Presence of Diethylenetriaminepentaacetic Acid in Aqueous Phase. *Solvent Extr. Ion Exch.* **1993**, *11* (3), 437-453.
- [18] Fu, X.; Hu, Z.; Liu, Y.; Golding, J.A. Extraction of sodium in bis(2,4,4-trimethylpentyl) phosphinic acid (Cyanex 272): Basic constants and extraction equilibria. *Solvent Extr. Ion Exch.* **1990**, *8* (4-5), 573-595.
- [19] Martell, A.E.; Smith, R.M. *NIST Critically Selected Stability Constants of Metal Complexes Database*; Version 8.0, 2004.
- [20] Bravard, F. Complexation of trivalent lanthanides with oxygen containing ligands: Studies regarding the chemistry of association and selectivity in solution. **2004**, CEA report, 26.
- [21] Shannon, R.D.; Prewitt, R.C.T. Effective ionic radii in oxide and fluorides. *Acta Crystallogr.* **1969**, *B25* (Pt. 5), 925-946.
- [22] Frullano, L.; Rohovec, J.; Peters, J.A.; Geraldès, C.F.G.C. *Structures of MRI Contrast Agents in Solution* in Contrast agents. 1: Magnetic Resonance Imaging, Kraus, V. Eds.; Topics in Current Chemistry, v. 221. Springer: Berlin, Germany. 25-60, 2002.

[23] Grimes, T.S.; Nilsson, M.; Nash, K.L. Lactic acid partitioning in TALSPEAK extraction systems. *Sep. Sci. Tech. Accepted*.

[24] Braley, J.B.; Grimes, T.S.; Nash, K.L. Insight to TALSPEAK: Exchanging HDEHP for HEH[EHP] and DTPA for TTHA. *Manuscript in preparation*.

[25] Miralles, N.; Sastre, A.; Martinez, M.; Aguilar, M. The aggregation of organophosphorus acid compounds in toluene. *Analytical Sciences* **1992**, 8 (6), 773-777.

[26] Nilsson, M.; Heydon, A.; Nash, K.L. Studies of the lactic acid concentration on extraction equilibria and kinetics in TALSPEAK chemistry. *Manuscript in preparation*.

[27] Kolarik, Z.; Koch, G.; Kuhn, W. Acidic organophosphorus extractants. XVIII. Rate of lanthanide (III) extraction by bis(2-ethylhexyl) phosphoric acid from complexing media. *Jour. Inorg. Nucl. Chem.* **1974**, 36 (4), 905-909.

[28] Tachimori, S.; Nakamura, H. Radiation effects of the separation of lanthanides and transplutonides by the TALSPEAK-type extraction. *J. Radioanal. Chem.* **1979**, 52 (2), 343-354.

[29] Harris, D.C. *Quantitative Chemical Analysis 3rd Ed.* W. H. Freeman and Company: New York, NY, 1991.

CHAPTER FIVE

PREFACE

Several proposals have been offered to explain the observed discrepancy between predicted and observed metal distribution in the TALSPEAK separations process, particularly as regards pH dependence of the extraction system. These suggestions have involved additional aqueous phase reactions, such as ternary complex formation or outer-sphere interaction of lactate with the metal-DTPA complex, or organic phase reactions, such as an extracted ternary complex or reverse micelle formation. The formation of reverse micelles would be sort of a worst case scenario. Micelle formation in the organic phase has been shown to be a precursor for third phase formation. Although criticality concerns should not be significant for the TALSPEAK process due to the lack of fissile material, third phase formation would greatly complicate the application of the technology.

This study continued the investigations of the extraction chromatographic chapter by examining the use of HEH[EHP] and TTHA in the solvent extraction system. Many of the same issues observed with TTHA in the extraction chromatographic system (significant retention of the light lanthanides in the aqueous phase) were observed in the solvent extraction studies. However; heavy lanthanide partitioning from TTHA seemed to be quicker and less dependent on lactate concentration. Very significant changes were observed using HEH[EHP] in a solvent extraction configuration. When HEH[EHP] is used in a solvent extraction configuration, metal distribution is predictable using known equations and equilibrium constants.

The origins of such behavior were intriguing. There are typically notable amounts of lactate and water in the extractant phase for conventional HDEHP-based TALSPEAK. This currently stands as the indirect evidence for the formation of reverse micelles in the organic phase. To further probe the HEH[EHP] system, the water content and concentration of lactate in the

organic phase were determined. The partitioning of water and lactate to the HEH[EHP]/n-dodecane organic phase was comparable to what is typically observed for the distribution of the two analytes when only n-dodecane or kerosene is present in the organic phase. Currently the indication is micelle formation occurs in the HDEHP organic phase. Since models thus far have not accounted for this, metal distribution is not predicted. The potential absence of micelles in the HEH[EHP] TALSPEAK may make this phosphonic acid extractant preferential to HDEHP. Ultimately, the entire process could be revolutionized.

CHAPTER FIVE

INSIGHT TO TALSPEAK: EXCHANGING HDEHP FOR HEH[EHP] AND DTPA FOR TTHA

Abstract

The UREX+ nuclear fuel reprocessing suite currently champions the TALSPEAK process for separation of the lanthanides from trivalent actinides. Although process development has been successful at several levels, modeling of the system using known equilibrium constants has proven difficult and slow phase transfer kinetics have been observed for heavier lanthanides. The slow kinetics are generally improved by the addition of lactate, but the mechanism of lactate participation is still largely unknown. This work shows that by exchanging the classically used holdback reagent (diethylenetriamine- N,N,N',N'',N''' -pentaacetic acid; DTPA) for triethylenetetramine- N,N,N',N'',N''',N'''' -hexaacetic acid (TTHA) some proposed mechanisms for the role of lactate can be eliminated. When bis-2-ethyl(hexyl) *phosphoric* acid (HDEHP) is replaced by bis-2-ethyl(hexyl) *phosphonic* acid (HEH[EHP]) lanthanide extraction by HEH[EHP] can be modeled with known thermodynamic equilibria. In addition, significantly lower concentrations of water, lactate and sodium in the organic phases are seen with HEH[EHP] than seen in TALSPEAK chemistry using HDEHP. The absence of water, lactate and sodium from the thermodynamically predictable HEH[EHP] system is taken as an indication of the presence of micelles when HDEHP is used as the organic extractant instead of HEH[EHP].

Introduction

For reprocessing or disposal purposes of spent nuclear fuel, removal of americium from the lanthanides is necessary step if transmutation is to be pursued. Lanthanides compete for fast-spectrum neutrons needed for fissioning americium. Considering the hard-acid^[1] nature and the comparable charge density of Am and the lanthanides the separation is unusually challenging. The most successful approaches to separations of the group have involved exploiting the slightly greater covalency of Am³⁺, resulting from the extension of the 5f orbitals.^[2-5] The interaction of nitrogen and sulfur donating ligands with Am³⁺ is stronger than with the lanthanides thus enabling group separation.

There are several viable approaches the separation of Am³⁺ from the lanthanides based on the manipulation of this chemistry. Unfortunately, the relatively polarizable molecular orbitals encountered in sulfur and pyridine based separations increase the propensity for radiolytic breakdown of the ligand.^[6-8] The most tested, and arguably least understood, method for separating trivalent actinides from trivalent lanthanides is the TALSPEAK (Trivalent Actinide-Lanthanide Separation by Phosphorus reagent Extraction from Aqueous Komplexes) solvent extraction process. The use of TALSPEAK chemistry lacks the radiolysis concerns; however, complex interactions seen in TALSPEAK separations chemistry make understanding the chemistry of the system challenging.

In TALSPEAK, group selectivity arises from the presence of a polyaminopolycarboxylate complexant in the aqueous phase. The most successful TALSPEAK separations have used bis-(2-ethylhexyl) phosphoric acid (HDEHP, organic extractant), diethylenetriamine-N,N,N',N'',N'''-pentaacetic acid (DTPA, holdback reagent), and lactic acid (carboxylic acid buffer). Structures

of these three species are shown in [Figure 5.1](#). Recent reports have addressed the basic chemistry of TALSPEAK and found metal distribution data cannot be modeled using known thermodynamic equilibria when the aqueous phase pH is greater than 3.6.^[9-11] The relatively high concentrations of water present, especially at concentrations of total lactate greater than 0.5 M, in the TALSPEAK organic phase suggest the formation of reverse micelles of HDEHP.

As an expansion of recently published extraction chromatographic work, this study aims to advance the understanding of TALSPEAK solution chemistry by comparing performance of triethylenetetramine- N,N,N',N'',N''',N''''-hexaacetic acid (TTHA) with DTPA and 2-ethylhexyl phosphonic acid mono-2-ethylhexyl ester acid (HEH[EHP]) with HDEHP. Structures of both DTPA and HEH[EHP] are shown in [Figure 5.1](#). Based on binding constants ([Figure 5.2](#)), the alternative use of TTHA may provide an improved separation factor between the lanthanides and americium. Since HEH[EHP] has a stronger P-C bond present (compared to HDEHP's three P-O bonds), the phosphonic acid should be more resistant to radiolytic degradation.

The use of HEH[EHP] is particularly helpful since the molecule is structurally analogous to HDEHP; therefore observed differences in metal partitioning can be explained primarily by the difference in the basicity of the extractants. If micelle formation in the organic phase is actually occurring, the decreased dimerization and higher pK_a of HEH[EHP] ($\log K_D = 3.37$; $pK_a = 4.51$) compared HDEHP ($\log K_D = 3.68$; $pK = 3.47$) may lead to less tendency for the phosphonic acid to aggregate.^[12] In the following, a profile of the TALSPEAK-relevant performance of TTHA and

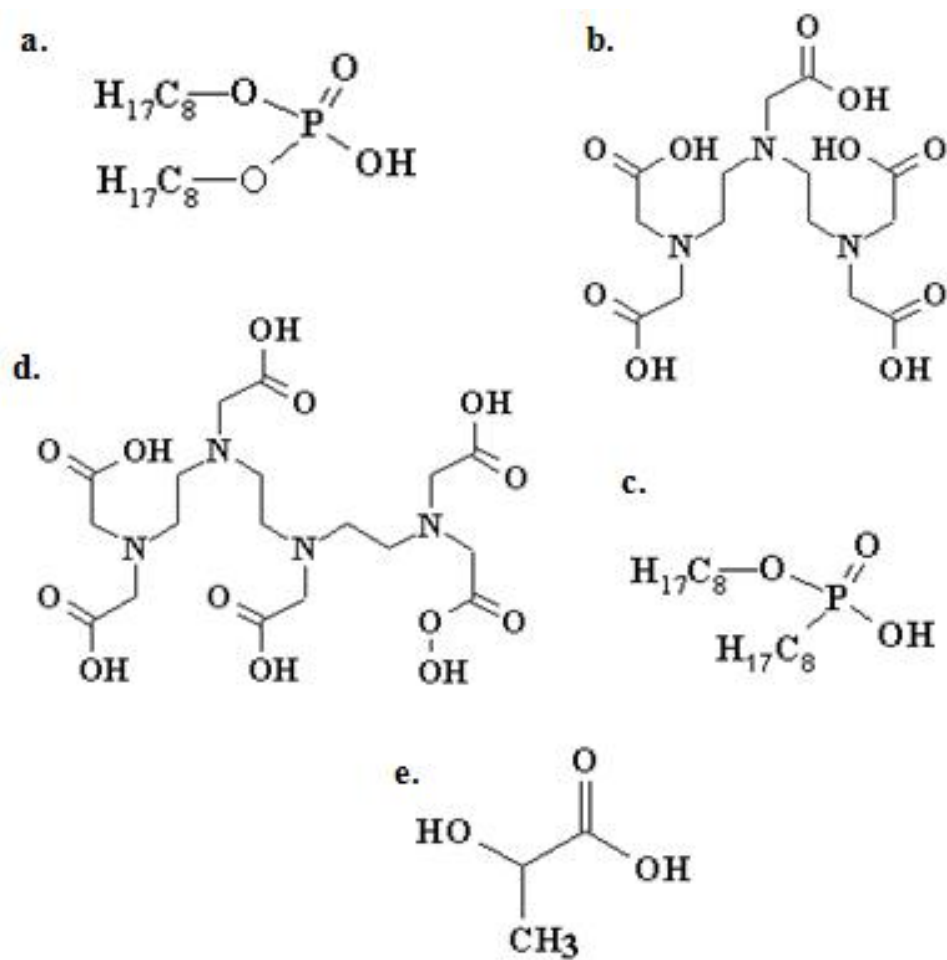


Figure 5.1. Structures of the components used in these studies; a: di(2-ethylhexyl) phosphoric acid (HDEHP) b: diethylenetriamine- N,N,N',N'',N'''-pentaacetic acid (DTPA) c: di(2-ethylhexyl) phosphonic acid (HEH[EHP]) d: triethylenetetramine- N,N,N',N'',N''',N''''-hexaacetic acid (TTHA) e: lactic acid (HL)

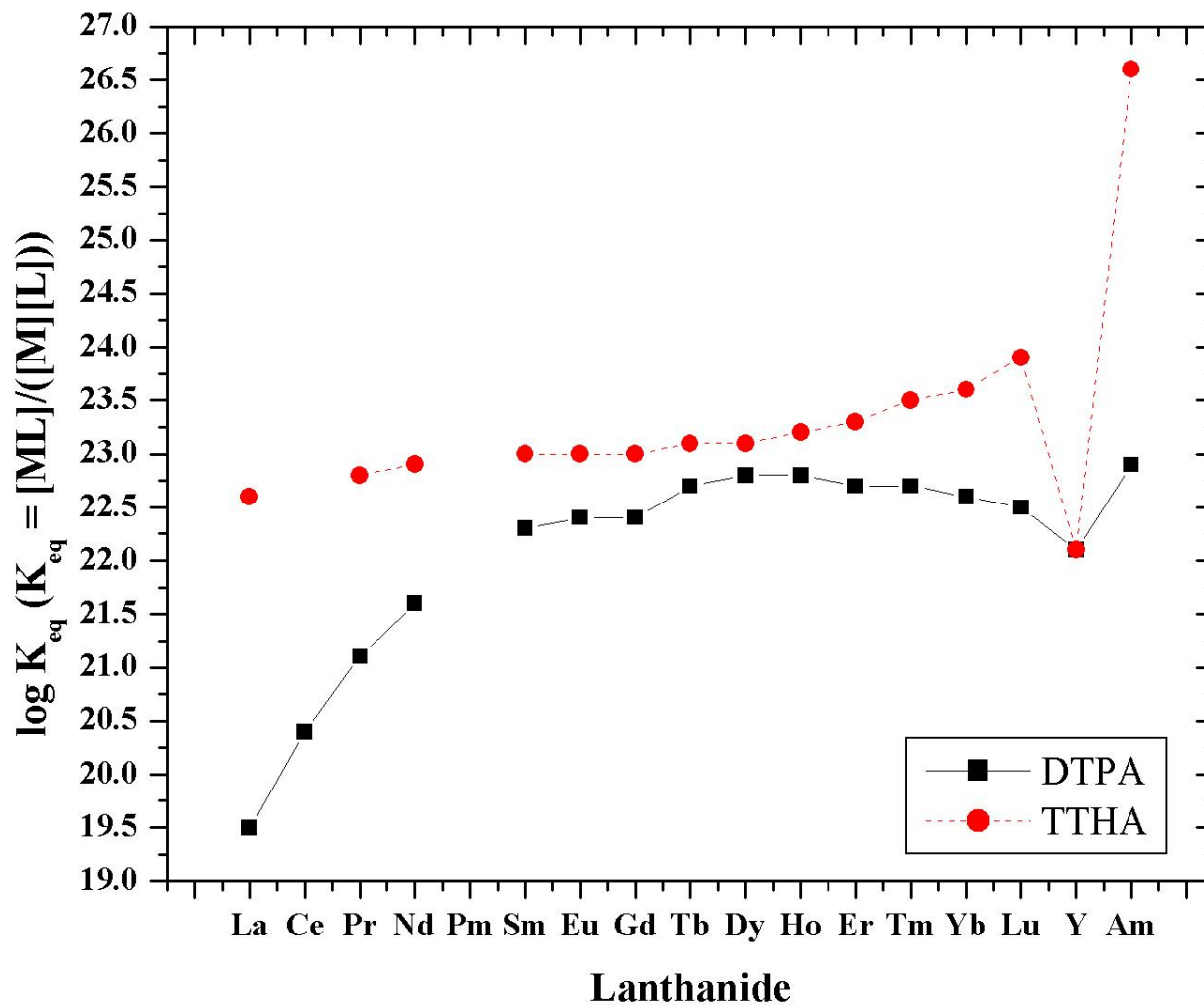


Figure 5.2. Equilibrium constants for DTPA and TTHA with the lanthanides and americium in 0.1 M ionic media at 25 °C.^[19]

HEH[EHP] will be described. The comparative differences of TTHA with DTPA and HEH[EHP] with HDEHP will also be emphasized.

Experimental

Materials

The HDEHP was obtained at 97% pure material from Sigma-Aldrich. The copper purification method was used to purify the sample to >99% as verified by potentiometric titrations.^[13] Eichrom Technologies provided HEH[EHP] (Albright & Wilson) at 90% purity. The third phase formation procedure was used to purify the material to >98% as verified by NMR.^[14] The n-dodecane was obtained from Alfa-Aesar (99% pure) and used as received. Sodium nitrate (Ricca Chemical Company) was dissolved in deionized water, filtered through a 1.0 μm membrane, recrystallized from H_2O and redissolved in H_2O to prepare a 5.28 mol NaNO_3/kg solution, as determined by using Eichrom cation exchange resins (H^+ form) and potentiometric titrations. Lanthanide oxides, 99.999%, purchased from Arris International, were used to prepare lanthanide nitrate stock solutions (La, Ce, Pr, Nd, Sm, Eu, Gd, Tb, Dy, Ho, Er, Tm, Yb, Lu, Y). Metal content, acid content and nitrate content of lanthanide solutions were determined using a HP Agilent 4500+ ICP-MS and cation-exchange resin coupled with potentiometric titration. Nitric acid solutions were prepared from Trace Metal Grade acids (Fisher Scientific) using deionized water obtained from a Milli-Q2 water purification system. Sodium lactate (mixture of *d/l* isomers) was obtained as an aqueous solution from J.T. Baker and solutions were standardized using cation-exchange chromatography (Dowex x50, H^+ form) with analysis by potentiometric titration. Stock solutions of polyaminopolycarboxylic acid were prepared by dissolving the solid acid in solution and adding 50% w/w sodium hydroxide (Sigma Aldrich) to raise the pH to 3.6. Analytical grade potassium hydrogen phthalate (KHP) was used

to standardize the base for potentiometric titrations. Radioactive $^{152/154}\text{Eu}$ and ^{24}Na was created by neutron activation of 99.999% Eu_2O_3 (Arris International) and recrystallized NaNO_3 , respectively, using a Teaching, Research, Isotopes General Atomics (TRIGA) reactor with a neutron flux of $5 \times 10^{12} \text{ n/cm}^2 \cdot \text{sec}$ at the Nuclear Radiation Center at WSU. The ^{241}Am tracer in 0.1 M HNO_3 solution was obtained from Pacific Northwest National Laboratory.

Methods

All aqueous solutions were prepared by weight. Experiments were conducted at a 1:1 aqueous/organic phase ratio with variations including pH, lactate and time. An attempt to control ionic strength was made by maintaining the concentration of NO_3^- at 1 M for all studies. Radiotracer experiments using $^{152/154}\text{Eu}$ and ^{241}Am were analyzed on a NaI(Tl) solid scintillation counter, a Packard Cobra-II auto gamma, for gross gamma counting. Radiotracer experiments using ^{14}C were analyzed using a Beckman LS6500 liquid scintillation counter for beta detection with 5 mL of EcoScint® scintillation fluid. Water distribution to the organic phase was examined through Karl Fisher analysis using a Metler Toledo Model 4200 KF titrator. The instrument was standardized immediately before analysis using 1000 ppm water standards. The calibrations were within 2-5% error before analysis.

The distribution ratios ($[\text{M}]_{\text{org}}/[\text{M}]_{\text{aq}}$) for nonradioactive metal ions were calculated by analyzing the aqueous phase before ($[\text{M}]_{\text{i, aq}}$) and after ($[\text{M}]_{\text{f, aq}}$) contact with the organic phase. Assuming no losses to sorption or precipitation, the difference between $[\text{M}]_{\text{i, aq}}$ and $[\text{M}]_{\text{f, aq}}$ defines the concentration of metal in the organic phase. The distribution ratio can then be defined as:

$$D_M = \frac{[\text{M}]_{\text{i, aq}} - [\text{M}]_{\text{f, aq}}}{[\text{M}]_{\text{f, aq}}} \quad (5.1)$$

The distribution ratios for extraction using radiotracer techniques were calculated by measuring the amount of radioactive of both the aqueous and organic phases at equilibrium. The counting efficiency is identical for both phases. Therefore; the distribution ratio is defined as the ratio of specific activity of metal in the organic phase compared to the aqueous phase:

$$D_M = \frac{[M]_{f,org}}{[M]_{f,aq}} \quad (5.2)$$

Previous work^[9] has shown reasonable agreement between distribution ratios obtained through ICP-MS or radiotracer methods; hence the assumption that there was no metal precipitation or sorption seems reasonable. The total concentration of all metal in solution was maintained at 1 mM to prevent extractant loading. To further confirm these observations for this study, experiments examining Eu distribution as a function of pH were performed using both radiotracer and inactive metal methodologies. Europium distribution values for both studies were consistent within error.

The following^[9] are valid for all experiments presented in this paper:

- i)* all solutions were prepared by weight
- ii)* experiments were performed in triplicate
- iii)* the aqueous/organic phase ratio was 1:1 using 0.5 mL of each phase
- iv)* concentrations of HDEHP or HEH[EHP] were maintained at 0.1 M
- v)* nitrate (NO_3^-) was present at 1 M to maintain ionic strength.
- vi)* contact times for distribution studies were 30 minutes (unless otherwise noted)

The effect of total lactate concentration (pH 3.6) on trans-lanthanide uptake kinetics was performed for all combinations of DTPA and TTHA with HDEHP and HEH[EHP]. A pH dependence study for lanthanide uptake from a DTPA aqueous phase to a HDEHP or HEH[HEP] organic phase was also examined. The partitioning of water and lactate into HDEHP or

HEH[HEP] organic phases as a function of total lactate concentration was also studied from a DTPA aqueous phase.

Results

Trans-lanthanide Kinetics Investigation

Reports regarding the liquid-liquid TALSPEAK system have shown kinetics to be impacted by the concentration of lactate, DTPA, organophosphorus acid or aqueous acid in the system.^[15-17] To develop some understanding regarding the impact of lactate on the kinetics of the phosphonic acid and TTHA, lanthanide distribution was monitored at the optimized TALSPEAK separations initial pH (3.6). To ensure appropriate comparison, HDEHP and DTPA studies were performed under comparable conditions. Metal distribution patterns are shown in [Figure 5.3](#). The concentration of each lanthanide was provided at 20 ppm; hence bringing the total metal in solution to just above 1 mM. All lactate concentrations noted are stating the total molar concentration of lactate.

pH Investigation

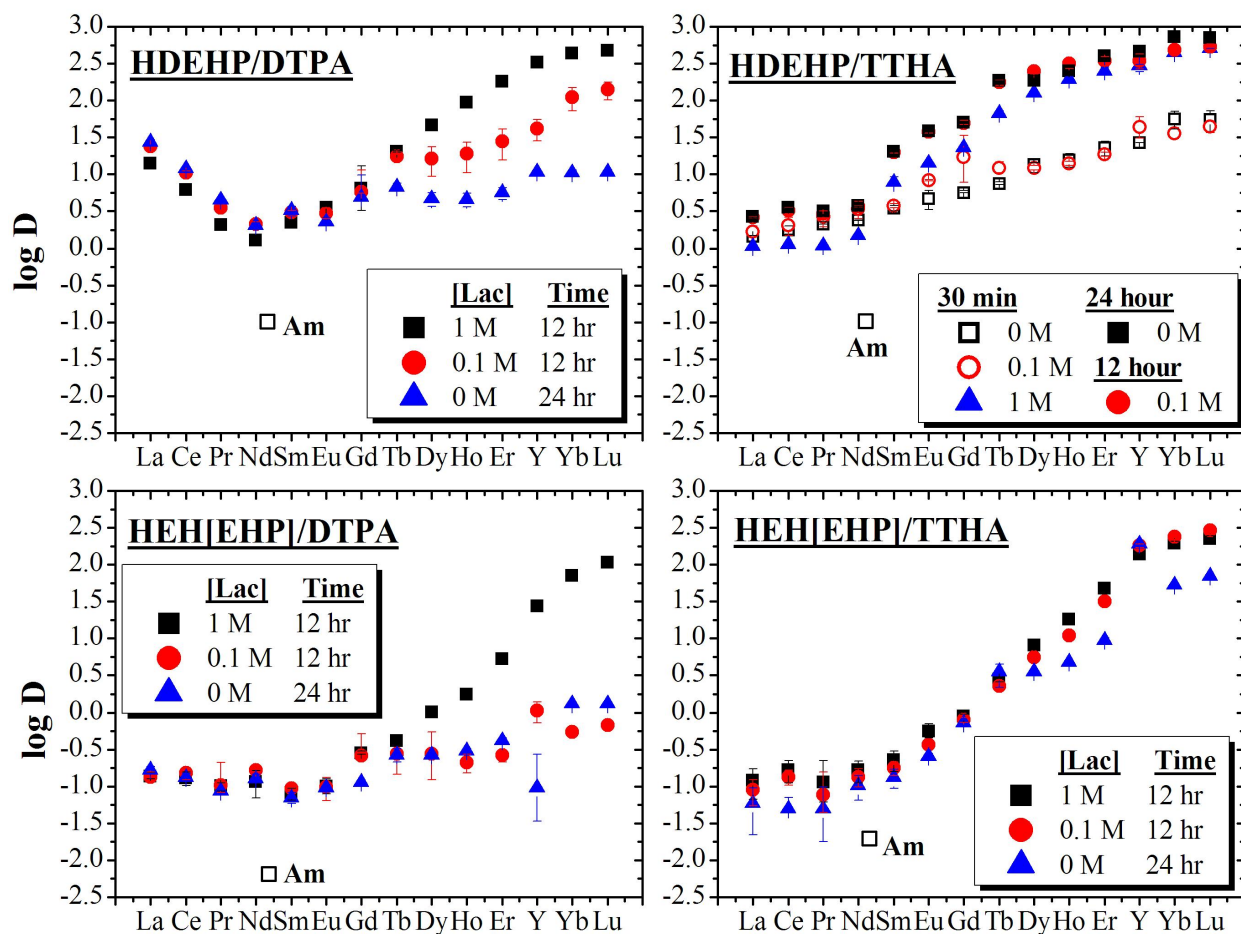


Figure 5.3. The affect of lactate concentration on the extraction kinetics of the lanthanides for several modifications of the TALSPEAK process. For all studies, the following were present. *Aqueous phase:* 1 M NO_3^- , pH = 3.6, 20 mM DTPA or TTHA *Organic Phase:* 0.1 M HDEHP/HEH[EHP] in n-dodecane. All lactate concentrations presented indicate the formal concentration of lactate. Additional data shown for the HDEHP/TTHA system as data was presentable with minimal overlap. Error bars indicate $\pm 1\sigma$ error.

Previous work has shown current thermodynamic data in the literature is insufficient to describe metal partitioning in the TALSPEAK system when the pH is greater than 2.5.^[9] An examination of ^{241}Am and $^{152/154}\text{Eu}$ metal ion partitioning as a function of pH was completed to

examine if the same experimental deviations from the predicted thermodynamic model were present using HEH[EHP] or TTHA. The formal concentration of lactate was 1 M for all studies and tracer europium was supplemented with inactive europium to bring the total europium metal concentration to 1 mM. The experimental results of the radiotracer studies and thermodynamic calculations are shown in [Figure 5.4](#) and [5.5](#). Europium extraction with HEH[EHP] displayed trends comparable to previously calculated models regardless the use of DTPA or TTHA as the holdback reagent. For a more extensive examination of the pH profiles for the rest of the lanthanides, only DTPA was utilized. A combination of modeling and previous literature eventually suggested the heavier lanthanides may not be reaching equilibrium when the pH was greater than 3.6 and contact time was limited to thirty minutes. Initial kinetics studies suggested more than 24 hours may be required for the heavier lanthanides under these conditions when partitioning is occurring at a higher pH. For this reason, a second contact was performed for 48 hours. [Table 5.1](#) displays the pH profile of several lanthanides after the thirty minute and 48 hour contact. [Figure 5.6](#) shows trend lines calculated using a previously reported simplified model (shown below) and equilibrium constants from the NIST database and trend lines calculated when the metal-DTPA β_{101} value is manipulated to fit experimental data.^[9,19] Metal-DTPA binding values obtained for the new β_{101} are compared with literature values in [Table 5.2](#).

Lactate, Sodium and Water Partitioning

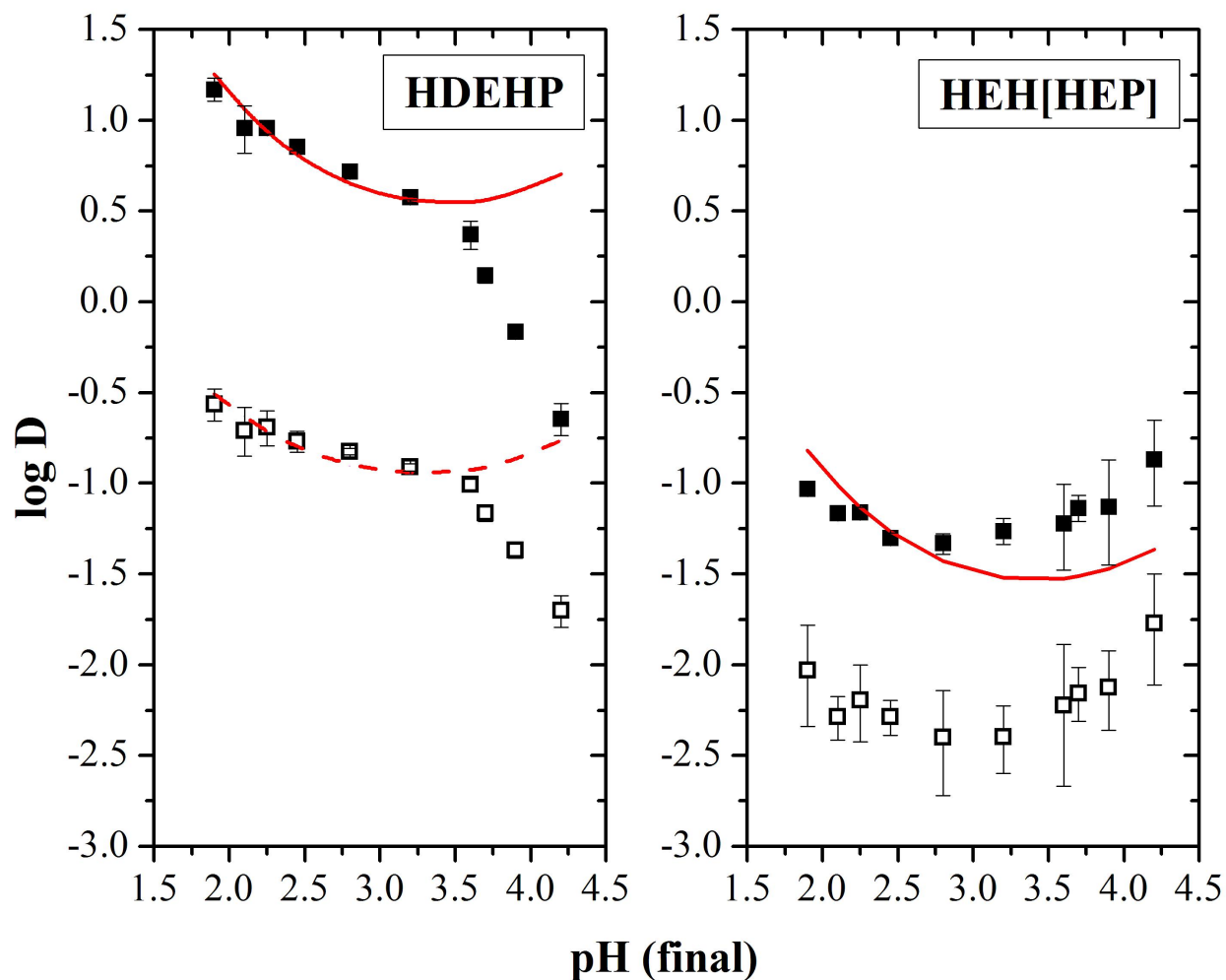


Figure 5.4. Distribution of europium and americium as a function of pH for several modifications of the TALSPEAK process after a thirty minute contact. For all studies the following were present: *Aqueous phase:* 1 M total lactic acid, 1 M NO_3^- , 20 mM DTPA *Organic phase:* 0.1 M HDEHP or HEH[EHP] in n-dodecane. Error bars indicate $\pm 3\sigma$ error. Thermodynamic equilibrium constants used in distribution calculations for DTPA and TTHA were at 0.1 and 0.5 M ionic strength, respectively. ■ Eu □ Am Solid lines indicate calculated trends for Eu. Dashed lines indicate calculated trends for Am.

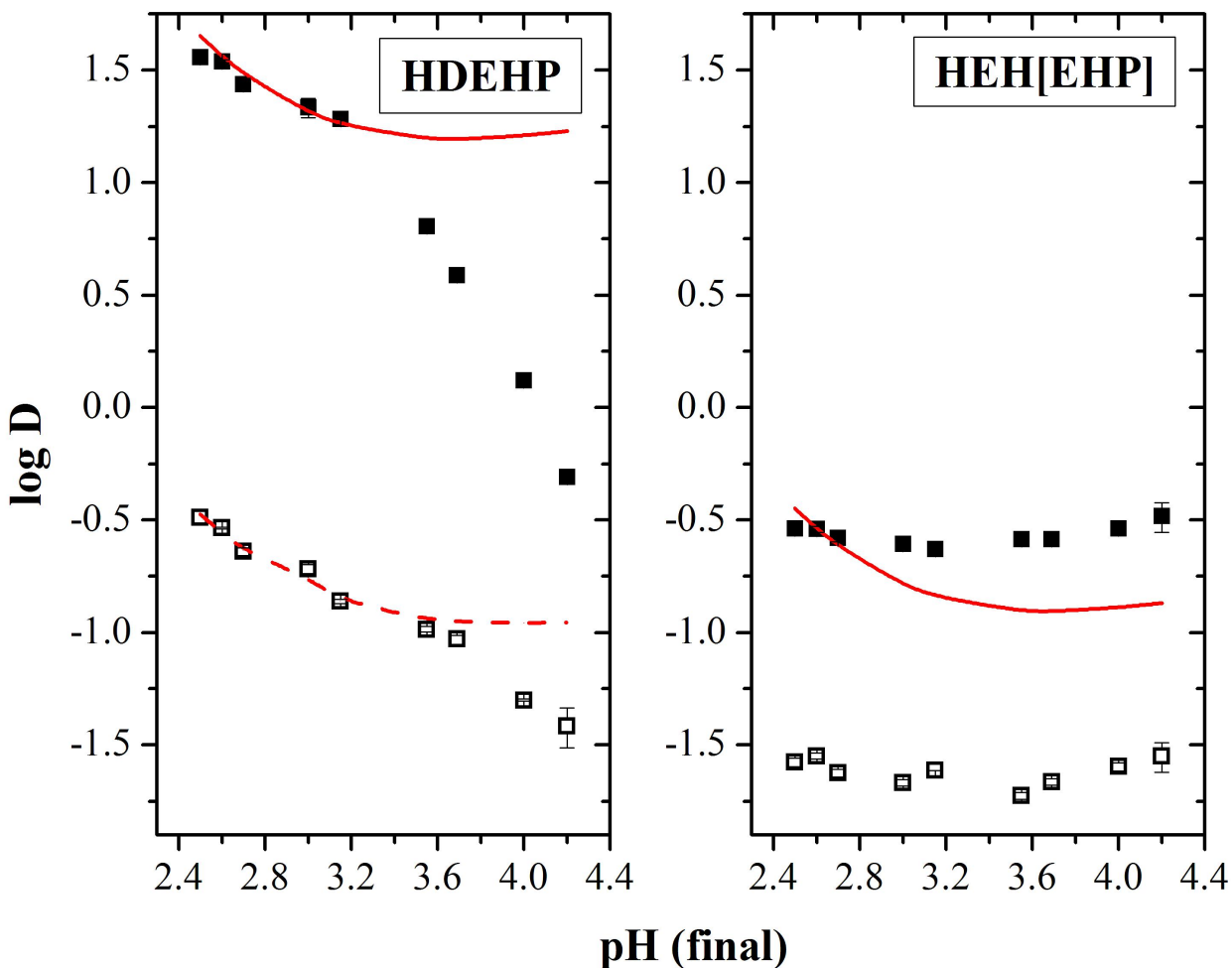


Figure 5.5. Distribution of europium and americium as a function of pH for several modifications of the TALSPEAK process after a thirty minute contact. For all studies the following were present: *Aqueous phase:* 1 M total lactic acid, 1 M NO_3^- , 20 mM TTHA *Organic phase:* 0.1 M HDEHP or HEH[EHP] in n-dodecane. Error bars indicate $\pm 3\sigma$ error. Thermodynamic equilibrium constants used in distribution calculations for DTPA and TTHA were at 0.1 and 0.5 M ionic strength, respectively. ■ Eu □ Am Solid lines indicate calculated trends for Eu. Dashed lines indicate calculated trends for Am.

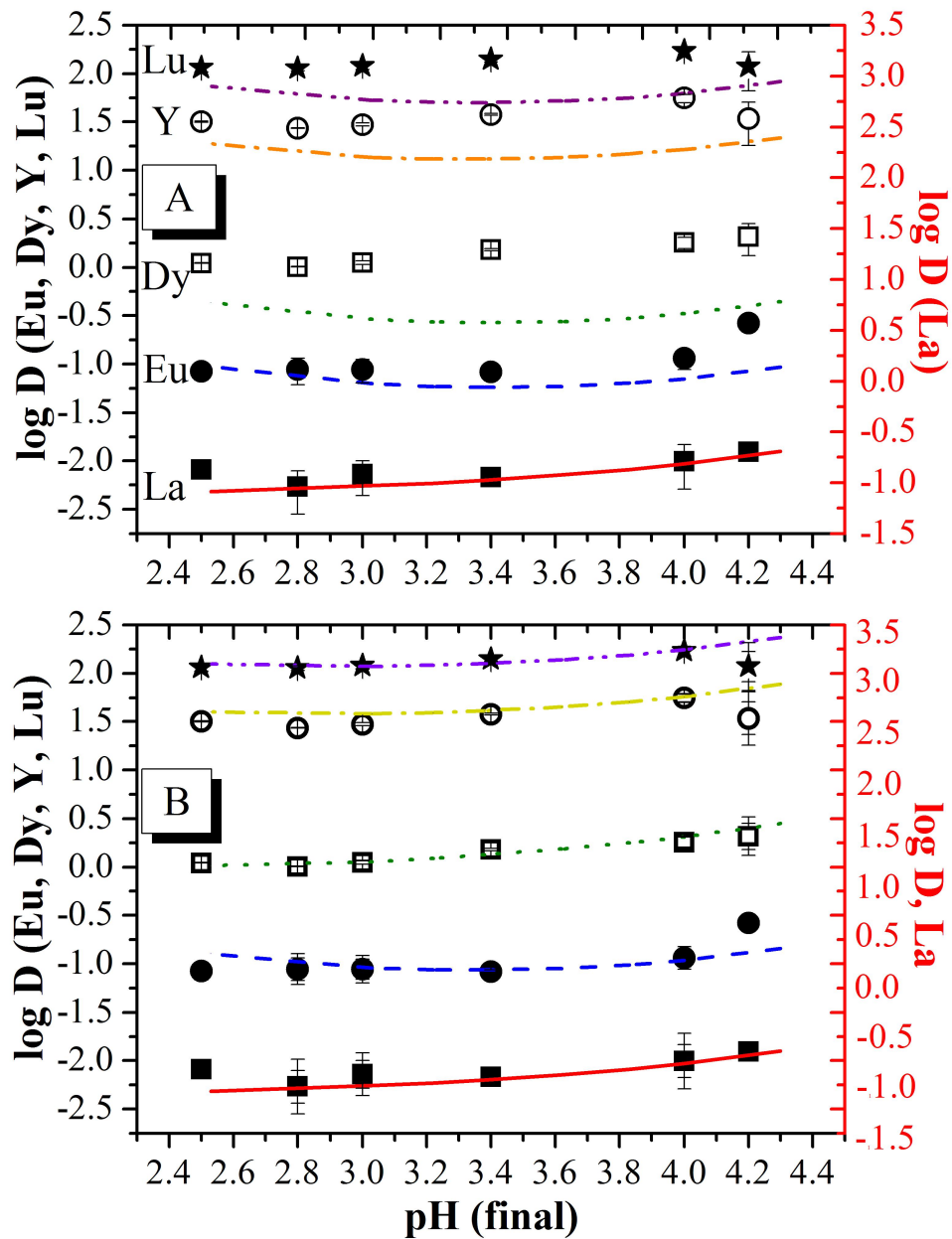


Figure 5.6. Distribution of select lanthanides + Y as a function of pH for the HEH[EHP]/DTPA TALSPEAK system using a 48 hour contact time. For all studies the following were present: *Aqueous phase:* 1 F Lactic acid, 1 M NO_3^- , 20 mM DTPA *Organic phase:* 0.1 M HDEHP or HEH[EHP] in n-dodecane. All error bars indicate $\pm 1\sigma$ error. a) Metal-DTPA constants included in calculations were at 0.1 M ionic strength. Lines indicate the calculated extraction patterns based on thermodynamic data. — La — — — Eu — — — — — Dy — — — — — Y — — — — — Lu b) Metal-DTPA constants included in calculations were manipulated to fit data. Lines here show calculated extraction patterns with adjustment to $\log \beta_{101}$ metal-DTPA equilibrium constant. — La — — — — — Eu — — — — — Dy — — — — — Y — — — — — Lu

Table 5.1. Distribution of select lanthanides + Y as a function of pH for the HEH[EHP]/DTPA TALSPEAK system for both 30 minute and 48 hour contact times. Error bars indicate $\pm 1\sigma$ error.

pH	D, La		D, Eu		D, Dy		D, Yb	
	30 min	48 hour	30 min	48 hour	30 min	48 hour	30 min	48 hour
2.5	0.97 ± 0.01	0.08 ± 0.01	0.063 ± 0.03	0.08 ± 0.01	1.80 ± 0.08	1.10 ± 0.01	103 \pm 3	120 \pm 10
2.8	0.83 ± 0.06	0.054 ± 0.02	0.033 ± 0.004	0.09 ± 0.02	0.7 \pm 0.1	1.013 ± 0.008	6.5 \pm 0.4	113 \pm 7
3.2	0.75 ± 0.04	0.089 ± 0.008	0.027 ± 0.008	0.09 ± 0.02	0.4 \pm 0.3	1.12 ± 0.05	5.7 \pm 0.4	119 \pm 9
3.6	0.9 ± 0.1	0.07 ± 0.01	0.26 ± 0.03	0.084 ± 0.003	1.4 \pm 0.2	1.51 ± 0.04	5 \pm 2	138 \pm 6
4.0	0.84 ± 0.09	0.127 ± 0.004	0.3 ± 0.1	0.11 ± 0.03	1.5 \pm 0.4	1.8 \pm 0.2	5 \pm 2	160 \pm 20
4.5	0.90 ± 0.04	0.12 ± 0.02	0.30 ± 0.08	0.26 ± 0.03	1.6 \pm 0.1	2.1 \pm 0.7	6.2 \pm 0.2	117 \pm 50

Table 5.2. Equilibrium constants for the MR_2^- species under various ionic strengths. “Model” value describes values used to fit lanthanide distribution shown in [Figure 3.5](#).

Lanthanide	$\log \beta_{101}$		
	0.1 M	0.5 M	Model
La	19.49	18.23	19.49
Eu	22.39	20.87	22.2
Dy	22.83	21.11	22.0
Y	22.05	20.39	21.5
Lu	22.46	20.77	22.0

The increase in lactate distribution has typically been accompanied by a significant increase in water partitioning to the organic phase.^[11] The observed behavior of the HEH[EHP]/DTPA system warranted further investigation to the amount of lactate and water partitioning to the organic phase as a function of increasing lactate concentration. [Figure 5.7](#) shows the partitioning of lactate and water with DTPA present in the aqueous phase for both HDEHP and HEH[EHP]. A study examining the lactate dependence of sodium extraction into HEH[EHP] was performed to compliment previous investigations involving HDEHP. An expansion of this work was completed observing the pH dependence of sodium extraction into HDEHP and HEH[EHP]. Sodium distribution into the organic phase for both lactate and pH dependences is shown in [Figure 5.8](#).

Discussion

Previous Uses of Phosphonic Acids and TTHA for TALSPEAK

The original Oak Ridge report, published in 1964, provided a brief examination of triethylenetetramine-N,N,N',N'',N''',N''''-hexaacetic acid (TTHA), [Figure 5.1](#).^[15] Initially, TTHA was shown to insufficiently compete with the organophosphorus acid for the americium. Stability constants reported for Am and the lanthanides have since shown TTHA should have significant promise. [Figure 5.2](#) shows the stability constants for DTPA and TTHA with the lanthanides and americium.^[19] Sufficient recovery of Am using DTPA ($\log K_{Am} = 22.9$) from HDEHP has been observed with separation factors as high as 100. If the reported stability constant for Am with TTHA ($\log K_{Am} = 26.6$) is correct, TTHA should be a more than

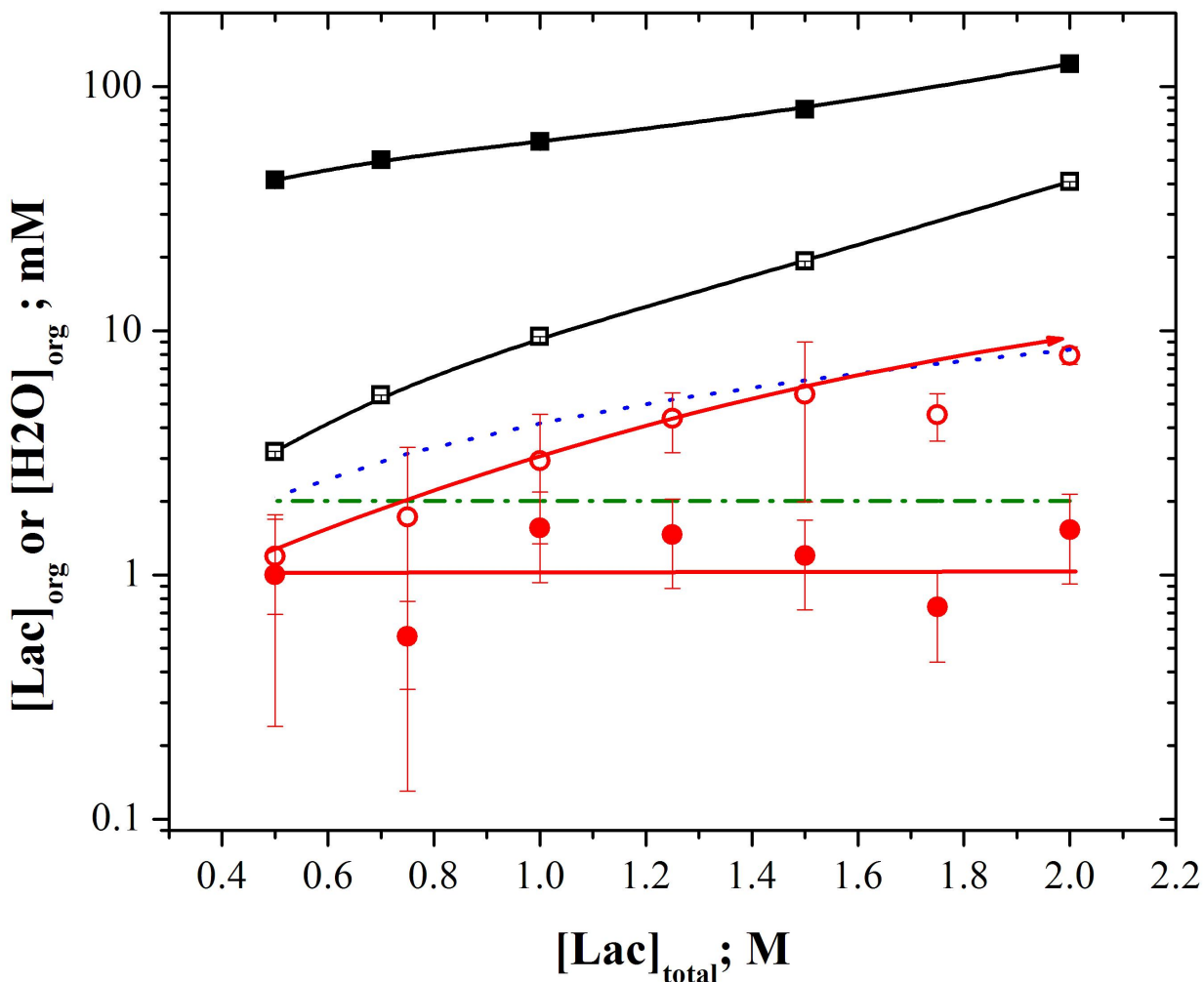


Figure 5.7. Water and lactate partitioning as function of formal lactate concentration. For all studies the following were present: *Aqueous phase*: 1 M total lactic acid, 1 M NO_3^- , 20 mM DTPA, $\text{pH}(\text{final}) = 3.5$ *Organic phase*: 0.2 M HDEHP or 0.1 M HEH[EHP] in n-dodecane. Samples were contacted for 15 minutes. Error bars indicate $\pm 1\sigma$ error. HDEHP- ■ H₂O □ HL HEH[EHP]- ● H₂O ○ HL ●● Calculated concentration of lactic acid in organic phase based on K_d into n-dodecane - - - Calculated concentration of water in organic phase based on K_d into kerosene.

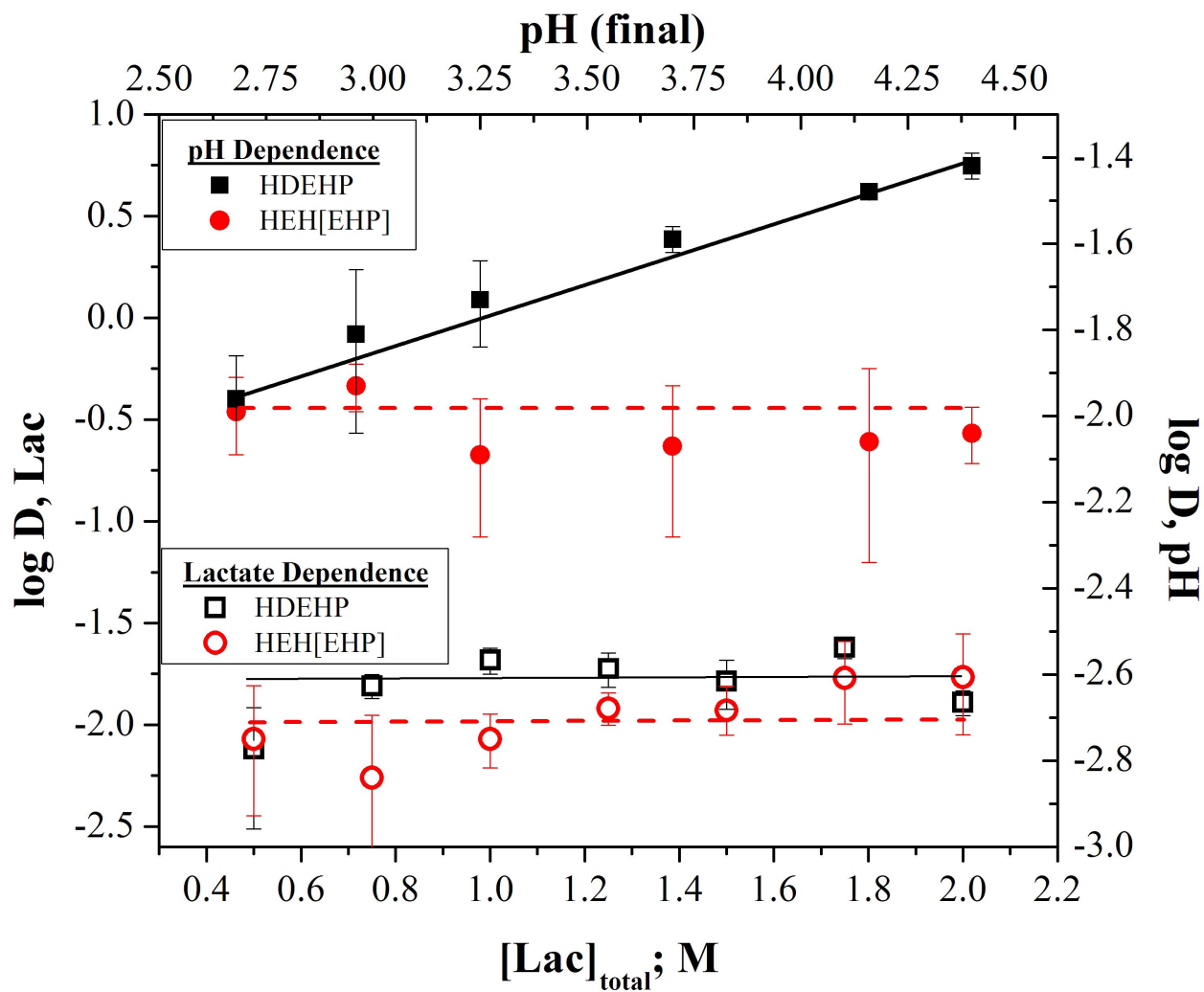


Figure 5.8. Sodium partitioning as function of formal lactate concentration or pH. For all lactate dependence studies the following were present: *Aqueous phase*: 1 M NO_3^- , 20 mM DTPA *Organic phase*: 0.1 M HDEHP or HEH[EHP] in n-dodecane. The pH was 3.5 for all lactate dependence studies. For pH dependence studies, the formal lactic acid concentration was 1 M. All data corresponding to pH dependence study are correlated to the top and right axes. All data corresponding to the lactate dependence study are correlated to the bottom and left axes. Samples were contacted for 15 minutes. Error bars indicate $\pm 1\sigma$ error.

sufficient competitor for HEDHP with americium under the right circumstances. One should expect that the separation factors between americium and the lanthanides should be orders of magnitude higher than observed with DTPA. Since TTHA has the ability to completely saturate the coordination sphere of a lanthanide with carboxylate and amine donor atoms, examining the kinetics behavior of TTHA could also progress understanding of kinetics issues observed for the heavier lanthanides in TALSPEAK.^[16,17,18]

The original Oak Ridge report also examined the performance of two phosphonic acids: 2-ethylhexyl (phenyl)phosphonic acid (HEH[ϕ P]) and decyl(decyl)phosphonic acid HD[DP].^[15] Separation factors for HEH[ϕ P] were comparable to those obtained by HDEHP, except the phosphonic acid gave considerably higher distribution coefficients. Studies with HD[DP] noted slightly lower separation factors and much lower distribution values compared to HEH[ϕ P]. These two phosphonic acid demonstrations are currently the only literature examples using a phosphonic extractant to perform TALSPEAK-type chemistry.

DTPA & TTHA Metal Binding

A steady decrease is observed in the ionic radii of the lanthanides from La³⁺ to Lu³⁺.^[20] This decrease leads to a change in coordination number from 9 for the lighter lanthanides compared to 8 for the heavier lanthanides.^[21] Under some circumstances larger coordination numbers can be observed.^[22] In solvent extraction, lower coordination numbers can be forced by extractant geometry. This change in coordination number leads to different binding behaviors for DTPA and TTHA depending on the lanthanide. Studies have shown all DTPA interaction sites (three N atoms of the diethylene backbone and five O atoms from carboxylate groups) bind to a

lanthanide. For lighter lanthanides with 9-coordinate possibilities, the additional coordination site is generally occupied by water. Studies have shown TTHA to bind in a 10-coordination fashion for the lightest lanthanides. For lanthanides heavier than neodymium, lanthanide-TTHA complexes have been shown to be 9-coordinate with one of the terminal carboxylates not coordinating to the metal center in both the solution and solid phases.^[22] Speciation calculations based on the pK_a 's of DTPA and TTHA from the NIST database at 0.1 M ionic allow calculation of the polyaminopolycarboxylate species available for analyte binding. The speciation diagram for TTHA in relevant TALSPEAK pH ranges is shown in [Figure 5.9](#). A comparable speciation diagram for DTPA has been provided previously.^[10]

Kinetics

It can be seen in [Figure 5.3](#) that the light lanthanides appear to be at equilibrium after 12 hours, but the heavy lanthanides need lactate to reach equilibrium within this time regardless the use of HDEHP or HEH[HEP] as the extractant. The removal of lactic acid is less dramatic for TTHA based systems. The argument could be presented that the mystery equilibrium present in “classical” HDEHP/DTPA TALSPEAK is partially responsible for the slow kinetics observed at low concentrations of lactate. However; metal partitioning studies, discussed below, will show the HEH[EHP]/DTPA system to be potentially absent of additional equilibria and *still* prone to slow heavy lanthanide distribution kinetics. Thus, kinetic challenges appear to be unrelated to equilibria involving currently uncharacterized reactions in the aqueous phase.

The pH dependence of several lanthanides after a 30 minute and 48 hour contact is shown in [Table 5.1](#). The distribution values of lighter and middle lanthanides (modeled by La and Eu)

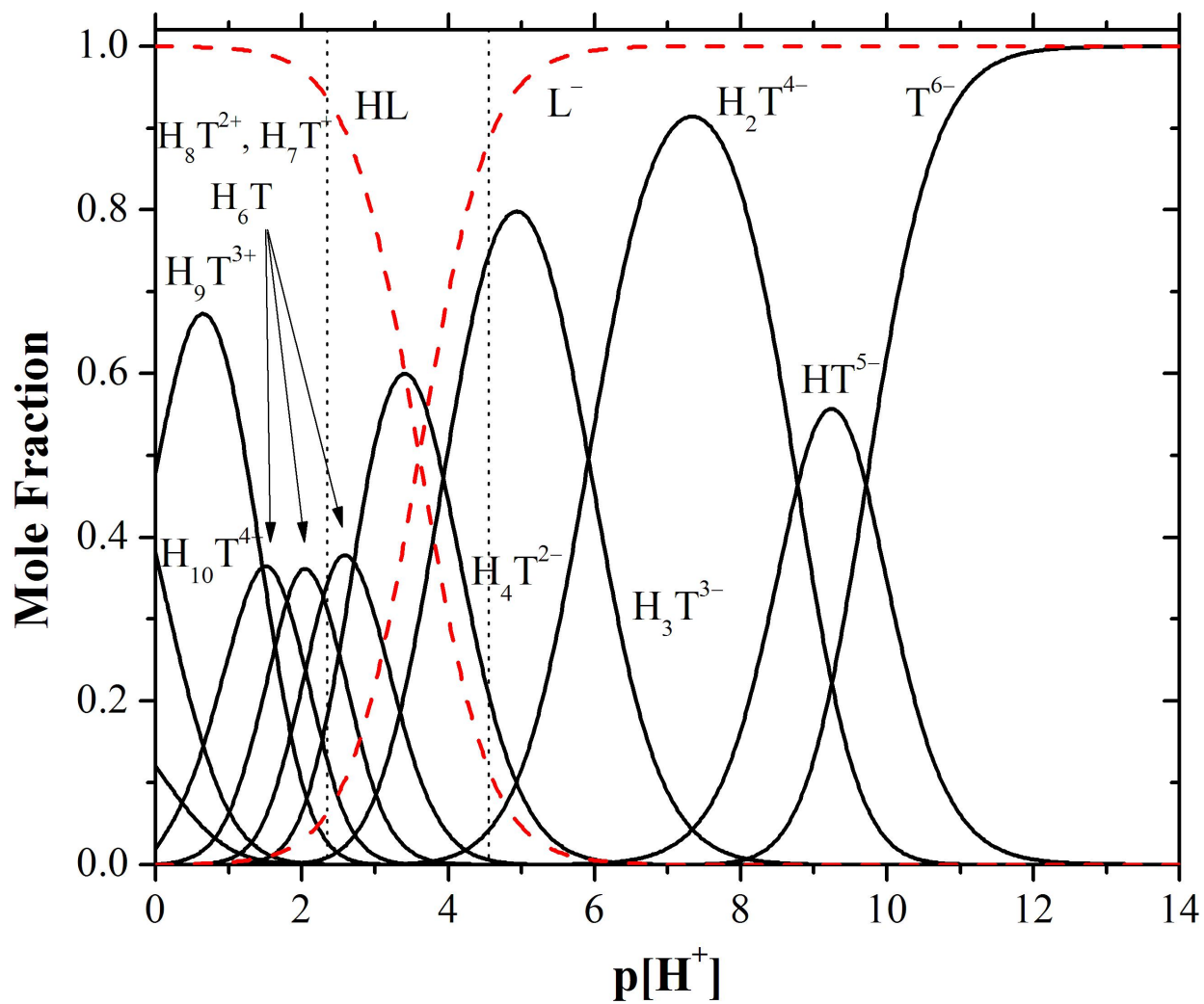


Figure 5.9. Speciation diagram showing DTPA and lactic acid calculated using protonation constants at 0.1 M ionic strength, 25.0°C.^[18] The dotted rectangle outlines approximate working conditions for the TALSPEAK system.

after 30 minutes and 48 hours are within error of each other. One should note the errors for the 30 minute contacts are much larger though. For the heavier lanthanides (shown by Dy and Yb), the difference in metal distribution when comparing the 30 minute and 48 hour contacts is shown in [Table 5.1](#). The distribution values of lighter and middle lanthanides (modeled by La and Eu) after 30 minutes and 48 hours are within error of each other. One should note the errors for the 30 minute contacts are much larger though. For the heavier lanthanides (shown by Dy and Yb), the difference in metal distribution when comparing the 30 minute and 48 hour contacts is substantially greater than for the lighter lanthanides.

The inherently complicated nature of the TALSPEAK aqueous phase makes understanding metal transfer from the aqueous to the organic phase unusually challenging. Studies examining the kinetic dependence of metal partitioning on H^+ , lactic acid, DTPA or HDEHP have been performed.^[16,17] These studies have acknowledged the seemingly catalytic impact of lactate on metal transfer kinetics; however, the specific mechanism for lactate participation is currently unknown.

Previous authors^[18] have suggested a ternary Ln-DTPA-Lactate complex could be formed as an intermediate before metal transfer to the organic phase. The reasoning for this being the addition of lactate could weaken DTPA-metal interactions; thus encouraging release of the metal. For a TTHA-metal complex, all metal coordination sites are occupied therefore making the formation of a ternary intermediate species extremely doubtful unless lability of the carboxylic acid groups allows binding of lactate. If both dissociation pathways participated in ternary complex formation, one may anticipate the system containing TTHA to be slower than the DTPA system because of the additional carboxylic acid groups available for binding. However, [Figure 5.3](#) shows metal partitioning in the system containing TTHA is generally faster

and less impacted by the concentration of lactate. Based on this observation, the probability of ternary complex formation seems unlikely.

Another possibility is for lactate to interact with DTPA or TTHA in an outer sphere mechanism to weaken the Ln-DTPA or Ln-TTHA complex and allow lanthanide partitioning into the organic phase. This interaction may explain some of the observations in lanthanide partitioning discussed below. The interactions of lactic acid with DTPA are currently under examination to elucidate if these are the focus for improved extraction kinetics at higher lactic acid concentrations.

Metal Partitioning in TALSPEAK

A general disagreement has been noted previously between calculated metal distribution values based on equilibrium constants and experimentally obtained values for HDEHP/DTPA TALSPEAK systems.^[10] The mismatch between model and experiment typically becomes more dramatic as the pH continues to increase. Figure 5.4 shows the pH profiles for Eu and Am for several variations of the TALSPEAK process. Theoretical distribution values are calculated based on the following simplified model:

$$D = \frac{\overline{[M(AHA)_3]}}{[M^{3+}] + [ML^{2+}] + [ML_2^+] + [ML_3] + [MR_2^-] + [MHR^-]} \quad (5.3)$$

An in depth discussion of this equation and the equilibrium constants necessary for application have been noted previously.^[9,10,19,23]

Most notable in Figure 5.4 is the comparable extraction behavior of the HEH[EHP] based TALSPEAK systems to the proposed model regardless the presence of DTPA or TTHA. Several hypotheses have been presented in the literature to account for the breach observed between

model and experiment when HDEHP is used as the organic extractant. These have included purely aqueous phase competition reactions such as the formation of a previously unreported $\text{Ln}(\text{Lac})_4^-$ species or mixed Ln-DTPA-Lac complexes. One should observe significant evidence for a lack of the ternary Ln-DTPA-Lac and $\text{Ln}(\text{Lac})_4^-$ species has been provided recently.^[24] Proposed complications of TALSPEAK in the organic phase have included a mixed $\text{Ln}(\text{Lac})_n(\text{AHA})_{3-n}$ extracted species, dramatic changes in the activity of the organic phase brought on by increased partitioning of lactate to the organic phase or the increase in Na^+ concentration at higher pH bringing an interruption in the dimeric structure of the organophosphorus acid based extractants. The results in [Figure 5.4](#) suggest the many discrepancies between the anticipated and observed behavior of the HDEHP-based TALSPEAK process are based purely in the organic phase.

To provide further confirmation of unanticipated results, the pH dependence of other lanthanides was examined. Calculated and experimental distribution of La, Eu, Dy, Lu and Y are shown in [Figure 5.6a](#) using the β_{101} (shown in Equation 4) for DTPA at 0.1 M ionic strength.

$$\beta_{101} = \frac{[\text{MR}^{2-}]}{[\text{M}^{3+}][\text{R}^{5-}]} \quad (5.4)$$

The values for $\log \beta_{101}$ at 0.1 M and 0.5 M ionic strength are shown in Table 2 and define the presence of the MR_2^- species. The modeling shows best agreement with the lightest lanthanides. Deviations from the distribution model are still observed for the middle to heavier lanthanides. However; when HEH[EHP] is utilized as the organic extractant the model predicts metal distribution that is too low. Previously, when the model was compared with HDEHP metal partitioning patterns, the model predicted higher lanthanide partitioning than was observed. The differences between observed and predicted metal partitioning for HDEHP seemed to be consistent for each lanthanide. Differences between observed and predicted metal partitioning

for HEH[EHP] are specific to the lanthanide being examined. The lanthanides with the greatest deviation from predicted behavior seems to correlate with lanthanides dependent on lactate for improved kinetics (Figure 5.3). Figure 5.6b provides the thermodynamically calculated and experimental distribution of La, Eu, Dy and Lu when the β_{101} value is manipulated to fit the extraction data. The $\log \beta_{101}$ values used to fit data in Figure 5.6b are also presented in Table 5.2.

By manipulating the strength of the β_{101} lanthanide-DTPA complex, a better alignment is observed between experimentally observed and calculated distribution values. The values used to fit the data seem to compare reasonably with what is known for lanthanide-DTPA complexes at 0.1 and 0.5 M ionic strength. The equilibrium constants for the β_{101} lanthanide-DTPA species in lactate media have been unexamined to date. Several possibilities exist to justify the manipulation to the β_{101} equilibrium constant required to fit the extraction data, including: activity affects, the hypothetical interaction of lactate on the outer sphere of the lanthanide-DTPA/TTHA complex or the presence of an undetermined equilibria in the aqueous phase. As stated in the kinetics section, NMR studies are currently underway to examine if signal broadening (an indication of interaction between two species) is observed when DTPA and lactate are present in solution together. This lactate-DTPA outer sphere interaction could be dependent on the concurrent binding of DTPA to a particular lanthanide. The improved modeling behavior for some lanthanides in Figure 5.6 provides further validation of metal extraction with HEH[EHP] having fewer extraneous equilibria than when metal extraction in TALSPEAK occurs with HDEHP.

Organic Phase Composition

To further advance understanding of the composition of the organic phase, lactate, sodium and water partitioning were performed for the phosphonic acid system. Although initially intended to be an inert buffer in TALSPEAK chemistry, the liquid-liquid system has shown lactate to impose kinetic benefits on this separation process. Previous work has shown there to be notable amounts of lactate, sodium and water partitioning into the HDEHP/1,4 diisopropylbenzene organic phase when lactate is present.^[11] To expand on these earlier studies, the lactate dependence for the distribution of water, lactate and sodium in HEH[EHP]/DTPA based TALSPEAK was performed. A further exploration of sodium partitioning as a function of pH and lactate for both HDEHP and HEH[EHP] has been completed.

Figure 5.7 shows the partitioning of lactate and water as a function of formal lactate concentration for both HDEHP and HEH[EHP] centered TALSPEAK. Also shown is the distribution coefficient (k_d) for water and lactate into n-dodecane or kerosene, respectively, in the absence of organic extractant. Water and lactate partitioning is within error or less than the k_d value when HEH[EHP] is present. This is notably less than water and lactate partitioning into HDEHP. Since extra water and lactate are lacking in the more thermodynamically predictable HEH[EHP] TALSPEAK, the excess water and lactate in the organic phase could possibly correlate with the discrepancies present between the extraction model and the observed distribution ratios.

The partitioning of sodium into the HDEHP organic phase is of significant interest. Consistent with the patterns for water and lactate partitioning, Figure 5.8 shows sodium partitioning by HDEHP is affected by the pH. Varying the concentration of lactate with HEH[EHP] in the organic phase produces no change in the amount of sodium extraction. One

should also note, the presented $\log K_{\text{ex}}$ for sodium extraction by HDEHP or HEH[EHP] in the literature (Eqn. 5) is -3.56 ± 0.08 in 1 M NaClO_4 or -5.46 ± 0.09 in 0.5 M NaNO_3 ,



respectively.^[25,26] The application of the HDEHP equilibrium constant to the conditions appropriate in this study (1 M NO_3^- , 0.1 M HDEHP, 20 mM DTPA) provides concentrations of the extracted $[\text{NaA}(\text{HA})_3]$ species of ranging from 0.46 to 39.4 mM as the pH is increased from 2.68 to 4.4. Of the 84 mM of Na^+ present in n-dodecane at a pH of 4.4, some of the remaining 40 mM could be accounted for by the presence of potential NaLactate in the organic phase (Figure 5.8). However; using values for lactate partitioning into the organic phase at a concentration of 1 M lactate at a pH of 3.6 using 0.1 M HDEHP, an insufficient presence of lactate seems available to completely account for the remaining sodium present in the organic phase. Changing the pH or concentration of lactate seems to have no impact on the extraction of sodium by HEH[EHP]. This makes the direct relationship observed between pH and sodium extraction for HDEHP seem all the more unique.

The final suggestion for the observed differences between HDEHP and HEH[EHP] based TALSPEAK involves the discussion of micellar aggregation of HDEHP in the organic phase. A reverse micelle is a state of molecular organization comprised of a nonpolar surface surrounding a polar core. For the purposes of an HDEHP micelle proposed here and previously^[11], the hydrophilic branched chains of HDEHP would be exposed to the n-dodecane. The core of the micelle would be composed of the more polar phosphoryl and phosphoric acid groups surrounding water and sodium. Lactate could also be present within the hydrophilic core or by forming the shell of the micelle with the carboxylic acid group pointing towards the aqueous core with the methyl group assisting in forming the hydrophobic exterior. This sort of

aggregation could account for the amount of water, sodium and lactate present. The log of the dimerization constant for HEH[EHP] is 3.37 in toluene media compared to 3.68 for HDEHP.^[12] The relative decrease of dimerization for HEH[EHP] could also describe a decreased tendency for HEH[EHP] to aggregate into larger organic oligomers that would be comprised of sodium, HDEHP, lactate and water.

Some systems have noted this type of reverse micelle microemulsion to be an initial step in the formation of third phases of biphasic extraction systems.^[27,28] The third phase arises when the organic phase splits into two components. One is typically a lighter phase comprised largely of diluent. The other is a heavy phase loaded with extractant, aqueous phase components and metal. Third phase formation raises concerns ranging from simple material handling to safety issues involving criticality.^[29] The ability to further prevent third phase formation through using HEH[EHP], while obtaining consistent separations regardless of pH, makes HEH[EHP] a serious candidate to replace HDEHP in the TALSPEAK process if HEH[EHP] maintains this behavior at higher concentrations of HEH[EHP].

Conclusions

The investigation of fundamental TALSPEAK solution chemistry was aided through the substitution of significant components (DTPA and HDEHP) for comparable ligands (TTHA and HEH[EHP]). Slow lanthanide phase-transfer kinetics appear to be unrelated to the unknown equilibria present in HDEHP based TALSPEAK. The equilibria responsible for the mismatch between thermodynamically predicted and experimentally observed lanthanide distribution appear to be tied previously undefined interactions between HDEHP, water, lactate and sodium.

The simplified behavior and comparable lanthanide/americium separation factors for TALSPEAK including HEH[EHP] may make the substitution of bis-2-ethyl(hexyl) *phosphonic* acid for bis-2-ethyl(hexyl) *phosphoric* acid an attractive solution to the unusual behavior of “classical” TALSPEAK. Work investigating the thermodynamic properties and optimization of this system are ongoing.

References

- [1] Aspinall, H. Chemistry of the f-Block Elements. Gordon & Breach: Australia. 5st Ed. 2001
- [2] Jensen, M. P.; Bond, A. H. Influence of aggregation on the extraction of trivalent lanthanide and actinide cations by purified Cyanex 272, Cyanex 301, and Cyanex 302. *Radiochim. Acta.* **2002**, *90* (4), 205-209.
- [3] Jensen, M. P.; Bond, A. H. Comparison of covalency in the complexes of trivalent actinide and lanthanide cations. *J. Am. Chem. Soc.* **2002**, *124* (33), 9870-9877.
- [4] Choppin, G. R.; Nash, K. L. Actinide separation science. *Radiochim. Acta.* **1995**, *70/71*, 225-236.
- [5] Kozimor, S.A.; Yang, P.; Batista, E.R.; Boland, K.S.; Burns, C.J.; Clark, D.L.; Conradson, S.D.; Martin Wilkerson, M.P.; Wolfsberg, L.E. Trends in covalency for d- and f-Element metallocene dichlorides identified using chlorine k-edge x-ray absorption spectroscopy and time-dependent density functional theory. *J. Am. Chem. Soc.* **2009**, *131* (34), 12125–12136.
- [6] Peterman, D.R.; Martin, L.R.; Klaehn, J.R.; Harrup, M.K.; Greenhalgh, M.R.; Luther, T.A. Selective separation of minor actinides and lanthanides using aromatic dithiophosphinic and phosphinic acid derivatives. *J. Rad. Nucl. Chem.* **2009**, *282* (2), 527-531.
- [7] Hill, C.; Guillaneux, D.; Berthon, L.; Madic, D. Sanex-Btp process development studies. *J. Nucl. Sci. Technol.* **2002**, *Suppl. 3*, 453-461.
- [8] Mincher, B. J.; Modolo, G.; Mezyk, S. P. Review article: The effects of radiation chemistry on solvent extraction: 1. Conditions in acidic solution and a review of TBP radiolysis. *Solvent Extr. Ion Exch.* **2009**, *27* (1), 1-25.
- [9] Nilsson, M.; Nash, K.L. Trans-lanthanide extraction studies in the TALSPEAK system: Investigating the effect of acidity and temperature. *Solvent Extr. Ion Exch.* **2009** *27* (3), 354-377.
- [10] Nilsson, M.; Nash, K.L. Review article: A review of the development and operational characteristics of the TALSPEAK process. *Solvent Extr. Ion Exch.* **2007** *25* (6), 665-710.

- [11] Grimes, T.S.; Nilsson, M.; Nash, K.L.; Lactic Acid Partitioning in TALSPEAK Extraction Systems. *Sep. Sci. Tech.* *Accepted*.
- [12] Miralles, N.; Sastre, A.; Martinez, M.; Aguilar, M. The aggregation of organophosphorus acid compounds in toluene. *Analytical Sciences*. **1992**, *8* (6), 773-777.
- [13] Partridge, J.A.; Jensen, R.C. Purification of Bis(2-ethylhexyl) Hydrogen phosphate by precipitation of copper(II) bis(2-ethylhexyl) phosphate. *J. Inorg. Nucl. Chem.* **1969**, *31* (8), 2547-2589.
- [14] Hu, Z.; Pan, Y.; Ma, W.; Fu, X. Purification of organophosphorus acid extractants. *Solvent Extr. Ion Exch.* **1995**, *13* (5), 965-976.
- [15] Weaver, B.; Kappelmann, F.A. Talspeak, A new method of separating americium and curium from the lanthanides by extraction from an aqueous solution of an aminopolyacetic acid complex with a monoacetic organophosphate or phosphonate. August 1964, ORNL-3559.
- [16] Kolarik, Z.; Koch, G.; Kuhn, W. Acidic organophosphorus extractants. XVIII. Rate of lanthanide (III) extraction by bis(2-ethylhexyl) phosphoric acid from complexing media. *Jour. Inorg. Nucl. Chem.* **1974**, *36* (4), 905-909.
- [17] Danesi, P.R.; Cianetta, C.; Horwitz, E.P. Distribution equilibriums of europium(III) in the system: bis(2-ethylhexyl)phosphoric acid, organic diluent-sodium chloride, lactic acid, polyaminocarboxylic acid, water. *Sep. Sci. Tech.* **1982** *17* (3), 507-519.
- [18] Nilsson, M.; Heydon, A.; Nash, K.L. Studies of the lactic acid concentration on extraction equilibria and kinetics in TALSPEAK chemistry. *Manuscript in preparation*.
- [19] Martell, A.E.; Smith, R.M. NIST Critically Selected Stability Constants of Metal Complexes Database; Version 8.0, 2004.
- [20] Bravard, F. Complexation of trivalent lanthanides with oxygen containing ligands: Studies regarding the chemistry of association and selectivity in solution. **2004**, CEA report, 26.
- [21] Shannon, R.D.; Prewitt, R.C.T. Effective ionic radii in oxide and fluorides. *Acta Crystallogr.* **1969**, *B25* (Pt. 5), 925-946.

[22] Frullano, L.; Rohovec, J.; Peters, J.A.; Geraldes, C.F.G.C. *Structures of MRI Contrast Agents in Solution* in Contrast agents. 1: Magnetic Resonance Imaging, Kraus, V. Eds.; Topics in Current Chemistry, v. 221. Springer: Berlin, Germany. 25-60, 2002.

[23] Sary, J. Separation of the transplutonium elements. *Talanta*. **1966**, *13* (3), 421-437.

[24] Leggett, C.J.; Liu, G.; Jensen, M.P. Do Aqueous Ternary Complexes Influence the TALSPEAK Process? *Solvent. Extr. Ion Exch.* 2010 *28* (3), 313-334.

[25] Gao, Z.; Sun, S.; Kong, W.; Wang, B.; Shen, J. Study on the Solvent Extraction of Sodium with HDEHP. *J. of Shandong University*. **1983**, *4*, 80.

[26] Komasaawa, I.; Otake, T.; Higaki, Y. Equilibrium studies of the extraction of divalent metals from nitrate media with Di-(2-ethylhexyl) Phosphoric Acid. *J. Inorg. Nucl. Chem.* **1981**, *43* (12), 3351-3356.

[27] Osseo-Asare, K. Aggregation, reversed micelles and microemulsions in liquid-liquid extraction: The tri-n-butylphosphate-diluent-water-electrolyte system. *Adv. Colloid Interface Sci.* **1991**, *37* (1-2), 123-173.

[28] Osseo-Asare, K. Microemulsions and third phase formation. **2002** In ISEC 2002, Proceedings of the International Solvent Extraction Conference; Sole, K.C., Cole, P.M., Preston, J.S., Robinson, D.J., eds., S. African Inst. Mining and Metallurgy: Marshalltown, South Africa, 118-124.

[29] Plaue, J.; Gelis, A.; Czerwinski, K.; Plutonium Third Phase Formation in the 30% TBP/Nitric Acid/Hydrogenated Polypropylene Tetramer System. *Sol. Extr. Ion Exch.* **2006**, *24* (2), 271-282.

CHAPTER SIX

CONCLUSIONS

Organophosphorus reagents have been crucial to f-element separations for the past 60 years. The combination of selectivity for f-elements and fewer issues with radiolysis has made organophosphorus extractants virtually irreplaceable in remediation of federal facilities contaminated with radioactive isotopes, including the nuclear weapons complex, and in nuclear fuel reprocessing. A few examples include trivalent actinide and lanthanide extraction in the TRUEX process (octyl(phenyl)-N,N-diisobutylcarbamoylmethyl-phosphine oxide, CMPO), uranium and plutonium extraction in the PUREX process (tri-n-butyl phosphate, TBP), and trivalent lanthanide extraction from trivalent lanthanides in the TALSPEAK process (bis-2-(ethyl)hexyl phosphoric acid, HDEHP). This dissertation is focused on the use of organophosphorus solvating extractants for proposed remediation of the Hanford site in south central Washington state and on cation exchange extractants for trivalent lanthanide separations from trivalent actinides. These reagents share a considerable affinity for the target metal ions (or their salts) and a substantial ability to support partitioning of these species into organic media.

Hanford Site Remediation

The objective of this investigation was to compare the abilities of an extraction chromatographic (EXC) decontamination of Hanford tank leachate solutions with the successful decontamination already displayed using liquid-liquid extraction. This decontamination in the liquid-liquid system was accomplished by selectively removing radioactive species (UO_2^{2+} and Eu(III), representative in general of oxidized and reduced actinide species) using TBP and tri-n-

octyl phosphine oxide (TOPO) in dodecane. The results from EXC studies using 60% $(m_{\text{TBP}})/(m_{\text{TBP}}+m_{\text{XAD7}})$ and 58% TOPO $(m_{\text{TOPO}})/(m_{\text{TOPO}}+m_{\text{XAD7}})$ impregnated XAD-7 resins were very comparable to liquid-liquid studies. All the extraction experiments involving the TBP-XAD7 system indicate that it is only suitable for complete decontamination of the HNO_3 leachate solutions when $[\text{Al}(\text{NO}_3)_3]$ is moderate to high. The results from the TOPO-XAD7 system indicate that complete decontamination is possible from solutions of low $[\text{HNO}_3]$ and $[\text{Al}(\text{NO}_3)_3]$. Considering that UO_2^{2+} was quantitatively extracted from all aqueous $\text{HNO}_3/\text{Al}(\text{NO}_3)_3$ solutions in both systems, the failure for these processes relates to their inability to remove the Eu(III) species.

The initial studies focused on the partitioning of nitric acid into TBP and TOPO impregnated resins as a function of varied $\text{Al}(\text{NO}_3)_3$. Results suggested $(\text{TBP})\cdot\text{HNO}_3$, $(\text{TBP})_2\cdot\text{HNO}_3$, $(\text{TOPO})\cdot\text{HNO}_3$, $(\text{TOPO})_2\cdot\text{HNO}_3$ species were present in the resin. The presence of the $(\text{TOPO})_2\cdot\text{HNO}_3$ species had not been reported before. This was related to the relatively low solubility of TOPO in aliphatic diluents. Typical liquid-liquid studies using an n-dodecane organic diluent use 0.1 M TOPO. The calculated concentration of 58% TOPO $(m_{\text{TOPO}})/(m_{\text{TOPO}}+m_{\text{XAD7}})$ was more than an order of magnitude higher (1.33 M). The observation of the 2:1 TOPO: HNO_3 both highlight some of the differences that can distinguish EXC from liquid-liquid separations.

Extraction chromatographic investigations expanded on initial liquid-liquid studies by examining the redox behavior of Np in such a system. To aid in this investigation, the partitioning of Th^{4+} , UO_2^{2+} and Eu^{3+} was studied to model the distribution behavior of An^{4+} , AnO_2^{2+} , and An/Ln^{3+} cations, respectively. Comparing uptake of redox active (Np) with redox-stable analogs UO_2^{2+} , Th^{4+} , Eu^{3+} allowed an approximation of the anticipated redox state of Np

in the sludge simulants for both potentially oxidizing and reducing conditions. These studies indicated Np would be a mixture of NpO_2^+ or NpO_2^{2+} depending largely on the concentration of acid. As $[\text{HNO}_3]$ increased, NpO_2^{2+} becomes more important. At the highest $\text{Al}(\text{NO}_3)_3$ and HNO_3 concentrations, NpO_2^{2+} appeared to be the sole oxidation state for Np in the system. Since Np partitioning was only truly controllable under oxidizing conditions, later decontamination investigations focused on the partitioning of Eu^{3+} , PuO_2^{2+} , NpO_2^{2+} and UO_2^{2+} from chromate containing media.

To encourage faster flow rates (and ultimately higher column throughput) the kinetics of the TOPO-XAD7 resin were improved by wetting the impregnated resin with n-dodecane. Previous work has shown that the uptake kinetics of impregnated solids (such as TOPO) can be improved by providing rearrangement capabilities when the solid extractant is dissolved in a diluent.[1] The uptake kinetics of the TOPO-XAD7 resin were greatly improved by decreasing the extractant concentration to 38% ($m_{\text{TOPO}}/m_{\text{TOPO}} + m_{\text{XAD7}}$) and wetting with n-dodecane. Langmuir isotherms and dynamic capacity determinations (breakthrough curves) showed the decreased concentration of TOPO on the resin led to a more efficient use of extractant. The Eu:TOPO stoichiometries for the 58% and 38% TOPO-XAD7 resins were 1:4 and 1:3.5, respectively. Creating an environment that more closely resembled a liquid-liquid extraction system by wetting the resin with n-dodecane and decreasing extractant concentration, led to Eu:TOPO stoichiometries that more closely resembled a liquid-liquid system (1:3).[2]

Chromatograms were developed examining individual Eu^{3+} , PuO_2^{2+} , NpO_2^{2+} , and UO_2^{2+} separations and separations in a simulated waste steam containing all species together using the kinetically preferential 38% ($m_{\text{TOPO}}/m_{\text{TOPO}} + m_{\text{XAD7}}$) resin. For all studies, quantitative loading (>99%) of all species was observed as well as quantitative recovery. The separation of trivalent

species (modeled by Eu^{3+}) from PuO_2^{2+} , NpO_2^{2+} , and UO_2^{2+} was achieved using 3 M HNO_3 , 1 mM KBrO_3 (to maintain redox actinides in the hexavalent state in the absence of Cr). Removal of hexavalent actinides was performed using 0.1 M 1-hydroxyethane 1,1-diphosphonic acid and 1 mM KBrO_3 .

Although the extraction chromatographic results were comparable to the liquid-liquid results, throughput and column blockage can be drawbacks to the implementation of chromatography on a large scale. Of course, extractant loss occurs in both liquid-liquid and extraction chromatographic methods. If the extractant were covalently bound to a polymer (instead of merely held in place by solubility preferences), chromatographic separations of nuclear fuel could become preferable. The next chapter examined the possibility of a resin with phosphate ester covalently bound to a polystyrene backbone.

Covalently Bonded Resins with Phosphate Ester Moieties

This investigation aimed to characterize the actinide uptake of the novel pPenta, pTris and pTris-Mono resins (Figure 6.1). This characterization was accomplished by examining uranium uptake from nitric acid, sodium nitrate and sodium carbonate media. Infrared spectra of the resins were obtained to compliment observations of partitioning studies. Although previous studies had indicated uptake of uranyl via a solvating mechanism through the phosphoryl oxygen, uranium partitioning studies indicated hydrolysis of the ethoxy groups forming phosphoric acid moieties.[3-6] Metal extraction would most likely occur through a cation

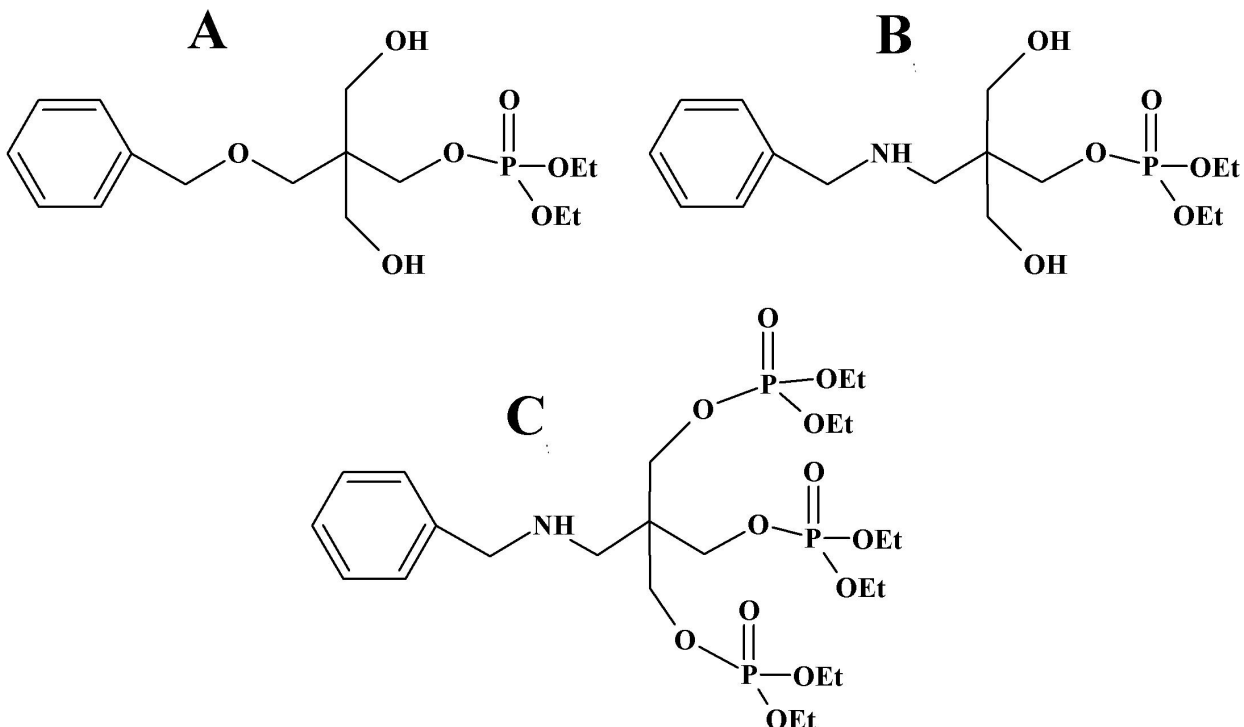


Figure 6.1. Structures of immobilized: a) pentaerythritol triethoxylate (*pPenta*) b) tris (hydroxymethyl) amino methane (*pTris*) c) mono-tris(hydroxymethyl)amino methane (*pTris-Mono*)

exchange mechanism at the acidic oxygen if this were the case. In this case, uptake should decrease as $[\text{HNO}_3]$ increases, though the pattern could be complex, as HNO_3 could compete with $\text{UO}_2(\text{NO}_3)_2$ for the extractant molecules.

For the *pPenta*, *pTris* and *pTris-Mono* resins, uranium extraction decreased as the concentration of nitric acid increased from 0.01 – 4 M HNO_3 . With neutral phosphate based extractants (such as TBP) increasing the nitric acid concentration typically increases metal extraction since the background anion (NO_3^-) complexes with the metal cation (UO_2^{2+}) to charge neutralize the cation for partitioning into the neutral organic phase.[7] Increasing the concentration of nitric acid typically decreases metal partitioning to the organic phase since the additional aqueous phase protons compete with the metal for the organic phase extractant. For

the pPenta, pTris and pTris-Mono resins, the decrease in metal partitioning observed as nitric acid increased indicated a cation exchange mechanism was occurring. Such an extraction mechanism would be possible if the ethoxy groups were hydrolyzing and the phosphoric acid was being formed. The literature has shown the hydrolysis of neutral phosphates slows as the chain length or branching of the chain increases. The short chain esters present in these resins would most likely hydrolyze quickly in the presence of acid.

Several other experiments were performed examining the batch uptake of the metal ions under various conditions that could establish the occurrence of hydrolysis. The uptake of uranium was examined for the three resins after a pre-equilibration with nitric acid was done. Performing the equilibration prior to metal partitioning resulted in an apparent increase in cation exchange metal partitioning trends; therefore providing further evidence for acid promoted hydrolysis of the phosphate ester. Another partitioning study examined the uptake of uranium in the presence of Eu^{3+} and Th^{4+} . The presence of Th^{4+} is particularly helpful, since Th^{4+} uptake will be preferential over UO_2^{2+} if the resin is participating through a cation exchange mechanism. If the resin is participating through a solvating mechanism, UO_2^{2+} uptake by the phosphate would be preferential (based on analogy with TBP solvent extraction) and no difference in UO_2^{2+} uptake would be observed regardless the presence of Eu^{3+} and Th^{4+} . In the presence of Eu^{3+} and Th^{4+} , UO_2^{2+} uptake was significantly decreased at low acid concentrations ($< 1 \text{ M HNO}_3$). When the concentration of HNO_3 is greater than 1 M, the partitioning of UO_2^{2+} is the same, within error, for systems with and without Eu^{3+} and Th^{4+} . These results indicated uranium uptake was occurring through a cation exchange mechanism when the concentration of HNO_3 was less than 1 M. At concentrations greater than 1 M HNO_3 , uranium extraction was occurring through a solvating mechanism.

Infrared spectra (IR) of the resin were examined before and after contact with 1, 2 and 4 M HNO₃ for the pTris resin. Spectra prior to contact with HNO₃ were in agreement with spectra acquired with the Alexandratos group. The presence of a phosphoryl stretch ($\nu_{\text{PO}} = 1280 \text{ cm}^{-1}$) and phosphoryl bend ($\nu_{\text{COP}}^* = 970\text{-}1050 \text{ cm}^{-1}$, $740\text{-}830 \text{ cm}^{-1}$) for an organophosphorus ester in the IR spectra were of particular importance for conveying the presence of a neutral phosphate ester.[8] A phosphoric acid wag (observable in solid phosphate acids, $\nu = 2500\text{-}2350 \text{ cm}^{-1}$) would indicate the presence of hydrolyzed functional groups. The IR active bands typical of phosphate esters were absent regardless the concentration of nitric acid. In some instances, the phosphoric acid wag was present. For the highest concentrations of acid, there appeared to be an absence of any functional groups.

The hydrolysis of the phosphate esters was disappointing considering the possible use of such a resin for the proposed acidic remediation of the Hanford site and other more common PUREX type applications. However; the experience with cation exchange materials provided another opportunity for extraction chromatography to compliment or advance understanding of liquid-liquid systems. The distribution of lanthanides in the TALSPEAK process is currently poorly understood. A study examining lanthanide partitioning using extraction chromatographic materials was proposed to study lanthanide partitioning from a TALSPEAK-type aqueous phase to extraction chromatographic materials.

Extraction chromatographic investigations of TALSPEAK chemistry

The examination of TALSPEAK chemistry using extraction chromatographic materials has not been reported previously. Previous reports had performed “proof-of-concept” investigations using aqueous phase conditions observed in liquid-liquid systems that provide the highest

separation factors and applying them to HDEHP immobilized on silica supports. While these separations were successful in providing the quantitative separation of Eu^{3+} from Am^{3+} , little was gained in understanding of the fundamental chemistry. A systematic examination of TALSPEAK chemistry was performed on a series of extraction chromatographic materials comprised of two different acidic organophosphorus extractants bis-(2-ethylhexyl) phosphoric acid (HDEHP), 2-ethylhexyl (2-ethylhexyl)phosphonic acid (HEH[EHP]), sorbed on Amberchrom CG-71, an aliphatic acrylic polymer. Only the initial studies of Weaver and Kappelmann examined the use of phosphonic acids to perform TALSPEAK separations.[9] This same previous study presented some separations of Am from the lanthanides using of triethylenetetramine-N,N,N',N'',N''',N''''-hexaacetic acid (TTHA) as the hold-back reagent in the aqueous phase. The results described Chapter 4 of this dissertation focused on the use of extraction chromatography, HEH[EHP] and TTHA as alternative TALSPEAK reagents.

The highest $\text{Am}^{3+}/\text{Eu}^{3+}$ separation factors were provided when the HEH[EHP] impregnated resin was coupled with TTHA in the aqueous phase (SF ~ 120). Unfortunately, simulated lanthanide waste studies showed TTHA will retain lanthanides lighter than Nd in the aqueous phase. This kind of retention is highly undesirable since most simulated waste will be comprised of lanthanides lighter than Gd. When TTHA concentrations were decreased to encourage partitioning of the light lanthanides to the resin, Am^{3+} partitioning to the resin increased as well. The conclusion was reached that even though $\text{Am}^{3+}/\text{Eu}^{3+}$ separations are cleaner with TTHA, DTPA is still the most complete hold-back reagent for applied nuclear fuel separations since the light lanthanides are not retained as strongly in the DTPA aqueous phase.

The dependence of the metal uptake on pH of the EXC system using HDEHP showed some very different patterns than were seen in the liquid-liquid system. Thermodynamic model

calculations based on equilibrium constants from the previous literature indicate that lanthanide and actinide distribution ratios should decrease slightly as the pH increases from 2 to 3.5. At pH above 3.5, the model predicts that metal partitioning should increase slightly.[10]

Experimentally, both EXC and liquid-liquid systems metal partitioning decreases at pH above 3.5, consistent with previous reports from the literature. Interestingly, europium uptake deviates more from the predicted thermodynamic model for the HDEHP extraction chromatographic system than the HDEHP liquid-liquid system. It is postulated that difference arises from potential micellar aggregation (not accounted for by the thermodynamic model) being more significant in an extraction chromatographic system neat extractant used in the EXC system could be more prone organizing into larger oligomers than the diluted extractant present in liquid-liquid systems.

Metal partitioning also decreased as pH increased when HEH[EHP] was used as the extractant as well, though the decrease was less drastic than that seen in the HDEHP system. The decreased deviation of the LN2 resin from thermodynamically predicted models was interesting. Two, nearly contradicting, explanations were suggested for this observation. 1) The dimerization constant for HEH[EHP] is about 2 times lower than that for HDEHP.[27] It is postulated that, a decreased tendency to dimerize may make HEH[EHP] less likely to associate into larger molecular clusters. 2) The higher pK_a of the phosphonic acid buffer (4.51) compared to the phosphoric acid buffer (3.47) could be more significant.[28] At a pH of 3.6, nearly 50 % of the HDEHP will have a tendency to exchange a proton for a sodium ion deprotonated. Therefore the organic phase may contain less $(HA)_2$ and more (Na^+AHA^-) (or some de-dimerized material like Na^+A^- in the organic phase). This de-dimerization may encourage micellization of the HDEHP. Sodium partitioning did increase into the HDEHP organic phase when the pH of

the aqueous phase was above 3.5. Interestingly, an increase in sodium extraction was not observed for the phosphonic acid. The phosphonic acid has a higher pK_a and probably remains as primarily $(HA)_2$ well beyond pH 4, hence less prone to de-dimerization and the formation of micelles. The experimental evidence suggest the latter hypothesis is more likely to be correct.

On an applied level, no real benefit was gained by perform TALSPEAK separations chromatographically. The information obtained regarding TTHA helped in understanding the complexity of group lanthanide separations. The potential of TTHA and the unique behavior of HEH[EHP] justified further examination in a more applied liquid-liquid extraction system.

The Examination of HEH[EHP] and TTHA for TALSPEAK Solvent Extraction Systems

The original Oak Ridge report introducing the TALSPEAK separations process examined multiple candidates to serve as organic phase extractants, aqueous complexants and carboxylic acid buffers.[9] The most successful TALSPEAK separations observed included bis-(2-ethylhexyl) phosphoric acid (HDEHP), diethylenetriaminepentaacetic acid (DTPA), and lactic acid as the acidic phosphorus extractant, the polyaminocarboxylic acid complexant, and the carboxylic acid buffer, respectively (Figure 6.2). While this system has shown sufficient recovery of Am with separation factors as high as 100, there are some concerns regarding the current process. The most apparent being slow kinetics of heavy lanthanide transfer to the organic phase and the potential formation of micelles in the organic phase. Micelle formation in the organic phase of liquid-liquid separations has been shown to be a precursory step to third-phase formation. The slow kinetics are generally improved by the addition of lactate, but the mechanism of lactate participation is still largely uncharacterized. This work shows by

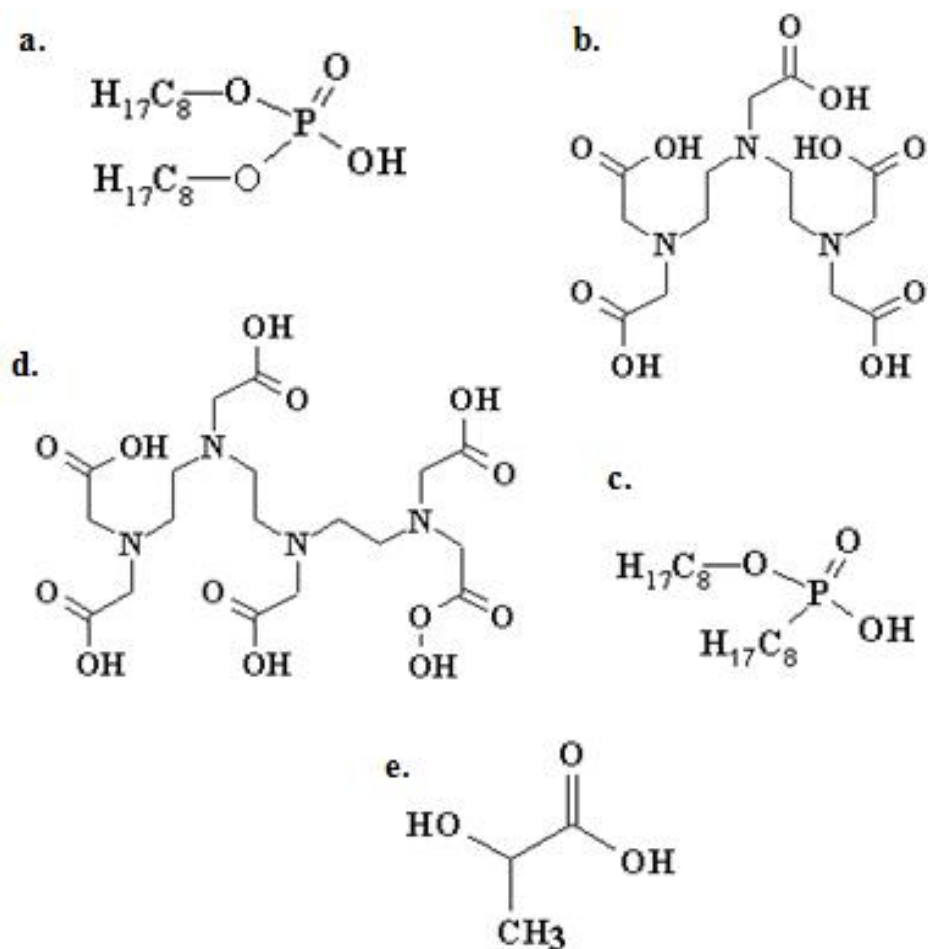


Figure 6.2 Structures of the components used in these studies; a: di(2-ethylhexyl) phosphoric acid (HDEHP) b: diethylenetriamine- N,N,N',N'',N'''-pentaacetic acid (DTPA) c: di(2-ethylhexyl) phosphonic acid (HEH[EHP]) d: triethylenetetramine- N,N,N',N'',N''',N''''-hexaacetic acid (TTHA) e: lactic acid (HL)

exchanging the classically used holdback reagent (DTPA) with TTHA some proposed mechanisms for the role of lactate can be eliminated. The replacement of HDEHP with analogous phosphonic acid, HEH[EHP], helped in understanding the significance of the HDEHP organic phase composition.

The lactate dependence of lanthanide transfer to an HDEHP or HEH[EHP] organic phase from a DTPA or TTHA aqueous media was helpful in understanding the mechanisms of lanthanide phase transfer. The previous literature has suggested the formation of a Ln-DTPA-

Lac ternary complex forming as an intermediate before metal transfer to the organic phase. Since TTHA saturates the coordination sphere of all lanthanides, this sort of ternary complex formation would likely be less possible for the TTHA aqueous complexant. However, results show the system containing TTHA is generally faster and less impacted by the concentration of lactate. Based on this observation, the probability of ternary complex formation seemed low. An alternative explanation was provided that lactate interacts with DTPA or TTHA in an outer sphere mechanism to weaken the Ln-DTPA or Ln-TTHA complex and allow lanthanide partitioning into the organic phase. Examining the interaction of lactate with the metal-DTPA complex was continued during the thermodynamic modeling of the system.

A general disagreement has been noted previously between calculated metal distribution values based on equilibrium constants and experimentally obtained values for HDEHP/DTPA TALSPEAK systems.[10] The mismatch between model and experiment typically becomes more dramatic as the pH continues to increase. However, when lanthanide extraction is performed using HEH[EHP] from an aqueous TALSPEAK media, the distribution patterns could be better modeled using known extraction equilibria. A further improvement to the model was observed if DTPA binding constants (originally used at 0.1 M) for the formation of the MR_2^- species were manipulated. The manipulations were within a range that could be reasonably accounted for by changing from a single-ion aqueous phase (where the NIST binding constants were determined) to a mixed electrolyte, high ionic strength media. The change required in the binding constant also could be related to the outer sphere interaction of DTPA with lactate.

The difference in lanthanide extraction trends between HDEHP and HEH[EHP] warranted further examination of the composition of the HEH[EHP] organic phase for comparison with previous studies that had examined the concentrations of water, lactate and sodium in the

HDEHP organic phase.[11] Water and lactate partitioning was within error or less than the K_d value when HEH[EHP] was used as the organophosphorus extractant. This was notably less than water and lactate partitioning into HDEHP from a TALSPEAK aqueous phase. Since extra water and lactate were lacking in the more thermodynamically predictable HEH[EHP] TALSPEAK, the excess water and lactate in the organic phase are thought to possibly correlate with the discrepancies present between the extraction model and the observed distribution ratios. The previous section discussing the extraction chromatographic behavior of TALSPEAK chemistry introduces the possibility of reverse micelle formation as the avenue for additional water, sodium and lactate in the organic phase of HDEHP-based TALSPEAK. The proposed reversed micelle would have a core composed of the more polar phosphoryl and phosphoric acid groups surrounding water and sodium. Lactate could also be present within the hydrophilic core or by forming the shell of the micelle with the carboxylic acid group pointing towards the aqueous core with the methyl group assisting in forming the hydrophobic exterior.

The application of HEH[EHP] (or a similar phosphonic acid) as a replacement for HDEHP currently offers possible benefits in advancing the stability of the separation. Significant work is remaining investigating the optimization and thermodynamic characteristics of this separation. Immediate future work includes the application of SANS spectroscopy to the HDEHP and HEH[EHP] organic phases to compare structural differences that may exist.

Overall Conclusions

This dissertation investigated the use of organophosphorus reagents for the remediation and reprocessing purposes of used nuclear fuel. Tri-n-octyl phosphine oxide provided the extraction

capabilities necessary to provide a clean-up of secondary waste arising from the Hanford site. The pPenta, pTris and pTris-Mono resins provided further insight to the qualities required for the development of a solvating extractant covalently bonded to a polymeric support,. The use of HEH[EHP], both in chromatographic and liquid-liquid methods, provided insight, and quite possibly an improvement, to the useful but incompletely understood TALSPEAK process. The successful application of these extractants to issues and questions posed throughout this dissertation indicates the continued use of organophosphorus reagents in f-element separations for many years to come.

References

- [1] Sulakova, J. Study of solid extractants for separation of minor actinides from high active liquid waste, Ph.D. Thesis, Czech Technical University: Prague, 179, 2007.
- [2] Foffart, J.; Duyckaerts, G. Extraction of lanthanides and actinides by alkylphosphine oxides. IV. Extraction of trivalent cations by tri-n-butylphosphine oxide or tri-n-octylphosphine oxide. *Analyt. Chim. Acta*, **1969**, *46* (1), 91-9.
- [3] Alexandratos, S.D.; Zhu, X. High-affinity ion-complexing polymer-supported reagent: Immobilized phosphate ligands and their affinity for the uranyl ion. *React. Polym.* **2007**, *67* (5), 375-382.
- [4] Alexandratos, S.D.; Zhu, X. Immobilized Tris(hydroxymethyl)aminomethane as a Scaffold for Ion-Selective Ligands: The Auxiliary group Effect on Metal Ion Binding at the Phosphate Ligand. *Inorg. Chem.* **2007**, *46* (6), 2931-2147.
- [5] Alexandratos, S.; Xiaoping, Z.; Polyols as scaffolds in the development of ion selective polymer-supported reagents: The effect of auxiliary groups on the mechanism of metal ion complexation. *Inorg. Chem.* **2008**, *47* (7), 2831-2836.
- [6] Alexandratos, S.; Xiaoping, Z. Immobilized phosphate ligands with enhanced ion affinity through supported ligand synergistic interaction. *Sep. Sci. & Tech.* **2008**, *43* (6), 1296-1309.
- [7] Alcock, K.; Best, G.F.; Hesford, E.; McKay, H.A.C. Tri-n-butyl phosphate as an extracting solvent for inorganic nitrates – V. *J. Inorg. Nucl. Chem.* **1958**, *6* (4), 328-333.
- [8] Smith, A.L. *Applied infrared spectroscopy: fundamentals, techniques, and analytical problem-solving*. Wiley:New York, NY. 1979.
- [9] Weaver, B.; Kappelmann, F.A. TALSPEAK, A new method of separating americium and curium from the lanthanides by extraction from an aqueous solution of an aminopolyacetic acid complex with a monoacetic organophosphate or phosphonate. August 1964, ORNL-3559.
- [10] Nilsson, M.; Nash, K.L. Trans-lanthanide extraction studies in the TALSPEAK system: Investigating the effect of acidity and temperature. *Solvent Extr. Ion Exch.* **2009**, *27* (3), 354-377.

[11] Grimes, T.S.; Nilsson, M.; Nash, K.L.; Lactic Acid Partitioning in TALSPEAK Extraction Systems. *Sep. Sci. Tech. Accepted for publication, 2010.*